Synthesis, characterization and biological studies of some organotin-dithiocarbamate complexes

Oluwasegun Jerry Adeyemi

orcid.org/0000-0002-7769-5264

Thesis submitted in fulfilment of the requirements for the degree *Doctor of Philosophy in Chemistry* at the North-West University

Promoter: Prof. D.C. Onwudiwe

Graduation: April 2019

Student number: 28570235

CERTIFICATE OF LANGUAGE EDITING

NORTH-WEST UNIVERSITY
YUNIBESITI YA BOKONE-BOPHIRIMA
NOORDWES-UNIVERSITEIT
MAFIKENG CAMPUS

Tel: +27 18 3892308

Fax: +27 18 3892052

E-mail: David.Isabirye@nwu.ac.za

Internet: http://www.nwu.ac.za

7 September 2018

This serves to confirm that I have read and edited the PhD thesis of Mr O.J. Adeyemi (student number 28570235) entitled:

"Synthesis, characterization and biological studies of organotin-dithiocarbamate complexes".

The candidate corrected the language errors identified to the satisfaction of the supervisor.

The document presentation is of an acceptable academic and linguistic standard.

Thank you

.....

Dr D.C. Onwudiwe

Supervisor

.....

Prof D.A. Isabirye

Language Editor

Faculty of Natural and Agricultural Sciences

DECLARATION

I declare that this doctoral thesis titled: "**Synthesis, characterization and biological studies of some organotin-dithiocarbamate complexes**" is solely owned by me, and has not been submitted to any other institution for the purpose of obtaining a degree or qualification, and all sources cited are acknowledged by comprehensive referencing.

Signature: 

Adeyemi, Oluwasegun Jerry

ABSTRACT

Organotin(IV)dithiocarbamate owe their functionality and usefulness to the individual attributes of the organotin and the dithiocarbamate moieties. The synergy exhibited by these moieties has resulted in the enhanced biological activity of the hybrid molecule. This thesis reports the synthesis, characterization and evaluation of the biological properties (including antimicrobial, antioxidant and anticancer activities) of series of organotin(IV) dithiocarbamate complexes. Organotin(IV) chlorides of various alky and aryl groups [R_nSnCl_{4-n}] (n = 1, 2; R = CH_3, C_4H_9, C_6H_5) were utilized, while the dithiocarbamate ligands [$^-S_2CNRR'$] (R= H, CH_3, C_2H_5, C_4H_9, C_3H_5 and R′= C_6H_5, C_6H_5-CH_2, CH_3-C_6H_5, C_2H_5-C_6H_5, C_3H_5) were constituted of different alkyl, allyl and aryl substituents, resulting in array of compounds with different stereochemistry. All the complexes were characterized using spectroscopic techniques (FTIR, ^1H and ^{13}C and ^{119}Sn NMR) and elemental analysis, and a few of them were further characterized by single crystal X-ray diffraction. The thermal decomposition properties of the complexes were studied using thermogravimetric analyser, and they displayed varying decomposition patterns to give tin sulfide residue of different phases. The antimicrobial properties of the complexes were studied using some gram positive bacteria (*Bacillus cereus and Staphylococcus aureus),* gram negative bacteria (*Escherichia coli, Klebsiella pneumonia* and *Pseudomonas aeruginosa*) and some fungi (*Candida albicans* and *Aspergillus flavus*). They showed great potential as antimicrobial agents better than their respective ligands, and compared favorably with other standard drugs used as control. The complexes also exhibited potentials as antioxidant agents from the study carried out using 2,2-diphenyl-1-picrylhydrazyl (DPPH) and reducing power assays methods. Furthermore, the preliminary *in vitro* cytotoxicity activity study of the complexes was tested against tumor cell line human cervix carcinoma (HeLa). Activity ranged from very good to moderate, for all tested

complexes. These complexes could be useful lead compounds in antibiotic, antioxidant and anticancer studies.

Key words: Organotin(IV); dithiocarbamate; antimicrobial; antioxidant; cytotoxicity

Word count: 311

DEDICATION

This thesis is dedicated to my amazing parents, Pastor and Mrs J.A. Adeyemi and my amiable blessing, Salome Joel. Few words on this page cannot capture my immense gratitude towards your support in achieving this great fit. Thank you for your encouraging words in times when things were not going so good and for the endless prayers and financial supports. I love you very much, and God bless you.

I also dedicate this thesis to every young person out there who comes in contact with this. Believe, work hard, be dedicated, trust God and the sky will be your limit.

ACKNOWLEDGEMENTS

Firstly, my heart is filled with gratitude to God for this immense grace in granting me the strength and wisdom needed to complete this research study.

I am grateful to my supervisor, Prof Damian Onwudiwe for his guidance and supervision during the rigorous research process. Also, I want to appreciate Prof. Moganavelli Singh, Dr Eric Hosten, Dr Anthony Ekennia, Dr Chinedu Anokwuru, Mr. Uwaoma Romanus, for their support in carrying out this research effectively. Thank you and God bless you.

My gratitude also goes to great mentors, friends and colleagues: Mr and Mrs Uche Obiofuma, Mr and Mrs Joel, Mr. Funsho Ogunsola, Pastor (Dr) Ademola Adeyinka, Dr (Mrs) Yemi Aremu, Dr. David Olusegun, Ayanfeoluwa Oyewo, Jesumayowa Ajidahun, Lynda Martins, and Mrs Felicia Bobinihi, Dr Jeje Osuntokun, Dr Emeka, for their intellectual and moral support.

I would also like to thank my siblings, Funmilola Ibikunle, Femi Adeyemi and Adeola Ademefun and their respective families, for their unending support of love. God bless you!

PUBLICATIONS

Part of this Thesis has been reported or submitted as follows:

J.O. Adeyemi, D.C. Onwudiwe, E.C. Hosten, Organotin(IV) complexes derived from N -ethyl-N -phenyldithiocarbamate: Synthesis, characterization and thermal studies, J. Saudi Chem. Soc. 1 (2017) 0–471. doi:10.1016/j.jscs.2017.08.004.

J.O. Adeyemi, D.C. Onwudiwe, A.C. Ekennia, R.C. Uwaoma, E.C. Hosten, Synthesis, characterization and antimicrobial studies of organotin(IV) complexes of N- methyl -N-phenyldithiocarbamate, Inorganica Chim. Acta. 477 (2018) 148–159. doi:10.1016/j.ica.2018.02.034.

J. Adeyemi, D. Onwudiwe, Organotin(IV) Dithiocarbamate Complexes: Chemistry and Biological Activity, Molecules. 23 (2018) 2571. doi:10.3390/molecules23102571.

J.O. Adeyemi, D.C. Onwudiwe, A.C. Ekennia, C.P. Anokwuru, N. Nundkumar, M. Singh, E.C. Hosten, Synthesis, characterization and biological activities of organotin(IV) diallyl dithiocarbamate complexes, Inorg. Chim. Acta. 485 (2019) 64–72.doi:10.1016/j.ica.2018.09.085.

J.O. Adeyemi, D.C. Onwudiwe, M. Singh, Synthesis, characterization, and cytotoxicity study of organotin(IV) complexes involving different dithiocarbamate groups; Journal of molecular structure. 1179(2019) 366 – 375. doi:10.1016/j.molstruc.2018.11.022

J.O. Adeyemi, D.C. Onwudiwe, Organotin(IV) N-butyl-N-phenyldithiocarbamate complexes: Synthesis,characterization, biological evaluation and molecular docking studies
Journal of molecular structure. (2019) Accepted

TABLE OF CONTENT

CERTIFICATE OF LANGUAGE EDITING ii
DECLARATION iii
ABSTRACT iv
DEDICATION vi
ACKNOWLEDGEMENTS vii
PUBLICATIONS viii
TABLE OF CONTENT ix
LIST OF FIGURES xiv
LIST OF TABLES xv
LIST OF SCHEMES xxi
LIST OF ABBREVIATIONS xxii
Chapter One 1
1.0. INTRODUCTION 2
1.1. Metals in Medicine 2
1.2. Organometallic Compounds 3
1.2.1. Organotin(IV) compounds 4
1.2.2. Organotin(IV) dithiocarbamate complexes 5
1.3. Problem Statement 7
1.4. Research Aim and Objectives 8
References 9
Chapter two 12
2.0 LITERATURE REVIEW 13
2.1 Chemistry Of Organotin(IV) Dithiocarbamate Complexes And Their Biological Relevance 13
2.2. Chemistry Of Organotin(IV) Dithiocarbamate Complexes 13
2.3. Structural geometry of organotin(IV) dithiocarbamate complexes 20
2.2. Thermal decomposition studies of organotin(IV) dithiocarbamate complexes 28

2.4. Biological applications of organotin(IV) dithiocarbamate complexes 31

2.4.1. Antimicrobial properties of organotin(IV) dithiocarbamate complexes 31

2.4.2. Antibacterial studies of organotin(IV) dithiocarbamate complexes 32

2.4.3. Antifungal studies of organotin(IV) dithiocarbamate complexes 34

2.4.4 Anticancer / Antitumor studies of organotin(IV) dithiocarbamate complexes 35

2.4.5. Other biological studies of organotin(IV) dithiocarbamate complexes 37

2.5 Limitation associated with toxicity of organotin(IV) compounds 38

References 39

Chapter three 46

3.0 SYNTHESIS AND CHARACTERIZATION OF ORGANOTIN(IV) DITHIOCARBAMATE COMPLEXES 47

3.1. Materials 48

3.2. Physical Measurements 48

3.2.1. X-ray crystallography 48

3.3. Complexes of Organotin(IV) and *N*-Methyl-*N*-Phenyldithiocarbamate 49

3.3.1. Synthesis of ammonium *N*-methyl-*N*-phenyldithiocarbamate (L^1) 49

3.3.2. Synthesis of the organotin(IV) *N*-methyl-*N*-phenyldithiocarbamate complexes [$RSnCl(L^1)_2$ and $R_2Sn(L^1)_2$ ($R = CH_3$, C_4H_9, C_6H_5)] 49

3.4. Results and discussion on the organotin(IV) *N*-methyl-*N*-phenyldithiocarbamate complexes 51

3.4.1. Synthesis of organotin(IV) *N*-methyl-*N*-phenyldithiocarbamate complexes 51

3.4.2. Infrared spectroscopic studies of organotin(IV)*N*-methyl-*N*-phenyldithiocarbamate complexes 52

3.4.3. Nuclear magnetic resonance studies of organotin(IV)*N*-methyl-*N*-phenyldithiocarbamate complexes 53

3.4.4. X-ray crystallography for complexes 3 and 4 54

3.4.5. Thermogravimetric Analysis (TGA) of organotin(IV)*N*-methyl-*N*-phenyldithiocarbamate complexes (1 – 5) 61

3.5 Complexes of organotin(IV)*N*-ethyl-*N*-phenyldithiocarbamate 65

3.5.1. Synthesis of ammonium *N*-ethyl-*N*-phenyldithiocarbamate, L^2 65

3.5.2. Synthesis of the organotin(IV) complexes of *N*-ethyl-*N*-phenyl dithiocarbamate ($[RSnCl(L^2)_2]$ and $[R_2Sn(L^2)_2]$ (R = CH_3, C_4H_9, C_6H_5)) 65

3.6. Results and discussion on the organotin(IV)*N*-ethyl-*N*-phenyldithiocarbamate complexes 67

3.6.1. Synthesis of organotin(IV) complexes of *N*-ethyl-*N*-phenyl dithiocarbamate 67

3.6.2. Infrared spectroscopic studies of the organotin(IV)*N*-ethyl-*N*-phenyldithiocarbamate complexes 68

3.6.3. Nuclear Magnetic Resonance studies of the organotin(IV)*N*-ethyl-*N*-phenyldithiocarbamate complexes 69

3.6.4. X-ray crystallographic studies of complexes 9 and 10 70

3.6.5. Thermogravimetric Analysis (TGA) of organotin(IV) *N*-ethyl-*N*-phenyldithiocarbamate complexes (6 – 11) 76

3.7. Complexes of organotin(IV) and *N*-butyl-*N*-phenyldithiocarbamate 81

3.7.1. Synthesis of ammonium *N*-butyl-*N*-phenyl dithiocarbamate, L^3 81

3.7.2. Synthesis of the organotin(IV) *N*-butyl-*N*-phenyl dithiocarbamate complexes, $RSnClL_2$ and R_2SnL_2 (R = CH_3, C_4H_9, C_6H_5) 81

3.8. Results and discussion on the organotin(IV) *N*-butyl-*N*-phenyldithiocarbamate complexes 83

3.8.1. Synthesis of organotin(IV)*N*-butyl-*N*-phenyldithiocarbamate complexes 83

3.8.2. FTIR spectral studies of organotin(IV) *N*-butyl-*N*-phenyl dithiocarbamate complexes 83

3.8.3. Nuclear Magnetic Resonance studies of the organotin(IV) and *N*-butyl-*N*-phenyldithiocarbamate complexes 83

3.8.4. X-ray crystallographic studies of the organotin(IV) and *N*-butyl-*N*-phenyldithiocarbamate complexes 84

3.8.5. Thermogravimetric analysis (TGA) of organotin(IV)*N*-butyl-*N*-phenyldithiocarbamate complexes (12 -15) 91

3.9. Complexes of organotin(IV) with mixed ligands of *N,N*-methylphenyl-*N,N*-ethyl phenyldithiocarbamate 93

3.9.1. Synthesis of the organotin(IV) complexes, $R_2SnL^1L^2$ (R = CH_3, C_4H_9, C_6H_5)..... 93

3.10 Results and discussion on the organotin(IV) *N,N*-methylphenyl-*N,N*-ethylphenyl dithiocarbamate complexes (16 - 18) 94

3.10.1. Synthesis of organotin *N,N*-methylphenyl-*N,N*-ethylphenyldithiocarbamate complexes 94

3.10.2. FTIR spectral studies of organotin(IV) *N,N*-methylphenyl-*N,N*-ethylphenyl dithiocarbamate complexes 95

3.10.3. Nuclear Magnetic Resonance studies of the organotin *N,N*-methyl phenyl-*N,N*-ethylphenyl dithiocarbamate complexes 95

3.10.4. X-ray crystallographic studies of dimethyl and dibutyl *N,N*-methyl phenyl-*N,N*-ethyl phenyldithiocarbamate complexes (16) and (17) 97

3.10.5. Thermogravimetric Analysis (TGA) of organotin(IV) *N,N*-methyl phenyl-*N,N*-ethyl phenyldithiocarbamate complexes (16, 17 and 18) 103

3.11. Mixed ligand complexes of dimethyltin(IV)*N,N*-alkylphenyl-*N,N*-butylphenyldithiocarbamate (19) and (20) (alkyl = CH_3 (L^1) and C_2H_5 (L^2))..... 106

3.11.1. Synthesis of the organotin(IV) complexes $R_2SnL^1L^3$ (R = CH_3) 106

3.12. Results and Discussion on the dimethyltin(IV) *N,N*-alkylphenyl-*N,N*-butyl phenyldithiocarbamate complexes 107

3.12.1. Synthesis of dimethyltin(IV) *N,N*-alkylphenyl-*N,N*-butyl phenyldithiocarbamate (19) and (20) 107

3.12.2. FTIR spectral studies of dimethyltin(IV) *N,N*-alkyl phenyl-*N,N*-butyl phenyldithiocarbamate (19) and (20) 107

3.12.3. Nuclear Magnetic Resonance studies of dimethyltin(IV) *N,N*-alkyl phenyl-*N,N*-butyl phenyldithiocarbamate (19) and (20) 107

3.12.4. Thermogravimetric analysis (TGA) of dimethyltin(IV) *N,N*-alkyl phenyl-*N,N*-butyl phenyldithiocarbamate (19) and (20) 109

3.13. Complexes of organotin(IV) with diallyldithiocarbamate 112

3.13.1. Synthesis of ammonium-*N, N*,-diallyldithiocarbamate, L^4 112

3.13.2. Synthesis of the organotin(IV) *N, N*,-diallyldithiocarbamate, $RSnClL_2$ and R_2SnL_2 (R = CH_3, C_4H_9 , C_6H_5)..... 112

3.14. Results and discussion on the organotin(IV) *N, N*,-diallyldithiocarbamate complexes (21 – 25)..... 114

3.14.1. Synthesis of organotin(IV) *N, N*,-diallyldithiocarbamate (R = CH_3, C_4H_9 , C_6H_5). 114

3.14.2. FTIR spectral studies of organotin(IV) *N, N*-diallyldithiocarbamate complexes.... 114

3.14.3. Nuclear Magnetic Resonance studies of organotin(IV) *N, N*,-diallyldithiocarbamate complexes..... 115

3.14.4. X-ray crystallography of organotin(IV) *N, N*,-diallyldithiocarbamate complexes 22 and 23 116

3.14.5. Thermogravimetric analysis of organotin(IV) *N, N*,-diallyldithiocarbamate complexes..... 122

3.15. Complexes of organotin(IV) and *p*-alkylphenyldithiocarbamate..... 126

3.15.1 Synthesis of sodium *p*-methyl phenyldithiocarbamate (L^5) 126

3.15.2. Synthesis of ammonium *p*-ethyl phenyldithiocarbamate (L^6)..... 126

3.16. Results and discussion on the organotin(IV) *p*-alkylphenyldithiocarbamate complexes (26 – 29) 128

3.16.1. Synthesis of organotin(IV) and *p*-alkylphenyldithiocarbamate..... 128

3.16.2. FTIR spectral studies of organotin(IV) *p*-alkylphenyldithiocarbamate complexes 129

3.16.3. Nuclear Magnetic Resonance studies of organotin(IV)*p*-alkylphenyldithiocarbamate complexes 129

3.16.4. Thermogravimetric Analysis (TGA) of organotin(IV) *p*-alkylphenyldithiocarbamate complexes..... 130

3.17. Complexes of organotin(IV) and benzyl dithiocarbamate 135

3.17.1. Synthesis of ammonium *N*-benzyldithiocarbamate (L^7) 135

3.18. Results and discussion on organotin(IV)*N*-benzyldithiocarbamate complexes..... 136

3.18.1. Synthesis of organotin(IV) *N*-benzyldithiocarbamate complexes..... 136

3.18.2. FTIR spectral studies organotin(IV) *N*-benzyldithiocarbamate complexes 136

3.18.3. Nuclear Magnetic Resonance studies of organotin(IV) *N*-benzyldithiocarbamate complexes 137

3.18.4. Thermogravimetric Analysis (TGA) of organotin(IV) *N*-benzyldithiocarbamate complexes 138

3.19. Chapter conclusion 141

References 142

Chapter four 146

4.0. Biological application of the synthesized complexes. 147

4.1 Introduction 148

4.2. Antimicrobial studies 150

4.2.1. Methodology for antimicrobial studies 150

4.2.2. Results of antimicrobial activities of ligand L^1 - L^7 and complexes 1–32 152

4.2.3. Discussion of the antimicrobial studies 154

4.3. Antioxidant activity 160

4.3.1. Methodology for antioxidant activity evaluation 160

4.3.2. Results of antioxidant activities of complexes 1 - 11 and 21 – 25. 161

4.3.3. Discussion of antioxidant activities 161

4.4. *In vitro* cytotoxicity assay 163

4.4.1. Methodology for cytotoxicity activity evaluation (MTT Assay) 163

4.3. Results of cytotoxicity study for complex 1 – 32 165

4.4.3. Discussion of cytotoxicity results 167

4.5. Chapter conclusion 170

References 171

Chapter five 174

5.0. Conclusion and recommendations 175

Appendices 177

LIST OF FIGURES

2.1:	Structure of carbamate (a) and dithiocarbamate (b)	**13**
2.2:	Structures of (a) thiram and (b) disulfiram	**14**
2.3	Resonance structure of dithiocarbamate	**16**
2.4	Thermal ellipsoidal plot of (a) triphenyltin(IV) *p*-bromo-*N*-methyl benzylaminedithiocarbamate and (b) triphenyltin(IV) *N*-methyl benzylamine dithiocarbamate with ellipsoidal displacement at 50% probability level (For clarity, H atoms were omitted).	**22**
2.5	ORTEP view of triphenyltin(IV) 4-hydroxypiperidine dithiocarbamate displacement ellipsoids drawn at 30% . (For clarity, H atoms were omitted).	**23**
2.6	Thermal ellipsoidal plot of dimethyltin(IV) bis[*p*-bromo-*N*-methyl benzylaminedithiocarbamate with ellipsoidal displacement at 50% probability level. (For clarity, H atoms were omitted).	**25**
2.7	Thermal ellipsoidal plot of dimethyltin(IV) bis(*p*-fluoro-*N*-methyl benzylaminedithiocarbamate) with ellipsoidal displacement at 50% probability level. (For clarity, H atoms were omitted).	**25**
2.8	The molecular structure $Sn\{S_2CN(CH_2)_4\}_2n\text{-}Bu_2$ and the atom numbering .(For clarity, H atoms were omitted).	**26**
2.9	(a)The molecular structure of dibutyltin (IV) 4-phenylpiperazine-1-dithiocarbamate, (b) dibutyltin*N*-benzyl-*N*-methyl-4-pyridyldithiocarbamate and (c) diphenyltin (IV) *N*-benzyl-*N*-methyl-3- pyridyldithiocarbamatethe atom numbering scheme (all hydrogen atoms are omitted for clarity)	**28**
2.10	The general mechanism for antimicrobial agent on microorganism.	**32**
3.1	List of complexes obtained from the reaction scheme 3.1	**51**
3.2	(a) Structure of dimethyltin(IV) *N*-methyl-*N*-phenyldithiocarbamate complex (3) drawn at 50% probability level displacement ellipsoids, and (b) thecrystal packing viewed along the best axis.	**56**
3.3	(a) Structure of dibutyltin(IV) *N*-methyl-*N*-phenyldithiocarbamate(4) drawn at 50% probability level displacement ellipsoids, and (b) the crystal packing viewed along the best axis (hydrogen atoms removed for clarity).	**58**
3.4	TG and DTG curves (with heating rate 10 ^{o}C/min) of complex 1 in N_2atmosphere (75 mL/min).	**63**
3.5	TG and DTG curves (with heating rate 10 ^{o}C/min) of complex 2 in N_2atmosphere (75 mL/min).	**63**
3.6	TG and DTG curves (with heating rate 10 ^{o}C/min) of complex 3 in	**63**

	N_2atmosphere (75 mL/min).	
3.7	TG and DTG curves (with heating rate 10 °C/min) of complex 4 in N_2 atmosphere (75 mL/min).	**63**
3.8	TG and DTG curves (with heating rate 10 °C/min) of complex 5 in N_2 atmosphere (75 mL/ min).	**64**
3.9	List of complexes 6 – 11 obtained from the reaction scheme 3.1 (with L^2)	**68**
3.10	The molecular structure of butyltin(IV) *N*-ethyl-*N*-phenyldithiocarbamatecomplex (9) with displacement ellipsoids drawn at 50% probability level (all hydrogen atoms are omitted for clarity).	**74**
3.11	The molecular structure of butyltin(IV) *N*-ethyl-*N*-phenyldithiocarbamatecomplex (10) with displacement ellipsoids drawn at 50% probability level (all hydrogen atoms are omitted for clarity).	**74**
3.12	Ortep diagram of 9showing the hydrogen interactions. Ellipsoids drawn at 50 % probability. Cg is the centroid of the phenyl ring C111—C116. Symmetry element: (i) 1-x, 1-y, 1-z.	**75**
3.13	Ortep diagram of 10 showing the hydrogen interactions. Ellipsoids drawn at 50 % probability. Cg is the centroid of the ring formed by Sn1, C11, S11 and S12. Symmetry element: (i) 1-X,1/2+Y,3/2-Z.	**75**
3.14	TG/DTG curves of complex 6 obtained in nitrogen atmosphere (75 mL/min), heating rate 10 °C/min.	**79**
3.15	TG/DTG curves of complex 7 obtained in nitrogen atmosphere (75 mL/min), heating rate 10 °C/min.	**79**
3.16	TG/DTG curves of complex 8 obtained in nitrogen atmosphere (75 mL/min), heating rate 10 °C/min.	**79**
3.17	TG/DTG curves of complex 9 obtained in nitrogen atmosphere (75 mL/min), heating rate 10 °C/min.	**79**
3.18	TG/DTG curves of complex 10 obtained in nitrogen atmosphere (75 mL/min), heating rate 10 °C/min.	**80**
3.19	TG/DTG curves of the complex 11 obtained in nitrogen atmosphere (75 mL/min), heating rate 10 °C/min	**80**
3.20	(a) Structure of dimethyltin(IV) and *N*-butyl-*N*-phenyl dithiocarbamate complex 13 drawn at 50% probability level displacement ellipsoids, and (b) the crystal packing viewed along the best axis.	**89**
3.21	(a) Structure of dibutyltin(IV) and *N*-butyl-*N*-phenyl dithiocarbamate complex 14 drawn at 50% probability level displacement ellipsoids, and (b) the crystal packing viewed along the best axis	**90**

3.22	TG/DTG curves of complex 12 obtained in nitrogen atmosphere (75 mL/min), heating rate 10 °C/min.	**92**
3.23	TG/DTG curves of complex 13 obtained in nitrogen atmosphere (75 mL/min), heating rate 10 °C/min.	**92**
3.24	TG/DTG curves of complex 14 obtained in nitrogen atmosphere (75 mL/min), heating rate 10 °C/min.	**92**
3.25	TG/DTG curves of complex 15 obtained in nitrogen atmosphere (75 mL/min), heating rate 10 °C/min.	**92**
3.26	The molecular structure of dimethyltin(IV) of *N,N*-methyl phenyl-*N,N*-ethyl phenyldithiocarbamatecomplex (16), with displacement ellipsoids drawn at 50% probability level (all hydrogen atoms are omitted for clarity).	**102**
3.27	The molecular structure of dibutyltin(IV) of *N,N*-methyl phenyl-*N,N*-ethyl phenyldithiocarbamatecomplex (17), with displacement ellipsoids drawn at 50% probability level (all hydrogen atoms are omitted for clarity).	**102**
3.28	TG/DTG curves of dimethyltin(IV) of *N,N*-methylphenyl-*N,N*-ethylphenyldithiocarbamate complexes (16) obtained under nitrogen atmosphere (75 mL/min), heating rate 10 °C/min.	**104**
3.29	TG/DTG curves of dibutyltin(IV) of *N,N*-methylphenyl-*N,N*-ethylphenyldithiocarbamate complexes (17) obtained under nitrogen atmosphere (75 mL/min), heating rate 10 °C/min.	**105**
3.30	TG/DTG curves of dibutyltin(IV) of *N,N*-methylphenyl-*N,N*-ethyl phenyldithiocarbamate complex complexes (18) obtained under nitrogen atmosphere (75 mL/min), heating rate 10 °C/min.	**105**
3.31	^{119}Sn NMR spectrum of dimethyltin(IV) *N,N*-methyl phenyl-*N,N*-butyl phenyldithiocarbamate (19).	**107**
3.32	^{119}Sn NMR spectrum of dimethyltin(IV) *N,N*-ethyl phenyl-*N,N*-butyl phenyldithiocarbamate (20).	**108**
3.33	TG/DTG curves of 19 obtained under nitrogen atmosphere (75 mL/min), heating rate 10 °C/min.	**110**
3.34	TG/DTG curves of 20 obtained under nitrogen atmosphere (75 mL/min), heating rate 10 °C/min.	**110**
3.35	Schematic representation of the positions of hydrogen atoms in the complexes.	**115**
3.36	^{119}Sn NMR spectrum of dimethyltin(IV) *N, N*,-diallyldithiocarbamate complexes (22).	**116**

3.37	(a) Structure of dimethyltin(IV) *N, N*,-diallyldithiocarbamate complex (22) drawn at 50% probability level displacement ellipsoids (hydrogen atoms are excluded for clarity), and (b) the crystal packing viewed along the best axis.	**118**
3.38	(a) Structure of dibutyltin(IV) *N, N*,-diallyldithiocarbamate complex (23) drawn at 50% probability level displacement ellipsoids (hydrogen atoms are excluded for clarity), and (b) the crystal packing viewed along the best axis.	**119**
3.39	TG/DTG curves of complex 21 obtained under nitrogen atmosphere (75 mL/min), heating rate 10 °C/min.	**123**
3.40	TG/DTG curves of complex 22 obtained under nitrogen atmosphere (75 mL/min), heating rate 10 °C/min.	**123**
3.41	TG/DTG curves of 22 obtained under nitrogen atmosphere (75 mL/min), heating rate 10 °C/min.	**124**
3.42	TG/DTG curves of complex 23 obtained under nitrogen atmosphere (75 mL/min), heating rate 10 °C/min.	**124**
3.43	TG/DTG curves of complex 23 obtained under nitrogen atmosphere (75 mL/min), heating rate 10 °C/min.	**124**
3.44	TG/DTG curves of complex 26 obtained under nitrogen atmosphere (75 mL/min), heating rate 10 °C/min.	**132**
3.45	TG/DTG curves of complex 27 obtained under nitrogen atmosphere (75 mL/min), heating rate 10 °C/min.	**133**
3.46	TG/DTG curves of complex 28 obtained under nitrogen atmosphere (75 mL/min), heating rate 10 °C/min.	**133**
3.47	TG/DTG curves of complex 29 obtained under nitrogen atmosphere (75 mL/min), heating rate 10 °C/min.	**134**
3.48	TG/DTG curves of complex 30 obtained under nitrogen atmosphere (75 mL/min), heating rate 10 °C/min.	**139**
3.49	TG/DTG curves of complex 31 obtained under nitrogen atmosphere (75 mL/min), heating rate 10 °C/min.	**140**
3.50	TG/DTG curves of complex 32 obtained under nitrogen atmosphere (75 mL/min), heating rate 10 °C/min.	**140**
4.1	Histogram showing antimicrobial activity of the complexes 1 – 5.	**157**
4.2	Histogram showing antimicrobial activity of the complexes 6 – 11	**158**
4.3	Histogram showing antimicrobial activity of the complexes 12 – 15.	**158**
4.4	Histogram showing antimicrobial activity of the complexes 16 – 20.	**158**

4.5	Histogram showing antimicrobial activity of the complexes 21 – 25.	**159**
4.6	Histogram showing antimicrobial activity of the complexes 26 – 29.	**159**
4.7	Histogram showing antimicrobial activity of the complexes 30 – 32.	**159**

LIST OF TABLES

3.1	Crystallographic data and refinement parameters for complexes 3 and 4	**59**
3.2	Selected interatomic distances and angles for complexes 3 and 4	**60**
3.3	Thermal analysis data of the complex 1-5	**62**
3.4	Crystal data, data collection and refinement parameters	**72**
3.5	Selected bond distances and angles for complexes 9 and 10	**73**
3.6	Thermal analysis data of complexes 6 -11.	**78**
3.7	Crystal data, data collection for and refinement parameters for complexes 13 and 14	**87**
3.8	Selected bond distances and angles for complexes 13 and 14	**88**
3.9	Thermal analysis data of complexes 12, 13, 14 and 15	**91**
3.10	Crystal data collection and refinement parameters of dimethyl (16) and dibutyl(17) complexes of *N,N*-methyl phenyl-*N,N*-ethyl phenyldithiocarbamate	**99**
3.11	Selected interatomic distances and angles dimethyl (16) and dibutyl (17) complexes of *N,N*-methyl phenyl-*N,N*-ethyl phenyldithiocarbamate	**100**
3.12	Thermal analysis data of organotin(IV) complexes of *N,N*-methyl phenyl-*N,N*-ethyl phenyldithiocarbamate (16, 17 and 18)	**104**
3.13	Thermal analysis data of complexes 19 and 20	**110**
3.14	Crystal data collection and refinement parameters	**120**
3.15	Selected interatomic distances and angles complex 22 and 23	**121**
3.16	Thermal analysis data of organotin(IV) *N, N*,-diallyldithiocarbamate complexes (22 -25)	**125**
3.17	Thermal analysis data of complexes 26 – 29	**132**
3.18	Thermal analysis data of complexes 30 – 32	**139**
4.1	Summary of antimicrobial screening of complexes 1–32	**152**
4.2	Antioxidant activities (μg/mL) of complexes 1-11 and 21 – 25.	**161**
4.3	Viabilities (%) of the HeLa cell lines at different concentration for complex 1 – 32.	**165**

LIST OF SCHEMES

2.1	Preparation of dithiocarbamates from primary and secondary amine	**15**
3.1	Synthesis of N-methyl-N-phenyl dithiocarbamate(L^1) and the organotin(IV) complexes [$RSnCl(L^1)_2$ and $R_2Sn(L^1)_2$ (R = CH_3, C_4H_9, C_6H_5)]	**51**
3.2	Organotin complexes of mixed ligand of dithiocarbamate $L^1$and L^2	**95**
3.3	Schematic route for the synthesis of the complexes.	**114**
3.4	Organotin(IV) complexes of *p*-alkyl phenyldithiocarbamate L^5 and L^6.	**128**
4.1	General mechanism of DPPH reduction from a hydrogen-donating antioxidant	**162**

LIST OF ABBREVIATIONS

Dithiocarbamate	**DTC**
Metal sulfide	**MS**
Fourier-transform infrared	**FTIR**
Thermal gravimetric analysis	**TGA**
Differential thermogravimetric	**DTG**
Nuclear magnetic resonance	**NMR**
Oak ridge thermal ellipsoid	**ORTEP**
2,2-diphenyl-1-picrylhydrazyl	**DPPH**
Reactive oxygen species	**ROS**
Dimethylsulfoxide	**DMSO**
Adenosine triphosphate	**ATP**
Gallic acid	**GA**
3-(4,5-Dimethylthiazol-2-Yl)-2,5-diphenyltetrazolium Bromide	**MTT**
human epithelial cells	**HeLa**
5-Fluorouracil	**5FU**
World health organization	**WHO**
Multi-Drug-Resistant	**MDR**

Chapter One

1.0. INTRODUCTION

1.1. Metals in Medicine

Metals have esteemed place in medicinal chemistry because they play crucial role in living systems. Their solubility in biological system is due to their easy loss of electrons to form positively charged species. It is in this ionic state that metals play their biological roles. Metal ions are electron deficient while most biological molecules such as DNA and proteins are rich in electrons. This attraction of the opposing charges leads to the affinity of metal ions for biological molecules. This also forms the basis for the interaction of metal ions with many other small molecules and ions crucial to life, such as oxygen [1]. Metal chemotherapy dates back to centuries ago. Copper was used to sterilize water around 5000 years ago in Egypt; the Arabians and the Chinese also used gold for various medicinal purposes [2]. Arsenic trioxide (ATO) has been used in traditional Chinese medicine as an antiseptic agent in the treatment of syphilis, psoriasis, and rheumatoid diseases [2,3]. In the 18^{th} and 19^{th} century, ATO was used mainly for the treatment of leukemia, and was also suggested for cancer therapy. The modern era of metal-based anticancer drugs began with the discovery of the platinum(II) complex, cisplatin [4].

In modern times, the various methods used in drug discovery arose due to the evolution of new diseases, loss in activity of known drugs, and the resistance of pathogens to already used drugs. Some of these methods are carried out by organic Chemists and involve synthetic approach, development of structural analogues of the existing drugs, fortuitous identification, and metal complex therapy etc. [5]. Metal complex formation has provided a therapeutic platform [6] for making innovative and novel drugs to tackle new emerging diseases [7], and also combat resistance in some cases. They are formed when a central metal atom is bonded to one or more Lewis bases (the ligand). The types of coordinated ligands, the oxidation state, and the coordination geometry of the complexes can be useful in identifying a variety of properties [1]. These diverse properties can affect the identity without altering the very nature of the organic fragment (ligand) in the search for the formation of new analogues [2]. Metal complexes are also relevant in catalysis, materials synthesis, and several other fields [8]. The general mechanism of a metal-ligand interaction as it relates to their actions in a biological system have been ascribed to the capacity of the ligands to control the reactivity of metals [2,9]. Ligands play major role in

determining the nature of secondary coordination sphere involved in the recognition of biological sites such as DNA, enzymes, and proteins. Metal-ligand bonds have much weaker covalent bond with high tendencies for ligand substitution and redox reaction in the biological medium before getting to the target site. The displaced ligand from this substitution may itself attack a targeted site and the controlled ligand not released can play a role in the mechanism of action [2,8]. Over time, metal derivatives became neglected in favor of more reliable organic compounds from natural or synthetic sources due to limited selectivity and associated toxicity. Therefore, leading to a decline in the use of metal based drugs even though some are still used till date. For example, in the treatment of rheumatoid arthritis, cytokine receptors and immunosuppressant have been used to replace auranofin, a metal based drug containing metals of Group II. Nevertheless, silver sulfadiazine is still an agent of choice for the prevention of burn infections [10].

However, the serendipitous discovery of cisplatin by Rosenberg in 1965 as an anti-proliferating agent and its successful usage in the treatment of testicular cancer has encouraged renewed interest in the use of metals as therapeutic agents. Examples of such metal derivatives with antitumoural potential are the organometallic complexes. Metal ions in anions and organic ligands have been found to create a spatial distribution, which make them effective to attack targeted constituents of cancer cell [11].

1.2. Organometallic Compounds

Organometallic compounds are compounds which possess at least one direct, covalent metal-carbon bond [12]. They possess distinct chemical properties such as structural diversity, catalytic and redox capacity, the possibility of ligand exchange and variety of available interactions that can be used for medical purposes [13]. Due to their great structural diversity which ranges from linear to octahedral and even beyond, they have been found to show promising biological activities. Organometallic compounds have shown far more diverse stereochemistry than organic compounds. For example, 30 stereoisomers are known to exist in an octahedral complex having six different ligands, which consequently results in providing control over key kinetic properties such as hydrolysis rate of ligands [14]. Furthermore, they are usually uncharged, kinetically stable and lipophilic with their metal atom existing in a low oxidation state. Thus,

organometallics, to a large extent, offer advantages in the design of novel medicinal compounds with new metal-specific modes of action, because of these primary differences compared to "classical coordination metal complexes" [13]. Hence, most of the classes of organometallics such as metallocenes, half-sandwich, carbene-, CO-, or π-ligands which have been used for biosensing and catalytic purpose now found application in medicinal field [14]. These compounds have been useful in gaining conceptual understanding of surprising structures, and as useful catalysts in organic chemistry and in industrial processes. Insights drawn from the chemistry of organometallics have provided platforms which has aided the interpretation of the chemistry of metal to metal surface in heterogeneous catalysis [12]. The organometallic field has also created links with biochemistry (in which acetyl CoA synthase was used to carry out organometallic catalysis), and with the chemistry of material science (in which organometallic compounds are continuously being preferred as the precursors source) for depositing materials on various substrates via thermal decomposition of the metal compound [12].

Organotin has contributed immensely to the study and the understanding of organometallic compounds which began in 1949, and this has led to their usage in diverse field of applications. Detailed studies on the structural understanding and changes which occur in solution and solid states or organotin compounds have been reported [15].

1.2.1. Organotin(IV) compounds

Organotin compounds are widely used organometallic compounds. They have been used over the last several decades for different industrial and agricultural applications such as pesticides, fungicides and anti-fouling agents [16]. These compounds were first discovered by Edward Frankland in 1894, with the first compound being diethyltindiiodide ($(C_2H_5)_2SnI_2$). Since tin is known to exist in two oxidation number, +2 and +4, organotin compounds can exist as organotin(II) (sp^2 hybridized) or organotin(IV) (sp^3 hybridized). However, the oxidation state of +IV have been found to be more stable than their +II state which often polymerizes. Organotin(II) are not so stable and, thus, oxidize easily to their +IV state. An example of a stable organotin(II) compound is bis(cyclopentadienyl)tin(II) [15]. Many organotin(IV) compounds are known and they conform to the general formula;

$$R_xSn(L)_{4-x},$$

Where R=alkyl or aryl substituents L= Organic or inorganic Ligand

Organotin(IV) compounds contain a tetravalent Sn centers with an anion usually oxide, hydroxide, chloride, fluoride, carboxylate or thiolate [17]. They possess distinct chemical properties such as structural diversity, catalytic and redox capacity, possibility of ligand exchange and a variety of different interactions with useful medicinal properties [13]. The presence of one or more covalent carbon-tin bond influences the activity of the whole compound. This activity is also dependent on the number and the nature of alkyl/aryl (R) substituents attached to the Sn atom [18]. Variations of the alkyl/aryl group substituent of the organotin(IV) have proven to show notable effects on their diverse properties [10,18]. Organotin(IV) compounds have shown great therapeutic activities on diverse tumor cells, but their mode of action still remains unclear [19]. They have been reported to show good biological activities as an antibacterial, antitumor, schizonticidal, antimalarial and as biocides in agriculture [20–23]. Organotin(IV) cation can readily form complexes with ligands possessing S, N, O and P donor atoms with various composition and stability [18]. One of such ligand is the dithiocarbamate group.

1.2.2. Organotin(IV) dithiocarbamate complexes

There are rapid increase in the number and diversity of sulfur containing compounds used in the preparation of novel coordination and organometallic compounds. This is due to the ease of modification, possible by introducing different organic substituents which in-turn cause variation in property around the donor group [24]. This form of interaction between metals and donor groups has led to the synthesis of complexes with diverse geometries and possible applications in biological science. Metal-thiolato compounds form the inorganic part of biologically active center of some enzymes and metalloproteins [24]. Sulfur containing ligands and organotin moieties have been combined to form complexes with various geometries and diverse biological applications [20,25]. This class of ligands have received much attention in recent times due to their similarities to biomolecules such as amino acids (e.g cysteine), enzymes, proteins, peptides and vitamins [26]. A notable example of such ligand, with diverse application, is the dithiocarbamate. The sulfur atoms of the dithiocarbamate ligand have large ionic radii [27], and

various modes of coordination are possible when combined with metal in complexation [28,29]. This has been attributed to the resonance which exists between the two sulfur atoms of the dithiocarbamate moiety [27]. Dithiocarbamates can stabilize different oxidation states of the main group metals and also give different geometries [30]. The properties of these ligands could be significantly influenced by little change in their structure [31]. Main group metal complexes of dithiocarbamate have a wide range of applications in separation and material science [31]. These complexes are also used as pesticides, fungicides, and as chemotherapeutics [32]. The molecular weight and the lipophilicity of organotin complexes have been reported to govern their antimicrobial activities [33]. These consequently reduces the polar nature of the metal center by the delocalization of electron and charge sharing with donor groups thereby enhancing permeability across the plasma membrane of the micorganisms [23].

Several reports have been made on the synthesis and application of organotin(IV) dithiocarbamates complexes which have led to their emergence as anti-cancer agents [34], antimicrobial agents [29,35–37], and a good single source precursor for SnS nanoparticles [38–40]. The unique stereo-electronic properties of organotin(IV) complexes containing sulfur donor ligands underline their relevance in the area of medicinal chemistry. The sulfur atoms as donor sites in molecules has been reported to play an important role in the transportation of the molecules to the targeted sites, as well as the enhancement of retention time [41,42]. The discovery of triphenyltin acetate as an antitumor agent in 1972 has led to a number of reports which highlights organotin compounds as potential biologically active metallopharmaceuticals [43], also showing good anti-tumorigenic abilities both *in vitro* and *in vivo*. Due to the toxic nature of some organotin(IV) compounds, their after effects might pose some challenges. However, the ligand fragments have the capacity to effectively modulate associated toxicity of the organotin(IV) moiety in the complexes with increased potency [41].

Organotin(IV) dithiocarbamate, therefore, owe their useful functionality in biological system to the individual attributes of the organotin(IV) and the dithiocarbamate moiety. The synergy exhibited by the individual moieties is expected to result in enhanced biological activity in the hybrid molecule [44]. Thus, our interest in the biological study of organotin(IV) dithiocarbamates complexes.

1.3. Problem Statement

Organisms are continuously adapting to cope better in their environment due to evolution by natural selection. Small organisms are not exempted from this, moreover they reproduce rapidly and thus adapt quickly. Regardless of how uncomfortable their environment may be, due to the introduction of foreign substances such as drugs, these organisms mutate by developing features/mechanisms to defend themselves by acquiring features that aid their survival. For example, microorganisms can develop features around their outer layer that prevent the movement of drugs into their cells or develop mechanisms which eject harmful unwanted material out from their cells [45]. These organisms develop adaptive features either by mutations or acquisition of mobile genetic elements carrying resistance genes for survival [46]. The mutated organisms then multiplies and spread among their population and this in turn leads to the emergence of resistance among such specie of microorganism [45].

Drug resistance by microorganism has continued to plaque our world due to the drop in the pace of the discovery of novel drugs, while the usage of the currently available drugs has continued to rise. This continuous use of large amounts of antibiotics to combat diseases in both animals and humans without further discoveries has led to the rapid development of resistance by microorganisms. Thus, the consistent misuse and abuse of the available antibacterial agents are the decisive cause of the increasing rates of the fast emergence of resistant microorganisms. Infrequent use at low dosage and short time would have helped reduce the pace at which this organism acquire resistance toward the available drugs, but this is not the case [46]. The discovery and development of new antimicrobial agents are locked in an evolutionary fight with natural resistance mechanism [47]. Therefore, due to the continuous emergence of resistance caused by Multi-Drug-Resistant (MDR) microorganism, effective, safe and cheap antibiotics are in demands. The mortality rate due to the effects of microbial infection continues to rise and this has been attributed to the unavailability and the affordability of suitable antimicrobial agent for the various resistant strain [48]. The list of some microorganism with drug resistant strains includes *Pseudomonas aeruginosa, Staphylococcus aureus, Streptococcus pyogenes;* multidrug-resistant *Mycobacterium tuberculosis, penicillin-resistant, carbapenem-resistant, Escherichia coli, Acinetobacter baumannii, Pseudomonas aeruginosa* and *Enterobacteriaceae*; sulfonamide-resistant, *penicillin*-resistant, and vancomycin resistant *P. aeruginosa* and several others [47]. Most of these strains have been identified as most vicious pathogens whose remedies are in

urgent demand [46]. It is therefore imperative to continue to search for alternative drugs that are effective, affordable and void of unwanted side effects in the quest to combat this menace.

Metal complex therapy has proved to be a viable platform which offers possible advantages/opportunities to metals and organic fragment synergism, by enhancing the activity of the organic ligand (with useful medicinal property) upon coordination with a metal ion. This complexation leads to longer residence time in the organism thereby allowing medicinal substances to efficiently reach their biological targets [49]. Organotin(IV) dithiocarbamate have shown useful antimicrobial activity which are of notable consideration. Variation of the alkyl/aryl group substituents of organotin(IV) moiety with an appropriate choice of dithiocarbamate ligand can have remakable effects on their biological activities [18]. Organotin(IV) compounds with less substituted alkyl are considered less toxic among these derivatives and have not achieved much commercial application as biological agents [17]. Thus, it is against this backdrop that the proposed research is designed to study the antimicrobial properties of some newly synthesized complexes alongside their potentials as antiradical and anti-tumoral agents.

1.4. Research Aim and Objectives

The aim of this research is to prepare a new class of organotin(IV) dithiocarbamate compounds with enhanced biological activity.

The aim will be achieved by accomplishing the following objectives:

- synthesize dithiocarbamate ligands from different primary and secondary amines,
- synthesize organotin(IV) complexes with the prepared dithiocarbamate ligands,
- characterize the complexes using different spectroscopic techniques (FTIR, ^{1}H, ^{13}C and ^{119}Sn NMR), elemental and thermal analyses (TGA and DTG) and single crystal X-ray diffraction techniques,
- investigate the biological activities of the new complexes formed, including antibacterial, antifungal, antioxidant and anticancer potency (cytotoxicity study).

References

[1] S.R. Pattan, S.B. Pawar, S.S. Vetal, U.D. Gharate, S.B. Bhawar, Indian Drugs. 49 (2012) 5.

[2] J. A. Obaleye, A.C. Tella, M.O. Bamigboye, A Search Antibact. Agents. (2012) 197.

[3] S. Tapio, B. Grosche, Mutat. Res. 612 (2006) 215.

[4] A.A. Warra, J. Chem. Pharm. Res. 3 (2011) 951.

[5] P.F. Salas, C. Herrmann, C. Orvig, Chem. Rev. 113 (2013) 3450.

[6] B. Deepthi, I.S. Babu, P. Venkatesh, S. Sharfudeen, V. Soumya, J. Chem. Pharm. Res. 2 (2010) 496.

[7] A. Casini, J. Inorg. Biochem. 109 (2012) 97

[8] P. J. Sadler, Adv. Inorg. Chem. (1991) 1.

[9] S.H. van Rijt, P.J. Sadler, Drug Discov. Today. 14 (2009) 1089.

[10] A. Alama, B. Tasso, F. Novelli, F. Sparatore, Drug Discov. Today. 14 (2009) 500.

[11] F. Alama, Angela; Tasso, Bruno; Novelli, Federica, Discov. Antitumour Agents. (2009) 50.

[12] R.H. Crabtree, The Organometallic Chemistry of the Transition Metals, 2005.

[13] G. Gasser, N. Metzler-Nolte, Curr. Opin. Chem. Biol. 16 (2012) 84.

[14] G. Gasser, I. Ott, N. Metzler-Nolte, J. Med. Chem. 54 (2011) 3.

[15] Alwyn G. Davies, Organotin chemistry, Wiley-VCH Verlag GmbH & Co. KGaA, Weinheim, Germany, 2004.

[16] B.A. Buck-Koehntop, F. Porcelli, J.L. Lewin, C.J. Cramer, G. Veglia, J. Organomet. Chem. 691 (2006) 1748.

[17] L. Pellerito, L. Nagy, Coord. Chem. Rev. 224 (2002) 111

[18] C. Pellerito, L. Nagy, L. Pellerito, A. Szorcsik, J. Organomet. Chem. 691 (2006) 1733.

[19] A. Szorcsik, L. Nagy, L. Pellerito, E. Nagy, F.T. Edelmann, J. Radioanal. Nucl. Chem. 252 (2002) 523.

[20] N. Awang, I. Baba, B.M. Yamin, World Appl. Sci. J. 12 (2011) 630.

[21] D.C. Menezes, F.T. Vieira, G.M. De Lima, J.L. Wardell, M.E. Cortés, M.P. Ferreira, M.A. Soares, A. Vilas Boas, Appl. Organomet. Chem. 22 (2008) 221.

[22] N. Khan, Y. Farina, L.K. Mun, N.F. Rajab, N. Awang, Polyhedron. 85 (2015) 754.

[23] F. Javed, M. Sirajuddin, S. Ali, N. Khalid, M.N. Tahir, N.A. Shah, Z. Rasheed, M.R. Khan, Polyhedron. 104 (2016) 80.

[24] S. Jabbar, I. Shahzadi, R. Rehman, H. Iqbal, Qurat-Ul-Ain, A. Jamil, R. Kousar, S. Ali, S. Shahzadi, M.A. Choudhary, M. Shahid, Q.M. Khan, S.K. Sharma, K. Qanungo, J. Coord. Chem. 65 (2012) 572.

[25] D.C. Menezes, G.M. De Lima, A.O. Porto, C.L. Donnici, J.D. Ardisson, A.C. Doriguetto, J. Ellena, Polyhedron. 23 (2004) 2103.

[26] L.A. Komarnisky, R.J. Christopherson, T.K. Basu, Nutrition. 19 (2003) 54.

[27] E.J. Mensforth, M.R. Hill, S.R. Batten, Inorganica Chim. Acta. 403 (2013) 9.

[28] S. Eckhardt, P.S. Brunetto, J. Gagnon, M. Priebe, B. Giese, K.M. Fromm, Chem. Rev. 113 (2013) 4708.

[29] M. Mahato, S. Mukherji, K. Van Hecke, K. Harms, A. Ghosh, H.P. Nayek, J. Organomet. Chem. 853 (2017) 27

[30] N. Azizi, F. Aryanasab, M.R. Saidi, Org. Lett. 8 (2006) 5275.

[31] P.J. Heard, Prog. Inorg. Chem. 53 (2005) 1.

[32] D. C. Onwudiwe, T. Arfin, C.A. Strydom, R. J. Kriek, Electrochim. Acta. (2013) 19.

[33] F. Shaheen, Zia-Ur-Rehman, S. Ali, A. Meetsma, Polyhedron. 31 (2012) 697.

[34] L. Tian, X. Liu, X. Zheng, Y Sun, D. Yan, L. Tu, Appl. Organomet. Chem. 25 (2011) 298

[35] N. Awang, N. Mokhtar, N.M. Zin, J. Chem. Pharm. Res. 7 (2015) 379.

[36] S. Shahzadi, S.U. Ahmad, S. Ali, S. Yaqub, F. Ahmed, J. Iran. Chem. Soc. 3 (2006) 38.

[37] Zia-ur-Rehman, N. Muhammad, S. Ali, I.S. Butler, A. Meetsma, Inorganica Chim. Acta. 376 (2011) 381 .[38] K. Ramasamy, V.L. Kuznetsov, K. Gopal, M.A. Malik, J. Raftery, P.P. Edwards, P. O'Brien, Chem. Mater. 25 (2013) 266.

[39] N. Singh, S. Bhattacharya, J. Organomet. Chem. 700 (2012) 69.

[40] E.R.T. Tiekink, Appl. Organomet. Chem. 22 (2008) 533.

[41] R. Kadu, H. Roy, V.K. Singh, Appl. Organomet. Chem. 29 (2015) 746.

[42] A. Al Bawab, A. Bozeya, F. Odeh, GSTF Int. J. Chem. Sci. 1 (2014) 32

[43] H. Iqbal, S. Ali, S. Shahzadi, Cogent Chem. 1 (2015) 1029039.

[44] A.B. Caballero, J.M. Salas, M. Sánchez-Moreno, Met. Ther. Leishmaniasis. (2014) 1.

[45] S. Advisory, Eur. Acad. Sci. Advis. Counc. (2014) 1.

[46] M. Bilal, T. Rasheed, H.M.N. Iqbal, H. Hu, W. Wang, X. Zhang, Int. J. Biol. Macromol. 103 (2017) 554.

[47] A. Regiel-Futyra, J.M. Dąbrowski, O. Mazuryk, K. Śpiewak, A. Kyzioł, B. Pucelik, M. Brindell, G. Stochel, Coord. Chem. Rev. 351 (2017) 76

[48] C. Kang, S. Kim, W.B. Park, H. Kim, E. Kim, M. Oh, K. Choe, K. Lee, Ris, Antimicrob. Agents Chemother. 49 (2005) 760.

[49] A.A. Sánchez-Delgado R.A., Mini-Review Med. Chem. 24 (2004).

Chapter two

2.0 LITERATURE REVIEW

2.1 Chemistry Of Organotin(IV) Dithiocarbamate Complexes And Their Biological Relevance

Organotin(IV) compounds are group of organometallics which owe their utility in coordination chemistry to their distinct chemical properties such as structural diversity, possibility for ligand exchange, catalytic and redox capacity. They also possess a variety of available interactions with useful medicinal properties. Their ability to complex with ligands possessing S, N, O and P donor atoms have led to the development of biologically useful derivatives like organotin(IV) dithiocarbamate. These complexes have excellent coordination chemistry and stability; thus, prompt diverse molecular structures with a wide range of useful biological activities. Therefore, in this review chapter, the useful chemistry of organotin(IV) dithiocarbamate complexes that accounts for their biological relevance in medicine is presented.

2.2. Chemistry Of Organotin(IV) Dithiocarbamate Complexes

Dithiocarbamates are half amide of dithiocabonic acids [1]. They belong to the carbamate family in which the two oxygen atoms have been replaced with sulfur atoms (Figure 2.1). They are mono-anionic chelating ligands, and are capable of forming stable complexes with a large number of the main group elements, all transition metals and also lanthanoids and actinides [2]. This is because of the presence of the anionic CS_2^- moiety which has a wide range of binding modes, thus possessing excellent coordination capacity. This excellent coordination and stability observed between dithiocarbamate ligands and a metal derivative like organotin salts is based on the fact that some metals (like tin) act as strong Lewis acids [3,4]. Thus, they easily complex with the electron rich sulfur dithiocarbamate ligand based on the Hard Soft [Lewis] Acid Base (HSAB) principle [5]. They show good solubility in water or organic solvents depending on the nature of the cation.

(R = Aryl, Alkyl, Alkylene and M = K^+/Na^+)

Figure 2.1: Structure of carbamate **(a)** and dithiocarbamate **(b).**

Various biological activities can be prompted when incorporated into other molecular structures. Thus, they are good pharmacophore and have shown to possess useful biological activities such as their usage as antifungal drugs [6,7]. Thiram (Figure 2.2 a): for food dressing and control of turf diseases and disulfiram (Figure 2.2 b): for the treatment of addiction to alcoholic drinks [6,7].

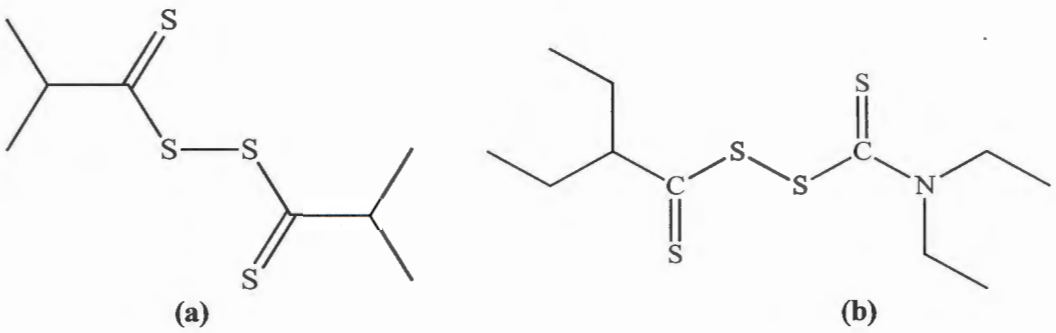

Figure 2.2: Structures of **(a)** thiram and **(b)** disulfiram.

Dithiocarbamate compounds are capable of inhibiting the growth of bacterial by altering the metabolic activities which take place in the bacteria. This ligand continues to receive increased attention due to the presence of the carbon-sulfur bond, which are useful in many products of biological and medicinal relevance [8]. This bond is also useful in the formation of organic intermediates with interesting chemistry [8,9]. Reports on their usage in protein folding, redox signaling and enzyme catalysis have been attributed to the strong nucleophilic character and peculiar properties of sulfur to undergo redox reaction [7]. They have found other usefulness in agriculture as pesticides, herbicides, and fungicides [10–12]. Some compounds of these classes have been commercialized such as zineb, maneb, nabam, ziram and ferbam[13]

The earliest record of dithiocarbamate synthesis involved the use of thiophosgene, chlorothioformate and an isothiocyanate [13]. This reaction had many drawbacks such as long reaction time, use of expensive and toxic reagents, and harsh reaction conditions. Several synthetic procedure have been developed involving one-pot condensation of amines, carbon disulfide and electrophiles such as alkyl halides, epoxides, carbonyl compounds and α,β-unsaturated compounds [13]. They have been prepared from both primary and secondary amines [14–16] as shown in Scheme 2.1. The respective amines react with carbon disulfide in the

presence of a base like potassium/sodium hydroxide or ammonium hydroxide to form the corresponding dithiocarbamate salts of sodium ion (K^+/Na^+) or ammonium ion (NH_4^+). In this reaction, the addition of the strong base helps catalyze the reaction, hence making an important impact on the dithiocarbamate (DTC) formation rate [6]. The dithiocarbamate obtained from secondary amines are more stable than the products obtained from primary amine, due to the presence of acidic hydrogen on the nitrogen [6]. The Na^+ or NH_4^+ salts of DTCs are reasonably stable compared to their corresponding carbamic acids. The sodium salts of DTCs are white crystalline solids which are soluble in water. These salts are usually stable for a long time, nevertheless whenever required; the solutions of DTCs are to be prepared freshly.

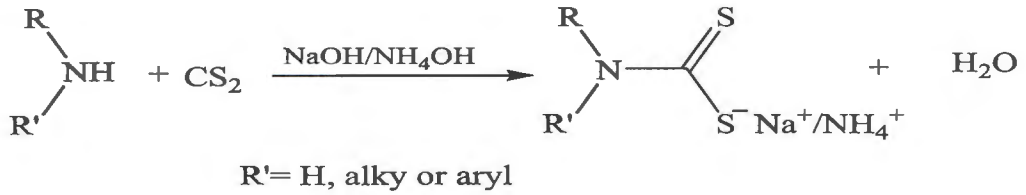

Scheme 2.1: Preparation of dithiocarbamates from primary and secondary amines.

Another reported method for the synthesis of dithiocarbamates which are soluble in organic solvents involves the reaction of two equivalents of secondary amine (in the absence of any base) with carbon disulfide. One equivalent of amine act as the base while the other as a neuclophile for the reaction to give the ammonium salt of the compound [17].

Several metal dithiocarbamate complexes have been synthesized simply by the reaction of dithiocarbamate ligand with the corresponding metal salts in an appropriate solvent [17–23]. The metal dithiocarbamate complexes formed are often via simple metathesis with the corresponding metal salts [24,25]. Some metal complexes of dithiocarbamates are colored, and this has been useful in facilitating their spectrophotometric studies especially in visible or near UV region. Most heavy metal dithiocarbamate compounds are sparingly soluble in solvents that are organic in nature such as chloroform, alcohols, dimethyl sulfoxide and dimethyl formamide [26,27].

With appropriate choice of the substituents on the secondary amine, and a right choice of cation, a unique modification in the stereo-electronic properties of the corresponding dithiocarbamate ligand can be obtained [28]. Dithiocarbamates are lipophilic and possess the ability to bind to metal ion as monodentate **(I)** (using one binding site of S), as bidentate **(II)** (using the two S

atoms in binding to the central metal atom or ion) or bidentate bridging ligands **(III)** (in which it binds to the metal ion with one sulfur and forms a bridge with adjacent molecule with the other sulfur) [29]. This is because DTC can exist in 3 different resonance forms [30] as shown in Figure 2.3. In the resonance form of the dithiocarbamate, there is a single bond between the nitrogen atom and the C bearing the two S atoms as presented in **(I)** and **(III)**, and the delocalization of the -1 charge between the carbon and two sulfur atoms. The lone pair on the nitrogen atom (N) in the 'thioureide' form is delocalized as shown in the form **(II)**, resulting in π (double bond) character between the N and the C bearing the two S groups with negative charges. The nitrogen is sp^2 hybridized in this resonance form. The resonance form **(II)** is described as a hard ligand because it can stabilize hard metal centers at higher oxidation states while both forms **(I)** and **(III)** can stabilize soft metals at lower oxidation states [17].

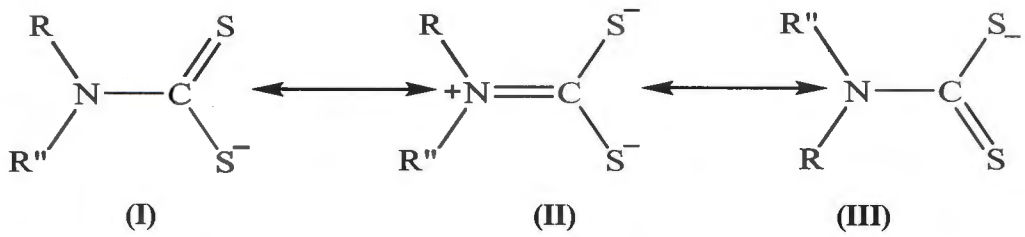

(I) (II) (III)

Figure 2.3: Resonance structure of dithiocarbamate.

The exceptional stability of dithiocarbamate is often explained by the outstanding contribution of resonance form **(II)** to the overall electronic structure, which ensures that this anion is an effective ligand for metal complexation. They exhibit various modes of coordination in homo and heteronuclear complexes, depending on the mode of attachment between the ligands and the metal ion [10]. The ease of replacement of hydrogen from -SH group in dithiocarbamates and their complexes in inorganic analysis is the main reason for their numerous applications. This usually occurs when a coordinate bond is formed through S, forming strongly colored complexes with a number of metals. This outstanding metal binding capacity of the dithiocarbamates were noted by Delepine [31].

The interesting chemistry of organotin(IV) dithiocarbamate results from the individual properties of both organotin and dithiocarbamate. As such, the chemistry and the application of these set of

complexes is believed to be the consequence of the synergistic activity of both the organotin and dithiocarbamate compounds. Generally, different methods have been used to prepare organotin complexes of dithiocarbamate, and there is no specific method of synthesis. However, organotin(IV) dithiocarbamate complexes have been mostly reported to be prepared *in situ*. The *in situ* method involves a one pot system in which the organotin(IV) compound is introduced into the flask containing freshly prepared dithiocarbamate, and allowed to react for a few hours [13]. Some organotin(IV) dithiocarbamate complexes prepared via this method have been reported. Basirah *et al.* synthesized organotin(IV) dithiocarbamate complexes using "*in situ*" insertion method, involving the reactions of bis-2-methoxyethyldithiocarbamate with some organotin compounds of the type R_xSnCl_x (where R= Bu, Me, Ph and x= 1, 2 or 3) [32]. Organotin compounds with the molecular formula $R_mSn[S_2CN(CH_3)(C_6H_{11})]_{4-m}$ (where m = 2, R = CH_3, C_2H_5; m = 3, R = C_6H_5) were reported by Awang *et al.* [33]. They also prepared organotin(IV) dithiocarbamate complexes derived from methoxyethyldithiocarbamate, with corresponding di and tri organotin chloride bearing alkyl group (R_3SnL and R_2SnL_2;L = R = C_6H_5 or C_4H_9) [34]. Kamaludin *et al.* reported some organotin(IV) *N*-butyl-*N*-phenyldithiocarbamate compounds using the dithiocarbamate derivatives obtained from *N*-butylamine and the corresponding organotin chloride in different ratios [35]. The number of anion (e.g. Cl^-) present in the organotin(IV) salt often determines the mole ratio of the dithiocabamate ligand to the organotin(IV) salts. This is because the chloride ions are labile and are easily replaced by the dithiocarbamate ligand. Thus, the molar ratio of the dithiocarbamate ligand to the organotin salt (for a substituted derivative) is 2:1 for di-substituted organotin(IV) salt, and 3:1 for a tri-substituted derivatives.

Various spectroscopic techniques have been used to characterize organotin compounds and they give insight on the geometry of the compounds. In infrared spectroscopy, specific bands aid in identifying the dithiocarbamate. Characteristic bands such as the υ(C=N), the υ(C-S) and υ(M-S) band are peculiar. The thiouride band is often found in the 1450-1550 cm^{-1} band region of the spectrum, which is associated with the vibration of C-N bond that display a partial double bond and a polar character. The υ(C-S) stretching vibrational band often appears in the 950-1000 cm^{-1} region, while the υ(M-S) stretching vibration band is found in the 350-450 cm^{-1} [36]. The movement of the C-N vibrational band after complexation with a metal to a higher frequency of about 15 cm^{-1} often indicate the delocalization of the electron cloud of the –NCSS group towards

the metal center [37]. Thus, giving the C-N bond a partial double bond character [38]. The υ(M—S) band usually appear in the far infra-red region, and indicates complexation [39]. In dithiocarbamate ligands, there are often two types of υ(C-S) band, the $\upsilon(CS_2)_{asym}$ and $\upsilon(CS_2)_{sym}$; and they appear around 1055 and 961 cm^{-1} respectively in dithiocarbamate ligands [40]. When these are replaced by strong singlet at approximately 1000 cm^{-1} in complexes, it indicates a symmetrical coordination of the dithiocarbamate moiety to the metal ions. However, the splitting of the same band within a difference of 20 cm^{-1} in the same region is ascribed to the monodentate binding mode of dithiocarbamate ligand [41].

The electronic spectra of organotin(IV) dithiocarbamate complexes are generally characterized by three principal bands which are attributed to (C=N) bond, the electron pair of sulfur and the metal-ligand (M-L) bond in the UV-visible absorption spectra [42]. From the dithiocarbamate moiety, the absorption band of (C=N) chromophore due to the intramolecular π-π* transition are found around 300 nm [32]. However, the movements of this peak to a lower/shorter wave length often reveal the involvement of the band in complex formation. This, therefore, shows the contribution of the NCS_2 group in the complexation of the dithiocarbamate ligand to the organotin moiety [42]. The existence of a non-bonding electron pair of the S atom in the range 240 - 261 nm have been attributed to n-π* transition [42]. Furthermore, the presence of a broad shoulder band in the complexes, which is usually found above 300 nm, is attributed to charge transition from the metal to the ligand (M-L). The absorption indicates an extended conjugation system due to the electronic transition between p-orbital of sulfur and 5d-orbital of tin metal [32,42,43].

NMR spectroscopy is one of the widely and often used technique for the prediction of geometry in organotin(IV) complexes. Parameters such as the coupling constant (J) [$^{n}J(^{119}Sn,^{1}H)$, $^{n}J(^{119}Sn,^{13}C)$], and the chemical shifts (δ) of ^{119}Sn NMR are obtained from this technique and these give useful information in solution state about the geometry of the tin center in the organotin complexes [44]. Studies have shown that the coordination of tri and dimethyl derivatives of tin(IV) compounds having ^{n}J (n = 1, 2) values are: tetra-coordinated in tin(IV) compounds, if the coupling constant (^{1}J) are predicted to be less than 400Hz and ^{2}J values should be less than 59 Hz; penta-coordinated, if the coupling constant (^{1}J) is between 450 and 670 Hz and ^{2}J values is between 65 and 80 Hz; and hexa-coordinated, if the coupling constant (^{1}J) is

greater than 670 Hz and ^2J values is greater than 83 Hz [44,45]. These observed J values could be utilized in the calculation of the bond angle (θ) of C–Sn–C in solution using Lockhart's equation (1), and the equation (2) for the phenyl and the butyltin(IV) compounds were proposed by Howard *et al.* [46].

$$\theta = 0.0105\,|^2J(^{119}\text{Sn}–^1\text{H})|^2 - 0.799\,|^2J(^{119}\text{Sn}–^1\text{H})| + 122.4 \quad (1)$$

$$|^1J(^{119}\text{Sn}–^{13}\text{C})| = 11.4\,\theta - 875 \quad (2)$$

(for methyl and ethyl derivatives).

$$|^1J(^{119}\text{Sn}–^{13}\text{C})| = (9.99 \pm 0.73)\theta - (746 \pm 100) \quad (3)$$

(for butyl derivatives).

$$|^1J(^{119}\text{Sn}–^{13}\text{C})| = (15.56 \pm 0.84)\theta - (1160 \pm 101) \quad (4)$$

(for phenyl derivatives).

These bond angles (θ) are attributed to tetra-coordinated geometry, if $\theta \leq 112°$; penta-coordinated, if $\theta = 115 - 130°$; and hexa-coordinated, if $\theta = 129 - 76°$ [44].

The tin chemical shift (^{119}Sn) values often indicate the number of coordination around the tin center and, thus, provide valuable information about the geometry of organotin(IV) complexes [44]. The shifts are however, found to be dependent on the nature of the group attached to Sn. Caution is important in this analysis because tin resonance is strongly dependent on factors such as temperature, concentration used and electronegativity of the ligands [44,47,48]. With an electron donating group, Sn atom becomes more shielded, thereby leading to an increase in the chemical shift value [44]. The spectra of ^{119}Sn NMR of an organotin complex usually show a singlet which is significantly lower in frequency than corresponding organotin(IV) salts [48]. The lower chemical shifts observed in the spectra of organotin complexes are due to the change in the coordination number and bond angle around the tin center, caused by possible presence of electronegative substituents and $d\pi–p\pi$ bonding effect. Hence, lower frequency upon coordination is an indication of increased coordination number [49]. The ^{119}Sn NMR shifts for

organotin complexes are either tetra-(δ = 200 to -60 ppm), penta-(δ = -90 to -190 ppm) or hexa (δ = -210 to -400 ppm)-coordinated [50]. Chemical shifts (δ) in the range of -600 to -700 nm suggest either 6- or 7-coordination geometry around the tin center. This has been attributed to a possible chemical equilibrium between octahedral and pentagonal-bipyramidal arrangement due to intra-molecular metal ligand bond [51].

X-ray single crystal technique, on the other hand, exploits the fact that X-rays (in the Ångström range, ~10^{-8} cm) are scattered (diffracted) by electron cloud of an atom with similar sizes to determine the three dimensional structures of molecules [52]. Accurate knowledge of molecular structures are known to aid the development of effective drugs [53] and therapeutic complexes. This is achieved by the growth of crystal, which when diffracted gives useful information such as bond distances, bond angles, and can clearly show the geometry of molecules. This analytical technique gives clearer information compared to spectroscopic techniques which are often limited. However, X-ray single crystal diffraction analysis is limited since the molecule is in the solid state and not much information is obtained about the behavior of the molecule in solution [54].

2.3. Structural Geometry of Organotin(IV) Dithiocarbamate Complexes

Several reports have been made on the structural geometry around the tin center in organotin(IV) complexes of dithiocarbamate [25]. This ranges from tetrahedral to octahedral geometries, depending on the nature of the ligand, the type and number of alkyl/aryl substituents on the organotin moiety. These complexes have shown rich diversity in coordination and the geometry around the tin center [55]. One important attribute of organotin(IV) halides is their propensity to have their coordination number increased from four to six by intermolecular association [43], and this property influences the geometry in the complexes. The geometries are not exactly perfect, but are distorted due to the asymmetric nature of the dithiocarbamate ligand, which consequently leads to unequal distances of the tin-sulfur bond. The ability of the dithiocarbamate ligand to bond to a central metal atom has led to several mode of coordination in this ligand via the two sulfur atoms present in the moiety. Thus, they favor a bidentate (chelate) coordination mode through the sulfur-metal bonds with bond angles between 65° and 80°; and this is dependent upon the metal ion and the size of the ligand [19]. The drawbacks in their ability to bind in a bidentate fashion has been attributed to the steric hindrance and lack of vacant orbital

for the metal center to coordinate with the second sulfur of the dithiocarbamate which subsequently results in a high activation barrier [56]. When this occurs, the geometry often shifts from the bidentate mode to anisobidenate or a monodentate binding mode. Thus, leading to various geometrical variations around the central metal atom [57]. Organotin(IV) compounds are confronted with a major structural issue often caused by the propensity of the tin metal atom towards high coordination, which could either be a weak or strong intramolecular coordination. This has been attributed to the availability of the empty 5d-orbital in the tetravalent tin atom [58].

Generally, the structural geometries of tin(IV) complexes are tetrahedral, trigonal pyramidal, or octahedral. For organotin(IV) compounds, the tri-substituted (R_3SnX) and the di-substituted (R_2SnX_2) derivatives often possess five and six coordinate geometries respectively [59,60]. Thus, the high coordination number mostly observed in organotin complexes of the formula R_nSnX_{4-n} (n = 1 - 3, X = halide, carboxylate, dithiocarbamate) with Lewis bases is due to the increase in the Lewis acid strength of the tin metal [61]. These geometries are often influenced by the mole ratio of the ligand to organotin(IV) salt used. This coordination geometries have been found to depend on the mode of bonding in the dithiocarbamate moiety, which is mostly monodentate or bidentate fashion [62].

Four coordinate geometries are common for the tri-substituted organotin complexes. These complexes are not completely tetrahedral but are distorted due to the distance of the second non-coordinated sulfur atom which often hangs as a "pendant" as shown in Figure 2.4. The structures of triphenyltin(IV) complexes of *p*-bromo-*N*-methylbenzylaminedithiocarbamate and *p*-fluoro-*N*-methylbenzylaminedithiocarbamate have been reported [63]. Both complexes contain discrete molecular units with the central tin atom bonded to the triphenytin moeties in a monodentate fashion, forming a supposed tetra-coordinated geometry as presented in Figures 2.4a and 4b. The bond lengths and angles observed show that in both complexes, the monodentate bond was through one of the sulfur atoms with distances [Sn1-S1 = 2.464(10) Å] 1 and [Sn1-S1 = 2.4671(4) Å] respectively. The bond length of the non-coordinating sulfur atoms was found below the van der Waal radii of 4.0 Å, but too weak because of the distances (S2 atoms are 3.022 Å and 3.066 Å). The bond angles in S1-Sn1-C7, and C1-Sn1-C13 in triphenyltin(IV) *p*-bromo-*N*-methylbenzylaminedithiocarbamate are 90.54°(9) and 114.62°(13); and in triphenyltin(IV)*N*-

methylbenzylaminedithiocarbamate, the S1-Sn1-C13 and C1-Sn1-C7 are 92.82°(2) and 119.75°(14) respectively, which showed a deviation from the expected 109.5°. The wider angles show deviation from the expected tetrahedral angle, and have been attributted to the infleunce of the proximity of the non-coordinated sulfur atoms in the complexes [63].

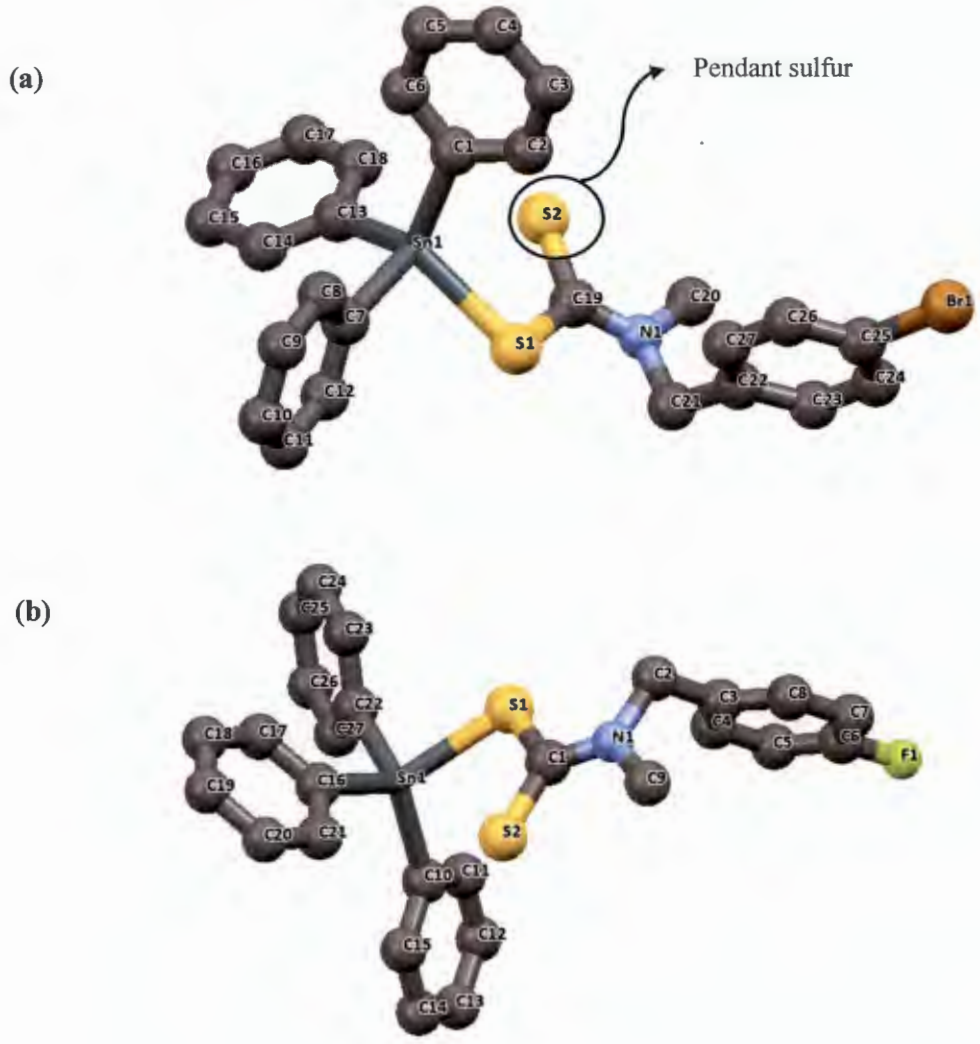

Figure 2.4: Thermal ellipsoidal plot of **(a)** triphenyltin(IV) *p*-bromo-*N*-methyl benzylaminedithiocarbamate and **(b)** triphenyltin(IV) *N*-methylbenzylaminedithiocarbamate with ellipsoidal displacement at 50% probability level (For clarity, H atoms were omitted). Redrawn from [63] with permission from Elsevier(Copyright 2018).

Yandav *et al.* reported a monodentate coordination for the organotin complex obtained from 4-hydroxypiperidine dithiocarbamate. The ligand imposes a distorted tetrahedral geometry around the tin center as shown in Figure 2.5 [64]. The covalent Sn–S bond distances are unequal with Sn1–S1 and Sn1–S2, having distances of 2.4757(7) and 3.0336(7) Å respectively. The longer distance (3.0336(7) Å) is significantly high, but less than the sum of the van der Waal radii of two atoms, which suggested a weak interaction for the Sn1---S2 bond. Thus, the geometry of the coordination around the tin atom suggests a deviation away from the regular tetrahedron to a trigonal bipyramidal structure due to the weak bond interaction of Sn1–S2. This complex have subtending angles for the atoms in the axial and equatorial positions smaller than the ideal tetrahedral, which supports the deviation towards trigonal bipyramidal (for equatorial substituents C19–Sn1–C13, 118.12°(10); S1–Sn1–C19, 112.75°(7); S1–Sn1–C13, 116.54°(7)).

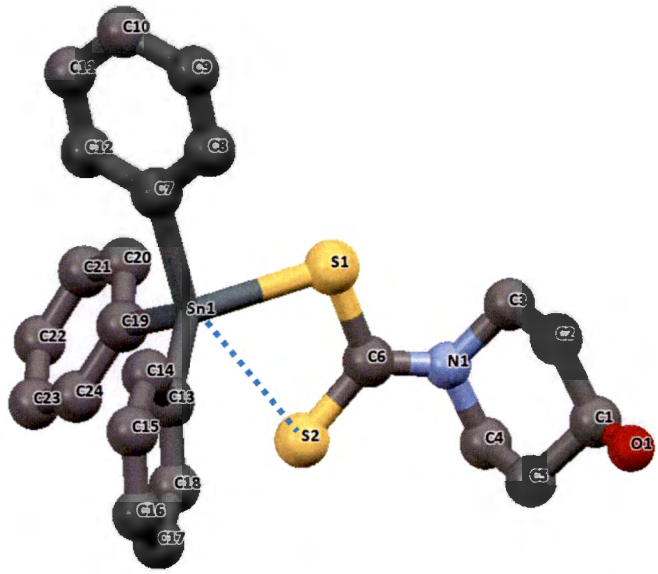

Figure 2.5: ORTEP view of triphenyltin(IV) 4-hydroxypiperidine dithiocarbamate displacement ellipsoids drawn at 30% . (For clarity, H atoms were omitted). Redrawn from [64] with permission from Elsevier (Copyright 2018).

Similarly, the structures of triphenyltin(IV) *N*-cyclohexyl-*N*-ethyl- and *N*-cyclohexyl-*N*-methyldithiocarbamate were reported to have anisobidentate coordination with one Sn-S short distance Sn(1)-S(2) = 2.9426(10) Å and another long Sn(1)-S(2) = 3.0134(8) Å, resulting in a

distortion in geometry. Thus, the geometry in both complexes about the Sn center is between tetrahedral and trigonal bipyramidal [65].

Some diorganotin(IV) salts have shown, from the crystallographic data obtained, the ability to bind in a monodentate fashion with dithiocarbamate ligand [66,67]. This is uncommon for most substituted diorganotin(IV) complexes which are often found to bond in a bidentate fashion. An example is the diorganotin(IV) complexes of *p*-bromo-*N*-methylbenzylaminedithiocarbamate and *p*-fluoro-*N*-methylbenzylaminedithiocarbamate. The structural data showed that the ligands are bonded in a monodentate fashion. In dimethyltin(IV)bis[*p*-bromo-*N*-methylbenzylamine dithiocarbamate complex (Figure 2.6), the bond distances of Sn1-S1 and Sn1-S2 were 2.530(2) and 2.515(19) Å respectively. Also, Sn1-S1 and Sn1-S3 for dimethyltin(IV)bis(*p*-fluoro-*N*-methylbenzylamine dithiocarbamate) (Figure 2.7), were 2.5139(7) and 2.5181(7) Å, respectively (Figure7). The dithiocarbamate ligands in dimethyltin complexes have structural motifs and bonds in similar fashion. The distance of the non-bonded sulfur atoms (S2 and S4) to the Sn atom in dimethyltin(IV)bis[*p*-bromo-*N*-methylbenzylamine dithiocarbamate are = 2.902 and 3.104 Å and in dimethyltin(IV)bis(*p*-fluoro-*N*-methylbenzylamine dithiocarbamate) are 2.997 and 3.023 Å respectively. They are relatively longer than the coordinated Sn-S distances, but significantly less than the sum of the van der Waal force. This weak interaction which exist between the S2 and S4 atoms with the tin metal forces the opening of the angle between the C-Sn-C, and the closing up of the angle between the S-Sn-S to a small value, which is less than the expected tetrahedral value of 109°. Hence, resulted into a distortion away from the expected tetrahedral geometry around the Sn center [66].

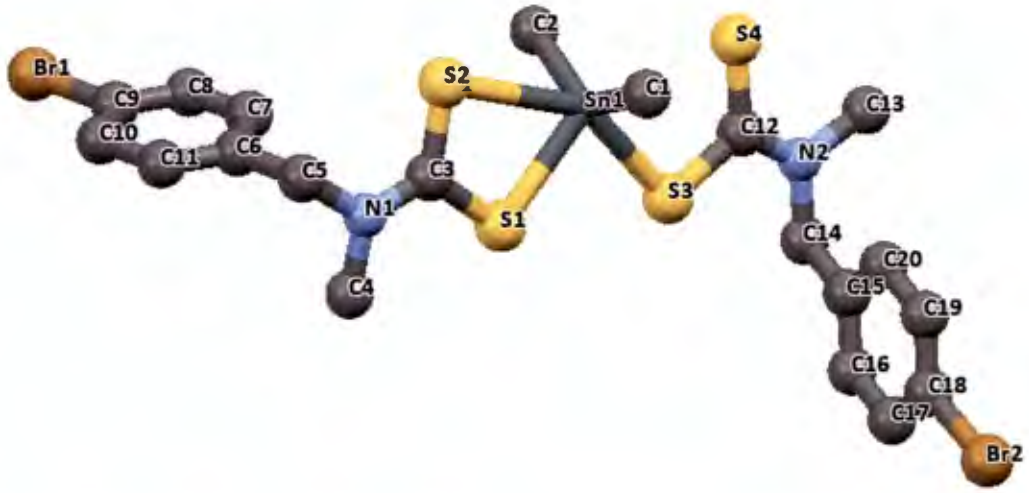

Figure 2.6: Thermal ellipsoidal plot of dimethyltin(IV) bis[*p*-bromo-*N*-methyl benzylaminedithiocarbamate with ellipsoidal displacement at 50% probability level. (For clarity, H atoms were omitted). Redrawn from [66] with permission from Elsevier (Copyright 2018).

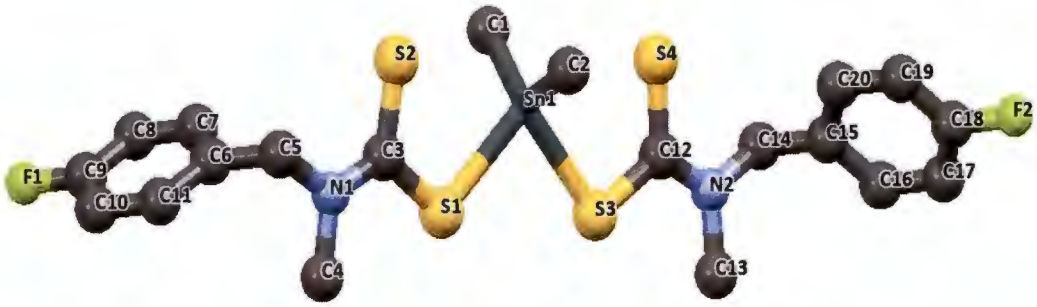

Figure 2.7: Thermal ellipsoidal plot of dimethyltin(IV) bis(*p*-fluoro-*N*-methyl benzylaminedithiocarbamate) with ellipsoidal displacement at 50% probability level. (For clarity, H atoms were omitted). Redrawn from [66] with permission from Elsevier (Copyright 2018).

A distorted tetrahedral geometry has also been reported for the organotin(IV) complex obtained from ammonium pyrrolidinedithiocarbamate ($[Sn\{S_2CN(CH_2)_4\}_2n\text{-}Bu_2]$ [67]. The

dithiocarbamate ligand was bonded to the adjacent side of the organotin moiety via a single sulfur atom at both ends as shown in Figure 2.8. The bond distances obtained for the Sn-S bond are Sn–S(1) = 2.534 Å and Sn–S(3) = 2.532 Å.

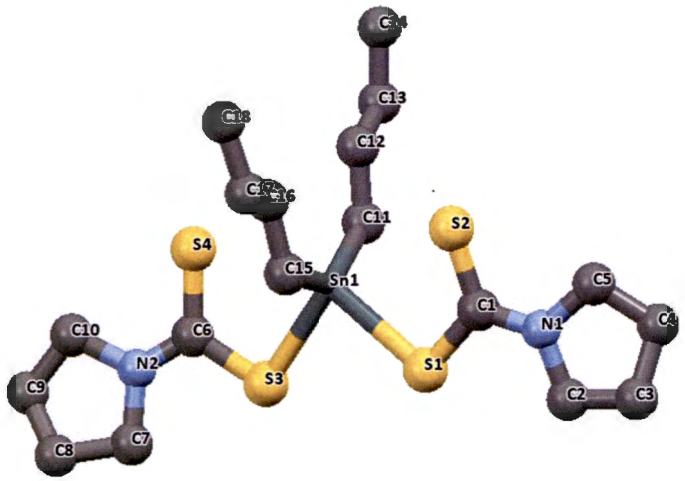

Figure 2.8: The molecular structure $Sn\{S_2CN(CH_2)_4\}_2n\text{-}Bu_2$ and the atom numbering. (For clarity, H atoms were omitted). Redrawn from [67] with permission from Elsevier (Copyright 2018).

When two groups of dithiocarbamate ligands bond with all the sulfur atoms present in a bidentate fashion, it often results in an octahedral geometry around the tin atom [68]. This class of organotin dithiocarbamate complexes is represented in Figure 2.9a-c. The molecular structure and structural data obtained for the dibutyltin(IV) complexes of 4-phenylpiperazine-1-dithiocarbamate $[(nBu)_2Sn(L^1)_2]$ and *N*-benzyl-*N*-methyl-4-pyridyldithiocarbamate $[(nBu)_2Sn(L^1)_2]$, as presented in Figure 9a-b, show that the metal occupy a twofold axis such that half of the molecule is found in the asymmetric unit. In the dibutyltin(IV) complexes, the two dithiocarbamate ligands bond through the two available sulfur (S11 and S13) in an unequal distance (2.533(1)-2.554(1) Å) to the tin atom and at a somewhat longer distances of 2.896(1)-2.971(1) Å respectively. The longer distances are well within the sum of the van der Waals radii of tin and sulfur (3.97 Å), and are considered as bonds. The distances of Sn-C bonds in these complexes observed in the range 2.140(2) - 2.145(5) Å are within the range found for diorganotin(IV) dithiocarbamates. For diphenyltin(IV) *N*-benzyl-*N*-methyl-3-pyridyldithiocarbamate $[(Ph)_2Sn(L^3)_2]$, similar unequal distances were observed as for Sn-S

bond, 2.593(1) and 2.680(1) Å. The Sn-C41 bond length is 2.139(4) Å. the geometry around these complexes are best described as distorted octahedral geometry [69].

(a)

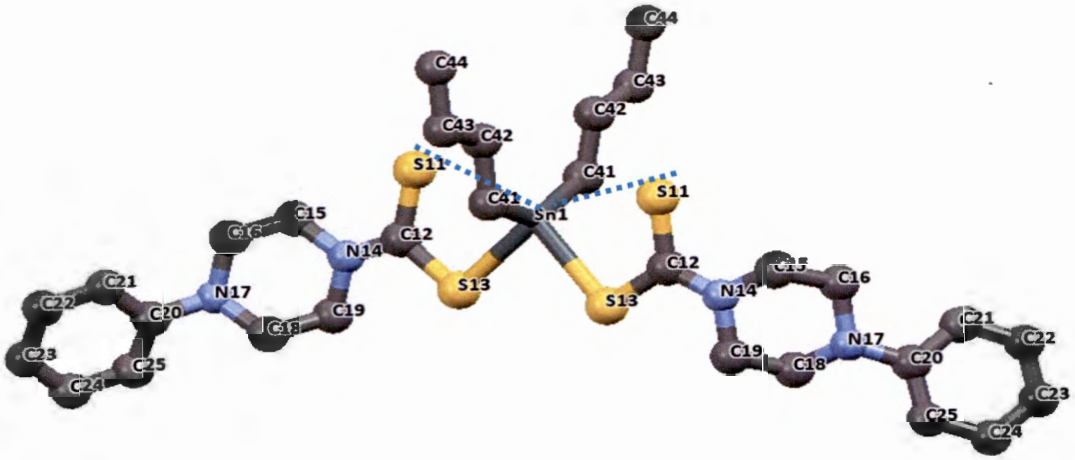

(b)

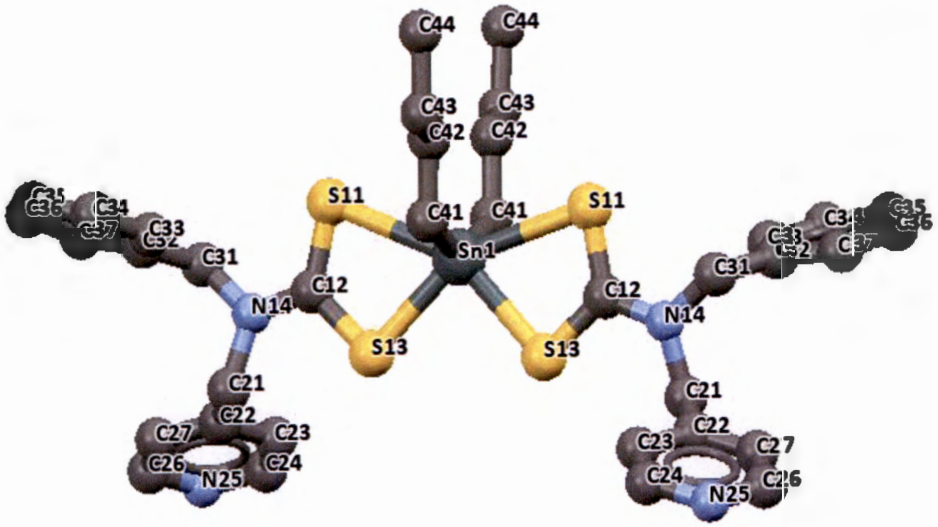

(c)

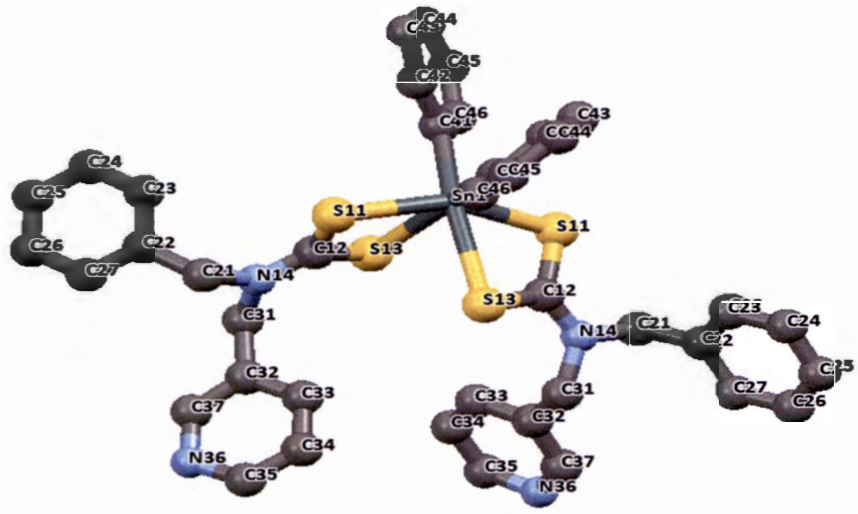

Figure 2.9: **(a)**The molecular structure of dibutyltin (IV) 4-phenylpiperazine-1-dithiocarbamate, **(b)** dibutyltin*N*-benzyl-*N*-methyl-4-pyridyldithiocarbamate and **(c)** diphenyltin (IV) *N*-benzyl-*N*-methyl-3- pyridyldithiocarbamatethe atom numbering scheme (all hydrogen atoms are omitted for clarity). Redrawn from [69] with permission from Elsevier (Copyright 2018).

Contrary to most known structures of diorganotin(IV) dithiocarbamate complexes, another structural motif exists in which one of the two dithiocarbamate ligands can bond to the central metal atom in a monodentate fashion and the other in a bidentate fashion (with second sulfur hanging as a pendant). This consequently results in five-coordinate geometry around the central Sn atom. An example is the dimethyltin(IV) complex of the *N,N*-dimethyldithiocarbamate ligand [62], in which one of the ligands is bonded in an anisobidentate fashion due to the unequal distances of the tin to sulfur bond (Sn-S(1) and Sn-S(3) 2.795 (1) and 2.489 (1) Å) and a bite angle of 67.56(2)°. The non-coordinating pendant sulfur atom S(4) possesses a distance of 3.532(1) Å. The geometry around the tin metal observed has been described as a distorted trigonal bipyramid. The two bulky groups of the tert-butyl ligand moiety has been suggested to be responsible for the five coordinate geometry around the Sn center [62].

2.2. Thermal Decomposition Studies of Organotin(IV) Dithiocarbamate Complexes

Thermogravimetric analyses of compounds are usually carried out in order to gain insight into the thermal properties and stability of the compounds; and in materials chemistry it helps ascertain the possible use of thio-complexes as single source precursors for metal sulfides

nanoparticles. In the case of organotin(IV) dithiocarbamate, a possible formation of tin sulfide is envisaged [64]. The thermochemistry of metal dithiocarbamates has shown, from its wide study, that the complexes either volatilize to leave a negligible amount of residue or decompose to yield metal sulfide [70].

The major techniques employed for the thermal study of a wide variety of metal dithiocarbamate complexes are TGA, STA and DSC [71]. These techniques have made it possible to study the trend within a group of complexes with relevant analytical and structural significance, and also classify them based on their thermal properties. A common intermediate that is associated with the thermal decomposition of metal dithiocarbamate is metal thiocyanate intermediate [72]. Metal thiocyanate has been reported as an intermediate for a number of transition metal dithiocarbamate complexes which often decomposes to give its corresponding metal sulfide as final residue [73–76]. The decomposition pattern of some organotin(IV) dithiocarbamate complexes can also progress via the tin thiocyanate intermediate to give a tin sulfide residue [77]. Thermal study data relating to the decomposition of tin dithiocarbamates are available [71], but it has been observed (generally) that there is no clear cut trend in the thermal decomposition pattern within this group of organotin(IV) complexes irrespective of structural similarity. Tin dithiocarbamates exhibit complicated thermochemistry and an unpredictable thermal decomposition pattern even for a series of structurally related complexes [71]. It is almost impossible to establish a trend among structurally related compounds because they do not follow similar decomposition pathway [71].

Two types of residue, including tin-sulfide or tin-oxide, are often obtained from the thermal decomposition of organotin dithiocarbamate complexes, and they are dependent on the decomposition condition (inert or in air) [78]. Tin sulfides can exist in three possible phases: SnS that exhibit layer structures, SnS_2 and Sn_2S_3 which has a mixed valence of Sn^{2+}/Sn^{4+} with a ribbon-like structure [79]. Tin sulfides have semiconducting properties; and due to its low toxicity, it is used as solar energy absorber in holographic recording and for infrared detection [80]. Tin sulfide in its various forms possesses the following band gaps: SnS (1.3 eV), SnS_2 (2.18 eV), and Sn_2S_3 (0.95 eV). The electronic band gap of SnS have attracted much attention because it lies between that of Ga and Si [80].

Tin sulfide nanoparticles of different morphologies such as rods, belts, and spheres have been produced via the thermal decomposition of organotin dithiocarbamate complexes under specific conditions [81]. Hence, it is imperative to understand the thermal behavior of organotin(IV)dithiocarbamate complexes [71]. New routes for making cheaper and microscale inorganic material with well-defined sizes and shapes have led to the continuous research in materials science. Dithiocarbamate complexes, on the other hand, have been regarded as a good single source materials for metal sulfides [82]. This is because they possess sulfur as the only heteroatom to the metal center (after their thermal decomposition), while avoiding the formation of undesired impurities like metal oxides to exclusively yield metal sulfide nanoparticles [83]. The product of the thermal decomposition of organotin dithiocarbamate has various applications. For example, tin oxides are used as light detectors (visible and infrared), solar cells, light emitting diodes and as gas sensors [78]. Tin sulfides have outstanding electronic and optical properties due to their narrow bad gap. They have been used to replace cadmium chalcogenides (due to toxicity) or silicon based sensor in low cost green photovoltaic devices [79].

Thermogravimetric analyses have been carried out (under nitrogen) on some organotin(IV) 4-hydroxypiperidine dithiocarbamate. The decomposition of these complexes proceeded via a single step decomposition regardless of the nature of the alkyl group attached. The final residue obtained for these set of complexes was found to be SnS [64]. Similarly, the TGA of (diphenyltin(IV)*N*-benzyl-*N*-methyl-3-pyridyldithiocarbamate and dibutyltin-4-ethoxycarbonyl piperidine-1-dithiocarbamate) at similar heating rate of 10 °C min^{-1} (to a temperature of 600 °C) under nitrogen gave a double decomposition pattern leaving SnS_2 and SnS residue respectively [69].

In the report of Menezes *et al.* [79], the thermal study of two organotin complexes of ammonium pyrrolidinedithiocarbamate with the formula $[Sn\{S_2CN(CH_2)_4\}_2\{C_6H_5\}_2]$ and $Sn\{S_2CN(CH_2)_4\}\{C_6H_5\}_3$ were carried out. The decomposition of these complexes were observed to proceed in a pseudo-single step which began at 207 and 233 °C (±2 °C) for $Sn\{S_2CN(CH_2)_4\}_2\{C_6H_5\}_2$ and $Sn\{S_2CN(CH_2)_4\}\{C_6H_5\}_3$ respectively, and terminates at about 350 °C in both cases. In $Sn\{S_2CN(CH_2)_4\}\{C_6H_5\}_3$, it was observed that the presence of an extra phenyl group increased temperature of decomposition by approximately 26 °C. The final residues of these decompositions were chemically and structurally characterized. The electron

probe micro analyzer (EPMA) results, clearly shows the presence of S and Sn as the major elements found in the residues. However, a minute amount of O_2 was observed and attributed to the formation of SnO_2 as a much lesser product. This O_2 was suggested to originate from the N_2, which was not completely free from moisture or oxygen. The pattern observed from the diffraction of these residues suggested the formation of a mixed phase γ-Sn_2S_3 and SnS for both orthorhombic phases, in view of the diffraction lines.

2.4. Biological Applications of Organotin(IV) Dithiocarbamate Complexes

2.4.1. Antimicrobial properties of organotin(IV) dithiocarbamate complexes

Generally, the antimicrobial mode of action of metal complexes involves the interference of the cell wall synthesis (alteration of the cell permeability) by the compounds, metabolic interference with various cellular enzymes, cellular impairment (due to denaturing of proteins), and alteration of the normal cell processes (due to the hydrogen bonding with active cellular enzymes) [84]. The pictorial presentation of this mechanism is shown in Figure 2.11. The stereo-electronic properties of sulfur containing ligands is one of the responsible factors for their good activities as antimicrobial agent which is enhanced upon coordination to metals [28]. However, the antimicrobial activities of organotin complexes are also governed by their molecular weight and lipophilicity [12]. Complex formation causes an increased antimicrobial activities [85], which, in turn, alters the polar nature of the metal by the delocalization of electron and charge sharing with sulfur donor groups. This electron delocalization enhances plasma membrane permeability for the complexes [86]. Rehman *et al.* have suggested the mechanism of complexes with organotin moiety within their structure to proceed either by inhibiting the active site for multiplication or by killing of the microorganism [87]. Gram positive bacteria are known to have a simpler cell wall compared to the more complex wall of the Gram negative bacterial, thus, are more induced by the complexes to give higher activity. The complexity observed in the Gram negative bacteria have been attributed to the outer-lipid membrane formed from lipopolysaccharide contributing to the antigenic specificity of the Gram negative bacterial [11].

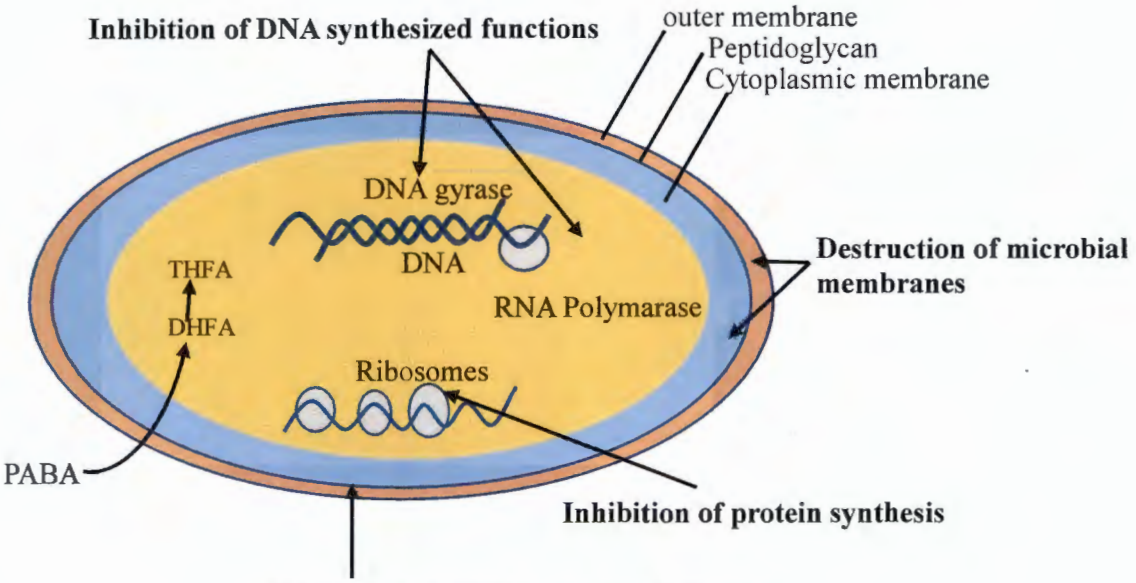

PABA = para-aminobenzoic acid
DHFA= dihydrofolic acid
THFA=tetrahydrofolic acid

Figure 2.10: The general mechanism for antimicrobial agent on microorganism. Copied and modified from Subbhankari *et al* [88].

2.4.2. Antibacterial studies of organotin(IV) dithiocarbamate complexes

Organotin(IV) dithiocarbamate complexes, due to their useful biological potentials, have been utilized as important pharmacophore in the development of metal based drugs [77]. Organotin as well as dithiocarbamate compounds, have been used in their uncombined state to develop several antimicrobial agents [6,7,67]. The potential activities of these compounds on individual basis, therefore indicates that both compounds can be combined to give a hybrid molecule with enhanced biological properties which could exert some synergistic biological activity[67,89]. Some currently used antibacterial drugs are known to contain metal fragment. These central metal ions help in maintaining proper structure and/or enhance their activities as antibiotics. Removal of the metal ions from these antibiotics could result into transformation and loss of activity [90]. Among this group of antibiotics with metal centers are bleomycin, streptonigrin, and bacitracin [90]. Drug resistance is a serious global challenge and remains the greatest threat to prevention and treatment of infectious diseases. According to WHO, antimicrobial resistance

is the opposition of a microorganism towards the drug that effectively treats the infection caused by the pathogen. Despite the various research and usage of antibiotics, most of them are often accompanied by the evolution of microbial resistance [91]. Hence, the need for continuous search for alternative drugs that can effectively combat pathogenic organism.

Awang *et al.* synthesized some organotin dithiocarbamate compounds bearing different alkyl and phenyl derivativeswhich were screened against four bacteria strains: *Staphylococcus aureus*, *Salmonella typhimurium*, *Pseudomonas aeruginosa* and *Bacillus subtilis*. The studied complexes generally gave moderate to good antibacterial activity. It was noted that the phenyl containing complex showed inhibitory effect on selected bacteria strains. Cytotoxicity assays of the compounds confirm the potential of these complexes for further research [33]. Furthermore, they synthesized some organotin complexes derived from methyltin(IV), butyltin(IV), phenyltin(IV), and methylcyclohexyldithiocarbamate and ethylcyclohexyldithiocarbamate ligands. These complexes were also screened for their antimicrobial properties against the ESKAPE bacteria, including *Enterococcus raffinosus*, *Staphylococcus aureus*, *Klebsiella sp.*, *Acinetobacter baumanni*, *Pseudomonas aeruginosa*, and *Enterobacter aerogenes,* using disc diffusion and microdilution methods. It was observed that phenyltin(IV) methylcyclohexyldithiocarbamate derivative showed good activity towards most bacteria tested, similar to ampicillin (2.5 mg/mL) in the minimum inhibitory concentration (MIC). Overall, all the complexes showed bacteriostatic effects at the minimum bactericidal concentration (MBC) higher than the MIC values, but phenyltin(IV) complex exhibited the best activity and has potential as an antibacterial agent upon further clinical investigation [92].

Good activities have been reported for dibutyltin(IV) and triphenyltin(IV) complexes of di-2-ethylhexyldithiocarbamate and *N*-methylbutyldithiocarbamate ligands [29]. These complexes were screened against some bacterial strains including *Escherichia coli, Staphylococcus aureus, Salmonella typhi and Bacillus cereus* using penicillin and streptomycin as positive and negative controls respectively. The complexes showed good antimicrobial activity and, thus, can be useful as anitibacterial agents [29]. Similarly, Adli *et al.* screened some organotin(IV) dithiocarbamate complexes of 1-methylpiperazinedithiocarbamate and *N*-methylcyclohexyldithiocarbamate against *Staphylococcus aureus, Bacillus cereus*, *Salmonella typhi* and *Escherichia coli*. The

microbial test carried out showed all synthesized complexes possessed great potential as antimicrobial agents [42].

2.4.3. Antifungal studies of organotin(IV) dithiocarbamate complexes

Although resistance to antibiotics by bacteria has become a widely recognized public health threat, not much is known about the effects of drug-resistance in fungal infections. Just as there has been increase in the discovery and usage of antibacterial drugs with increase in high-risk patients, discoveries of the widespread and increasing rates of serious invasive fungal infections have also been recorded. However, the available antifungals have become less effective against certain infections due to emergence of drug-resistance [93]. There are increase in the number of deaths caused by Aspegillosis (a variety of diseases caused by fungi infection of the genus *Aspergillus*), which have been attributed to the action of immunosuppressive drugs, diseases, cancer or AIDs. In the treatment of aggressive aspergillosis, liposomal amphotericin B and Voriconazole are the first choice drugs which can be dangerous to the kidney and liver. Resistance to antifungal drugs in conventional treatment has been found to be related to target alterations of the drug, ergosterol biosynthesis interference and/or increase in the expression of drug efflux pumps. These reasons have made the need for alternative drugs very important and synthesis of metal-based drugs might provide a novel platform for new alternative antifungal agents, either alone or in combination with already used drugs to overcome resistance [94]. Trioganotin(IV) complexes containing methoxyl and dioxolane moieties have been isolated, and screened by Ferreira *et al.* against *Aspergillus flavus, Aspergillus niger, Aspergillus parasiticus* and *Penicillium citrinum*. Good antifungal activities were observed which were in correlation with a study on the structural-activity relationship (SAR) carried out. The complexes with the triphenyltin group showed noteworthy biocidal activity andof them exhibited a nanomolar inhibition concentration in terms of IC_{50} [95]. Some tin(IV) complexes of pyrrolidinedithiocarbamate, $[Sn\{S_2CN(CH_2)_4\}_2Cl_2]$, $[Sn\{S_2CN(CH_2)_4\}_2Ph_2]$, $[Sn\{S_2CN(CH_2)_4\}Ph_3]$, $[Sn\{S_2CN(CH_2)_4\}_2n\text{-}Bu_2]$, $[Sn\{S_2CN(CH_2)_4\}Cy_3]$ have been screened for antifungal activities using agar disc diffusion against human pathogenic fungi (*Candida albicans*). The complexes were active with inhibition zones $\geq$ 11 mm, intermediate inhibition zones within the range 11 – 9 mm and resistant $\leq$ 9 mm. The inhibition zone for the commercial nystatin was 14 mm and was used to compare the activities of the complexes. The *C. albicans*

exhibited resistance against pyrrolidinedithiocarbamate ligand, but showed moderate activities with most of the tin(IV) complexes. Complexes $[Sn\{S_2CN(CH_2)_4\}_2Cl_2]$ and $[Sn\{S_2CN(CH_2)_4\}_2n\text{-}Bu_2]$ showed the highest activities. The penetration of the complexes through the yeast membrane was attributed to the size and structure of the complexes. The two chlorine atoms in complex $[Sn\{S_2CN(CH_2)_4\}_2Cl_2]$ were attributed to its ease of penetration across the cell membrane compared to other complexes [67]. Organotin(IV) complexes of methyl- and ethylisopropyldithiocarbamate including: dimethyltin(IV) methylisopropyl dithiocarbamate, dibuthyltin(IV) methylisopropyldithiocarbamate, triphenyltin(IV) methylisopropyldithiocarbamate, dimethyltin(IV) ethylisopropyldithiocarbamate, dibutyltin(IV) ethylisopropyldithiocarbamate, triphenyltin(IV) ethylisopropyldithiocarbamate have been synthesized and their biological activities were evaluated. The antifungal activities of these complexes were screened against three species of fungi namely *Aspergillus niger, Candida albicans,* and *Saccharomyces cerevisiae* using qualitative disc diffusion and quantitative broth microdilution method. Very good antifungal activities were observed for all the fungi tested. Minimum inhibitory concentration (MIC) values obtained for these compounds were better than streptomycin against *B. cereus*, *S. aureus*, and *S. mutans* [96].

2.4.4 Anticancer / Antitumor studies of organotin(IV) dithiocarbamate complexes

Metal complexes have, overtime, proven to be useful in the fight against cancer. Cisplatin, an inorganic complex of platinium discovered by Bernet Rosenberge, exhibits antitumor characteristics, and remains one of the world's bestselling anticancer drugs. This discovery led to changes in the course of therapeutic management of several tumors, such as those of the ovaries, testes, head and neck [97]. However, this spectacular clinical activity of cisplatin has been found to be limited by significant side effects such as DNA damage and the emergence of drug resistance [98]. Because of this usual accompanied side effect of the platinum based antitumor drugs, further research for alternative metal based drugs with improved antitumor activities such as the non-platinium based anticancer complex have been initiated. Good activities have been recorded with metals such as copper, gold [99], gallium, germanium, tin, ruthenium, iridium, lanthanum [100], but none has entered the clinical trial stage till date. Among the afore mentioned, gold and tin derivatives have gained increased interest and have appeared very promising as potential anticancer drugs [101]. Hence, the continual search for novel

chemotherapeutic agents with decreased toxic side-effects and improved specificity. *In vitro* screening of new coordination complexes, followed by careful selection of best active anticancer compounds, remains the best way of identifying potential antitumor agents. The underlying mechanism of the organotin compounds involve the inhibition of F1F0 ATP synthase [102,103]. F1F0 ATP synthase have been found to be harmful to all forms of life [103]. In their uncombined form as ordinary salts, organotin compound such as tributyltin(IV) chloride have been reported to inhibit ATP synthases by targeting the Na^+ channel. Likewise, oxidative phosphorylation and ATP synthesis in the mitochondria have been suggested to be suppressed by the dibutyltin(IV) dichloride [104]. Other reports have suggested their mechanism of action to involve binding to both DNA base and phosphate contrary to the cisplatin which could bind to DNA with a cross link. This can induce DNA damage by inhibiting DNA and protein synthesis while increasing RNA synthesis, thereby affecting structural selectively [105]. These observed mode of actions have been suggested to hinder the usage of organotin compounds as an improved antitumor agents due to the cellular targets of this compounds in their mechanism regardless of the mitochondrial oxidative phosphorylation [106]. Nevertheless, there is a need to further understand how to modulate these toxic effects.

Various studies with interesting results have been conducted on the *in vitro* antitumor properties of organotin(IV) complexes of dithiocarbamate against a wide panel of tumor cell lines of human origin [107]. Series of phenyltin(IV) dithiocarbamates of the formula $Ph_{4-n}Sn(S_2CNEt_2)_n$, where n=1–3, were evaluated for their cytotoxicity against L1210 mouse leukaemia cell line. About 50% growth inhibition ratings of 0.3 μM was found compared with 0.6 and 1.2 μM for the drugs cisplatin and carboplatin respectively. It was discovered that when chloride was introduced, as in $PhSn(S_2CNEt_2)_2Cl$ and $Ph_2Sn(S_2CNEt_2)Cl$, it resulted in low toxicity. Nevertheless, it was found to still exert more cytotoxic effect than drugs containing Pt metal [25]. In other study, organotin dithiocarbamates with general formula $(ArCH_2)_2Sn(S_2CNR'_2)Cl$ and $(ArCH_2)_2Sn(S_2CNR'_2)_2$ were evaluated against various panels of human cancer cell lines. It was reported that the group with chloride were more cytotoxic than their counterparts without chloride substituents, i.e. $(ArCH_2)_2Sn(S_2CNR'_2)_2$. From this study it was suggested that the ease of hydrolysis of the former might be the reason for such behavior. The complex, $(4\text{-}NC\text{-}C_6H_4CH_2)_2Sn[S_2CN(CH_2CH_2)_2NCH_3]Cl$, was found to be the most cytotoxic compound in the series, and more cytotoxic than cisplatin [40]. Some binuclear diphenyltin(IV) dithiocabamate

macrocyclic complexes have been synthesized through a self-assembly process involving novel diamino precursors 4,4′-bis(2-(alkylamino)acetamido)diphenyl ethers, CS_2 and Ph_2SnCl_2. Using the 3-(4,5-dimethylthiazol-2-yl)-2,5-diphenyltetrazolium bromide (MTT) assay, cytotoxic activity was carried out against HEP 3B (hepatoma) and IMR 32 (neuroblastoma). The complexes were very active against both cell lines and cytotoxicity data having better 16-fold potency compared to cisplatin. The flow cytometric analysis of annexin V–propidium iodide-stained cells of L5, 4 and 6 was found to possess the ability to induce apoptosis in HEP 3B and IMR 32 cells, which is a requirement for major cancer therapy. The binuclear complex show an extraordinary potency which can be correlated to result from the higher LUMO energy together with the great charge value on the Sn(IV) center [28].

Organotin compound of the type R_3SnCl and R_2SnCl_2 (R = C_6H_5 or C_4H_9) with dithiocarbamate ligand of methoxyethyldithiocarbamate have been evaluated for their *in vitro* anti-proliferative activities against HL-60 cell lines. The results showed that both complexes exhibited high cytotoxicities toward HL-60 cell lines with the IC_{50} values below 1 mM. These complexes were found to possess high anti-proliferative effects; thus, in correlation with an earlier finding of Awang *et al.* (2010). The potency against the HL-60 cells and the IC_{50} of triphenyltin(IV) complex was much less than the dibutyltin(IV) complex which displayed a higher potential. It was concluded that both complexes have the potential of becoming good antitumor agents due to their potent cytotoxic effect at micromolar concentrations [34].

2.4.5. Other biological studies of organotin(IV) dithiocarbamate complexes

The biological applications of organotin(IV) dithiocarbamate are not only limited to the highlighted areas, other biological activities of organotin(IV)dithiocarbamates have also been reported. Organotin(IV) dithiocarbamate have shown good activities as antileishmainial agent. Series of complexes of di- and tri- organotin(IV) dithiocarbamates with 4,4-trimethylenedipiperidine-1- carbodithioate have shown better antilaishmanial activity above the currently used standard drugs. Their high activities have been attributed to low binding energy with enzyme trypanothione synthetase. It was concluded that, with further clinical investigations the synthesized complex have a promising potential for the treatment of leishmaniasis [108].

Promising insecticidal activities have been obtained in a study involving complexes of triorganotin(IV) dithiocarbamates of the formula $R_3SnS_2CNR_2$ (where R = Cy, Ph; NR_2' = NEt_2,N(*n*-Bu)$_2$,N(i-Bu)$_2$, N(*n*-Pr)$_2$,N$(CH_2)_5$, NH(*n*-Pr), NH(*n*-Bu), NH(*i*-Bu)). This was achieved against the second larval instar of the *Anopheles stephensi* and *Aedes aegypti* mosquitoes. The studies showed no significant activities with triphenyltin and tricyclohexyltin derivatives, but showed moderate action against the larvae of both species [109].

The scavenging potential for radicals of some organotin(IV) dithiocarbamate complexes of cyclohexylcarbamodithioic acid have been studied. This was achieved using 2,2-diphenyl-1-picrylhydrazyl (DPPH) radical assay. The IC_{50} values and the percentage inhibition of both the ligand and complexes were obtained and compared with a known antioxidant agent (butylated hydroxytoluene). The ligand itself showed a good radical scavenging potential which were enhanced upon coordination to the respective organotin(IV) salts [11].

2.5 Limitation associated with toxicity of organotin(IV) compounds

Several reports have been made about the diverse use of organotin compounds as biological agents with better activity. Nevertheless, most of these compounds have not been cleared for clinical practice because most derivatives are generally very toxic [106]. They often leave undesirable effects on the nervous, reproductive, endocrine and other systems of animals. Some of which includes cognitive impairment in learning and memory [105]. One factor that increases the toxicity of organotin is the number of alky groups present within the moiety [106]. The bulkiness and the number of these alky groups affect the toxicity of the molecule which in turn affects their hydrophilicity at large [110]. Trimethyltin have been used as stabilizers in PVC, as disinfectants and as insecticides but has a strong neurostatic effect and have been reported to impair spatial memory in rat and mice [105]. Dibutyltin has also shown neurostatic effect by aggregating on the brain cell cultures.

In platinum chemotherapy, sulfur containing molecules have been used as chemo-protectants due to their anticancer potential and the ability to modulate cisplatin nephrotoxicity [28]. The mechanism of this modulation is still unknown, but there are reports that proposes the DNA to be the probable targets of the cytotoxic activity [106,111]. Therefore, regardless of the associated toxicity, organotin(IV) compounds and it derivatives can have their toxicities modulated by a judicious choice of the ligand (like dithiocarbamate) coordinated to the organotin(IV) moiety to

minimize this drawbacks [106]. This is one of the factors that informed the judicious choice of dithiocarbamate as complementing ligand in the synthesis of the organotin(IV) compoounds

References

[1] B.S. Garg, R. Dixit, A.L. Singh, J. Therm. Anal. 36 (1990) 2567–2582.

[2] G. Hogarth, ChemInform 44 (2013) no-no.

[3] D.J. Lewis, P. Kevin, O. Bakr, C.A. Muryn, M.A. Malik, P. O'Brien, Inorg. Chem. Front. 1 (2014) 577–598.

[4] A.S.L. Barbosa, J. de S. Guedes, D.R. da Silva, S.M.P. Meneghetti, M.R. Meneghetti, A.E. da Silva, M.V. de Araujo, M.S. Alexandre-Moreira, T.M. de Aquino, J.P. de Siqueira Junior, R.S.A. de Araújo, R.M.D. da Cruz, F.J.B. Mendonça-Junior, J. Inorg. Biochem. 180 (2018) 80–88.

[5] D.C. Onwudiwe, P.A. Ajibade, Polyhedron 29 (2010) 1431–1436.

[6] S. Kanchi, P. Singh, K. Bisetty, Arab. J. Chem. 7 (2014) 11–25.

[7] N. Lal, Chem. Biol. Interface 4 (2014) 321–340.

[8] A.S. Shahvelayati, F. Adhami, J. Org. Chem. 4 (2009) 244–246.

[9] B. Movassagh, B. Shokri, Int. J. Org. Chem. 2 (2012) 248–253.

[10] N. Singh, S. Bhattacharya, J. Organomet. Chem. 700 (2012) 69–77.

[11] S. Jabbar, I. Shahzadi, R. Rehman, H. Iqbal, Qurat-Ul-Ain, A. Jamil, R. Kousar, S. Ali, S. Shahzadi, M.A. Choudhary, M. Shahid, Q.M. Khan, S.K. Sharma, K. Qanungo, J. Coord. Chem. 65 (2012) 572–590.

[12] F. Shaheen, Zia-Ur-Rehman, S. Ali, A. Meetsma, Polyhedron 31 (2012) 697–703.

[13] A.Z. Halimehjani, A. Dadras, M. Ramezani, E. V. Shamiri, S.E. Hooshmand, M.M. Hashemi, J. Braz. Chem. Soc. 26 (2015) 1500–1508.

[14] S. Kanchi, P. Singh, K. Bisetty, Arab. J. Chem. 7 (2014) 11–25.

[15] A. Manohar, V. Venkatachalam, K. Ramalingam, S. Thirumaran, G. Bocelli, J. Chem. Crystallogr. 28 (1998) 861–866.

[16] A.A. Aly, A.B. Brown, T.M.I. Bedair, E.A. Ishak, J. Sulfur Chem. 33 (2012) 605–617.

[17] A.R. Roffey, Dithiocarbamate Complexes as Single Source Precursors to Metal Sulfide Nanoparticles for Applications in Catalysis, 2012.

[18] B.S. Garg, A.L. Singh, R. Dixit, Transit. Met. Chem. 13 (1988) 351–355.

[19] P.J. Heard, Prog. Inorg. Chem. 53 (2005) 1–69.

[20] A. Gölcü, Transit. Met. Chem. 31 (2006) 405–412.

[21] J. Sedlacek, L.M.D.R.S. Martins, P. Danek, A.J.L. Pombeiro, B. Cvek, J. Appl. Biomed. 12 (2014) 301–308.

[22] A.C. Ekennia, D.C. Onwudiwe, L.O. Olasunkanmi, A.A. Osowole, E.E. Ebenso, Bioinorg. Chem. Appl. 2015 (2015).

[23] D.C. Onwudiwe, J.N. Mugo, M. Hrubaru, E. Hosten, J. Sulfur Chem. 36 (2015) 36–47.

[24] G. Hogarth, in:, Prog. Inorg. Chem. Vol. 53, 2005, pp. 71–561.

[25] E.R.T. Tiekink, Appl. Organomet. Chem. 22 (2008) 533–550.

[26] B.S. Garg, R.K. Garg, M.J. Reddy, 99 (1995) 97–99.

[27] E.A. Hassan, S.E. Zayed, Phosphorus, Sulfur Silicon Relat. Elem. 189 (2014) 300–323.

[28] R. Kadu, H. Roy, V.K. Singh, Appl. Organomet. Chem. 29 (2015) 746–755.

[29] M.H. Sainorudin, N.M. Sidek, N. Ismail, M.Z.H. Rozaini, N.A. Harun, T.N. Sabiqah Tuan Anuar, A.A. Abd Rahman Azmi, F. Yusoff, GSTF J. Chem. Sci. 2 (2015) 1–9.

[30] E. Khan, U.A. Khan, A. Badshah, M.N. Tahir, A.A. Altaf, J. Mol. Struct. 1060 (2014) 150–155.

[31] M. Delepine, Compt. Rend., 144 (1907) 1125-1127

[32] A. Basirah, M. Faizuddin, A. Hasan, N.M. Sidek, W.M. Khairul, N. Ismail, J. Appl. Sci. Res. 9 (2013) 5562–5567.

[33] N. Awang, I. Baba, B.M. Yamin, M.S. Othman, N.F. Kamaludin, Am. J. Appl. Sci. 8 (2011) 310–317.

[34] N. Awang, N.F. Kamaludin, I. Baba, K.M. Chan, N.F. Rajaajab, A. Hamid, Orient. J. Chem. 32 (2016) 101–107.

[35] N.F. Kamaludin, N. Awang, I. Baba, A. Hamid, C.K. Meng, Pakistan J. Biol. Sci. 16 (2013) 12–21.

[36] K. K.Venugopal, Rameshbabu, J. Sreeramulu, World J. Pharm. Res. 4 (2015) 2278 – 4357.

[37] D.C. Onwudiwe, M. Hrubaru, E.E. Ebenso, J. Nanomater. 2015 (2015).

[38] F. Cotton, J. McCleverty, Inorg. Chem. 3 (1964) 1398–1402.

[39] M. Shahid, T. Ruffer, H. Lang, S.A. Awan, S. Ahmad, J. Coord. Chem. 62 (2009) 440–445.

[40] H.D. Yin, S.C. Xue, Appl. Organomet. Chem. 20 (2006) 283–289.

[41] F. Bonati, R. Ugo, J. Organomet. Chem. 10 (1967) 257–268.

[42] H.K. Adli, N.M. Sidek, N. Ismail, W.M. Khairul, Chiang Mai J. Sci. 40 (2013) 117–125.

[43] R. Sharma, N.K. Kaushik, Indian J. Chem. - Sect. A Inorganic, Phys. Theor. Anal. Chem. 43 (2004) 769–772.

[44] M. Sirajuddin, S. Ali, V. Mckee, RSC Adv. 4 (2014) 57505–57521.

[45] T.P. Lockhart, W.F. Manders, Inorg. Chem. 25 (1986) 583–585.

[46] W.F. Howard, R.W. Crecely, W.H. Nelson, Inorg. Chem. 24 (1985) 2204–2208.

[47] T. Sedaghat, K. Goodarzi, Main Gr. Chem. 4 (2005) 121–126.

[48] T. Sedaghat, Z. Shokohi-pour, J. Coord. Chem. 62 (2009) 3837–3844.

[49] J. Otera, J. Organomet. Chem. 221 (1981) 57–61.

[50] M. Sirajuddin, S. Ali, M.N. Tahir, Inorganica Chim. Acta 439 (2016) 145–158.

[51] R.C.R. Chagas, J.R. Da Silveira Maia, V.P. Ferraz, Main Gr. Met. Chem. 34 (2011) 131–137.

[52] T.M. Picknett, S. Brenner, in:, Encycl. Genet., Elsevier, 2001, p. 2154.

[53] J.-M. Rondeau, H. Schreuder, in:, C.G. Wermuth, D. Aldous, P. Raboisson, D. Rognan (Eds.), Pract. Med. Chem. (Fourth Ed., Fourth Edi, Academic Press, San Diego, 2015, pp. 511–537.

[54] G. Johansson, Pure Appl. Chem. 60 (1988) 1773–1784.

[55] S. Shahzadi, S. Ali, J. Iran. Chem. Soc. 5 (2008) 16–28.

[56] G. Hogarth, Mini Rev. Med. Chem. 12 (2012) 1202–1215.

[57] D. Cardell, G. Hogarth, S. Faulkner, Inorganica Chim. Acta 359 (2006) 1321–1324.

[58] S.M. Abbas, S. Ali, S.T. Hussain, S. Shahzadi, J. Coord. Chem. 66 (2013) 2217–2234.

[59] H. Iqbal, S. Ali, S. Shahzadi, Cogent Chem. 1 (2015) 1029039–1029039.

[60] P. Sebatian, D. Iv, Malaysian J. Anal. Sci. 15 (2011) 106–112.

[61] Alwyn G. Davies, Organotin Chemistry, Wiley-VCH Verlag GmbH & Co. KGaA, Weinheim, Germany, 2004.

[62] Kimoon Kim and James Ibers, Acta Cryst. 7 (1987) 2317–2319.

[63] N. Khan, Y. Farina, L.K. Mun, N.F. Rajab, N. Awang, J. Mol. Struct. 1076 (2014) 403–410.

[64] R. Yadav, M. Trivedi, R. Chauhan, R. Prasad, G. Kociok-Köhn, A. Kumar, Inorganica Chim. Acta 450 (2016) 57–68.

[65] N. Awang, I. Baba, B.M. Yamin, World Appl. Sci. J. 12 (2011) 630–635.

[66] N. Khan, Y. Farina, L.K. Mun, N.F. Rajab, N. Awang, Polyhedron 85 (2015) 754–760.

[67] D.C. Menezes, F.T. Vieira, G.M. de Lima, A.O. Porto, M.E. Cortés, J.D. Ardisson, T.E. Albrecht-Schmitt, Eur. J. Med. Chem. 40 (2005) 1277–1282.

[68] S. Shahzadi, S. Ali, J. Iran. Chem. Soc. 5 (2008) 16–28.

[69] A.N. Gupta, V. Kumar, V. Singh, A. Rajput, L.B. Prasad, M.G.B. Drew, N. Singh, J. Organomet. Chem. 787 (2015) 65–72.

[70] K.S. Siddiqi, S.A.A. Nami, Y. Chebude, J. Braz. Chem. Soc. 17 (2006) 107–112.

[71] J.O. Hill, S. Chirawongaram, J. Therm. Anal. 41 (1994) 511–518.

[72] A.S. Rozenberg, V.R. Stepanov, Rus. Chem. Bull. 45 (1996) 1336–1343.

[73] Damian C. Onwudiwe; Peter A. Ajibade, Asian J. Chem. 25 (2013) 10057–10061.

[74] V.T. Yilmaz, T.K. Yazicilar, H. Cesur, R. Ozkanca, F.Z. Maras, Synth. React. Inorg. Met. Chem. 33 (2003) 589–605.

[75] P.A. Ajibade, D.C. Onwudiwe, J. Mol. Struct. 1034 (2013) 249–256.

[76] A.C. Ekennia, D.C. Onwudiwe, A.A. Osowole, J. Sulfur Chem. 36 (2015) 96–104.

[77] J.O. Adeyemi, D.C. Onwudiwe, A.C. Ekennia, R.C. Uwaoma, E.C. Hosten, Inorganica Chim. Acta 477 (2018) 148–159.

[78] G.O. Siqueira, A.D.O. Porto, G.M. De Lima, T. Matencio, J. Organomet. Chem. 715 (2012) 48–53.

[79] D.C. Menezes, G.M. De Lima, A.O. Porto, C.L. Donnici, J.D. Ardisson, A.C. Doriguetto, J. Ellena, Polyhedron 23 (2004) 2103–2109.

[80] K. Ramasamy, V.L. Kuznetsov, K. Gopal, M.A. Malik, J. Raftery, P.P. Edwards, P. O'Brien, Chem. Mater. 25 (2013) 266–276.

[81] J. Gaur, S. Jain, S. Chand, N.K. Kaushik, 2014 (2014) 50–54.

[82] B.F. Ali, W.S. Al-Akramawi, K.H. Al-Obaidi, A.H. Al-Karboli, Thermochim. Acta 419 (2004) 39–43.

[83] B. Arul Prakasam, M. Lahtinen, A. Peuronen, M. Muruganandham, E. Kolehmainen, E. Haapaniemi, M. Sillanpää, Inorganica Chim. Acta 425 (2015) 239–246.

[84] A.C. Ekennia, D.C. Onwudiwe, A.A. Osowole, L.O. Olasunkanmi, E.E. Ebenso, J. Chem. 2016 (2016) 1–12.

[85] Y. Anjaneyulu, R.P. Rao, Synth. React. Inorg. Met. Chem. 16 (1986) 257–272.

[86] F. Javed, M. Sirajuddin, S. Ali, N. Khalid, M.N. Tahir, N.A. Shah, Z. Rasheed, M.R. Khan, Polyhedron 104 (2016) 80–90.

[87] W. Rehman, M.K. Baloch, A. Badshah, Eur. J. Med. Chem. 43 (2008) 2380–2385.

[88] P. Subbhankari Prasad Chakraborty, Pramanik, S. Roy, Int. Jounal Life Sci. Pharma Res. 2 (2012).

[89] S.M. Mamba, A.K. Mishra, B.B. Mamba, P.B. Njobeh, M.F. Dutton, E. Fosso-Kankeu, Spectrochim. Acta - Part A Mol. Biomol. Spectrosc. 77 (2010) 579–587.

[90] L.J. Ming, Med. Res. Rev. 23 (2003) 697–762.

[91] P.F. Salas, C. Herrmann, C. Orvig, Chem. Rev. 113 (2013) 3450–3492.

[92] N. Awang, N. Mokhtar, N.M. Zin, J. Chem. Pharm. Res. 7 (2015) 379–383.

[93] N. Bhalodia, V. Shukla, J. Adv. Pharm. Technol. Res. 2 (2011) 104.

[94] D.C. Menezes, F.T. Vieira, G.M. De Lima, J.L. Wardell, M.E. Cortés, M.P. Ferreira, M.A. Soares, A. Vilas Boas, Appl. Organomet. Chem. 22 (2008) 221–226.

[95] I.P. Ferreira, G.M. De Lima, E.B. Paniago, W.R. Rocha, J.A. Takahashi, C.B. Pinheiro, J.D. Ardisson, Polyhedron 79 (2014) 161–169.

[96] N. Awang, N.H. Zakri, N.M. Zain, J. Chem. Pharm. Res. 8 (2016) 862–866.

[97] R.A. Nash, Altern. Ther. Health Med. 11 (1999) 18–25.

[98] N. Farrell, Compr. Coord. Chem. II 11 (2012) 809–840.

[99] A.H. and A.A. Rafique S., Idrees M., Nasim A., Biotechnol. Mol. Biol. Rev. Vol. 5 (2010) 38–45.

[100] A.R. Anindiya Bagchi, Prosenjit Mukhergee, Int. J. Recent Adv. Pharm. Res. 5(3) (2015) 171–180.

[101] A. Alama, B. Tasso, F. Novelli, F. Sparatore, Drug Discov. Today 14 (2009) 500–508.

[102] M.J. Selwyn, in:, Organotin Compd. New Chem. Appl., 1976, pp. 204–226.

[103] K. Cain, D.E. Griffiths, Biochem. J. 162 (1977) 575–580.

[104] K. Cain, R.L. Hyams, D.E. Griffiths, FEBS Lett. 82 (1977) 23–28.

[105] L. Niu, Y. Li, Q. Li, Inorganica Chim. Acta 423 (2014) 2–13.

[106] C. Pellerito, L. Nagy, L. Pellerito, A. Szorcsik, J. Organomet. Chem. 691 (2006) 1733–1747.

[107] M.K. Amir, S. Khan, Zia-Ur-Rehman, A. Shah, I.S. Butler, Inorganica Chim. Acta 423 (2014) 14–25.

[108] S. Ali, Zia-Ur-Rehman, Muneeb-Ur-Rehman, I. Khan, S.N.A. Shah, R.F. Ali, A. Shah, A. Badshah, K. Akbar, F. Bélanger-Gariepy, J. Coord. Chem. 67 (2014) 3414–3430.

[109] G. Eng, X. Song, Q. Duong, D. Strickman, J. Glass, L. May, Appl. Organomet. Chem. 17 (2003) 218–225.

[110] S.K. Hadjikakou, N. Hadjiliadis, Coord. Chem. Rev. 253 (2009) 235–249.

[111] R. Yadav, M.K. Awasthi, A. Singh, G. Kociok-Köhn, M. Trivedi, R. Prasad, M. Shahid, A. Kumar, J. Mol. Struct. 1145 (2017) 197–203.

Chapter three

3.0 SYNTHESIS AND CHARACTERIZATION OF ORGANOTIN(IV) DITHIOCARBAMATE COMPLEXES

Chapter Summary

Novel organotin(IV) dithiocarbamate complexes have been synthesized by the reaction of six different derivatives of organotin(IV) chloride with various dithiocarbamate ligands prepared from both primary and secondary amines. The syntheses were mostly carried out *in-situ* in a one pot system except where stated otherwise. A general method used in the preparation of the entire complexes involved ethanol solution, due to the insolubility of the organotin salt in water. The complexation reaction proceeded via the replacement of the chloride ions of the organotin(IV) salts with the respective dithiocarbamate ligands. The resulting complexes were characterized using various spectroscopic techniques. The structures of some of the complexes were established by single crystal X-ray diffracton.

In this chapter, the complexes have been grouped into eight different sections based on the ligand type:

- Section one: complexes of *N*-methyl-*N*-phenyldithiocarbamate (L^1)
- Section two: complexes of *N*-ethyl-*N*-phenyldithiocarbamate (L^2)
- Section three: complexes of *N*-butyl-*N*-phenyldithiocarbamate (L^3)
- Section four: complexes of*N,N*-methylphenyl-*N,N*-ethylphenyldithiocarbamate (L^1L^2)
- Section five: complexes of *N,N*-alkylphenyl-*N,N*-butylphenyldithiocarbamate (L^1L^3) and (L^2 L^3) (alkyl = CH_3, C_2H_5)
- Section six: complexes of *N,N*-diallyldithiocarbamate (L^4)
- Section seven: complexes of *p*-alkyl phenyldithiocarbamate (alkyl = CH_3, L^5; C_2H_5, L^6)
- Section eight: complexes of benzyl dithiocarbamate (L^7)

3.1. Materials

All Chemicals and solvents used in this work were purchased from Sigma-Aldrich chemical Co, ACE chemicals or Merck, and were of high purity. These chemicals were used as received without further purification. They include *N*-methylaniline, *N*-ethylaniline, *N*-butylaniline,*N,N*-diallylamine, *p*-methylaniline, *p*-ethylaniline, benzylamine, ammonium hydroxide, carbon disulfide, methyltin(IV) trichloride, dimethyltin(IV) dichloride, butyltin(IV) trichloride, dibutyltin(IV) dichloride, phenyltin(IV) trichloride, diphenyltin(IV) dichloride, tetrahydrofuran (THF), ethanol, acetone, diethylether, chloroform, dichloromethane, methanol, and toluene.

3.2. Physical Measurements

Melting point measurement was carried out using Stuart melting point smp10. C, H, N, and S percentages were determined by Elementar, Vario EL Cube, set up for CHNS analysis. Infrared spectra were recorded in the range of 4000–300 cm^{-1} on a Bruker alpha-P FTIR spectrophotometer. The ^{1}H and ^{13}C Nuclear magnetic resonance (NMR) spectra were recorded on a 600 MHz Bruker Avance III NMR spectrometers at room temperature in chloroform. For the ^{1}H NMR, multiplicities of signals are given as: (s = singlet, d = doublet, t = triplet, q = quartet, m= multiplet). ^{119}Sn NMR was recorded on a Bruker Ascend 500MHz Avance III HD equipped with BBO Probe, and the chemical shifts were measured with reference to $(CH_3)_4Sn$ as an external standard. Thermogravimetric analysis was performed using SDTQ 600 Thermal analyser. Known masses of the samples were loaded into an alumina cup and respective weight losses (as a function of temperature) were recorded. The experiment was carried out under N_2 flow, and a heating rate of 10 °C/min was maintained from ambient temperature to 700 °C.

3.2.1. X-ray Crystallography

The single crystal analysis of some of the complexes was carried out at 200 K using a Bruker Kappa Apex II diffractometer with monochromated Mo Kα radiation (λ = 0.71073 Å). Data collection was done using APEX2 and SAINT [1] for cell refinement and data reduction. The structure was resolved and refined by least-squares procedures using SHELXT–2014 [2] and SHELXL-2016 [3] with SHELXLE as a graphical interface respectively. Numerical method using SADABS [1] was used for data correction of absorption effect. All non-hydrogen atoms were anisotropically resolved. Carbon-bound H atoms were placed in calculated positions and

were included in the refinement in the riding model approximation, with U_{iso}(H) set to 1.2U_{eq}(C). The H atoms of the alkylgroups were allowed to rotate with a fixed angle around the C---C bonds to best fit the experimental electron density (HFIX 137 in the SHELX program suite (Sheldrick, 2015)), with U_{iso} (H) set to 1.5U_{eq}(C).

3.3. Complexes of Organotin(IV) and *N*-Methyl-*N*-Phenyldithiocarbamate

3.3.1. Synthesis of ammonium *N*-methyl-*N*-phenyldithiocarbamate (L^1)

Ammonium *N*-methyl-*N*-phenyldithiocarbamate (L^1)was prepared following a similar procedure described previously with slight modification[4]. *N*-methylaniline (1.08 mL, 0.01 mol) was introduced into a round-bottomed flask in an ice bath, followed by the addition of ammonium hydroxide solution (3 mL, 0.01 mol) with continuous stirring for approximately 5 min. To this mixture, carbon disulfide (0.60 mL, 0.01 mol) was added dropwise and the solution was stirred for 5 h, resulting into a faint yellowish precipitate as product.

3.3.2. Synthesis of the organotin(IV) *N*-methyl-*N*-phenyldithiocarbamate complexes [$RSnCl(L^1)_2$ and $R_2Sn(L^1)_2$ (R = CH_3, C_4H_9, C_6H_5)]

About 20 mL ethanol solution of the respective organotin(IV) chloride ($RSnCl_3$ and R_2SnCl_2) was reacted with 20 mL ethanol solution of the ligand in 1: 2 mole ratio (organotin:dtc) in ice for 2 h. The resultant white precipitates were filtered, washed with ethanol and dried under vacuum.

(1) [$(C_4H_9)ClSn(L^1)_2$]: Yield: 2.75 g (78.0%); M.pt.: 190 - 192 °C; Selected FTIR, υ (cm^{-1}): 1490 (C-N), 971, 962 (C=S), 2955 (aliphatic C-H), 3048 (aromatic C-H), 552 (Sn-C), 403 (Sn-S); ^{1}H NMR ($CDCl_3$): δ ppm = 7.39 - 7.19 (m, 10H, N-$C_6\underline{H}_5$), 3.67 (s, 6H, N–$C\underline{H}_3$), 0.97 (t, 3H, $CH_2CH_2CH_2C\underline{H}_3$), 1.43 (m, 2H, $CH_2CH_2C\underline{H}_2CH_3$), 1.99 (m, 2H, $CH_2C\underline{H}_2CH_2CH_3$), 2.38 (t, 2H, $C\underline{H}_2CH_2CH_2CH_3$); ^{13}C NMR ($CDCl_3$) δ ppm = 147.3, 129.4, 128.1, 125.8 (-$\underline{C}_6H_5$), 47.4 (N-$\underline{C}H_3$), 205.3 (-CS_2), 13.9 ($CH_2CH_2CH_2\underline{C}H_3$), 25.3 ($CH_2CH_2\underline{C}H_2CH_3$), 29.3 ($CH_2\underline{C}H_2CH_2CH_3$), 30.9 ($\underline{C}H_2CH_2CH_2CH_3$); ^{119}Sn NMR ($CDCl_3$): δ ppm = -203.45;
$C_{20}H_{25}ClN_2S_4Sn$ (575.96): C, 41.71; H, 4.38; N, 4.86; S, 22.27. Found: C, 40.91; H, 4.08; N, 4.99; S, 22.57.

(2) $[(C_6H_5)ClSn(L^1)_2]$: Yield: 3.10 g (84%); M.pt.: 179 – 181 °C; Selected FTIR, υ (cm^{-1}): 1491 (C-N), 1002, 996 (C=S), 2806 (aliphatic C-H), 3039 (aromatic C-H), 553 (Sn-C), 448 (Sn-S); ^1H NMR ($CDCl_3$) δ ppm = 7.40 - 7.12 (m, 10H, -$C_6\underline{H}_5$), 3.52 (s, 6H, N–$C\underline{H}_3$), 7.99 - 7.56 (m, 5, Sn-$C_6\underline{H}_5$); ^{13}C NMR ($CDCl_3$) δ = 142.34, 135.09, 129.11, 128.07 (N-$\underline{C}_6H_5$), 50.01 (-CH_3), 200.03 (-CS_2), 135.09- 122.12 (Sn-$\underline{C}_6H_5$) ppm; ^{119}Sn NMR ($CDCl_3$): δ ppm = -286.57;
$C_{22}H_{21}ClN_2S_4Sn$ (595.93): C, 44.35; H, 3.55; N, 4.70; S, 21.53 Found: C, 43.95; H, 4.01; N, 4.91; S, 22.03. .

(3) $[(CH_3)_2Sn(L^1)_2]$: Single crystal for X-ray analysis was obtained in dichloromethane-ethanol solution (3:1). Yield: 2.79 g (85%); M.pt.: 121 – 122 °C; Selected FTIR, υ (cm^{-1}): 1488 (C-N), 1002 (C=S), 2912 (aliphatic C-H), 3005 (aromatic C-H), 555 (Sn-C), 420 (Sn-S); ^1H NMR ($CDCl_3$) δ ppm = 7.31 - 7.22 (m, 10H, N-$C_6\underline{H}_5$), 3.67 (s, 6H, N–$C\underline{H}_3$), 1.51 (s, 6H, Sn-$C\underline{H}_3$); ^{13}C NMR ($CDCl_3$) δ ppm = 146.70, 129.49, 128.30, 125.95 (-$\underline{C}_6H_5$), 46.49 (N-$\underline{C}H_3$), 202.82 (-$\underline{C}S_2$), 14.04 (Sn-$\underline{C}H_3$); ^{119}Sn NMR ($CDCl_3$): δ ppm = -312.93;
$C_{18}H_{22}N_2S_4Sn$ (513.97): C, 42.11; H, 4.32; N, 5.46; S, 24.98. Found: C, 41.21; H, 4.92; N, 5.56; S, 23.48.

(4) $[(C_4H_9)_2Sn(L^1)_2]$: Single crystal for X-ray analysis was obtained in dichloromethane-ethanol solution (4:1).Yield: 2.70 g (73%); M.pt.: 130 – 132 °C; Selected FTIR, υ (cm^{-1}): 1489 (C-N), 963 (C=S), 2914 (aliphatic C-H), 3036 (aromatic C-H), 554 (Sn-C), 407 (Sn-S); ^1H NMR ($CDCl_3$) δ ppm = 7.39 - 7.19 (m, 10, N-C_6H_5), 3.68 (s, 6H, N–CH_3), 0.95 (t, 6H, $CH_2CH_2CH_2C\underline{H}_3$), 1.46 (m, 4H, $CH_2CH_2C\underline{H}_2CH_3$), 1.93 (m, 4H, $CH_2C\underline{H}_2CH_2CH_3$), 2.04 (t, 4H, $C\underline{H}_2CH_2CH_2CH_3$); ^{13}C NMR ($CDCl_3$) δ ppm = 146.91, 129.46, 128.18, 126.01 (N-$\underline{C}_6H_5$), 46.46 (N-$\underline{C}H_3$), 203.80 (-$\underline{C}S_2$), 13.86 ($CH_2CH_2CH_2\underline{C}H_3$), 26.49 ($CH_2CH_2\underline{C}H_2CH_3$), 28.66 ($CH_2\underline{C}H_2CH_2CH_3$), 33.39 ($\underline{C}H_2CH_2CH_2CH_3$); ^{119}Sn NMR ($CDCl_3$): δ ppm = -268.07;
$C_{24}H_{34}N_2S_4Sn$ (598.1): C, 48.25; H, 5.74; N, 4.69; S, 21.46. Found: C, 48.15; H, 5.66; N, 4.21; S, 20.96.

(5) $[(C_6H_5)_2Sn(L^1)_2]$: Yield: 2.65 g (68%), M.pt.: 183 – 185 °C; Selected FTIR, υ (cm^{-1}): 1482 (C-N), 996 (C=S), 2987 (aliphatic C-H), 3055 (aromatic C-H), 553 (Sn-C), 418 (Sn-S); ^1H NMR ($CDCl_3$) δ ppm = 7.42 - 7.11 (m, 10H, N-$C_6\underline{H}_5$), 7.98-7.72 (m, 10H, Sn-$C_6\underline{H}_5$), 3.59 (s, 6H, N–$C\underline{H}_3$); ^{13}C NMR ($CDCl_3$) δ ppm = 146.97, 129.50, 128.64, 125.76 (N-$\underline{C}_6H_5$), 47.29 (N-CH_3),

202.06(-CS_2), 135.80 - 128.33, (Sn-$\underline{C}_6H_5$); ^{119}Sn NMR ($CDCl_3$): δ ppm = -312.04; $C_{28}H_{26}N_2S_4Sn$ (638.0): C, 52.76; H, 4.11; N, 4.39; S, 20.12. Found: C, 51.96; H, 3.98; N, 4.01; S, 21.01.

3.4. Results and Discussion on The Organotin(IV) *N*-methyl-*N*-phenyldithiocarbamate Complexes

3.4.1. Synthesis of organotin(IV) *N*-methyl-*N*-phenyldithiocarbamate complexes

The ligand ammonium *N*-methyl-*N*-phenyldithiocarbamate [L^1] was prepared by equimolar amount of *N*-methylaniline , carbon disulfide and ammonium hydroxide. This gave a pale yellow precipitate which was washed severally and filtered in cold ethanol to remove unwanted materials. The complex synthesis then proceeded by the by the replacement of the equivalent number of chloride ions of the organotin(IV) chloride by the dithiocarbamate ligand, Scheme 3.1. The organotin(IV) complexes in Figure 3.1 were obtained as white/faint-yellow, air stable and crystalline solids with melting points ranging from 121 - 192 °C.

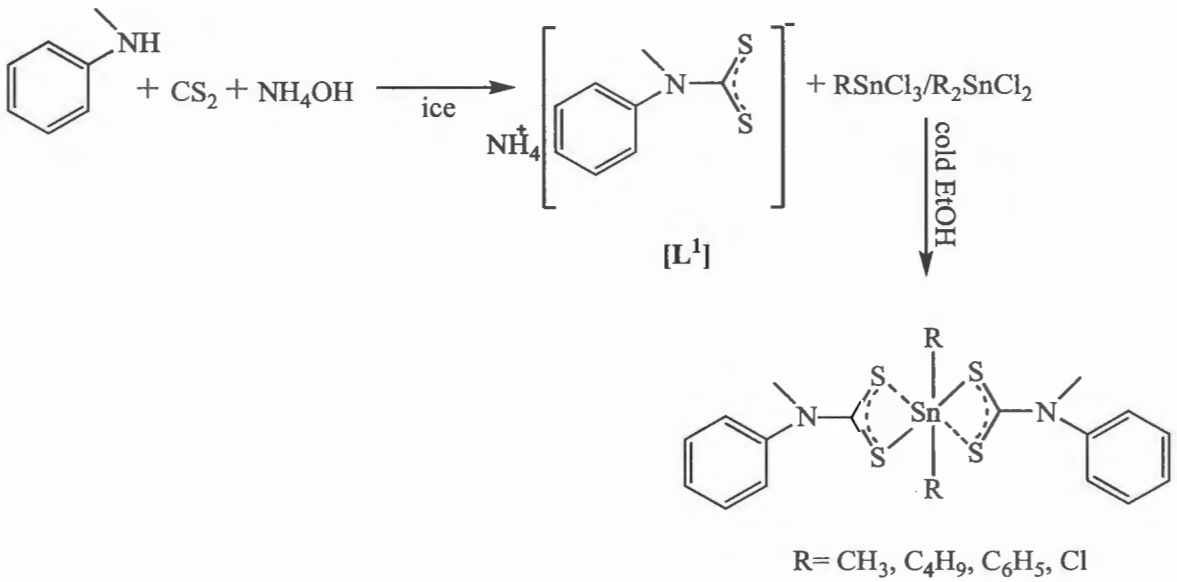

R= CH_3, C_4H_9, C_6H_5, Cl

Scheme 3.1: Synthesis of organotin(IV) *N*-methyl-*N*-phenyl dithiocarbamate complexes, [$RSnCl(L^1)_2$ and $R_2Sn(L^1)_2$ (R = CH_3, C_4H_9, C_6H_5)].

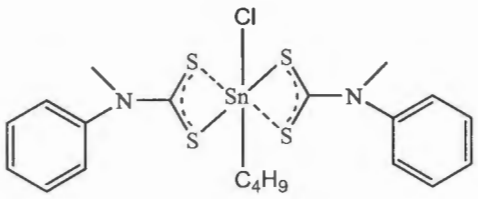

(1) $[(C_4H_9)ClSn(L^1)_2]$

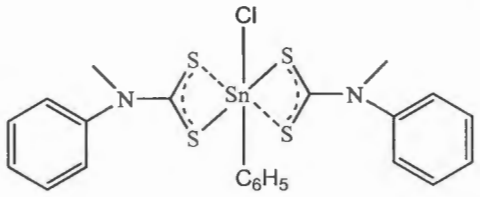

(2) $[(C_6H_5)ClSn(L^1)_2]$

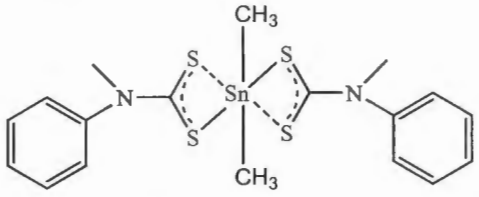

(3) $[(CH_3)_2Sn(L^1)_2]$

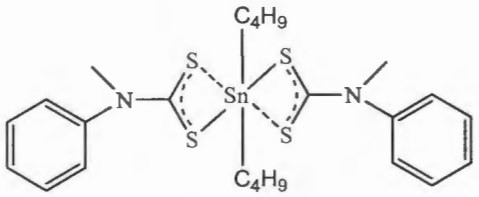

(4) $[(C_4H_9)_2Sn(L^1)_2]$

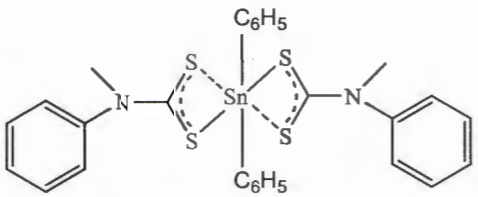

(5) $[(C_6H_5)_2Sn(L^1)_2]$

Figure 3.1: List of complexes obtained from the reaction scheme 3.1.

3.4.2. Infrared spectroscopic studies of organotin(IV)*N*-methyl-*N*-phenyldithiocarbamate complexes

The IR spectra of the organotin(IV) dithiocarbamate complexes, offered useful information about the coordination mode and structure of the dithiocarbamate. The assignment of the spectral bands was carried out based on established peaks of similar structures in literature [5,6]. The C-N vibrational frequency of the thioureide band was observed in each of the complexes in the range 1491 – 1482 cm^{-1}. The coordination of the ligand to the organotin moieties resulted in the bands occurring at higher frequencies, thus prompting a double bond character in the thioureide bond (N–CSS) due to the delocalization of electrons towards the central Sn atom[7]. The vibrational

frequency of C-N in the spectra of the complexes with a chloride ion within their molecule possesses slightly higher frequencies than others with no chlorine ion. This could be due to the electron withdrawing abilities of the chloride ion, which increases the positive charge on nitrogen atom in the thioureide bond [8,9]. The C–S vibration bands were observed as a single peak in the region 960 – 1010 cm^{-1} in complexes **3**, **4** and **5**, suggesting a bidentate mode; but as a splitted peak (in this region) for complexes **1** and **2** indicating an anisodentate coordination [8]. The vibrational bands in the region 448 – 403 cm^{-1} in the spectra of all the complexes were attributed to the presence of Sn-S, thus indicating the coordination of the sulfur atoms of the dithiocarbamate ligands to the central tin atom of the organotin [5].

3.4.3. Nuclear magnetic resonance studies of organotin(IV)*N*-methyl-*N*-phenyldithiocarbamate complexes

The ^{1}H NMR of the complexes gave two singlet signals in the range 3.68 – 3.52 ppm, assigned to the methyl group on the nitrogen atom of the dtc. The multiplets downfield around 7.42 – 7.11 ppm are due to the aromatic protons in the dtc moiety [10]. The signal of the protons of the CH_3 group attached to the Sn center in complex 3 was observed as a singlet upfield at 1.51 ppm [11]. The chemical shifts for the protons of the butyl groups in complexes **1** and **4** appeared in the range 2.38 – 0.95 ppm [10,12]. This decrease in the resonant values along the chain is due to the shielding of protons of the butyl group attached to the Sn metal centre which weakens along the carbon chain through the carbon nuclei [13]. The aromatic protons of the phenyl groups of the organotin moiety resonated in the range 7.99-7.52 ppm for complexes **2** and **5** [12,14].

The ^{13}C NMR spectra of the complexes gave signals due to the quaternary carbon ($-CS_2$) of the dtc moiety in the range 205.29 – 200.03 ppm, and the carbon atoms of the $-CH_3$ group attached to the nitrogen atom appeared in the range 50.01 – 46.46 ppm [15]. The somewhat downfield shift of the signals of the thioureide carbon is due to electron distribution over the bond existing in the $-CNS_2Sn$ region [16]. The somewhat upfield signal value of the carbon atom of the CH_3 group is attributed to its bonding to the electron rich nitrogen. The signals for the carbon atoms of the phenyl moiety resonated between 147.33 and 125.76 ppm in all the complexes [16]. In complex **3**, the carbon signals due to the methyl group of the organotin moiety resonated around 14.04 ppm. The resonant peaks due to the butyl groups in complexes **1** and **4** appeared in the

range 33.39 – 13.86 ppm [13], while the peaks due to the phenyl group in complexes **2** and **5** resonated between 135.08 and 122.12 ppm [15].

In ^{119}Sn NMR, certain chemical shift ranges have been established for different coordination and they give insight into the geometry of the compounds. In tetra-, penta-, or hexa-coordinated organotin complexes, the chemical shift ranges which, respectively, corresponds to this geometry includes: δ = 200 to -60, δ = -90 to -190 and δ = -210 to -400 ppm [17]. They are dependent on factors such as electronegativity of the ligand, temperature and concentration employed in the experiment. From the observed chemical shifts values of the complexes, hexa-coordinated geometry around the Sn metal is suggested in all the complexes.

3.4.4. X-ray crystallography for complexes 3 and 4

Information about the crystal structure and refinement parameters has been summarized in Table 3.1. Useful bond angles and lengths needed for the description and prediction of the geometry are presented in Table 3.2. The ORTEP plots showing the structure and numbering of the complexes and their respective crystal packing are shown in Figures 3.2 and 3.3.

3.4.4.1. Structural description of dimethyltin(IV) *N*-methyl-*N*-phenyldithiocarbamate complex (3)

Two groups of *N*-methyl-*N*-phenyldithiocarbamate ligand bond through the available sulfur atoms to the opposite side of the Sn atom in a bidentate chelating fashion, resulting in a six coordinate geometry around the Sn center as shown in Figure 3.2a. This complex **(3)** is monomeric, possessing four molecules per unit cell as shown in the packing diagram in Figure 3.2b. The Sn-S bond distances are Sn1-S11 [2.5199(7)], Sn1-S12 [2.9785(6)], Sn1-S21 [2.5259(5)] and Sn1-S22 [2.9479(7)]. The observed Sn-S bond distances showed that Sn1-S12 and Sn1-S22 are longer than the Sn1-S11 and Sn1-S21, hence resulting into an asymmetric molecule [18] with bonds which are anisobidentate in nature [19]. This anisobidentate bond also emerged due to the slight opening of the C-Sn-C bond angle (142.06) towards 180° moving away from 109°. If/when the C-Sn-C bond angle becomes linear, the nature of the bond becomes isobidentate [20]. The stronger Sn-S bonds have shorter bond lengths with an acute angle cis to each other, and subtending at 83.80(2)°, while the longer Sn-S bonds are weak bonds possessing

an angle of 146.16(2)° which is less from being co-linear with each other [6]. Both types of Sn-S bond lengths (the longer and the shorter) from the observed interatomic distances are longer than the expected sum of the covalent radii of a typical Sn-S bonds (2.42 Å), but well below the expected van der Wall radii (3.97Å) [18]. The increased coordination around the Sn atom has resulted in a significant change from the bite angle of the chelating dithiocarbamate ligand which in turn results in the different bond distances observed [18]. The observed C-S bond distances (S11-C11 [1.7419(16)], S12-C11 [1.6861(16)], S21-C21 [1.7432(16)], S22-C21 [1.6876(16)]) with an average value of 1.7147 (16) is shorter compared to a typical C-S bond (1.81 Å). This is indicative of a partial double bond character of the C-S bond characteristic of the dithiocarbamate ligands [21]. The bond between Sn and the attached methyl groups also significantly contribute to the observed distortion in the octahedral geometry for the complex. These -CH_3 groups (C3-Sn1-C4) are attached to tin axially with a bond angle of 142.06(8)°, showing a deviation from a cis-trans pathway of the C–Sn–C bond which is expected at 134° [18].The inter-atomic bond angles of the Sn-C bond (from Table 2) show the association between the Sn-C and Sn-S bonds. The bond angles S12-Sn1-C3 [83.40(60)], S12-Sn1-C4 [84.79(5)], S22-Sn1-C3 [86.12(6)], S22-Sn1-C4 [83.99(5)] reveals the bending of the Sn-C bonds towards the Sn-S bond with a higher distance. This was attributed to electronic (repulsion in the metal center and the bonding electron pair of the S atoms) and steric reasons [22]. The expected octahedral geometry observed due to the six coordination is distorted around the tin centre due to unequal bond distances and the asymmetric nature of the dithiocarbamate ligands. Hence, this geometry is described as skew trapezoidal-bipyramidal [7].

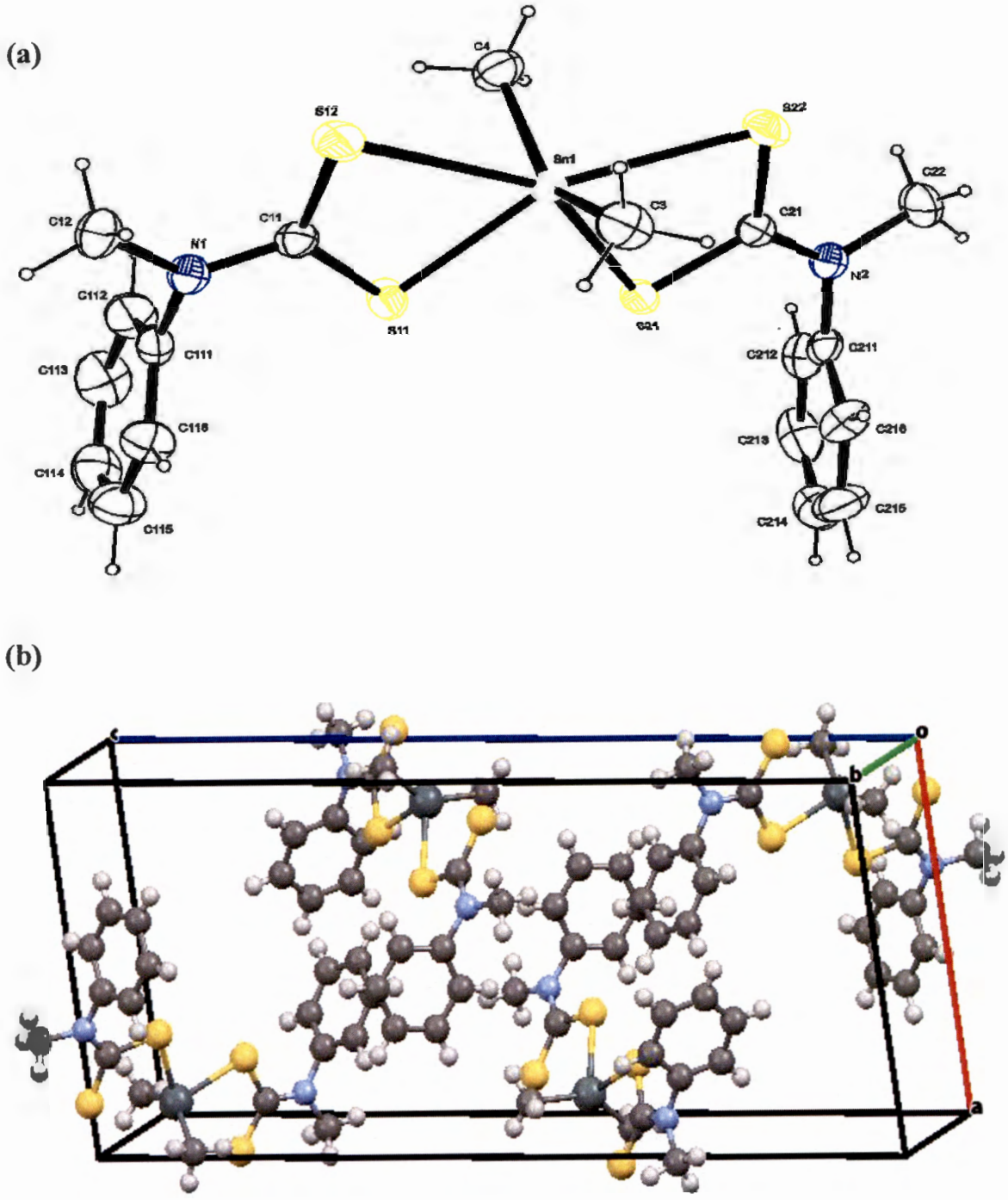

Figure 3.2: (a) Structure of dimethyltin(IV) *N*-methyl-*N*-phenyldithiocarbamate complex (**3**) drawn at 50% probability level displacement ellipsoids, and **(b)** the crystal packing viewed along the best axis.

3.4.4.2. Structural description of dibutyltin(IV)*N*-methyl-*N*-phenyldithiocarbamate complex (**4**)

The structure from the ORTEP plot in Figure 3.3a shows the coordination of dithiocarbamate ligands through sulfur atoms to the metal center in a monodentate fashion at the adjacent sides of the complex. The dibutyltin(IV) complex (**4**) is triclinic with two molecules per unit cell as shown in the crystal packing diagram presented in Figure 3.3b. The Sn-S bond distances observed are Sn1-S11 [2.5179(8)], Sn1-S12 [3.0275(8)], Sn1-S21 [2.507(7)] and Sn1-S22 [3.0465(9)]. These distances are similar to complex **3**, and results in the complex being asymmetrical. The longer bond could be regarded as a real bond because the length falls significantly below the sum of the van der Wall radii (3.97Å) [18]. The strong steric interaction of the two bulky butyl moiety attached to the Sn center might be responsible for this weak bond because it reduces the propensity for the coordination of the second pendant S atom [23]. The bulky size of the alkyl substituent and the phenyl ring may also play a role in preventing the Sn-S formation. These longer/weak bonds creates an anisobidentate mode of binding instead of a bidentate mode of binding with the Sn center and are less from being co-linear, possessing a bond angle of 148.29(2) cis to each other. This anisobidenate bonding is also supported by the slight opening of the C-Sn-C bond angle (137.7)°. The stronger Sn-S bonds are those with shorter bond distances with an acute angle cis to each other and subtending at 83.10(2)°[6]. The bite angles of the sulfur atoms to the tin center results in a very significant distortion away from the expected octahedral geometry. The average value of the C-S bond (Table 3.2) was 1.715 (3)Å, which is shorter compared to a typical C-S bond (1.81 Å). This shows the partial double bond character often attributed to dithiocarbamate complexes [21]. The C–Sn–C bond which is expected at 134° for the alkyl (C31-Sn1-C41) groups attached to the tin center was found axially at 137.7(6)°, showing a slight deviation from the cis-trans pathway of this bond [20]. The bond angles S12-Sn1-C31 [83.13(7)], S12-Sn1-C41 [87.4(5)], S22-Sn1-C31 [82.69(7)], S22-Sn1-C41 [84.30(7)] reveals the bending of the Sn-C bonds towards the Sn-S bond with a longer distance which is probably due to the bulkiness of this alky substituent. The distortion observed in this complex has been attributed to the several coordinations around the tin metal which, in turn, resulted in changes in the interatomic distances and angles [21]. Therefore, the geometry around the Sn atom in this complex (**4**) is best described as distorted skew trapezoidal-bipyramidal owing to the closeness of the double bonded sulfur atom, and this is similar to what has been reported for dibutyltin complexes [7,23].

(a)

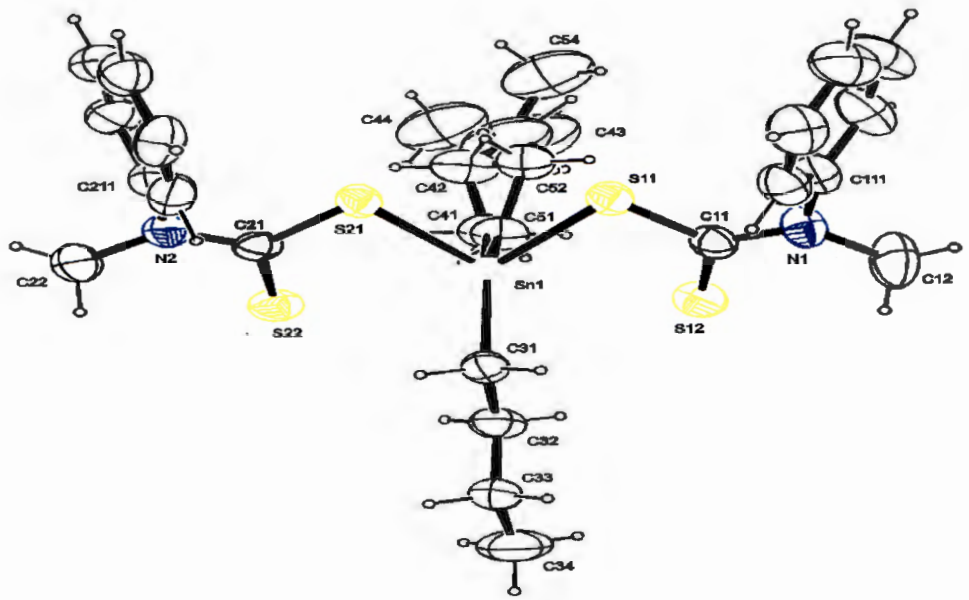

(b)

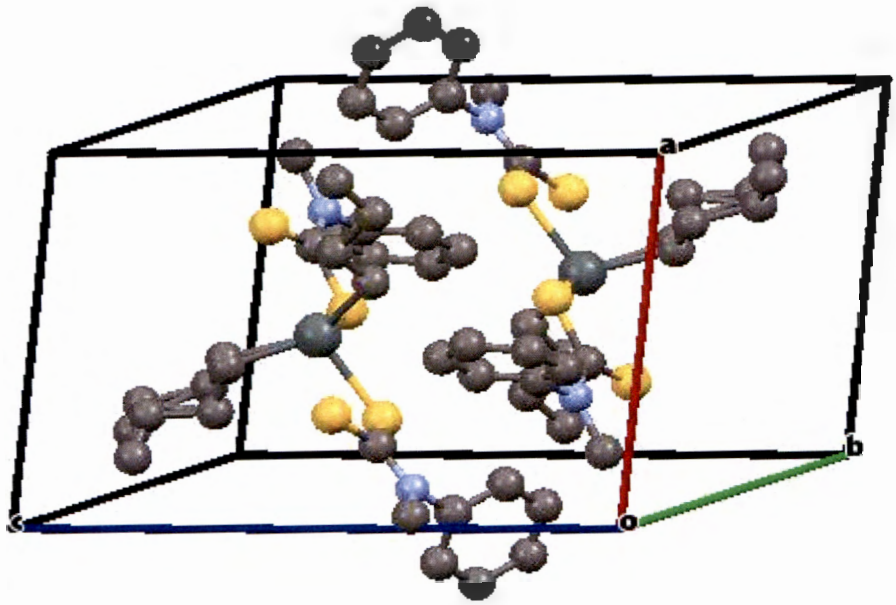

Figure 3.3: **(a)** Structure of dibutyltin(IV) *N*-methyl-*N*-phenyldithiocarbamate**(4)** drawn at 50% probability level displacement ellipsoids, and **(b)** the crystal packing viewed along the best axis (hydrogen atoms removed for clarity).

Table 3.1: Crystallographic data and refinement parameters for complexes **3** and **4**

Parameters	**Complex 3**	**Complex 4**
Empirical formula	C_{18} H_{22} N_2 S_4 Sn	C_{24} H_{34} N_2 S_4 Sn
Formula weight	513.33	597.48
Crystal size (mm)	0.22 x 0.34 x 0.52	0.22 x 0.34 x 0.52
Crystal system	monoclinic	triclinic
Crystal habit	colorless needle	colorless needle
Space group	P21/c	P-1
a (Å)	11.1556(6)	10.9795(5)
b (Å)	7.7350(4)	11.8505(5)
c (Å)	25.9770(12)	13.4456(6)
β (°)	96.257(2)	94.122(2)
U (Å^3)	2228.2(2)	1424.39(12)
Z	4	2
*D*calc (g cm^{-3})	1.530	1.393
F(000)	1032	612
θ range (°)	1.8 - 28.3	1.7 - 28.3
Index range	-14:14;-10:9;-33:34	-14:14;-15:15;-17: 17
Total, unique reflections	91346,5549,	48933,7058
Observed reflections *I*> 2σ(*I*)	5128	6130
Number of parameters refined	230	296
Final *R*, w*R2*	0.0186, 0.0441	0.0279, 0.0740
Goodness-of-fit (GOF)	0.00	0.00

Table 3.2: Selected interatomic distances and angles for complexes **3** and **4**

Complex 3		**Complex 4**	
Bond distances (Å)		**Bond distances (Å)**	
Sn1-S11	2.5199(7)	Sn1-S11	2.5179(8)
Sn1-S12	2.9785(6)	Sn1-S12	3.0275(8)
Sn1-S21	2.5259(5)	Sn1-S21	2.5073(7)
Sn1-S22	2.9479(7)	Sn1-S22	3.0465(9)
Sn1-C3	2.121(2)	Sn1-C31	2.137(2)
Sn1-C4	2.1193(17)	Sn1-C41	2.16(2)
S11-C11	1.7419(16)	S11-C11	1.741(2)
S12-C11	1.6861(16)	S12-C11	1.685(3)
S21-C21	1.7432(16)	S21-C21	1.745(3)
S22-C21	1.6876(16)	S22-C21	1.690(3)
N1-C11	1.337(2)	N1-C11	1.339(4)
N1-C12	1.466(2)	N1-C12	1.475(5)
N1-C111	1.444(2)	N1-C111	1.449(4)
N2-C21	1.335(2)	N2-C21	1.342(3)
N2-C22	1.470(2)	N2-C22	1.465(4)
N2-C211	1.440(2)	N2-C211	1.439(3)
Bond angles (°)		**Bond angles (°)**	
S11-Sn1-S12	65.11(2)	S11-Sn1-S12	64.19(2)
S11-Sn1-S21	83.80(2)	S11-Sn1-S21	83.10(2)
S11-Sn1-S22	148.62(2)	S11-Sn1-S22	147.29(2)
S11-Sn1-C3	105.71(6)	S11-Sn1-C31	105.14(7)
S11-Sn1-C4	101.61(5)	S11-Sn1-C41	107.4(7)
S12-Sn1-S21	148.49(2)	S12-Sn1-S21	147.27(3)
S12-Sn1-S22	146.16(2)	S12-Sn1-S22	148.29(2)
S12-Sn1-C3	83.40(6	S12-Sn1-C31	83.13(7)
S12-Sn1-C4	84.79(5)	S12-Sn1-C41	87.4(6)
S21-Sn1-S22	65.24(2)	S21-Sn1-S22	64.28(2)
S21-Sn1-C3	101.16(6)	S21-Sn1-C31	105.65(7)
S21-Sn1-C4	107.56(6)	S21-Sn1-C41	104.4(6)
S22-Sn1-C3	86.12(6)	S22-Sn1-C31	82.69(7)
S22-Sn1-C4	83.99(5)	S22-Sn1-C41	84.3(7)
C3-Sn1-C4	142.06(8)	C31-Sn1-C41	137.7(6)
Sn1-S11-C11	93.80(5)	Sn1-S11-C11	95.04(9)
Sn1-S12-C11	79.97(5)	Sn1-S12-C11	79.47(8)
Sn1-S21-C21	93.65(6)	Sn1-S21-C21	95.43(8)
Sn1-S22-C21	80.99(6)	Sn1-S22-C21	78.93(9)
C11-N1-C12	121.45(14)	C11-N1-C12	120.8(2)
C11-N1-C111	121.13(13)	C11-N1-C111	121.9(2)
C12-N1-C111	117.27(13)	C12-N1-C111	117.2(2)
C21-N2-C22	121.42(15)	C21-N2-C22	121.8(2)
C21-N2-C211	121.01(13)	C21-N2-C211	121.3(2)
C22-N2-C211	117.49(14)	C22-N2-C211	116.9(2)
S11-C11-S12	121.03(9)	S11-C11-S12	120.67(15)
S11-C11-N1	116.90(11)	S11-C11-N1	117.25(19)
S12-C11-N1	122.06(12)	S12-C11-N1	122.08(19)
S21-C21-S22	120.05(9)	S21-C21-S22	120.96(14)
S21-C21-N2	117.51(12)	S21-C21-N2	116.67(19)
S22-C21-N2	122.42(12)	S22-C21-N2	122.4(2)
Symmetry element i: -X, 1/2+Y, 1/2-Z			

3.4.5. **Thermogravimetric Analysis (TGA) of organotin(IV)*N*-methyl-*N*-phenyldithiocarbamate complexes (1 – 5)**

The Thermogravimetric analysis of the complexes carried out under nitrogen presented two types of decomposition patterns as shown in Figures 3.4 – 3.8, and the data obtained are summarized in Table 3.3. Complexes **1**, **2**, **4** and **5** gave two-step decomposition, while complex 3 gave a single-step decomposition. The differential thermogravimetric graph (DTG) for complexes **4** and **5** showed melting points at 129 and 187 °C respectively, as observed in Figures 3.7 and 3.8. The first step decomposition for complexes **1**, **2**, **4** and **5** occurred in the temperature ranges 98 – 144, 77 – 161, 160 – 399 and 116 – 192 °C respectively. This loss in mass was found to be 3.30, 2.50, 2.50 and 2.56% of the respective starting masses of complexes **1**, **2**, **4**, and **5**. The mass losses are in agreement with the calculated estimations of the mass of $-CH_3$ group in complexes (1) 2.72%, (2) 2.50%, (4) 2.50% and (5) 2.36%. The final step for the complexes gave decompositions in the range 193 – 290, 203 – 427, 206 – 373, 249 – 325°C respectively for complexes **1**, **2**, **4**, and **5**. The mass of the final residue found for these complexes were 26.03, 25.70, 23.90 and 22.18% of the respective starting masses, and were in agreement with the calculated value of the SnS residue in each case (complex (1) 24.84%, (2) 25.70%, (4) 23.90% and (5) 23.46%). In complex **3**, the decomposition occurred as a single step in the temperature range of 160 – 399 °C, to give a residue which was 28.8% of the starting mass. This was found to be in good agreement with the estimated theoretical mass of SnS (28.8%).

From the observed data in Table 3.3, there are similarities in the decomposition pattern of these complexes except complex **3**. However, all the complexes gave tin sulfide as the final residue, showing their potential as precursor for SnS nanoparticles. The different thermal decomposition observed for complex **3** shows the likely variation in the decomposition pattern of structurally related organotin(IV) dithiocarbamate complexes[24].

Generally, a relationship between the decompositions of the complexes and the interatomic distances can be deduced. It is possible that the decompositions occurred on the side with the longest/weakest Sn–S bond due to a weak force of attraction. Furthermore, amongst the synthesized precusors, complex **2** gave a more stable thermal behavior as regards to the structural analogue of this group of complexes with its final decomposition terminating at 427 °C. Thus, the pyrolysis of this group of compounds was achieved in the temperature ranges which correspond to the formation of thermally stable products, between 190 and 373 °C.

Table 3.3: Thermal analysis data of the complex **1-5**

Complexes:	**1**	**2**	**3**	**4**	**5**
Temp range of decomp. (°C):					
First stage Second stage	98 – 143 193 – 290	77 – 161 203 – 427	160 – 399 ———	116 – 192 206 - 373	108 – 154 249 – 325
DTG peak T(°C):					
First stage Second stage	137 247	113 399	304	185	138 315
Melting point:	———	———	———	129	186
Products Obtained:					
First decomp. Second decomp.	$[(C_6H_5)_2(CH_3)(CN)_2S_4]ClSn(C_4H_9)$ SnS	$[(C_6H_5)_2(CH_3)(CN)_2S_4]ClSn(C_6H_5)$ SnS	SnS ———	$[(C_6H_5)_2(CH_3)(CN)_2S_4]Sn(C_4H_9)_2$ SnS	$[(C_6H_5)_2(CH_3)(CN)_2S_4]Sn(C_6H_5)_2$ SnS
Mass of residue (mg) Found (Calc):					
First stage Second stage	4.08 (4.18) 1.10 (1.05)	16.60 (16.) 4.37 (4.37)	3.16 (3.16) ———	16.00 (16.01) 4.00 (4.05)	9.07 (9.05) 2.06 (2.18)

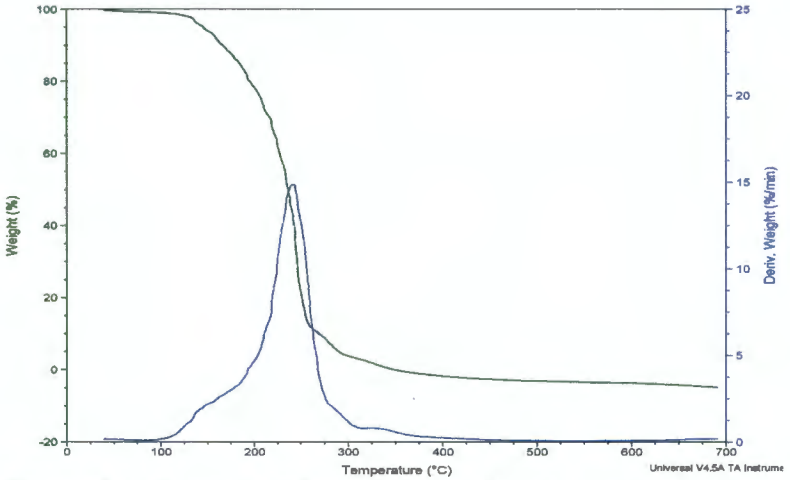

Figure 3.4: TG and DTG curves (with heating rate 10 °C/min) of complex **1** in N_2 atmosphere (75 mL/min).

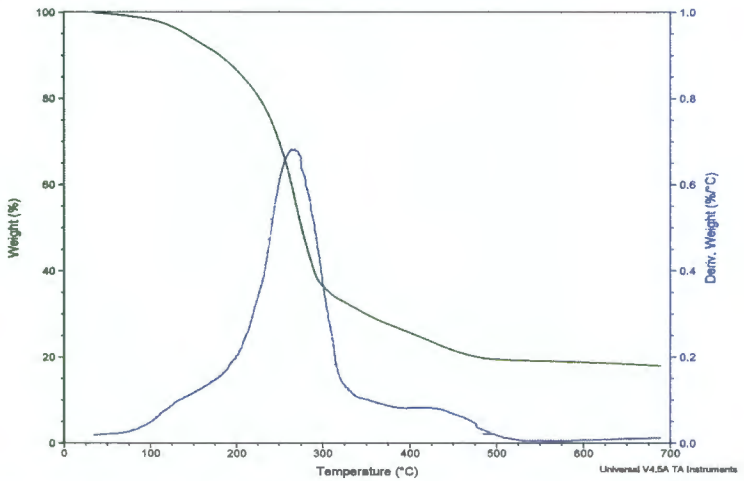

Figure 3.5: TG and DTG curves (with heating rate 10 °C/min) of complex **2** in N_2 atmosphere (75 mL/min).

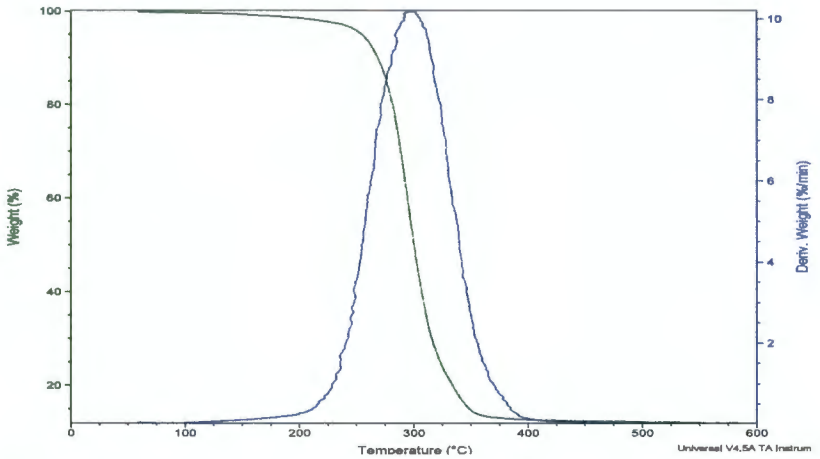

Figure 3.6: TG and DTG curves (with heating rate 10 °C/min) of complex **3** in N_2 atmosphere (75 mL/min).

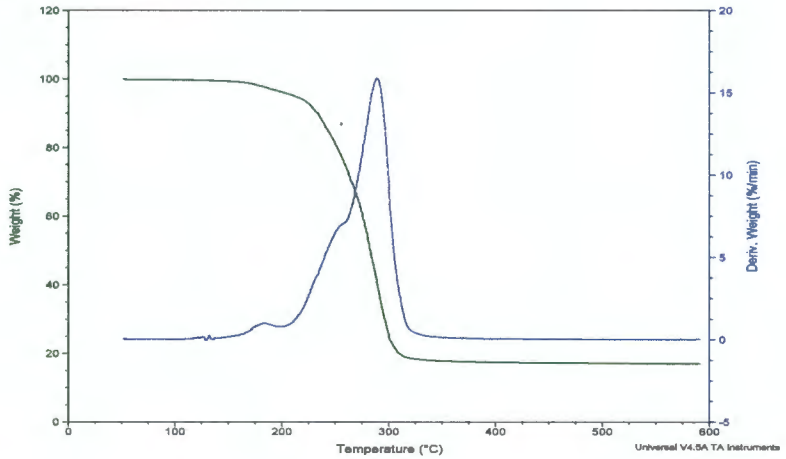

Figure 3.7: TG and DTG curves (with heating rate 10 °C/min) of complex **4** in N_2 atmosphere (75 mL/min).

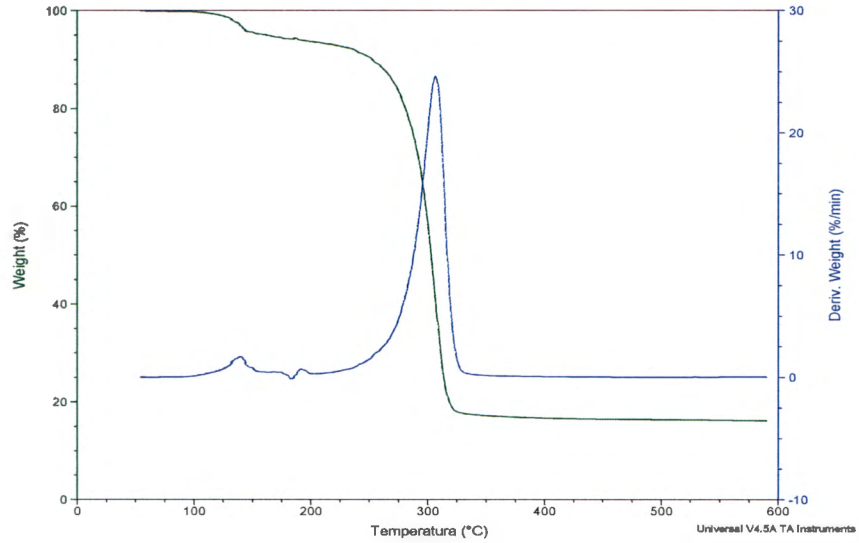

Figure 3.8: TG and DTG curves (with heating rate 10 °C/min) of complex **5** in N_2 atmosphere (75 mL/ min).

3.5 Complexes of organotin(IV)*N*-ethyl-*N*-phenyldithiocarbamate

3.5.1. Synthesis of ammonium *N*-ethyl-*N*-phenyldithiocarbamate, L^2

The ligand was prepared by a slightly modified procedure described previously [25]. *N*-ethyl aniline (1.26 mL, 0.01 mol) was introduced into a round bottom flask placed inside an ice bath at approximately 2 °C. To this, cold ammonia solution (3 mL, 0.01 mol) was added with continuous stirring. After about 5 min, carbon disulfide (0.6 mL, 0.01 mol) was added drop wise to the mixture. The solution was stirred for 4 h, given a faint yellowish precipitate, which was filtered, rinsed with cold ethanol and stored under reduced temperature.

3.5.2. Synthesis of the organotin(IV) complexes of *N*-ethyl-*N*-phenyl dithiocarbamate ($[RSnCl(L^2)_2]$ and $[R_2Sn(L^2)_2]$ (R = CH_3, C_4H_9, C_6H_5))

Respective organotin(IV) chloride (0.005 mol) of the formula $RSnCl_3$ and R_2SnCl_2 were dissolved in 10 mL cold ethanol, and added drop wise to the freshly prepared solution of ammonium-*N*-ethyl-*N*-phenyl dithiocarbamate, L^2. The solution was stirred for about 2 h in an ice bath. White precipitates were formed for all the complexes except the $[PhSnCl(L^2)_2]$ which gave a pale yellowish precipitate. These precipitates were filtered and washed with excess ethanol. The obtained precipitates were dried under vacuum for 24 h. Recrystallization was achieved in a mixture of dichloromethane and ethanol.

(6) $[(CH_3)SnCl(L^2)_2]$: Yield: 0.87 g (36%); M.pt.: 189-191 °C; Selected FTIR, υ(cm^{-1}): 1457(C=N), 1274 (C_2-N), 1003, 1021 (C=S), 2965 (-CH), 3058 (=CH), 552 (Sn-C), 411 (Sn-S); ^{1}H NMR ($CDCl_3$) δ = 7.40- 7.22 (m, 10H, N-$C_6\underline{H}_5$), 4.14 (q, 4H, N-$C\underline{H}_2$), 1.25 (t, 6H, –$C\underline{H}_3$), 2.17 (s, 3H, Sn-$C\underline{H}_3$); ^{13}C NMR ($CDCl_3$) δ = 145.12, 129.40, 128.27, 126.93 (-$\underline{C}_6H_5$), 54.22 (N-$\underline{C}H_2$), 12.23 (-$\underline{C}H_3$), 206.87 (-$\underline{C}S_2$), 30.91 (Sn-$\underline{C}H_3$); ^{119}Sn NMR ($CDCl_3$): δ ppm = -250.10;

$C_{19}H_{23}N_2S_4Sn$ (561.95): C, 40.62; H, 4.13; N, 4.99; S, 22.83; Found: C, 41.02; H, 5.10; N, 4.89; S, 21.98.

(7) $[(C_4H_9)SnCl(L^2)_2]$: Yield: 2.95g (78%); M.pt.: 196-198 °C; Selected FTIR, υ (cm^{-1}): 1498 (C=N), 1273 (C_2-N), 1003, 1019 (C=S), 2953 (-CH), 3115 (=CH), 553 (Sn-C), 447 (Sn-S); ^{1}H

NMR ($CDCl_3$) δ = 7.43 – 7.31 (m, 10H, N-$C_6\underline{H}_5$), 3.74(q, 4H, N-$C\underline{H}_2$), 1.10(t, 6H, –$C\underline{H}_3$), 0.86(t,-$C\underline{H}_3$ (C4)), 1.33 (m, 2H, $C\underline{H}_2$ (C3)), 1.70 (qt, 2H, $C\underline{H}_2$ (C2)), 2.19 (t, 2H, Sn-$C\underline{H}_2$); ^{13}C NMR ($CDCl_3$) δ = 129.94, 129.55, 127.25, 125.61 (N-C_6H_5), 52.64 (N-CH_2), 14.20(-CH_3) 206.97 (-CS_2), 21.07 ((C4) $\underline{C}H_3$), 30.93 ((C3) $\underline{C}H_2$), 39.91 ((C2) $\underline{C}H_2$), 40.05 ((C1) $\underline{C}H_2$);^{119}Sn NMR ($CDCl_3$): δ ppm = -207.33;

$C_{22}H_{29}ClN_2S_4Sn$ (603.9); C, 43.76; H, 4.84; N, 4.64; S, 21.24; Sn, 19.66; Found: C, 42.96; H, 5.04; N, 4.44; S, 21.04;

(8) $[(C_6H_5)SnCl(L^2)_2]$: Yield: 3.15 (82%); M.pt.: 209 – 210 °C; Selected FTIR, υ (cm^{-1}): 1445 (C=N), 1275 (C_2-N), 996, 1003 (C=S), 2960(-CH), 3043 (=CH), 588 (Sn-C), 448 (Sn-S); ^1H NMR ($CDCl_3$) δ = 7.42 – 7.11 (m, 10H, N-$C_6\underline{H}_5$), 7.89-7.87 (m, 5H, Sn-$C_6\underline{H}_5$), 4.07 (q, 4H, N-$C\underline{H}_2$), 1.21 (t, 6H, –$C\underline{H}_3$); ^{13}C NMR ($CDCl_3$) δ = 144.96, 129.47, 128.45, 126.30 (N-$\underline{C}_6H_5$), 135.82, 134.51, 129.37, 126.88 (Sn-$\underline{C}_6H_5$), 54.22 (N-$\underline{C}H_2$), 12.24(-$\underline{C}H_3$) 201.65 (-$\underline{C}S_2$);^{119}Sn NMR ($CDCl_3$): δ ppm = -312.40;

$C_{24}H_{25}ClN_2S_4Sn$ (623.96): C, 46.20; H, 4.04; N, 4.49; S, 20.56; Found: C, 47.00; H, 4.09; N, 5.10; S, 19.96

(9) $[(CH_3)_2Sn(L^2)_2]$: Single crystals suitable for X-ray diffraction analyses were obtained from dichloromethane-ethanol (4:1) solvent system. Yield: 3.15 g (82%); M.pt.: 167 – 169 °C; Selected FTIR, υ(cm^{-1}): 1461 (C=N), 1281 (C_2-N), 1000, 1006 (C=S), 2978 (-CH), 3126 (=CH), 551 (Sn-C), 450 (Sn-S); ^1H NMR ($CDCl_3$)δ = 7.41 – 7.10 (m, 10H, N-$C_6\underline{H}_5$), 4.19 (q, 4H, N-$C\underline{H}_2$), 1.51 (s, 3H, Sn –$C\underline{H}_3$), 1.22 (t, 6H, –$C\underline{H}_3$); ^{13}C NMR ($CDCl_3$) δ = 144.72, 129.44, 128.36, 127.03 (-$\underline{C}_6H_5$), 53.13 (N-$\underline{C}H_2$), 12.14 (-CH_3), 14.23 (Sn-$\underline{C}H_3$), 202.12 (-$\underline{C}S_2$);^{119}Sn NMR ($CDCl_3$): δ ppm = -345.45;

$C_{20}H_{26}N_2S_4Sn$ (541.40): C, 44.37; H, 4.84; N, 5.17; S, 23.69; Found: C, 43.90; H, 5.01; N, 4.99; S, 23.99.

(10) $[(C_4H_9)_2Sn(L^2)_2]$: Single crystals suitable for X-ray diffraction analysis were obtained from dichloromethane-ethanol (3:1) solvent system. Yield: 3.35g (87%); M.pt.: 121 – 122 °C; Selected FTIR, υ(cm^{-1}): 1488 (C=N), 1272 (C_2-N), 1003, 1020 (C=S), 2952 (-CH), 3037 (=CH), 553 (Sn-

C), 447 (Sn-S); ^{1}H NMR ($CDCl_3$) δ = 7.31 – 7.17 (m, 10H, N-$C_6\underline{H}_5$), 4.21 (q, 2H, N-CH_2), 1.25 (t, 3H, –$C\underline{H}_3$), (C_4H_9 moiety); 0.94(t, 6H, -$C\underline{H}_3$), 1.47 (m, 4H, $C\underline{H}_2$), 1.94 (qt, 2H, $C\underline{H}_2$), 2.05 (t, 2H, Sn-$C\underline{H}_2$); ^{13}C NMR ($CDCl_3$) δ = 144.95, 129.40, 128.24, 127.07 (N-$\underline{C}_6H_5$), 53.10 (N-$\underline{C}H_2$), 12.20 ($NCH_2\underline{C}H_3$)) 203.08 (-$\underline{C}S_2$), (C_4H_9 moiety) 13.89 ($\underline{C}H_3$), 26.46 ($\underline{C}H_2$), 28.62 ($\underline{C}H_2$), 33.49 ($\underline{C}H_2$); ^{119}Sn NMR ($CDCl_3$): δ ppm = -333.14;

$C_{26}H_{38}N_2S_4Sn$ (626.09): C, 49.92; H, 6.12; N, 4.48; S, 20.50; Found: C, 48.42; H, 5.81; N, 5.48; S, 21.50.

(11) $[(C_6H_5)_2Sn(L^2)_2]$: Yield: 3.27g (81%); M.pt: 121-122 °C ; Selected FTIR, υ(cm^{-1}): 1462 (C=N), 1275 (C_2-N), 996, 1003 (C=S), 2973 (-CH), 3043 (=CH), 552 (Sn-C), 444 (Sn-S); ^{1}H NMR ($CDCl_3$)δ = 7.41 - 7.21 (m, 10H, N-$C_6\underline{H}_5$), 7.98 - 7.72 (m, 10H, Sn-$C_6\underline{H}_5$), 4.09 (m, 4H, N-$C\underline{H}_2$), 1.19 (t, 6H, –$C\underline{H}_3$); ^{13}C NMR ($CDCl_3$)δ = 149.92, 129.87, 128.73, 126.87 (N-$\underline{C}_6H_5$), 144.93, 135.45, 134.50, 128.22 (Sn-$\underline{C}_6H_5$), 54.22 (N-$\underline{C}H_2$), 12.23 (-$\underline{C}H_3$), 201.59 (-$\underline{C}S_2$);^{119}Sn NMR ($CDCl_3$): δ ppm = -310.12;

$C_{30}H_{30}N_2S_4Sn$ (666.03): C, 54.14; H, 4.54; N, 4.21; S, 19.27; Found: C, 53.54; H, 5.10; N, 4.29; S, 20.79.

3.6. Results and discussion on the organotin(IV)*N*-ethyl-*N*-phenyldithiocarbamate complexes

3.6.1. Synthesis of organotin(IV) complexes of *N*-ethyl-*N*-phenyl dithiocarbamate

The ligand $\mathbf{L^2}$ was synthesized in a similar fashion according to the reaction procedure presented in scheme 3.1. It is unstable at room temperature but stable under cold condition, preferably in a refrigerator, but relatively more stable than L^1 at both conditions. The ligand L^2 is less soluble with higher number of carbon on the nitrogen atom. The organotin complexes synthesized (see Figure 3.9) were air stable and crystalline solids with melting points ranging from 121 –210 °C. The complexes were obtained as white solid except for complex **11** which gave a pale yellow precipitate. All complexes were soluble in dichloromethane, chloroform, dimethylsulfoxide and sparingly soluble in alcohols.

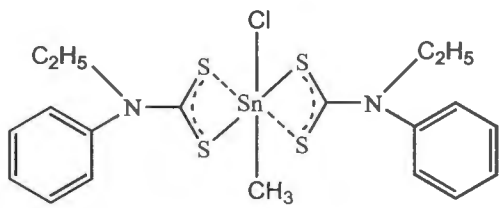

(6) $[(CH_3)ClSn(L^2)_2]$

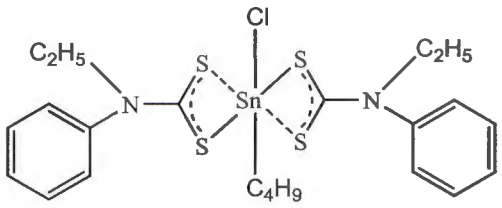

(7) $[(C_4H_9)ClSn(L^2)_2]$

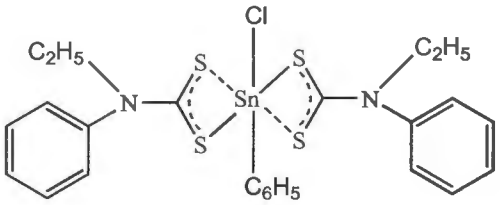

(8) $[(C_6H_5)ClSn(L^2)_2]$

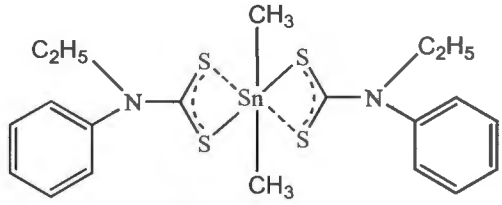

(9) $[(CH_3)_2Sn(L^2)_2]$

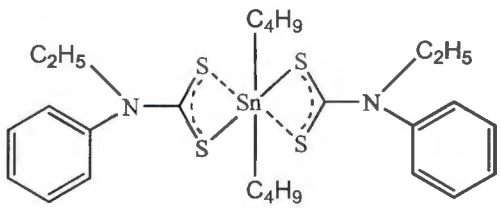

(10) $[(C_4H_9)_2Sn(L^2)_2]$

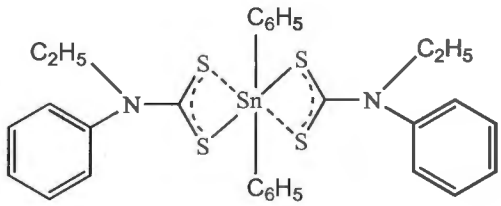

(11) $[(C_6H_5)_2Sn(L^2)_2]$

Figure 3.9: List of complexes **6 – 11** obtained from the reaction scheme 3.1 (with $\mathbf{L^2}$).

3.6.2. Infrared spectroscopic studies of the organotin(IV)*N*-ethyl-*N*-phenyldithiocarbamate complexes

In the IR spectra of the complexes, the strong ν(C–N) band was found in the region 1461-1498 cm^{-1}[26]. This high stretching vibration has been ascribed to an increase in the carbon-nitrogen double bond character due to delocalization of electrons toward metal atom in each of the complexes [15]. Thus, indicates a significant contribution of the thioureide form [27]. Bonati and Ugo proposed that a single symmetric peak for ν(C-S) around 1000 ± 70 cm^{-1} region indicates a bidentate mode of coordination, while the splitting of this peak within a difference of 20 cm^{-1} indicates a monodentate or anisobidentate mode of coordination [26]. Splitted absorption bands

of ν(C-S) stretching vibrations were observed in the range 996 – 1021 cm^{-1}, thus, indicating a monodentate mode of coordination through the sulfur atom of the dithiocarbamate moiety. The ν(Sn–S) bands (found in the far infrared region) was observed around 411 – 450 cm^{-1}. This band indicates coordination between the organotin compounds and the ligand molecule [28,29]. The ν(C-H) stretching frequency for the ethyl group in the dithiocarbamate moiety were observed in the range 2952 – 2978 cm^{-1} [16] and the ν(=C-H) stretching frequencies from the aromatic ring appeared in the 3037-3124 cm^{-1} region [15].

3.6.3. Nuclear Magnetic Resonance studies of the organotin(IV)*N*-ethyl-*N*-phenyldithiocarbamate complexes

The ^{1}H NMR of the complexes showed a quartet in the region 3.74 – 4.21 ppm, corresponding to the two protons of the methylene (-CH_2-) from the *N*-ethyl substituent of the dithiocarbamate moiety [14]. The proton of the methyl (-CH_3) group of the *N*-ethyl substituents resonated as triplet in the region 1.24 – 1.10 ppm [2]. The aromatic proton of the dithiocarbamate moiety for all the complexes appeared as multiplet around 7.43 – 7.11 ppm [15,30]. A strong singlet which is ascribed to the methyl proton from the organotin moiety resonated at 2.17 and 1.51 ppm in the spectra of complexes **9** and **6** respectively [31]. The slightly higher shift of the methyl group of complex **6** is due to the high electronegativity of chlorine atom which was unsubstituted in the organotin moiety. In complexes **7** and **10**, protons due to the butyl substituent of the organotin resonated in the region 2.19 – 0.86 ppm [10,12], while the phenyl protons from the organotin moiety of complexes **8** and **11** appeared as multiplet in the region 7.98 – 7.72 ppm. This observed shift is due to the deshielding which occurred upon complexation [12,14].

The ^{13}C NMR spectra of the complexes showed signals for the methylene (-CH_2-) and methyl (-CH_3) carbon atoms in the range 54.22 – 52.64 ppm and 14.20 – 12.14 ppm, respectively, for the ethyl substituent of the dithiocarbamate moiety [16]. In all the complexes, weak signals due to the carbon of the -NCS_2 appeared around 201.59 – 206.97 ppm [14,28]. This -NCS_2 resonance is often found in free dithiocarbamate ligands at a higher field above 205 ppm, but shifts slightly downfield upon complexation [32]. This downfield shift is due to the contribution of $R_2N^{+}{=}CS_2^{2-}$ resonance form in the complexes. In complex **9**, the carbon of the methyltin resonated at 14.23 ppm. The butyl carbon atoms bonded to the Sn atom in complexes **7** and **10** resonated within 33.49 – 13.89 ppm range [13]. The signals which resonate around 144 – 126 ppm in complexes **8**

and **11** were ascribed to the aromatic carbons of the phenyl group [15]. In these complexes, the ^{119}Sn NMR spectra showed a singlet in the range -207 to -345 ppm, which suggests a hexa-coordinated geometry about the tin center.

3.6.4. X-ray crystallographic studies of complexes 9 and 10

Suitable single crystals were obtained for X-ray diffraction analysis of both methyl and butyltin(IV) *N*-ethyl-*N*-phenyldithiocarbamatecomplexes (**9** and **10)** from dichloromethane-ethanol solvent system. Useful crystallographic data and geometric parameters are summarized in Table 3.4. Selected bond lengths and angles are given in Table 3.5. The ORTEP plot of the complexes with the structure and the numbering scheme given in Figures 3.10 and 3.11 showed the central tin atom bonded to the two ligands (*N*-ethyl-*N*-phenyldithiocarbamate) to form a five coordinate compound. The complexes are non-centrosymmetrical with four molecules in the asymmetric unit cell. Both complexes exist as a monomer in which one of the dithiocarbamate ligands formed a chelate, while the other dithiocarbamate bonded to the central tin atom through one of the sulfur atoms and the second sulfur atom existed as a pendant [33]. Structures of organotin complexes having one or more dithiocarbamate ligands are rarely symmetrically bonded to the tin center of the organotin moiety [34,35]. The bidentate dithiocarbamate were attached to the Sn center atom in an anisobidentate fashion. In complex **9**, Sn1-S11 is significantly shorter [2.5193 (5) Å] than the Sn1-S12 [2.9135 (6) Å], with a bite angle of [65.50 (2)]. Similarly, in complex **10**, Sn1-S12 is significantly shorter [2.5250 (7) Å] than Sn1-S11 [2.8619 (8) Å] with a bite angle of [66.39 (2)]. The second dithiocarbamate which coordinates in a monodentate fashion to the tin atom has a Sn-S21 bond length of 2.5193(5) and 2.5318(8) Å in complexes **9** and **10** respectively. A non-bonding distance between the Sn central atom of the organotin moiety and S22 atom at 3.12 (6) and 3.12 (9) Å was observed in complexes**9** and **10** respectively. This has been attributed to a change in one of the short Sn-S bond arising from the weak coordination of a sulfur atom in the dithiocarbamate moiety, thus leading to a change in position approximately orthogonal to the Sn-S22 plane [34].

Around the Sn atom, the geometry can be best described as a distorted trigonal bipyramid: in the dimethyltin group moiety, atoms C3 and C4 and the sulfur atom S11 occupied the equatorial position, while the sulfur atoms S12 and S21 are axial to each other with an angle [S12-Sn1-S21] 144.91 (2)°. Similarly, in the dibutyltin group moiety, atoms C31, C41 and S12 occupied the

equatorial position, while S11 and S21 are axial to each other with an angle [S11-Sn1-S21] 147.88 (3)°. The percentage along the trigonal bipyramid to square pyramid Berry pseudorotation is 18.8 and 16.7 in complexes **9** and **10** respectively. Similar mode of coordination for this complex have been reported [20, 36]. The C–S bond are typically observed for a single C–S bond lengths at 1.82 Å, which is usually longer than the C=S double bond of the distance 1.67 Å [36]. Incomplex**9**, the C–S bond lengths were observed at 1.7445(18) Å [S11-C11] and 1.7457(18) Å [S21-C21] and incomplex**10**, at 1.7411(3) Å [S12-C11] and 1.740(3) Å [S21-C21]. These observed bond lengths showed a significant difference from the expected. The observed differences from the expected and the values of the C-S bond is an indication of a partial double bond character within this bond. The C-N bonds were observed at 1.336(2) Å [C11–N1] and 1.342(2) Å [N2-C21] in complex **9**. However in **10** the bond distance for C-N bonds were1.337(3) Å [C11–N1] and 1.339(2) Å [N2-C21] from the two dithiocabamate moieties bonded to both sides. These distances deviate from the reported value of a simple C-N at 1.47 Å, but are similar to others reported in literature [32].

The ORTEP diagram showing the hydrogen interactions for complexes **9** and **10** is shown in Figure 3.12 and 3.13 respectively. In complex **9**, the dihedral angle between the two planes formed by the dithiocarbamate ligands is 7.2(1)°. The phenyl groups make dihedral angle of 83.5(1) and 83.6(1)° with the dithiocarbamate planes. The four S atoms form a plane with a RMS deviation of 0.0132 Å with the Sn atom 0.0112(3) Å from the plane. Each dithiocarbamate ligand has one intramolecular C---H...S hydrogen interaction between a S atom and an H from the ethyl group with lengths of 2.57 and 2.61 Å to S11 and S22 respectively as presented in Figure 3.12. Between adjacent molecules, there are two C214---H214...π ring interactions with the C111—C116 phenyl ring. The hydrogen to centroid distance is 2.82 Å. Similarly for **10**, the dihedral angle between the two planes formed by the dithiocarbamate ligands is 15.55(9)°. The phenyl groups make dihedral angle of 68.07(10) and 82.11(8)° with the respective dithiocarbamate planes. The Sn and non-bonding S22 atoms lie 0.231(1) and 0.738(3) Å above the plane formed by the bonding S11, S12 and S21 atoms. Each dithiocarbamate ligand has one intramolecular C---H...S hydrogen interaction between a S atom and an H from its ethyl group with lengths of 2.48 and 2.60 Å to S11 and S22 respectively, as shown in Figure 3.13.There is one intermolecular C215—H215…π ring interaction of length 2.88 Å to the centroid formed by the Sn1, S11, C11 and S12 atoms.

Table 3.4: Crystal data, data collection and refinement parameters

Complex	**9**	**10**
Empirical formula	$C_{20}H_{26}N_2S_4Sn$	$C_{26}H_{38}N_2S_4Sn$
Formula weight	541.38	625.53
Crystal size (mm)	0.24 x 0.41 x 0.56	0.28 x 0.38 x 0.61
Crystal system	monoclinic	monoclinic
Crystal habit	colorless needle	colorless needle
Space group	P21/c	P21/c
a (Å)	13.5000(7)	15.1480(8)
b (Å)	13.3490(7)	14.2260(7)
c (Å)	13.8105(7)	15.1519(8)
β (°)	107.894(2)	114.322(2)
U (Å^3)	2368.4(2)	2975.4(3)
Z	4	4
*D*calc (g cm^{-3})	1.518	1.396
F(000)	1096	1288
θ range (°)	2.2-28.4	2.1-28.3
Index range	-18:18;-14:17;-18:18	-20:20;-19:18;-20:20
Total, unique reflections	33990,5887	146426,7409
Observed reflections *I*> 2σ(*I*)	5024	6116
Number of parameters refined	248	302
Final *R*, w*R2*	0.0220, 0.0500	0.0294,0.0799
Goodness-of-fit (GOF)	1.03	1.12

Table 3.5: Selected bond distances and angles for complexes **9** and **10**

(9)		(10)	
Bond distances (Å)		**Bond distances (Å)**	
Sn1-S11	2.5193(5)	Sn1-S11	2.8619(8)
Sn1-S12	2.9135(6)	Sn1-S12	2.5250(7)
Sn1-S21	2.5193(5)	Sn1-S21	2.5318(8)
Sn1-C3	2.113(2)	Sn1-C31	2.150(3)
Sn1-C4	2.112(2)	Sn1-C41	2.142(3)
S11-C11	1.7445(18)	S11-C11	1.693(3)
S12-C11	1.6832(19)	S12-C11	1.741(3)
S21-C21	1.7457(18)	S21-C21	1.740(3)
S22-C21	1.6806(19)	S22-C21	1.690(3)
N1-C11	1.336(2)	N1-C11	1.337(3)
N1-C12	1.479(3)	N1-C12	1.481(4)
N1-C111	1.442(2)	N1-C111	1.442(4)
N2-C21	1.342(2)	N2-C21	1.339(3)
N2-C22	1.481(2)	N2-C22	1.478(4)
N2-C211	1.443(2)	N2-C211	1.442(4)
Bond angles (°)		**Bond angles (°)**	
S11-Sn1-S12	65.50(2)	S11-Sn1-S12	66.39(2)
S11-Sn1-S21	79.42(2)	S11-Sn1-S21	147.88(3)
S11-Sn1-C3	110.87(6)	S11-Sn1-C31	88.22(8)
S11-Sn1-C4	108.31(7)	S11-Sn1-C41	87.26(8)
S12-Sn1-S21	144.91(2)	S12-Sn1-S21	82.31(2)
S12-Sn1-C3	86.34(6)	S12-Sn1-C31	109.41(8)
S12-Sn1-C4	85.86(6)	S12-Sn1-C41	104.94(8)
S21-Sn1-C3	106.65(6)	S21-Sn1-C31	95.91(8)
S21-Sn1-C4	106.49(7)	S21-Sn1-C41	108.51(8)
C3-Sn1-C4	132.19(10)	C31-Sn1-C41	140.04(12)
Sn1-S11-C11	93.45(6)	Sn1-S11-C11	82.10(9)
Sn1-S12-C11	81.78(6)	Sn1-S12-C11	92.08(9)
Sn1-S21-C21	97.86(6)	Sn1-S21-C21	97.18(10)
C11-N1-C12	123.73(15)	C11-N1-C12	120.3(2)
C21-N2-C22	121.94(16)	C21-N2-C22	122.2(2)
C11-N1-C111	119.73(16)	C11-N1-C111	122.5(2)
C12-N1-C111	116.31(14)	C12-N1-C111	116.9(2)
C21-N2-C211	120.72(15)	C21-N2-C211	121.4(2)
C22-N2-C211	116.77(15)	C22-N2-C211	116.2(2)
S11-C11-S12	119.26(10)	S11-C11-S12	119.26(14)
S11-C11-N1	118.09(14)	S11-C11-N1	122.3(2)
S12-C11-N1	122.65(14)	S12-C11-N1	118.4(2)
N1-C12-C13	112.95(17)	N1-C12-C13	113.8(3)
S21-C21-S22	120.11(10)	S21 -C21-S22	120.96(16)
S21-C21-N2	116.07(14)	S21-C21-N2	116.4(2)
S22-C21-N2	123.81(14)	S22-C21-N2	122.6(2)
N2-C22-C23	113.18(18)	N2-C22-C23	112.8(3)

Symmetry element i: -X, 1/2+Y, 1/2-Z

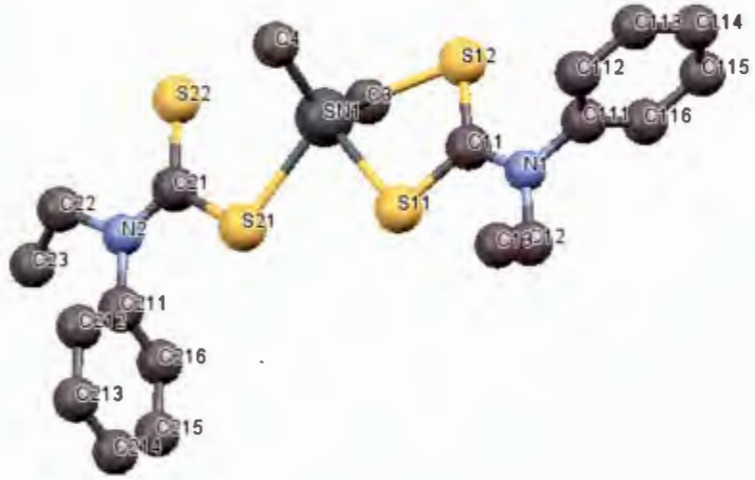

Figure 3.10: The molecular structure of butyltin(IV) *N*-ethyl-*N*-phenyldithiocarbamate complex **(9)** with displacement ellipsoids drawn at 50% probability level (all hydrogen atoms are omitted for clarity).

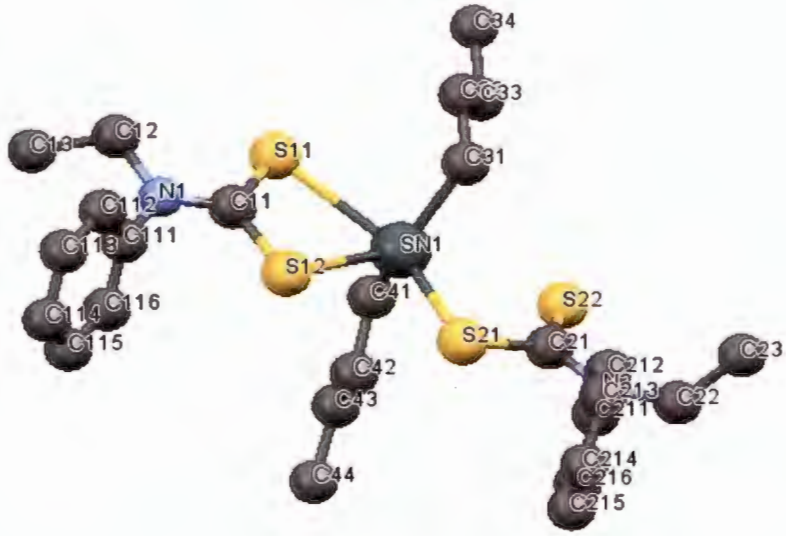

Figure 3.11: The molecular structure of butyltin(IV) *N*-ethyl-*N*-phenyldithiocarbamate complex **(10)** with displacement ellipsoids drawn at 50% probability level (all hydrogen atoms are omitted for clarity).

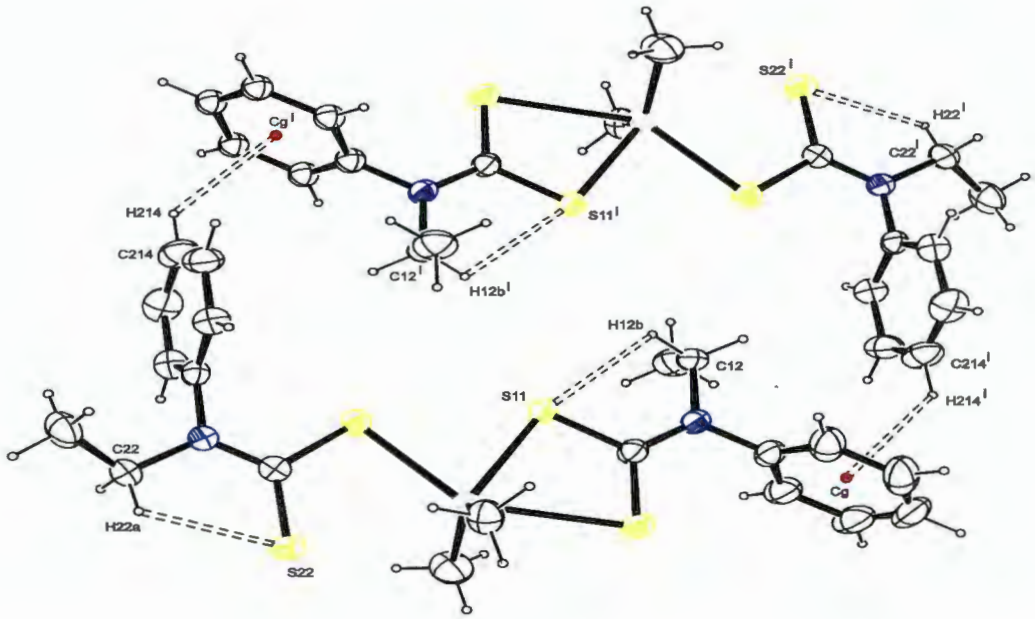

Figure 3.12: Ortep diagram of **9** showing the hydrogen interactions. Ellipsoids drawn at 50 % probability. Cg is the centroid of the phenyl ring C111—C116. Symmetry element: (i) 1-x, 1-y, 1-z.

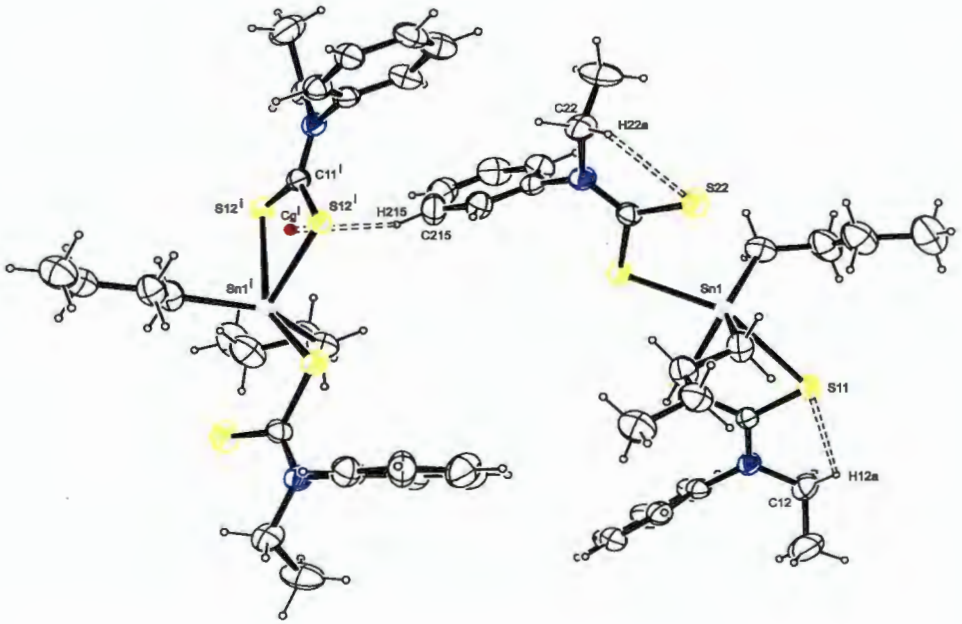

Figure 3.13: Ortep diagram of **10** showing the hydrogen interactions. Ellipsoids drawn at 50 % probability. Cg is the centroid of the ring formed by Sn1, C11, S11 and S12. Symmetry element: (i) 1-X,1/2+Y,3/2-Z.

3.6.5. Thermogravimetric Analysis (TGA) of organotin(IV) *N*-ethyl-*N*-phenyldithiocarbamate complexes (6 – 11)

The TGA graphs of the complexes in the temperature range of 50 – 700 °C are presented in Figures 3.14 – 3.19, while the summary of the thermal data are presented in Table 3.6. Complexes **6** and **8** showed a three step decomposition pathway respectively while complex **7** showed a two-step decomposition pathway. The literature reports on the thermal decomposition pathway of organotin(IV) dithiocarbamate revealed that this group of complexes, even those structurally related, possess an unpredictable and complicated decomposition pathways. Hence, the difficulty in rationalizing their thermal decomposition pattern [24]. However from the data obtained, a reasonable understanding of the stability can be deduced. From the graph obtained for complex **6**, the first step decomposition occurred in the temperature range 181 – 232 °C, with a mass loss of about of about 29.22% of the starting mass. The mass found here agree well with the obtained formula weight attributed to the loss of one ligand moiety [$S_2CN(C_2H_5)(C_6H_5)$] from the complex. As observed from the obtained crystal structures which predict the geometry of this group of complexes to have a five coordinate geometry with a pendant sulfur, it is possible that this decomposition occurred on the side with a single Sn–S bond due to a weak force of attraction. The second decomposition step occurred in the range 234 – 250 °C due to the elimination of CH_3 group and the chloride ion from the organotin moiety (CH_3Cl). The mass found at this stage is 63.06% of the starting mass. This was followed by a final decomposition step in the temperature range 262 – 310 °C with an approximate weight loss of 75%. The mass found here showed the formation of SnS as the residue (25.0% of the starting weight) and agrees with the calculated value (26.68%).

The first step of decomposition in complex **7** occurred in the temperature range of 132 – 226 °C, with an approximate weight loss of 65.48%. Mass of the residue left after this stage corresponded to the formation of isothiocyanate intermediate (34.51%). This intermediate immediately decomposed with a mass loss of 23.06% in the temperature range of 228 – 235 °C, leading to the formation of SnS. The mass found was in good agreement with the calculated (24.69%). Complex **8** decomposed with 12.33% weight loss in the first step in 107 – 163 °C temperature range, which corresponded to the release of the phenyl group ($-C_6H_5$) attached to the organotin moiety. At the temperature of maximum rate of decomposition, the DTG showed the formation of the metal isothiocyanate intermediate in the 246 – 281 °C range, with an

approximate weight loss of 66.48% of the starting mass. The third stage involved the instant decomposition of this isothiocyanate into SnS within 288 – 342 °C range. The percentage mass of the residue found (23.59%) corresponded to SnS, and was in good agreement with the calculated (24.02%).

Figures 3.17 – 3.19 present the overlapped TG/DTG curves of the diorganotin(IV) dithiocarbamate complexes: **9**, **10**, and **11**. The calculated weight losses were compared to the observed weight losses of the different decomposition steps on the basis of possible decomposition intermediates and volatilized groups. Complexes **9** and **10** showed similar thermal behaviour, with both complexes displaying a two-step decomposition pattern as evident in their DTG curves. The first step of degradation in complex **9** occurred in the temperature range of 170 – 289 °C, with an approximate weight loss of 39%. In complex **10**, about30% of the complex was degraded in the range 144 – 286 °C. These weight losses correspond to the decomposition of the organic moiety in the complexes, and the formation of metal thiocyanate intermediate. In the second step, the metal thiocyanate intermediate degraded in the range 290 – 308 °C with an approximate weight loss of 72% for complex **9**. Similarly, in the temperature range of 287 – 327°C, the metal thiocyanate intermediate of complex **10** degraded with an approximate weight loss of 78%. The decomposition of the metal thiocyanate intermediate in each case yielded SnS residue which was found to be in good agreement with the calculated weight.

In complex **11**, a single-step decomposition pattern was observed between 109 – 285 °C, with an approximate weight loss of 79% (Figure 3.19). The weight of the residue obtained after the decomposition process was 0.53 mg (20% of the starting weight) and was in good agreement with calculated value of 0.58 mg (22% of the starting mass) for SnS.

From the thermal study carried out, complexes **8** and **10** were more stable than the other complexes in this group. Thus, the pyrolysis of thesegroup of compounds was achieved in a temperature range corresponding to the formation of thermally stable products, 109 and 342 °C.

Table 3.6: Thermal analysis data of complexes **6 -11.**

Complexes						
	6	**7**	**8**	**9**	**10**	**11**
Temp. range of decomp. (°C)						
First stage	181 – 232	132 – 226	107 – 163	170 – 289	144 – 286	109 – 285
Second stage	234 – 250	228 – 235	246 – 281	290 – 308	287 – 327	—
Third stage	262 – 310	—	288 – 342	—	—	—
DTG peak T(°C)						
First stage	208	208	139	253	277	280
Second stage	248	230	269	308	327	—
Third stage	294	—	307	—	—	—
Melting point	—	—	206	—	—	—
Products obtained						
1st decomp.	$CH_3Sn[S_2CN(C_2H_5)(C_6H_5)]$	NCS_2Sn	$Sn[S_2CN(C_2H_5)(C_6H_5)]_2$	NCS_2Sn	NCS_2Sn	SnS
2nddecomp.	Cl	SnS	Cl	SnS	SnS	—
3rddecomp	$Sn[S_2CN(C_2H_5)(C_6H_5)]$	—	NCS_2Sn	—	—	—
	SnS		SnS			
Mass of residue (mg) Found (Calc.)						
First stage	1.61 (1.61)	0.86 (0.86)	5.91 (5.91)	3.90 (3.89)	5.40 (5.92)	0.53 (0.58)
Second stage	1.46 (1.46)	0.57 (0.61)	2.27 (2.26)	2.77 (2.80)	4.08 (4.27)	—
Third stage	0.58 (0.61)	—	1.59 (1.62)	—	—	—

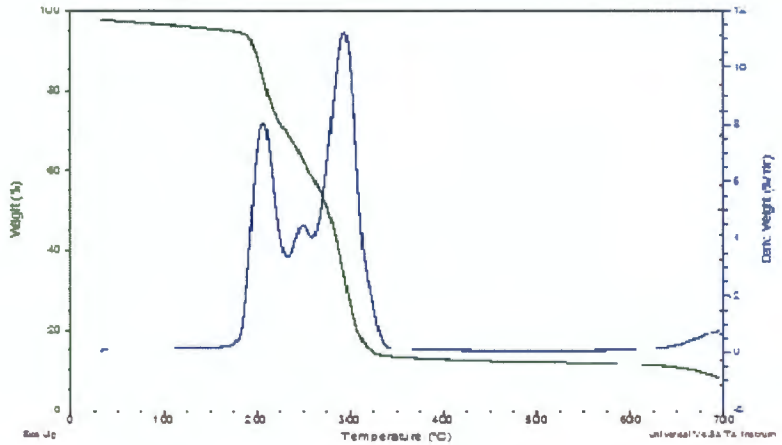

Figure 3.14:TG/DTG curves of complex **6** obtained in nitrogen atmosphere (75 mL/min), heating rate 10 °C/min.

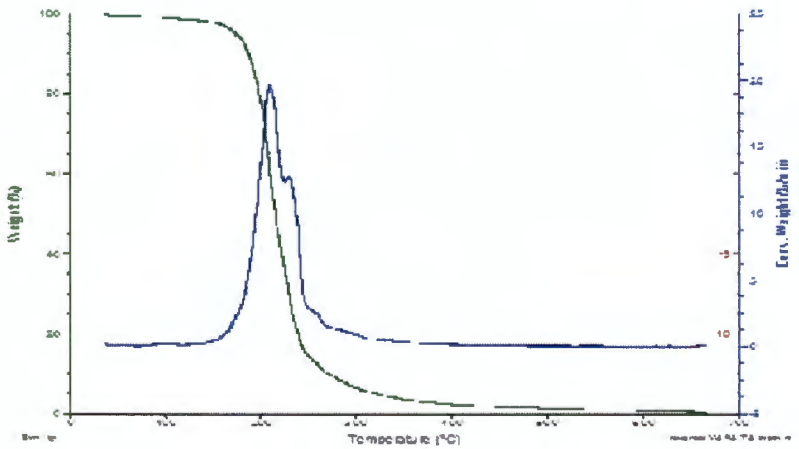

Figure 3.15: TG/DTG curves of complex **7** obtained in nitrogen atmosphere (75 mL/min), heating rate 10 °C/min.

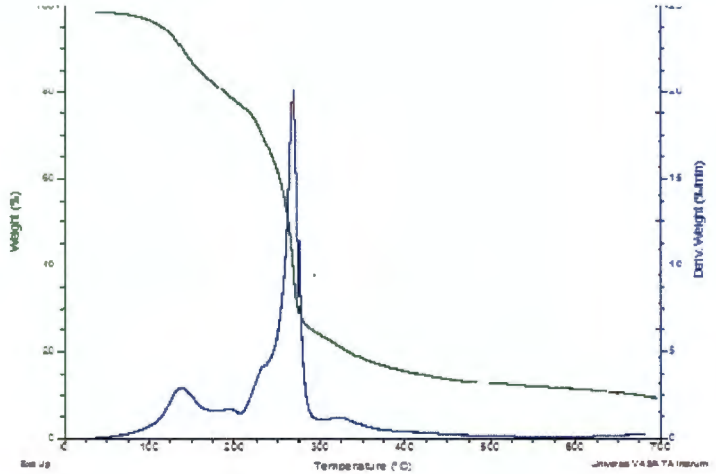

Figure 3.16:TG/DTG curves of complex **8** obtained in nitrogen atmosphere (75 mL/min), heating rate 10 °C/min.

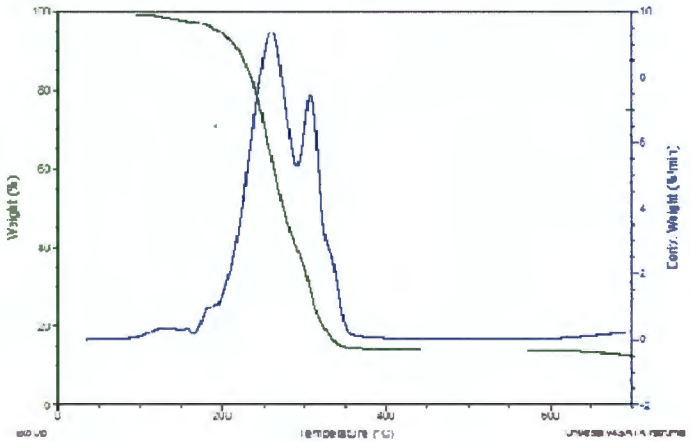

Figure 3.17:TG/DTG curves of complex **9** obtained in nitrogen atmosphere (75 mL/min), heating rate 10 °C/min.

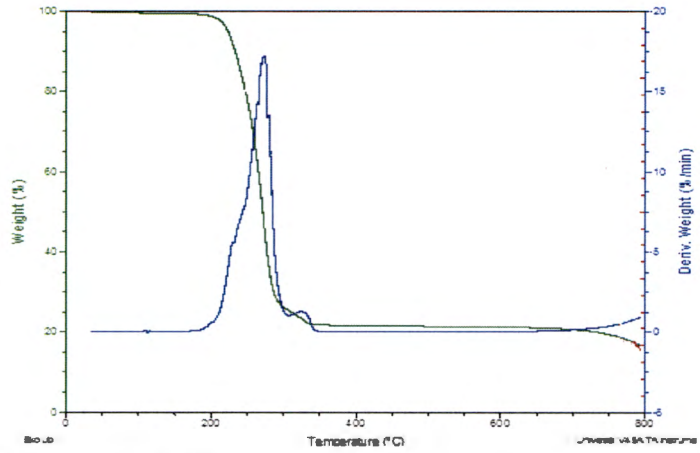

Figure 3.18: TG/DTG curves of the complex **10** obtained in nitrogen atmosphere (75 mL/min), heating rate 10 °C/min.

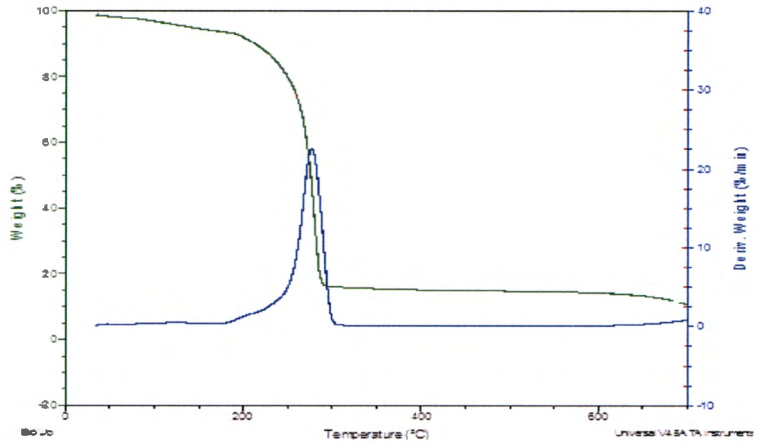

Figure 3.19: TG/DTG curves of the complex **11** obtained in nitrogen atmosphere (75 mL/min), heating rate 10 °C/min.

3.7. Complexes of organotin(IV) and *N*-butyl-*N*-phenyldithiocarbamate

3.7.1. Synthesis of ammonium *N*-butyl-*N*-phenyl dithiocarbamate, L^3

The ligand was prepared by a slightly modified procedure described previously [37]. *N*-butyl aniline (1.60 mL, 0.01 mol) was introduced into a round bottom flask placed inside an ice bath at low temperature of approximately 2 °C. To this, cold ammonia solution (3 mL, 0.01 mol) was added with continuous stirring. After about 5 min, carbon disulfide (0.6 mL, 0.01 mol) was added dropwise to the mixture. The solution was stirred for 4 h, given a faint yellowish precipitate.

3.7.2. Synthesis of the organotin(IV) *N*-butyl-*N*-phenyl dithiocarbamate complexes, $RSnClL_2$ and R_2SnL_2 ($R = CH_3, C_4H_9, C_6H_5$)

Respective organotin(IV) chloride (0.005 mol) of the formula $RSnCl_3$ and R_2SnCl_2 were dissolved in 10 mL cold ethanol and added dropwise to the freshly prepared solution of ammonium-*N*-butyl-*N*-phenyldithiocarbamate. The solution was stirred for about 2 h in an ice bath. White precipitates were formed for all the complexes. These precipitates were filtered, washed with excess ethanol and dried under vacuum. Recrystallization was achieved in a mixture of dichloromethane and ethanol.

(12) $[(C_4H_9)ClSn(L^3)_2]$: Yield: 2.56 g (63.84%); M.pt.: 229 – 230 °C; Selected FTIR, υ(cm^{-1}): 1442 (C=N), 1291 (C_2-N), 1001 (C=S), 2958 (-CH), 3020 (=CH), 519 (Sn-C), 356 (Sn-S); ^{1}H NMR ($CDCl_3$) δ ppm = 7.31–7.23 (m, 10H, N-C6H5), 4.05 (t, 4H, N-$CH_2CH_2CH_2CH_3$), 1.92 (m, 4H, N-$CH_2CH_2CH_2CH_3$), 1.58 (m, 4H, N-$CH_2CH_2CH_2CH_3$), 1.24 (t, 6H, N-$CH_2CH_2CH_2CH_3$), 2.09 (t, 2H, Sn-$CH_2CH_2CH_2CH_3$), 1.84 (m, 2H, Sn-$CH_2CH_2CH_2CH_3$), 1.38 (m, 2H, Sn-$CH_2CH_2CH_2CH_3$), 0.89 (t, 3H, Sn-$CH_2CH_2CH_2CH_3$); ^{13}C NMR ($CDCl_3$) δ ppm = 203.36 (CS_2), 145.22, 129.20, 127.01, 126.31 (N-C_6H_5), 58.10 (N-$CH_2CH_2CH_2CH_3$), 30.93 (N-$CH_2CH_2CH_2CH_3$), 19.89 (N-$CH_2CH_2CH_2CH_3$), 13.87 (N-$CH_2CH_2CH_2CH_3$), 31.67 (Sn-$CH_2CH_2CH_2CH_3$), 28.59 (Sn-$CH_2CH_2CH_2CH_3$), 20.30 (Sn-$CH_2CH_2CH_2CH_3$), 13.91(Sn-$CH_2CH_2CH_2CH_3$); ^{119}Sn NMR ($CDCl_3$) δ ppm = -316.15.

$C_{26}H_{37}ClN_2S_4Sn$ (660.1) = C, 47.31; H, 5.65;N, 4.24; S, 19.43; Found = C, 47.21; H, 6.05; N, 4.04; S, 20.40.

(13) $[(CH_3)_2Sn(L^3)_2]$: Yield: 2.51 g (67.77%); M.pt.: 207–208°C; Selected FTIR, υ (cm^{-1}): 1443 (C=N), 1237 (C_2-N), 1001 (C=S), 2921 (-CH), 3084 (=CH), 518 (Sn-C), 357 (Sn-S); ^{1}H

NMR (CDCl3) δ ppm = 7.38–7.16 (m, 10H, N-$C_6\underline{H}_5$), 4.11 (t, 4H, N-$C\underline{H}_2CH_2CH_2CH_3$), 2.06 (m, 4H, N-$CH_2C\underline{H}_2CH_2CH_3$), 1.66 (m, 4H, N-$CH_2CH_2C\underline{H}_2CH_3$), 1.25 (t, 6H, N-$CH_2CH_2CH_2C\underline{H}_3$), 1.57 (t, 6H, Sn-$C\underline{H}_3$); ^{13}C NMR ($CDCl_3$) δ ppm = 202.48 ($CS_2$), 145.08, 129.40, 128.30, 126.98 (N-$\underline{C}_6H_5$), 58.16 (N-$\underline{C}H_2CH_2CH_2CH_3$), 28.98 (N-$CH_2\underline{C}H_2CH_2CH_3$), 19.92 (N-$CH_2CH_2\underline{C}H_2CH_3$), 13.72 (N-$CH_2CH_2CH_2\underline{C}H_3$), 14.38 (Sn-$\underline{C}H_3$); ^{119}Sn NMR ($CDCl_3$): δ ppm = -314.20;

$C_{24}H_{34}N_2S_4Sn$ (598.1) = C, 48.24; H, 5.74; N, 4.69; S, 21.47; Found = C, 47.94; H, 5.14; N, 4.29; S, 22.04.

(14) [$(C_4H_9)_2Sn(L^3)_2$]: Yield: 2.86 g (69.41%); M.pt.: 215–217 °C; Selected FTIR, υ(cm^{-1}): 1440 (C=N), 1237 (C_2-N), 1001 (C=S), 2921(-CH), 3238 (=CH), 518 (Sn-C), 357 (Sn-S); ^{1}H NMR ($CDCl_3$) δ ppm = 7.41-7.26 (m, 10H, N-$C_6\underline{H}_5$), 4.14 (t, 4H, N-$C\underline{H}_2CH_2CH_2CH_3$), 1.65 (m, 4H, N-$CH_2C\underline{H}_2CH_2CH_3$), 1.33 (m, 4H, N-$CH_2CH_2C\underline{H}_2CH_3$), 0.89 (q, 6H, N-$CH_2CH_2CH_2\underline{C}H_3$), 1.94 (t, 4H, Sn-$C\underline{H}_2CH_2CH_2CH_3$), 1.45 (m, 4H, Sn-$CH_2C\underline{H}_2CH_2CH_3$), 1.23 (m, 4H, Sn-$CH_2C\underline{H}_2CH_2CH_3$), 0.91 (t, 6H, Sn-$CH_2CH_2CH_2\underline{C}H_3$); ^{13}C NMR ($CDCl_3$) δ ppm = 203.40 (-$CS_2$),145.24, 129.52, 128.18, 126.33 (N-C_6H_5), 58.12 (N-$\underline{C}H_2CH_2CH_2CH_3$), 28.98 (N-$CH_2\underline{C}H_2CH_2CH_3$), 19.90 (N-$CH_2CH_2\underline{C}H_2CH_3$), 13.88 (N-$CH_2CH_2CH_2\underline{C}H_3$), 31.69 (Sn-$\underline{C}H_2CH_2CH_2CH_3$), 28.89 (Sn-$CH_2\underline{C}H_2CH_2CH_3$), 27.89 (Sn-$CH_2CH_2\underline{C}H_2CH_3$); 13.90 (t, 6H, Sn-$CH_2CH_2CH_2\underline{C}H_3$); ^{119}Sn NMR ($CDCl_3$): δ ppm = -320.18;

$C_{30}H_{46}N_2S_4Sn$ (681.67) = C, 52.86; H, 6.80; N, 4.11; S, 18.82; Found C, 52.90; H, 6.28; N, 3.91; S, 19.02.

(15) [$(C_6H_5)_2Sn(L^3)_2$]: Yield: 3.01 g (69.83%); M.pt.: 220–221°C; Selected FTIR, υ(cm^{-1}): 1445 (C=N), 1244 (C_2-N), 999 (C=S), 2915 (-CH), 3100 (=CH), 517 (Sn-C), 354 (Sn-S); ^{1}H NMR ($CDCl_3$) δ ppm = 7.87-7.65 (q, 10H, Sn-$C_6\underline{H}_5$), 7.42-7.26 (m, 10H, N-$C_6\underline{H}_5$), 4.13 (t, 4H, N-$C\underline{H}_2CH_2CH_2CH_3$), 1.61 (m, 4H, N-$CH_2C\underline{H}_2CH_2CH_3$), 1.35 (m, 4H, N-$CH_2CH_2C\underline{H}_2CH_3$), 0.89 (t, 6H, N-$CH_2CH_2CH_2\underline{C}H_3$); ^{13}C NMR ($CDCl_3$) δ ppm = 201.95 (-$\underline{C}S_2$), 145.24, 129.52, 128.18, 126.33 (N-$\underline{C}_6H_5$), 150.18, 142.00, 135.81, 134.46 (Sn-$\underline{C}_6H_5$), 59.31 (N-$\underline{C}H_2CH_2CH_2CH_3$), 28.99 (N-$CH_2\underline{C}H_2CH_2CH_3$), 19.84 (N-$CH_2CH_2\underline{C}H_2CH_3$), 13.69 (N-$CH_2CH_2CH_2\underline{C}H_3$); ^{119}Sn NMR ($CDCl_3$): δ ppm = -319.48;

$C_{34}H_{38}N_2S_4Sn$ (722.1) = C, 56.59; H, 5.31; N, 3.88; S, 17.77; Found = C, 56.09; H, 5.03; N, 4.01; S, 17.99.

3.8. Results and discussion on the organotin(IV) *N*-butyl-*N*-phenyldithiocarbamate complexes

3.8.1. Synthesis of organotin(IV)*N*-butyl-*N*-phenyldithiocarbamate complexes

The synthesis of ligand $\mathbf{L}^3$ followed similar reaction procedure presented in scheme 3.1. However, the ligand is less stable compared to $\mathbf{L}^1$ and $\mathbf{L}^2$ due to the increased number of carbon attached to the N-atom. Also, the ammonium salts of the dithiocarbamate of *N*-alkyl-*N*-phenyl derivatives are less stable at room temperature; thus, the ligand was complexed with the respective organotin(IV) salts after rinsing. All complexes obtained were stable at room temperature. They were obtained as white solids and are soluble in dichloromethane, chloroform, dimethylsulfoxide and sparingly soluble in alcohols. These complexes are all air stable and crystalline solids with melting points ranging from 207–230°C.

3.8.2. FTIR spectral studies of organotin(IV) *N*-butyl-*N*-phenyl dithiocarbamate complexes

The IR spectra of the ligand has been reported and was carefully compared to the corresponding complexes [25]. Studies on the lengthening of the *N*-alkyl moiety of the complexes have been shown to be accompanied with a decrease in the frequency of C-N band [38]. The lower values observed for this band is due to the length of the *N*-butyl group of the ligand moiety. This stretching vibrational band of C–N was found in the range 1445 – 1440 cm^{-1} in all the complexes, and have been attributed to the delocalization of electron towards the tin centre of the complexes [7]. A single peak observed for the vibrational band of C–S in the frequency range of 1001 – 999 cm^{-1} suggested a bidentate mode of coordination [9]. Other important bands which supported the complex formation are the Sn–S band found around 357 – 354 cm^{-1} and the Sn–C stretching band for the alkyl moiety attached to the tin centre found around 552– 517 cm^{-1} [39].

3.8.3. Nuclear Magnetic Resonance studies of the organotin(IV) and *N*-butyl-*N*-phenyldithiocarbamate complexes

In the ^1H NMR spectra of the complexes, signals from the ligand moiety ascribed to the methylene and methyl protons of the *N*-butyl group where found in the spectra of all the complexes in the range 4.14 - 1.25 ppm. These frequencies are somewhat higher than for free methylene and methyl protons, and it is due to their close proximity to the electronegative

nitrogen, consequently resulting in increase in the chemical shifts. The terminal methyl protons resonated at lower field due to the strength of dishielding which decreases with increase in the distance from the thioureide bond [40]. Signals attributed to the protons of the phenyl rings of the ligand moiety, in all the complexes, were observed in the region 7.48–7.16 ppm as multiplet. Proton signals from the alkyl group of the organotin moiety were found in the spectrum of the dimethyl complex **13** as a strong singlet at 1.57 ppm, in the butyl complexes **12** and **14** in the range 2.01 – 0.89 ppm [12], and as a complex multiplet for the phenyl derivative **15** in the region 7.87-7.65 ppm [41].

The ^{13}C NMR spectra of the complexes showed the carbon signal of the thioureide bond in the range of 203 – 201 ppm due to an increase in the π-bond order in $-NCS_2$ moiety [41]. From the ligand fragment, carbon signals attributed to the *N*-butyl group resonated for the methylene carbon around 59, 28 and 19 ppm; while the terminal methyl carbon resonated around 13 ppm [25]. The aromatic carbon resonated in the range of 145 – 126 ppm in all the complexes, while the alkyl derivatives on the tin centre resonated at 14.38 ppm in complex **13** (methyl carbon) and in the range 31.69 –13.90 ppm in complexes **12** and **14** (butyl carbons). The carbon signals due to the aromatic carbons in the phenyltin complex **15** resonated in the region 150 – 134 ppm.

In these complexes, the ^{119}Sn NMR spectra showed a singlet in the range -310 to -330 ppm which suggests a hexa-coordinated geometry about the tin center.

3.8.4. X-ray crystallographic studies of the organotin(IV) and *N*-butyl-*N*-phenyldithiocarbamate complexes

Crystallographic information about the structure and the refinement parameters of complexes **13** and **14** are summarized in Table 3.7. Selected bond angles needed for the description of the geometry about the tin atom are presented in Table 3.8. The respective numbering of atom in the structure of the complexes observed in the ORTEP plot and the crystal packing diagram of the complexes are shown in Figure 3.20 – 3.21.

3.8.4.1. Structural description of dimethyltin(IV)*N*-butyl-*N*-phenyldithiocarbamate complex (**13**)

From the ORTEP plot of complex **13**, the dithiocarbamate ligand was bonded to the central organotin moiety via the four sulfur atoms as shown in Figure 3.20 (a). This consequently

resulted in a six coordinate geometry about the central metal. One of the butyl group from the ligand was disordered which may be due to the bulky nature of the complexes. In the crystal packing diagram in Figure 3.20(b), complex **13** is monomeric with two molecules of the complex in a unit cell. Studies have shown that dithiocarbamate complexes are rarely symmetrical, which is due to the unequal distance of the Sn-S bond amongst other reasons [34,35,42]. In this complex, the differences in the Sn-S bond distances showed Sn1-S12 and Sn1-S22 bonds to be longer than Sn1-S11 and Sn1-S21 bond, and, thus, contributes to the asymmetric nature of this molecule [42]. The bond distances observed for Sn-S are Sn1-S11 [2.5242(5)], Sn1-S12 [2.9350(5)], Sn1-S21 [2.5198(5)] and Sn1-S22 [2.9962(5)]. These Sn-S bonds are longer than the expected sum of the covalent radii of a typical Sn-S bonds (2.42 Å) but are well below the expected van der Wall radii (3.97A), hence, are true bonds [18]. The Sn-S bonds are anisobidentate in nature due to the slight opening of the C-Sn-C bond angle (138.84) towards 180°, moving away from 109° [19]. However, if the bond angle of C-Sn-C becomes linear, the mode of coordination becomes isobidenate [43]. This observed bond angle between C-Sn-C showed a deviation from a cis-trans pathway of the C–Sn–C bond which was expected at 134°, thus contributed to the distortion of the expected octahedral geometry [42]. A typical C-S has a bond length of 1.81 Å. However, the average distance of C-S found was 1.7171(16) Å, which is shorter than a typical C-S bond suggesting a partial double bond character usually found in dithiocarbamate complexes [21]. From the bond angles observed for S12-Sn1-C3 [84.41(5) °], S12-Sn1-C4 [84.25(5) °], S22-Sn1-C3 [82.53(5) °], S22-Sn1-C4 [83.77(5) °], there exists a relationship between the Sn-C bonds and the Sn-S bond (i.e. the bending of Sn-C bonds towards the longer Sn-S). This relationship originates due to stearic reason and the repulsion between the metal center and the bonding electron pair of sulfur atoms [22]. The number of coordination around the tin metal resulted in a significant change in the bite angle of the chelating dithiocarbamate ligand which, consequently, gave rise to different bond distances [21]. Therefore, the six coordination here appeared as a distorted octahedral geometry due to the asymmetric nature of the dithiocarbamate ligand and the unequal Sn-S bond lengths. Thus this geometry is best described as skew trapezoidal-bipyramidal [7].

3.8.4.2. Structural description of dibutyltin(IV)*N*-butyl-*N*-phenyldithiocarbamate complex (**14**)

From the ORTEP plot of complex **14** shown in Figure 3.21(a), the dithiocarbamate ligand is bonded to the adjacent sides of the tin metal from the organotin moiety via three of the four

available sulfur atoms from the ligand, while the remaining sulfur atom hangs as a pendant. Thus, a five coordinate geometry about the tin metal was observed [33]. Furthermore, the crystal packing diagram in Figure 3.2(b), shows the complex to be monomeric with four molecules per unit cell. In this complex, the bond Sn1-S21 was found to be significantly shorter [2.5128(6) Å] than Sn1-S22 [2.9723(7) Å] with a bite angle of [81.05(2) °]. This, therefore, results in an anisobidentate coordination with the tin atom at this side of the complex. A monodentate coordination, with a bond length of 2.5193(5) Å, was observed between one of the sulfur atoms and the tin atom on the second dithiocarbamate group. However, a contact distance of 3.2078(8) Å was observed in the pendant sulfur atom with the Sn metal which was due to a change in one of the short Sn-S bonds originating from a weak coordination by a sulfur atom in the dithiocarbamate moiety. Consequently, it caused a change in position approximately orthogonal to the Sn-S12 plane [34]. In the dibutyltin, atoms C31, C41 and S21 are all in equatorial position, while S11 and S22 are axial to each other with an angle [S11-Sn1-S22] 145.88(2)° around the tin atom. Thus, the geometry around the central tin atom is best described as distorted trigonal bipyramidal. Complexes with similar structure have been reported for organotin dithiocarbamate [20, 36]. Here, the average distance observed for the C-S bond is 1.713 (2) Å, which is shorter than a typical C-S bond suggesting a partial double bond character similar to what was observed for complex 13. The C-N bonds distances were observed at 1.341(3) A° [N1–C11] and 1.470(3) A° [N2–C12] from the two dithiocarbamate moieties on the adjacent sides of the complex. These bond lengths deviated from the value of a typical C-N bond [1.47 A°], but similar to those observed for other dithiocarbamate complexes.

Table 3.7: Crystal data, data collection for and refinement parameters for complexes **13** and **14**

Complex	**13**	**14**
Empirical formula	$C_{24}H_{34}N_2S_4Sn$	$C_{30}H_{46}N_2S_4Sn$
Formula weight	597.48	681.64
Crystal size (mm)	0.35 x 0.37 x 0.40	0.28 x 0.38 x 0.61
Crystal system	monoclinic	monoclinic
Crystal habit	colorless needle	colorless needle
Space group	P-1 (No.2)	P21/c (No.14)
a (Å)	9.4834(6)	10.5361(3)
b (Å)	11.6483(7)	18.0744(5)
c (Å)	13.1870(8)	18.0525(5)
β (°)	90.743(2)	94.005(1)
U (Å^3)	1393.54(15)	3429.41(17)
Z	2	4
Dcalc (g cm^{-3})	1.424	1.320
F(000)	612	1416
θ range (°)	1.5 – 28.3	1.6 -28.4
Index range	-12: 11 ; -15: 14 ; -17:15	-14: 14 ; -24: 24 ; -24: 24
Total, unique reflections	37128, 6923	48198, 8545
Observed reflections $I > 2\sigma(I)$	6358	8545
Number of parameters refined	314	338
Final R, w$R2$	0.0201, 0.0489	0.0281, 0.0696
Goodness-of-fit (GOF)	1.03	1.03

Table 3.8: Selected bond distances and angles for complexes **13** and **14**

13		**14**	
Bond distances (Å)		**Bond distances (Å)**	
Sn1-S11	2.5242(5)	Sn1-S11	2.5114(7)
Sn1-S12	2.9350(5)	Sn1-S21	2.5128(6)
Sn1-S21	2.5198(5)	Sn1-S22	2.9723(7)
Sn1-S22	2.9962(5)	Sn1-C31	2.137(2)
Sn1-C3	2.1236(18)	Sn1-C41	2.140(2)
Sn1-C4	2.1219(17)	S11-C11	1.743(2)
S11-C11	1.7455(15)	S12-C11	1.690(2)
S12-C11	1.6900(16)	S21-C21	1.746(2)
S21-C21	1.7432(16)	S22-C21	1.683(2)
S22-C21	1.6897(17)	N1-C11	1.341(3)
N1-C11	1.344(2)	N1-C12	1.470(3)
N1-C12	1.481(2)	N1-C111	1.446(3)
N1-C111	1.444(2)	N2-C21	1.334(3)
N2-C21	1.333(2)	N2-C22	1.475(3)
N2-C22	1.491(3)	N2-C211	1.446(3)
N2-C211	1.446(3)		
Bond angles (°)		**Bond angles (°)**	
S11-Sn1-S12	65.56(1)	S11-Sn1-S21	81.05(2)
S11-Sn1-S21	85.77(1)	S11-Sn1-S22	145.88(2)
S11-Sn1-S22	150.62(2)	S11-Sn1-C31	105.62(6)
S11-Sn1-C3	106.01(5)	S11-Sn1-C41	105.79(6)
S11-Sn1-C4	104.87(5)	S21-Sn1-S22	64.93(2)
S12-Sn1-S21	151.31(2)	S21-Sn1-C31	84.96(6)
S12-Sn1-S22	143.82(1)	S21-Sn1-C41	108.06(6)
S12-Sn1-C3	84.41(5)	S22-Sn1-C31	95.91(8)
S12-Sn1-C4	84.25(5)	S22-Sn1-C41	87.99(6)
S21-Sn1-S22	64.86(1)	C31-Sn1-C41	133.22(8)
S21-Sn1-C3	105.39(5)	Sn1-S11-C11	99.15(8)
S21-Sn1-C4	103.40(5)	Sn1-S22-C21	80.55(8)
S22-Sn1-C3	82.53(5)	Sn1-S21-C21	94.31(7)
S22-Sn1-C4	83.77(5)	C11-N1-C12	122.89(19)
C3-Sn1-C4	138.84(7)	C21-N2-C22	121.59(19)
Sn1-S11-C11	93.21(5)	C11-N1-C111	120.31(18)
Sn1-S12-C11	80.96(5)	C12-N1-C111	116.75(18)
Sn1-S21-C21	94.32(6)	C21-N2-C211	122.14(18)
Sn1-S22-C21	79.86(5)	C22-N2-C211	116.26(18)
C11-N1-C12	120.41(14)	S11-C11-S12	121.58(13)
C21-N2-C22	121.71(17)	S11-C11-N1	115.66(16)
C11-N1-C111	123.15(13)	S12-C11-N1	122.76(17)
C12-N1-C111	116.33(13)	N1-C12-C13	113.10(19)
C21-N2-C211	121.99(15)	S21 -C21-S22	119.99(13)
C22-N2-C211	115.58(16)	S21-C21-N2	116.72(16)
S11-C11-S12	120.02(9)	S22-C21-N2	123.29(17)
S11-C11-N1	118.07(12)	N2-C22-C23	112.66(19)
S12-C11-N1	121.91(12)		
N1-C12-C13	112.63(14)		
S21-C21-S22	120.82(9)		
S21-C21-N2	116.59(13)		
S22-C21-N2	122.58(13)		
N2-C22-C23	111.03(19)		

Symmetry element i: -X, -Y, -Z -X, 1+Y, 1/2-Z

(a)

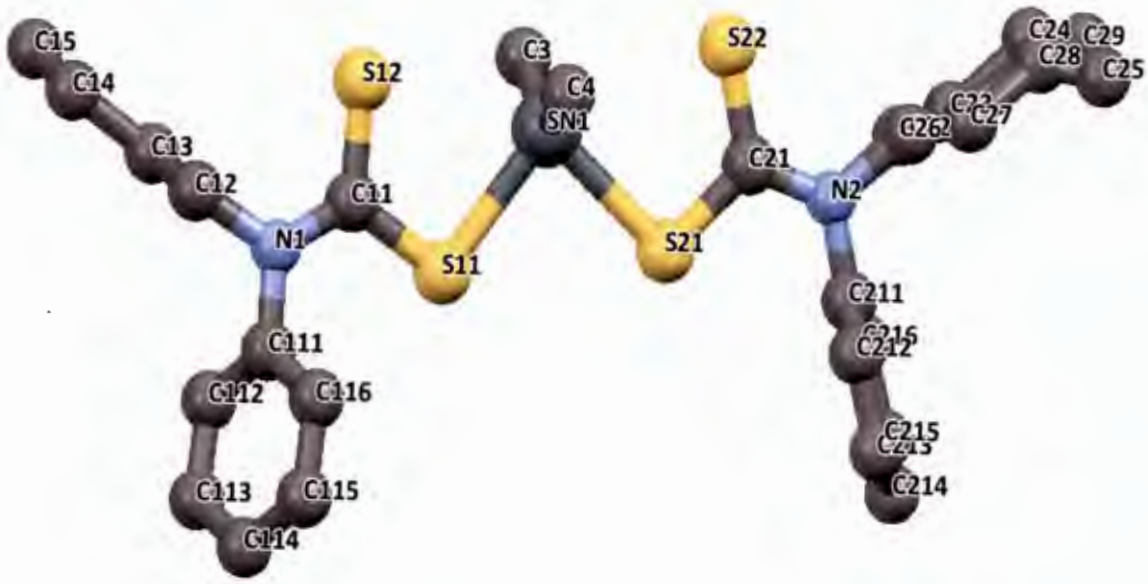

(b)

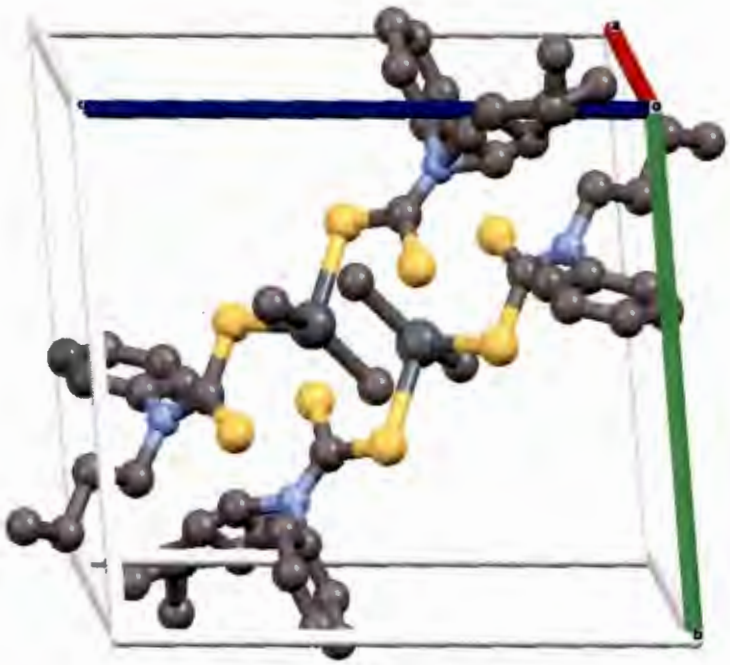

Figure 3.20: (a) Structure of dimethyltin(IV) *N*-butyl-*N*-phenyldithiocarbamate complex **(13)** drawn at 50% probability level displacement ellipsoids, and **(b)** the crystal packing viewed along the best axis.

(a)

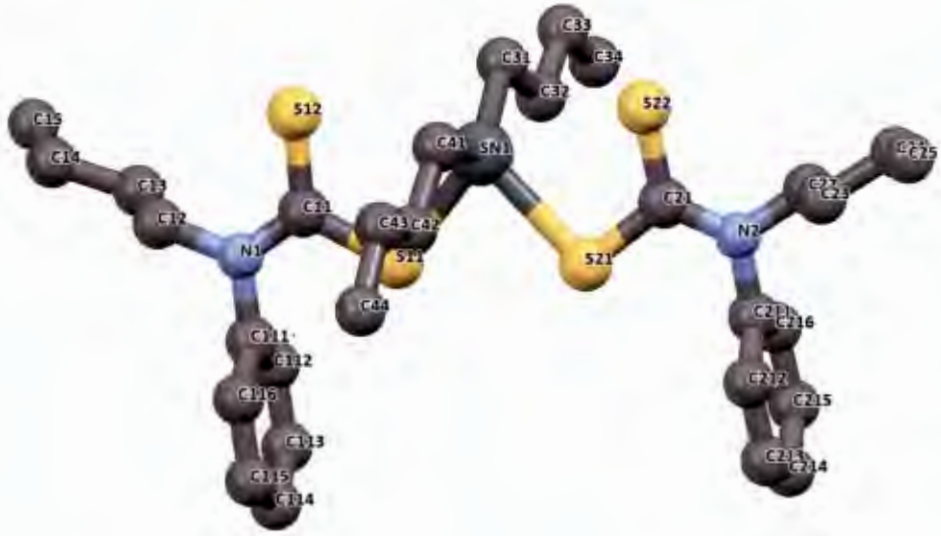

(b)

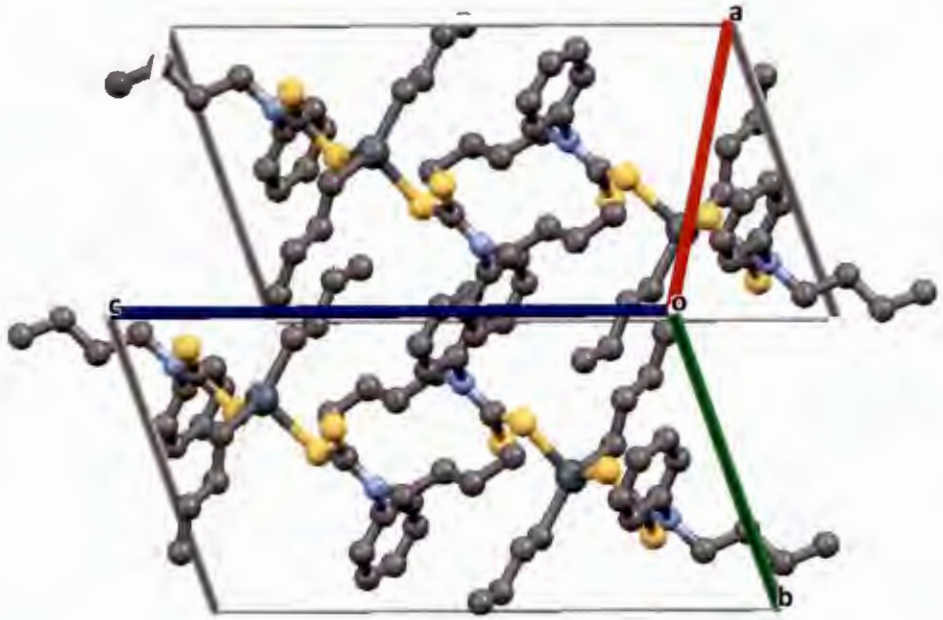

Figure 3.21: (a) Structure of dibutyltin(IV)*N*-butyl-*N*-phenyldithiocarbamate complex (**14**) drawn at 50% probability level displacement ellipsoids, and **(b)** the crystal packing viewed along the best axis

3.8.5. Thermogravimetric analysis (TGA) of organotin(IV)*N*-butyl-*N*-phenyldithiocarbamate complexes (12 -15)

A study of the thermal properties of the complexes was achieved by TGA/DTG analysis under nitrogen in the temperature range of 50 to 750 °C. The thermogravimetric graphs of the complexes as presented in Figures 3.22 – 3.25. Different compositional changes, based on mass losses, observed are summarized in Table 3.9. The complexes followed similar pattern, involving a single decomposition step except for complex **13,** which showed a two step decomposition pathway. Complexes **12, 14** and **15**, decomposed at varying temperature ranges of 112 – 298, 100 – 317 and 119 – 319 °C leaving residues with masses of about 22.67, 21.01 and 20.27% of the starting materials respectively. These values were found to agree well with the calculated value of SnS, which are 24.21, 22.00 and 20.78% respectively.

Complex **13** followed a two-step decomposition pattern. The first step occurred in the temperature range of 120 – 290 °C, due to the decomposition of the organic fragment of the complex. The mass found at this stage was 34.35% of the initial mass and a further decomposition occurred in a second and final step in the temperature range of 291 – 320 °C, which was about 23.65% of the starting mass. The mass of the residue was in good agreement with the calculated value of SnS (25.0%).

Complexes **13** and **15** gave more stable thermal behavior amogst these group of complexes with their final decomposition temperatures terminating at approximately 320 °C. Thus, pyrolysis amogst these complexe was achieved between 112 and 320 °C, which corresponded to the formation of thermally stable products.

Table 3.9: Thermal analysis data of complexes**12, 13, 14** and **15.**

Compounds	12	13	14	15
Temp. range of decom. (°C)				
1st stage 2nd stage	112 – 298 ———	120 – 290 291 – 320	100 – 317 ———	119– 319 ———
DTG peak T(°C)				
1st stage 2nd stage	283 ———	286 310	307 ———	318 ———
Prod. Obtained				
1st decomposition 2nd decomposition	SnS ———	$NCSSn(CH_3)_2$ SnS	SnS ———	SnS ———
Mass of res.(mg) Found (Calc)				
1st stage 2nd stage	2.50 (2.67) ———	3.48 (3.48) 2.40 (2.55)	5.95 (6.23) ———	2.37 (2.43) ———

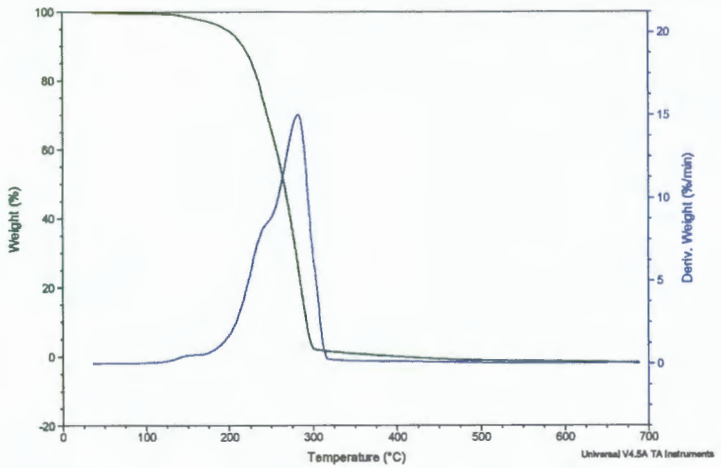

Figure 3.22: TG/DTG curves of complex **12** obtained in nitrogen atmosphere (75 mL/min), heating rate 10 °C/min.

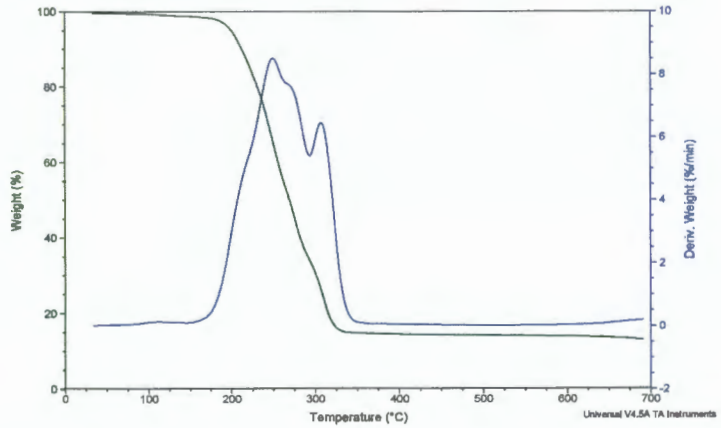

Figure 3.23: TG/DTG curves of complex **13** obtained in nitrogen atmosphere (75 mL/min), heating rate 10 °C/min.

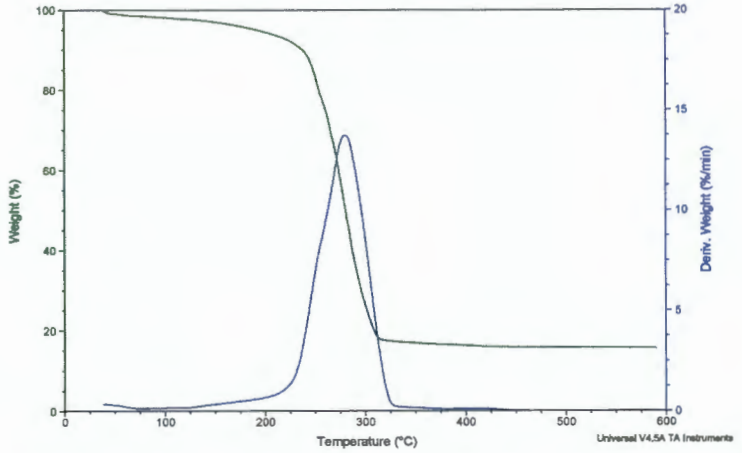

Figure 3.24: TG/DTG curves of complex **14** obtained in nitrogen atmosphere (75 mL/min), heating rate 10 °C/min.

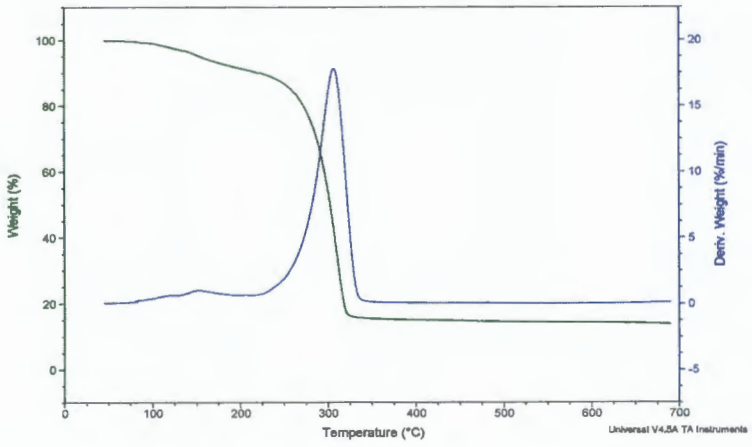

Figure 3.25: TG/DTG curves of complex **15** obtained in nitrogen atmosphere (75 mL/min), heating rate 10 °C/min.

3.9. Complexes of organotin(IV) with mixed ligands of *N,N*-methylphenyl-*N,N*-ethyl phenyldithiocarbamate

3.9.1. Synthesis of the organotin(IV) complexes, $R_2SnL^1L^2$ (R = CH_3, C_4H_9, C_6H_5)

The ligands $\mathbf{L^1}$ and $\mathbf{L^2}$ (0.005 mol) were separately dissolved in 10 mL of ethanol and then mixed together in a 100 mL round bottom flask. While stirring the solution of the two ligands in ice, ethanolic solution of the respective organotin(IV) salts (0.005 mol) was added and stirred for 2 h. The resultant white precipitates were filtered, washed with cold ethanol severally and dried under vacuum.

(16) $[(CH_3)_2Sn_2L^1L^2]$: Single-crystals suitable for X-ray diffraction analyses were obtained from dichloromethane-ethanol (4:1) solvent system; Yield: 2.54 g, (80.12%); M.pt.: 215–217 °C; Selected FTIR, υ (cm^{-1}): 1443 (C=N), 1236 (C_2-N), 1001 (C=S), 2911(-CH), 3033(=CH), 552 (Sn-C), 446 (Sn-S); ^{1}H NMR ($CDCl_3$) δ = 7.32–7.26 (m, 5H, $C_6\underline{H}_5$–N(CH_3)), 7.23–7.10 (m, 5H, $C_6\underline{H}_5$–N(C_2H_5)), 4.13 (q, 2H, $CH_3C\underline{H}_2$–N(C_6H_5)), 1.32 (t, 3H, $C\underline{H}_3CH_2$–N(C_6H_5)), 3.60 (s, 3H, $C\underline{H}_3$–N(C_6H_5)), 1.51 (s, 6H, Sn-($C\underline{H}_3$)$_2$); ^{13}C NMR ($CDCl_3$) δ = 202.90, 202.14 ($\underline{C}S_2$), 146.10, 129.49, 128.41,126.67, ($\underline{C}_6H_5$–N(CH_3));144.07,129.45,128.37, 125.97 ($\underline{C}_6H_5$–N(C_2H_5)), 53.20 ($CH_3\underline{C}H_2$–N(C_6H_5)), 12.15 ($\underline{C}H_3CH_2$–N(C_6H_5)), 46.47 ($\underline{C}H_3$–N(C_6H_5)), 14.24 (Sn–($\underline{C}H_3$)$_2$); ^{119}Sn NMR ($CDCl_3$): δ ppm = -311.96.

$C_{19}H_{24}N_2S_4Sn$ (527.38): C, 43.27; H, 4.59; N, 5.31; S, 24.32; Found: C, 43.12; H, 4.21; N, 4.99; S, 24.02%.

(17) $[(C_4H_9)_2SnL^1L^2]$: Single-crystals suitable for X-ray diffraction analyses were obtained from dichloromethane-ethanol (4:1) solvent system; Yield: 2.67 g, (74.37%); M.pt.: 222 – 223 °C; Selected FTIR, υ (cm^{-1}): 1488 (C=N), 1235 (C_2-N), 1001 (C=S), 2917(-CH), 3032 (=CH), 553 (Sn-C), 427 (Sn-S); ^{1}H NMR ($CDCl_3$) δ = 7.32–7.26(m, $C_6\underline{H}_5$–N(CH_3)), 7.23–7.10 (m, $C_6\underline{H}_5$–N(CH_3CH_2)), 4.13 (q, 2H, $CH_3C\underline{H}_2$–N(C_6H_5)), 1.32 (t, 3H, $C\underline{H}_3CH_2$–N(C_6H_5)), 3.61 (s, 3H, $C\underline{H}_3$–N(C_6H_5)), 2.10 (t, 4H, Sn-$C\underline{H}_2CH_2CH_2CH_3$), 1.87 (m, 4H, Sn-$CH_2C\underline{H}_2CH_2CH_3$), 1.37 (m, 4H, Sn-$CH_2CH_2C\underline{H}_2CH_3$), 0.89 (t, 6H, Sn-$CH_2CH_2CH_3\underline{C}H_3$); ^{13}C NMR ($CDCl_3$) δ = 202.87, 202.97 ($\underline{C}S_2$), 146.93, 129.46,128.30,126.03, ($\underline{C}_6H_5$–N(CH_3); 144.96,129.42, 127.09, 126.00 ($\underline{C}_6H_5$–N(C_2H_5), 53.12($CH_3\underline{C}H_2$–N(C_6H_5)), 12.21 ($\underline{C}H_3CH_2$–N(C_6H_5)), 46.47 ($\underline{C}H_3$–N(C_6H_5)), 33.44 (Sn-$\underline{C}H_2CH_2CH_2CH_3$), 28.51 (Sn-$CH_2\underline{C}H_2CH_2CH_3$), 26.49 (Sn-$CH_2CH_2\underline{C}H_2CH_3$), 13.89 (Sn-$CH_2CH_2CH_2\underline{C}H_3$); ^{119}Sn NMR ($CDCl_3$): δ ppm = -318.85.

$C_{25}H_{36}N_2S_4Sn$ (611.54): C, 49.10; H, 5.93; N, 4.58; S, 20.97; Found: C, 48.90; H, 5.53; N, 4.50; S, 21.08%

(18) $[(C_6H_5)_2SnL^1L^2]$: Yield: 3.01 g, (79.62%), M.pt.: 223–225°C; Selected FTIR, υ (cm^{-1}): 1461 (C=N), 1233 (C_2-N), 995 (C=S), 2970(-CH), 3036 (=CH), 552 (Sn-C), 447 (Sn-S);^{1}HNMR ($CDCl_3$) d = 7.98–7.80 (m, 10H, $C_6\underline{H}_5$–Sn), 7.39–7.30 (m,5H,$C_6\underline{H}_5$–N(CH_3)),7.27–7.13(m, 5H, $C_6\underline{H}_5$–N(CH_2CH_3)), 4.01 (q, 2H, $CH_3C\underline{H}_2$–N(C_6H_5)), 1.28 (t, 3H, $C\underline{H}_3CH_2$–N(C_6H_5)), 3.62 (s, 3H, $C\underline{H}_3$–N(C_6H_5));^{13}C NMR ($CDCl_3$) d = 202.15, 201.56 ($\underline{C}S_2$), 147.05, 134.34, 129.21, 125.81, ($\underline{C}_6H_5$–N(CH_3)) 146.96,131.51, 128.85,125.01($\underline{C}_6H_5$–N(CH_2CH_3)) 149.55, 135.83, 134.73, 125.11 ($\underline{C}_6H_5$–Sn), 54.24 ($CH_3\underline{C}H_2$–N(C_6H_5)), 12.38 ($\underline{C}H_3CH_2$–N(C_6H_5)) 47.31 ($\underline{C}H_3$–N(C_6H_5)), ; ^{119}Sn NMR ($CDCl_3$): δ ppm = -318.62.

$C_{29}H_{28}N_2S_4Sn$ (651.52): C, 53.46; H, 4.33; N, 4.30; S, 19.69; Found: C, 52.96; H, 4.03; N, 3.99; S, 20.09 %.

3.10 Results and discussion on the organotin(IV) *N,N*-methylphenyl-*N,N*-ethylphenyl dithiocarbamate complexes (16 - 18)

3.10.1. Synthesis of organotin *N,N*-methylphenyl-*N,N*-ethylphenyldithiocarbamate complexes

Complexes derived from mixed ligand sources have shown better stability in reaction media than those from a single ligand source whenever a competition arises in such reaction medium [44]. Although this is an established fact, nonetheless, certain properties and factors play vital roles in the preference of formation. This includes coordination number of the metal and its electronic structure, nature of the donor ligands and their mutual effects in a mixed ligand, structure and geometry of the complex and the mixed complex's coordination equilibria in solution amongst other factor [44,45]. For these complexes, equimolar amount of $\mathbf{L^1}$ and $\mathbf{L^2}$, and the organotin salts (of the formula R_2SnCl_2) were stirred in cold ethanol to give the respective complexes as presented in scheme 3.2. All complexes obtained were stable at room temperature. They were white, crystalline solids, and soluble in dichloromethane, chloroform, dimethylsulfoxide, but sparingly soluble in alcohols.

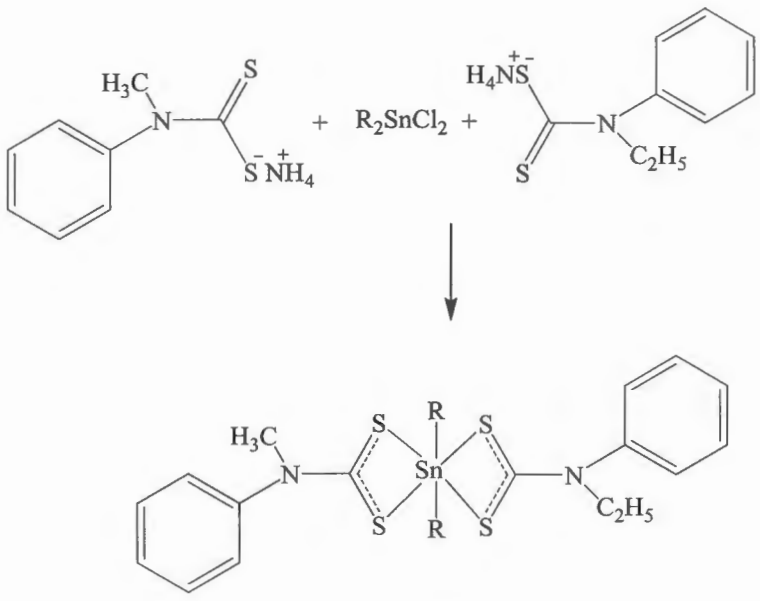

R= CH_3 **(16)**, C_4H_9 **(17)**, and C_6H_5**(18)**

Scheme 3.2: Organotin complexes of mixed ligand of dithiocarbamate $\mathbf{L^1}$ and $\mathbf{L^2}$

3.10.2. FTIR spectral studies of organotin(IV) *N,N*-methylphenyl-*N,N*-ethylphenyl dithiocarbamate complexes

The vibrational mode of the C–S, which often suggests the mode of coordination (either monodentate or bidentate), was found as a single peak for these complexes around 1001 – 995 cm^{-1} and the stretching vibrational band of C–N appeared around 1488 –1443 cm^{-1}. The single peak found for the vibrational mode of C–S suggest a bidentate mode of coordination [9]. The frequency range of the stretching C–N vibrational band suggest a double bond character which may be due to the delocalization of electron towards the tin center of the complexes [7]. Other important peaks are the Sn–S peak found around 447 – 427 cm^{-1}, which supports the coordination of the organotin moiety to the dithiocarbamate salt, thus confirmed the complex formation. The Sn–C stretching band for the alkyl group attached to the tin centre appeared around 552 – 553 cm^{-1} [39].

3.10.3. Nuclear Magnetic Resonance studies of the organotin *N,N*-methyl phenyl-*N,N*-ethylphenyl dithiocarbamate complexes

The chemical shifts values for each of the complexes were found in their expected regions in the ^1H NMR spectra. The influence of the methyl and ethyl substituents are evidently observed in the chemical shift of each complex obtained. In the dithiocarbamate moiety, a singlet ascribed to the proton of the methyl group attached to the electronegative nitrogen was

found in the region 3.62 – 3.60 ppm. Quartets in the region around 4.13 – 4.01 ppm were observed in all the complexes, and have been ascribed to the methylene protons. However, triplets in the region 1.53 – 1.28 ppm, ascribed to the methyl protons of the ethyl group bonded to the nitrogen atom, were observed in the complexes [46]. These methyl protons are found in the lower field because the magnitude of the dishielding often decreases with increased distance from the metal centre of the thioureide bond [40]. The proton of the aromatic ring in the ligand moiety were found as multiplets in the region 7.39 – 7.10 ppm. The chemical shifts of the organotin group were also found in their expected region. The methyl group of complex **16** was found as a singlet at 1.51 ppm, and the phenyl group of complex **18** as complex multiplet around 7.98–7.80 ppm. For the dibutyltin(IV) derivative of complex **17**, the chemical shift in the region 2.10 – 0.89 ppm were observed similar to what has been reported for dibutyltin complex [47].

In the ^{13}C NMR spectra of all the complexes, two distinct peaks (due to the different organic substituents resulting into variation in the magnetic equivalence) associated with the thioureide carbon (-NCS_2) of each of the ligand moiety were observed between 202 and 201 ppm. These signals indicate the contribution of the double bond character to a formally single N–C bond in the dithiocarbamate moiety. That is the admixture of the sp^2 hybridized state to the sp^3 orbitals of the nitrogen atom, thus a considerable δ^+ surplus charge is localized on the nitrogen atom, while a δ^- charge is delocalized through the four-membered metallochelate ring –CS_2M [48]. The dithiocarbamate group with greater trans-influence has more shielded – CS_2 and, thus, has a greater electronic density [49]. Methylene carbons in the complexes resonates around 53 and 54 ppm, and the CH_3 of the ethyl moiety resonated around *ca.* 12 ppm due to the electronegative nitrogen and the thioureide pie-system [16]. Two sets of peaks were found in the aromatic region ascribed to the aromatic carbons of the ligands: between 147 and 144 ppm for $\mathbf{L^2}$, which are of low intensity and 130 -125 ppm for $\mathbf{L^1}$, which are of high intensity. The non-equivalence nature of the two aromatic ring due to different alkyl groups on the nitrogen atom resulted in this two region occurring at different environment on the spectra [16]. For the organotin(IV) moieties in the complexes, the methyl carbon of complex **16** resonated at approximately 14 ppm and the butyl carbon of complex **17** resonated in the region 33.44 – 13.89 ppm. The carbon due to the phenyl moiety of complex **18** resonated around 149 – 125 ppm.

The resonant frequency of the ^{119}Sn NMR of the complexes is significantly lower in than the corresponding organotin(IV) salts [11]. In these complexes, the shifts (δ) observed ranged from -311 to -318 ppm, which suggested a hexa-coordinated geometry around the tin centre.

3.10.4. X-ray crystallographic studies of dimethyl and dibutyl *N,N*-methyl phenyl-*N,N*-ethyl phenyldithiocarbamate complexes (16) and (17)

Single crystals of complexes **16** and **17** were obtained from dichloromethane-ethanol (4:1) solvent system. Useful crystallographic data and geometric parameters have been summarized in Table 3.10. The bond lengths and angles from the analysis of the complexes have been summarized in Table 3.11. Figures 3.26 and 3.27 show the ORTEP plot with the structure and numbering of each of the complexes.

3.10.4.1. Structural description of complex **16**

Complex **16**, as presented in Figure 3.26, showed a five coordinate geometry about the central tin atom which is centrosymmetrical with four molecules in the asymmetric unit cell. A portion of the molecule exhibits positional disorder. The atoms involved are S4A, S4B, C5A, C5B, C6A and C6B, and they are disordered over two positions. The disordered S atoms have a major component that is present 78.261(3)% of the time and both of these atoms were refined anisotropically. The minor component was also successfully refined anisotropically. The disordered methyl and ethyl atoms have a major component that is present 62.761(5) % of the time and all of these atoms were also refined anisotropically. The above-mentioned atoms had thermal displacement parameter constraints applied to them. This disorder was consistent with what was observed in the NMR spectrum of this complex.

The complex has one of the ligands (with the *N*-ethyl group) forming a chelate with the central tin atom through the available sulfur atoms. The second dithiocarbamate unit with the *N*-methyl group was bonded through a single sulfur atom thereby leaving the second sulfur to hang as a pendant [33]. The sulfur–tin bond are rarely symmetrical for dithiocarbamate complexes [34,35]. Hence, Sn1-S1 is significantly longer [2.9178 (8)Å] than the Sn1-S2 [2.5317 (7)Å], with a bite angle of [65.680 (17)]. The unequal distances of the Sn-S bond in the chelate unit of this complex make the complex unsymmetrical. The second unit of the ligand was bonded to the tin atom in a monodentate fashion through a sulfur atom (S3) with a bond length of [2.5285 (7)Å]. The non-boding distance observed for the pendant S4 atom resulted from the change observed in Sn-S bond of one the short distances due to weak

coordination of a sulfur atom in the ligand moiety, which consequently changed the position approximately orthogonal to the Sn-S2 plane [34]. This occurrence of the pendant sulfur S4 in the complex have resulted due to steric demands or lack of vacant orbitals in the tin center for coordination (electronic reasons). Thus, no enough space for the coordination of the second sulfur, which consequently leads to high activation barrier [50]. The dimethyltin moiety with C3 and C4 atoms along with the S2 atom occupy an equatorial position while S1 and S3, [S1-Sn1-S3], are axial to each other with an angle of 149.212 (18)°. This arrangement results in a geometry around the central tin atom best described as a distorted trigonal bipyramidal geometry which is similar to what has been reported [20, 36]. A typical observed single C-S bond length is found at 1.82 Å, which is longer than that observed for a double bond at 1.67 Å [36]. In this complex, the average distance observed from the values in Table 3.10 for the C-S bond is 1.72 Å. This is signifcantly shorter than the value expected for a single (C-S) bond, but also longer than the expected for a double bond (C=S). Hence, indicative of a partial double bond character within the thiouride bond. There is also a deviation from the expected value of a simple C-N bond which is expected at 1.47 Å. The N1-C1 and N2-C2 have a bond distance of 1.341 (2) and 1.339 (3) Å respectively, which is shorter compared to the distance observed in a simple C-N, but similar to what has been reported in literature [32].

3.10.4.2. Structural description of complex **17**

From the crystallographic parameter obtained, and shown in Table 3.9, complex **17** was triclinic, having two molecules per unit cell. Portions of the molecule in the asymmetric unit exhibits extensive positional disorder, but consistent with what was observed in the corresponding NMR spectrum of this complex. The distortion observed in this complex has been attributed to the coordination around the tin metal which, in turn, resulted in changes in the interatomic distances and angles [21]. From the ORTEP plot in Figure 3.27, both dithiocarbamate ligands coordinated in a monodentate fashion with the central tin atom. The bond distance are Sn1-S1 [2.5077 (5)], Sn1-S3 [3.1254 (7)], Sn1-S2 [2.5019 (5)] and Sn1-S4 [3.1365 (6)] which, thus, make the complex asymmetrical. The shorter bonds can be clearly observed, but the longer bond lengths are a non-bonding distance observed for the pendants S3 and S4. This is due to the change observed in Sn-S bond of one the short distances and is attributed to weak coordination of a sulfur atom in the ligand moiety. These bonds are significantly lower than the sum of the Van der Waal radii (3.97A) [18]. Although these

bonds are weak, however, they are true bonds. These weak bonds may be due to the strong steric interaction of the two butyl groups on the Sn atom which reduces the chances of the second sulfur from coordinating with the metal centre [23]. This, thus, made the complex anisobidentate in coordination due to this unequal Sn-S bond length. The slight opening of the C-Sn-C bond angle which is at 136.86 (8)° further supports the anisobidentate nature of this coordination [20]. The short distance have the strongest bond of the two types of Sn-S bond and this angles S2-Sn1-S1 are subtending to each other at 81.825 (16)° which thus contributes to the distortion of the complexes away from the usual octahedral geometry. In this complex, the average distance observed for the C-S bond is 1.716 Å which is indicative of a partial double bond character within the thioureide bond.The C3–Sn–C7 bond angle is expected at 134° for the alkyl (C31-Sn1-C41) groups attached to the tin center was found axially at 136.86 (8)°, showing a slight deviation from the cis-trans pathway of this bond [18]. The deviations observed in the crystallographic data for this complex is due to the bulky coordination and the number of coordination on the tin metal [21]. Here, the geometry around the Sn center is best described as a distorted skew trapezoidal-bipyramidal similar to what has been reported[7,23]. This may be due to the large contact distance of one of the long Sn-S bond around the tin center.

Table 3.10: Crystal data collection and refinement parameters of dimethyl **(16)** and dibutyl(**17**) complexes of *N,N*-methyl phenyl-*N,N*-ethyl phenyldithiocarbamate

Complex	**16**	**17**
Empirical formula	C19 H24 N2 S4 Sn	C23H30.40N2S4Sn·2(CH3)
Formula weight	526.60	611.89
Crystal size (mm)	0.35 × 0.21 × 0.14	0.33 × 0.16 × 0.12
Crystal system	monoclinic	Triclinic
Crystal habit	Plate, clear colourless	Flat, clear colourless
Space group	P 21/c (14)	P -1
a (Å)	11.042 (3)	10.949 (9)
b (Å)	7.895 (2)	11.756 (9)
c (Å)	26.355 (7)	13.458 (10)
β (°)	96.955 (7)	68.346 (2)
U (Å^3)	2280.8 (11)	1424.65 (19)
Z	4	2
*D*calc (g cm^{-3})	1.534	1.426
F(000)	1060	628.8
θ range (°)	2.7–28.4	2.3–28.3
Index range	-14:14;-10:10;-35: 35	-14:14;-15:15; -17:17
Total, unique reflections	36539,5734	45832,7104
Observed reflections *I*> 2σ(*I*)	6130	6632
Number of parameters refined	254	311
Final *R*, w*R2*	0.0248, 0.0594	0.026,0.066

Table 3.11: Selected interatomic distances and angles dimethyl **(16)** and dibutyl**(17)** complexes of *N,N*-methyl phenyl-*N,N*-ethyl phenyldithiocarbamate

17		**16**	
Bond distances (Å)		**Bond distances (Å)**	
Sn1-S1	2.5077 (5)	Sn1-S1	2.9178 (8)
Sn1-S2	2.5019 (5)	Sn1-S2	2.5317 (7)
Sn1-S3	3.1254 (7)	Sn1-S3	2.5285 (7)
Sn1-S4	3.1365 (6)	Sn1-C3	2.117 (2)
Sn1-C3	2.1472 (19)	Sn1-C4	2.123 (2)
Sn1-C7	2.1359 (18)	S1-C1	1.6913 (19)
S1-C1	1.744 (2)	S2-C1	1.743 (2)
S3-C1	1.6832 (19)	S3-C2	1.743 (2)
S2-C2	1.7414 (18)	S4B-C2	1.758 (11)
S4-C2	1.6879 (19)	N1-C1	1.341 (2)
N1-C1	1.343 (2)	N1-C5A	1.476 (3)
N1-C24A	1.472 (3)	N1-C8	1.440 (2)
N1-C11	1.446 (3)	N2-C2	1.339 (3)
N2-C2	1.345 (2)	N2-C7	1.482 (3)
N2-C23A	1.473 (2)	N2-C14	1.444 (3)
N2-C17	1.473 (2)		
Bond angles (°)		**Bond angles (°)**	
S2-Sn1-S1	81.825 (16)	S1-Sn1-S2	65.680 (17)
C3-Sn1-S1	106.97 (6)	S1-Sn1-S3	149.212 (18)
C3-Sn1-S2	105.64 (6)	S1-Sn1-C3	84.07 (7)
C7-Sn1-S1	105.22 (5)	S1-Sn1-C4	85.63 (7)
C7-Sn1-S2	106.69 (5)	S2-Sn1-S3	84.05 (2)
C7-Sn1-C3	136.86 (8)	S2-Sn1-C3	107.21 (7)
C1-S1-Sn1	95.55 (6)	S2-Sn1-C4	100.61 (7)
C2-S2-Sn1	96.18 (7)	S3-Sn1-C3	100.57 (7)
C1-N1-C11	121.83 (17)	S3-Sn1-C4	106.31 (6)
C1-N1-C24A	122.05 (18)	C3-Sn1-C4	142.94 (9)
C1-N1-C24B	122.05 (18)	Sn1-S1-C1	81.33 (7)
C11-N1-C24A	116.12 (17)	Sn1-S2-C1	92.85 (7)
C11-N1-C24B	116.12 (17)	Sn1-S3-C2	93.23 (7)
C2-N2-C17	121.22 (15)	C1-N1-C5A	121.44 (17)
C2-N2-C23A	121.59 (17)	C1-N1-C8	120.66 (16)
C2-N2-C23B	121.59 (17)	C5A-N1-C8	117.81 (16)
C17-N2-C23A	117.15 (16)	C2-N2-C14	121.22 (16)
C17-N2-C23B	117.15 (16)	C7-N2-C14	117.33 (17)
S3-C1-S1	120.54 (11)	S1-C1-S2	120.67(15)
N1-C1-S1	116.65 (14)	S1-C1-N1	122.15 (15)
N1-C1-S3	122.81 (15)	S2-C1-N1	117.92 (14)
S4-C2-S2	121.08 (11)	S4A-C2-S3	120.76 (14)
N2-C2-S2	116.52 (14)	N2-C2-S3	117.20 (15)
N2-C2-S4	122.40 (14)	S4-C2-N2	121.96 (17)

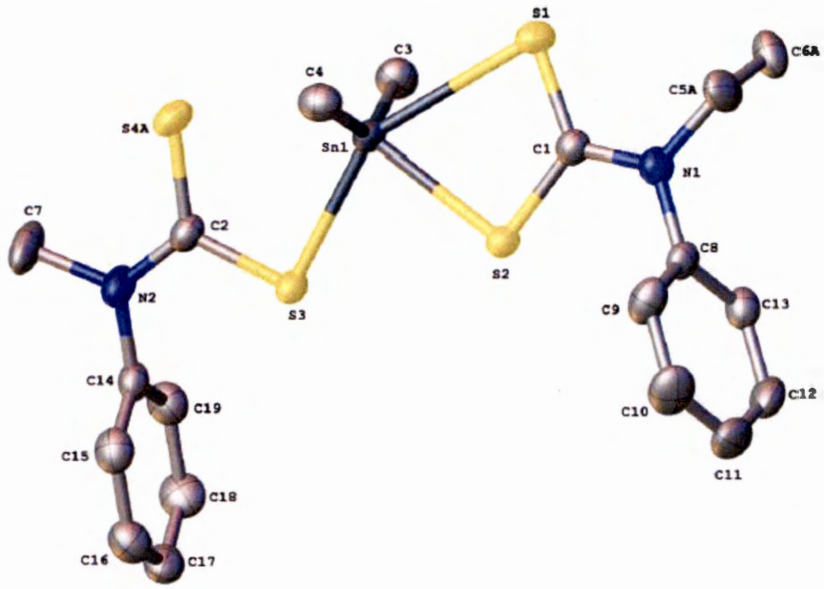

Figure 3.26: The molecular structure of dimethyltin(IV) *N,N*-methyl phenyl-*N,N*-ethyl phenyldithiocarbamatecomplex **(16),** with displacement ellipsoids drawn at 50% probability level (all hydrogen atoms are omitted for clarity).

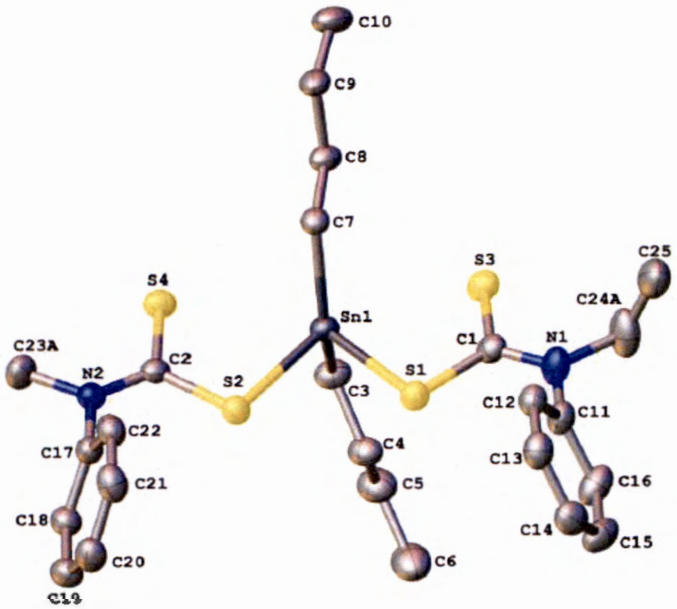

Figure 3.27: The molecular structure of dibutyltin(IV)*N,N*-methyl phenyl-*N,N*-ethyl phenyldithiocarbamatecomplex **(17),** with displacement ellipsoids drawn at 50% probability level (all hydrogen atoms are omitted for clarity).

3.10.5. Thermogravimetric Analysis (TGA) of organotin(IV) *N,N*-methyl phenyl-*N,N*-ethyl phenyldithiocarbamate complexes (16, 17 and 18)

The composition of each of the complexes changed based on mass losses upon thermal treatment as presented in the thermogravimetric plot. Figures 3.28 – 3.30 show the decomposition profile of each complex and the data obtained from these graphs are summarized in Table 3.12. Complexes **16** and **17** followed a two-step decomposition pattern, while complex 18 showed three-step decomposition. The first decomposition step for complex **16** and **17** have been attributed to the loss of some organic fragment in the temperature range of 85 – 211 and 96 – 200°C respectively. At the end of this step, masses found for these complexes were about 50 and 70% of the starting masses for complexes **16** and **17** respectively. The second (and final) step led to further decomposition in the temperature range of 218 – 299 and 210 – 320°C for complexes **16** and **17** respectively to give SnS residue. The masses of residues found at the end of the decomposition were 24.72 and 22.05% of the starting masses for complexes **16** and **17** respectively. These values were found to agree well with the calculated value of SnS which are 28.02% and 24.60%.

In the TGA of complex 18, the first step of decomposition occurred in a temperature range 91 – 201 °C, resulting in the loss of organic fragment which corresponded to one of the ligand fragment of the dithiocarbamate. Mass left after the first decomposition was found to be 71.95% of the starting mass of the complex. This step was followed by a second decomposition which occurred in the range 202 – 245 °C, and attributed to the two aryl groups attached to the tin atom. The mass found at this stage corresponds to about 60% of the starting mass. The final stage gave a residue of SnS in the range of 253 – 297°C, which was about 21% of the starting mass and agreed with the calculated (23.0%) value of the residue.

Generally, the stability of these complexes was influenced by their bond strengths which is also related to bond lengths between the atoms within the molecules of these complexes. Thus, the thermal fission occurred by the removal of one ligand moiety having the weakest (farthest) SnS bond. Furthermore, complex **18** gave a more stable thermal behavior compared to the structural analogue of this group of complexes with its final decomposition terminating at 297°C. Thus, the pyrolysis of this group of compound was achieved at a temperature range which corresponded to the formation of thermally stable products.

Table 3.12: Thermal analysis data of organotin(IV) complexes*N,N*-methyl phenyl-*N,N*-ethyl phenyldithiocarbamate **(16, 17** and **18)**

Compounds	**16**	**17**	**18**
Temp. range of decomp. (°C)			
1st stage 2nd stage 3rd stage	85 – 211 218 – 299 ———	96 – 200 210 – 320 ———	91 – 201 202 – 245 253 – 297
DTG peak T(°C)			
1st stage 2nd stage 3rd stage	210 270 ———	190 256 ———	198 236 283
Prod. Obtained			
1st decomposition 2nd decomposition 3rd decomposition	$(NCS)_2Sn(CH_3)_2$ SnS ———	$(C_4H_9)_2SnL^2$ SnS ———	$(C_6H_5)_2SnL^2$ SnL^2 SnS
Mass of res.(mg) Found (Calc)			
1st stage 2nd stage 3rd stage	6.89 (6.89) 3.45 (3.92) ———	11.46 (11.60) 3.72 (4.07) ———	3.28 (3.28) 2.55 (2.70) 0.96 (1.05)

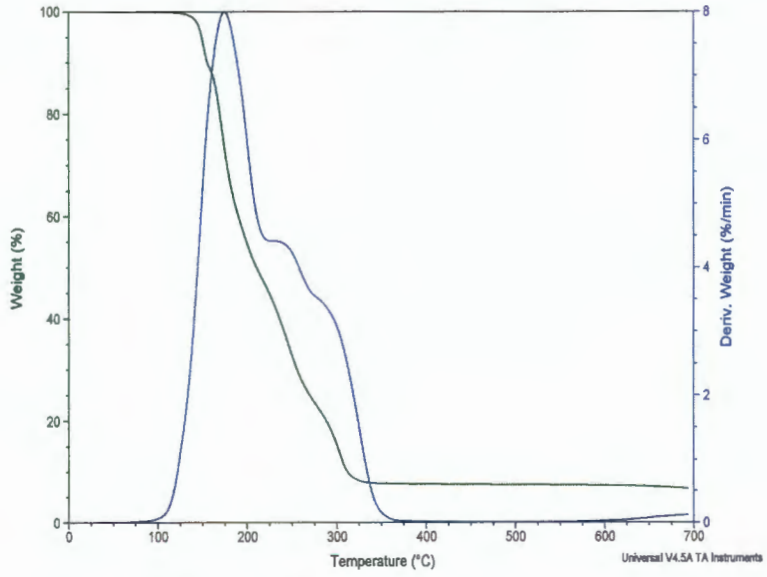

Figure 3.28: TG/DTG curves of dimethyltin(IV)*N,N*-methylphenyl-*N,N*-ethylphenyldithiocarbamate complexes **(16)** obtained under nitrogen atmosphere (75 mL/min), heating rate 10 °C/min.

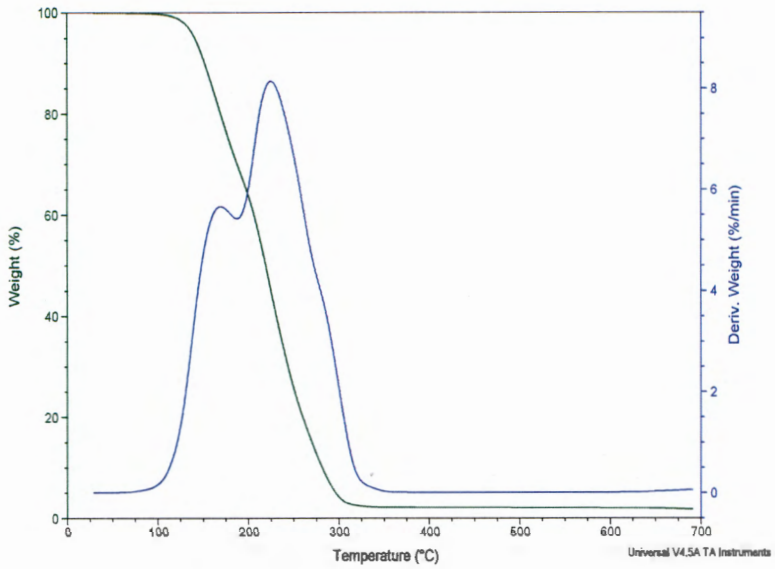

Figure 3.29: TG/DTG curves of dibutyltin(IV)*N,N*-methylphenyl-*N,N*-ethylphenyldithiocarbamate complexes **(17)** obtained under nitrogen atmosphere (75 mL/min), heating rate 10 °C/min.

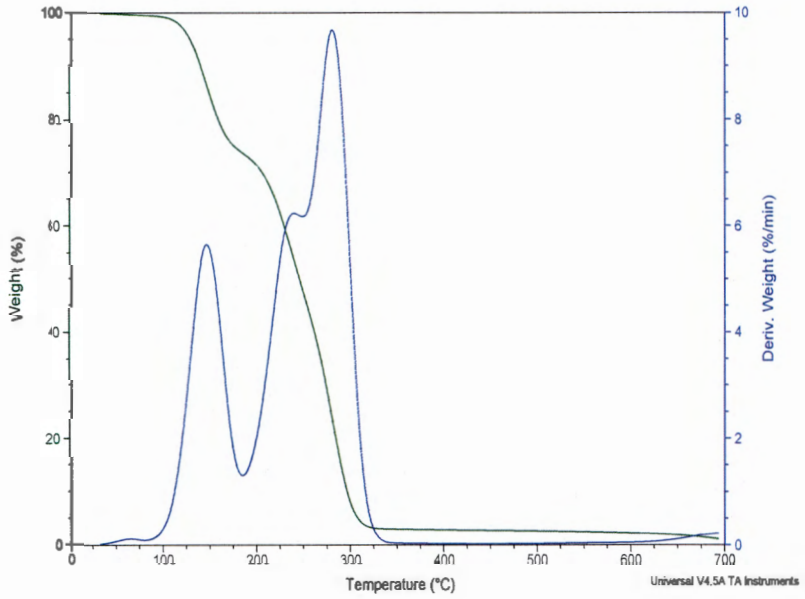

Figure 3.30: TG/DTG curves of dibutyltin(IV)*N,N*-methylphenyl-*N,N*-ethyl phenyldithiocarbamate complex complexes **(18)** obtained under nitrogen atmosphere (75 mL/min), heating rate 10 °C/min.

3.11. Mixed ligand complexes of dimethyltin(IV)*N,N*-alkylphenyl-*N,N*-butylphenyldithiocarbamate (19) and (20) (alkyl = CH_3 (L^1) and C_2H_5 (L^2))

3.11.1. Synthesis of the organotin(IV) complexes $R_2SnL^1L^3$ (R = CH_3)

The ligands $\mathbf{L^1}$ or $\mathbf{L^2}$ and $\mathbf{L^3}$ (0.005 mol) were dissolved separately in 10 mL of ethanol and mixed together in a 100 mL round bottom flask. Ethanolic solution of the dimethyltin(IV) dichloride (0.005 mol) was added to the solution of $\mathbf{L^1/L^2}$ and $\mathbf{L^3}$ in ice, then stirred for 2 h. The resultant white precipitates were filtered, washed with cold ethanol severally and dried under vacuum.

(19) $[(CH_3)_2SnL^1L^3]$: Yield: 2.67 g, (80.66%), M.pt.: 193–194 °C; Selected FTIR, υ (cm^{-1}): 1505 (C=N), 1236 (C_2-N), 1008 (C=S), 2943 (-CH), 2925 (=CH), 566 (Sn-C), 417 (Sn-S);^{1}H NMR ($CDCl_3$) δ = 7.50–7.44 (m, $C_6\underline{H}_5$–N(CH_3)), 7.35 –7.19 (m, $C_6\underline{H}_5$–N(C_4H_9), 3.84 (s, $C\underline{H}_3$–N(C_6H_5)), 4.13 (t, 2H, $CH_3CH_2CH_2C\underline{H}_2$–N($C_6H_5$)), 1.73 (m, 2H, $CH_3CH_2C\underline{H}_2CH_2$–N($C_6H_5$)), 1.38 (m, 2H, $CH_3C\underline{H}_2CH_2CH_2$–N($C_6H_5$)), 0.95 (t, 2H, $C\underline{H}_3CH_2CH_2CH_2$–N($C_6H_5$)), 1.47 (s, Sn-($C\underline{H}_3$)$_2$); ^{13}CNMR ($CDCl_3$) δ = 202.98, 202.45 ($\underline{C}S_2$), 146.77, 129.96, 128.30, 126.98, ($\underline{C}_6H_5$–N(CH_3)), 146.07, 129.35, 128.35, 126.93, ($\underline{C}_6H_5$–N(C_4H_9); 46.49 (C_6H_5–N($\underline{C}H_3$)), 58.16 (N-$\underline{C}H_2CH_2CH_2CH_3$), 28.97 (N-$CH_2\underline{C}H_2CH_2CH_3$), 19.91 (N-$CH_2CH_2C\underline{H}_2CH_3$), 13.72 (N-$CH_2CH_2CH_2\underline{C}H_3$),14.38 (Sn-$\underline{C}H_3$).^{119}Sn NMR ($CDCl_3$): δ ppm = -313.21.

$C_{21}H_{28}N_2S_4Sn$ (555.4) = C, 45.41; H, 5.08; N, 5.04; S, 23.09; Found = C, 45.21; H, 5.01; N, 4.99; S, 23.03;

(20) $[(CH_3)_2SnL^2L^3]$: Yield: 3.67 g, (76.03%), M.pt.: 198–200°C; Selected FT-IR, υ (cm^{-1}): 1485 (C=N), 1236 (C_2-N), 1000 (C=S), 2943 (-CH), 2925(=CH), 557 (Sn-C), 434 (Sn-S);^{1}H NMR ($CDCl_3$) δ = 7.49–7.39 (m, $C_6\underline{H}_5$–N(CH_3)), 7.35–7.19 (m, $C_6\underline{H}_5$–N(C_4H_9), 4.23 (q, 2H, $CH_3C\underline{H}_2$–N(C_6H_5)), 1.66 (t, 3H, $C\underline{H}_3CH_2$–N(C_6H_5)), 4.13 (t, 2H, $CH_3CH_2CH_2C\underline{H}_2$–N($C_6H_5$)), 1.69 (m, 2H, $CH_3CH_2C\underline{H}_2CH_2$–N($C_6H_5$)), 1.33 (m, 2H, $CH_3C\underline{H}_2CH_2CH_2$–N($C_6H_5$)), 0.92 (t, 2H, $C\underline{H}_3CH_2CH_2CH_2$–N($C_6H_5$)), 1.53 (s, Sn-($C\underline{H}_3$)$_2$); ^{13}C NMR ($CDCl_3$) δ = 202.45, 202.17 ($\underline{C}S_2$), 145.07, 129.93, 128.31, 126.98 (t, CH_3CH_2–N($\underline{C}_6H_5$)), 144.76, 129.90, 127.05, 126.36 ($\underline{C}_6H_5$–N(C_4H_9); 53.13 ($CH_3\underline{C}H_2$–N(C_6H_5)), 12.15 ($\underline{C}H_3CH_2$–N(C_6H_5)), 58.16 (N-$\underline{C}H_2CH_2CH_2CH_3$), 28.98 (N-$CH_2\underline{C}H_2CH_2CH_3$), 19.92 (N-$CH_2CH_2C\underline{H}_2CH_3$), 14.24 (N-$CH_2CH_2CH_2\underline{C}H_3$), 14.39 (Sn-$\underline{C}H_3$); ^{119}Sn NMR ($CDCl_3$): δ ppm = -312.49

$C_{22}H_{30}N_2S_4Sn$ (569.5) = C, 46.40; H, 5.31; N, 4.92; S, 22.52; Found = C, 46.10; H, 5.72; N, 4.44; S, 22.07.

3.12. Results and Discussion on the dimethyltin(IV) *N,N*-alkylphenyl-*N,N*-butyl phenyldithiocarbamate complexes

3.12.1. Synthesis of dimethyltin(IV) *N,N*-alkylphenyl-*N,N*-butyl phenyldithiocarbamate (19) and (20)

Both complexes are white, crystalline and air-stable. They are soluble in dichloromethane, chloroform, dimethylsulfoxide, sparingly soluble in alcohols and insoluble in *n*-hexane.

3.12.2. FTIR spectral studies of dimethyltin(IV) *N,N*-alkyl phenyl-*N,N*-butyl phenyldithiocarbamate (19) and (20)

The IR spectra of the complexes showed the expected absorption bands for dithiocarbamate complexes. The absorption bands around 1505 and 1485 cm^{-1} were due to the stretching vibration of the C-N bond of the thioureide moiety. The single band found at 1008 and 1000 cm^{-1} in each of the complexes were ascribed to the stretching vibration of the C-S bond. The higher value observed for the C-N bond have been attributed to the increase in the double bond character of this bond [7]. The appearance of a single band of C-S bond in the spectrum of each complex indicated a bidentate mode of bonding [9]. Bands found between 566 – 557 and 434 – 417 cm^{-1} suggest the presence of Sn-C and Sn-S bonds respectively [39].

3.12.3. Nuclear Magnetic Resonance studies of dimethyltin(IV) *N,N*-alkyl phenyl-*N,N*-butyl phenyldithiocarbamate (19) and (20)

From the ^1H NMR spectra, the influences of the various alkyl groups on the dithiocarbamate moiety were observed in the chemical shift of the complexes. In both complexes, multiplets in the region between 7.50 – 7.19 ppm were observed for the proton signals in the aromatic rings. The appearance of peaks in two different ranges within this environment was due to the non-equivalence nature emerging from the different alkyl derivatives on the nitrogen atom [46]. The signals due to the protons of the methyl group in complex **19** was found at 3.84 ppm due to its bonding to the electronegative N atom [15], while the methyelene and the methyl protons for complex **20** were found at 4.23 and 1.66 ppm respectively [25]. The chemical shift for the methyl group is somewhat lower due to dishielding which decreases with increase in distance from the metal centre of the thioureide bond [40]. The proton signals in the range of 4.14 and 0.92 ppm were found for both complexes and have been

attributed to the methylene and methyl protons in the *N*-butyl group on both complexes[25]. A strong signal at *ca.* 1.5 ppm was found in both complexes and this has been ascribed to the protons of the methyl group on the organotin moiety [13].

In the ^{13}C NMR spectra, two thioureide carbon peaks were observed between 202.98 – 202.17 ppm, due to the different alkyl substituents on the dithiocarbamate which affected the magnetic equivalence of the complexes. The lower values of these peaks have also been associated with the contribution of the double bond character existing within the thiouriede group. Therefore, dithiocarbamate moiety with the greater trans-influence has more shielded $-CS_2$ and, thus, has a greater electronic density [49]. The methyl carbon of the dithiocabamate moiety for complex **19** resonated at 46.49 ppm, while the methylene and the methyl carbon of complex **20** appeared at 53.13 and 12.15 ppm respectively [25]. The carbon signals associated with *N*-butyl group in the dithiocarbamate moieties of both complexes resonated in the range 58.16 – 13.72 ppm [25]. The resonant values of these carbons reduce along the chain away from the electronegative N atom due to reduction of the deshielding effect [25]. The carbon of the aromatic rings, due to the non-equivalence of both dithiocarbamate moieties on the adjacent sides of the tin metal, resonated in two regions within 145 – 125 ppm [16]. The carbon of the methyl group in the organotin moiety in both complexes resonated at *ca.* 14 ppm.

In these complexes, the ^{119}Sn NMR spectra showed a singlet at approximately-313 ppm (Figures 3.31 and 3.32), which suggested a hexa-coordinated geometry about the tin center.

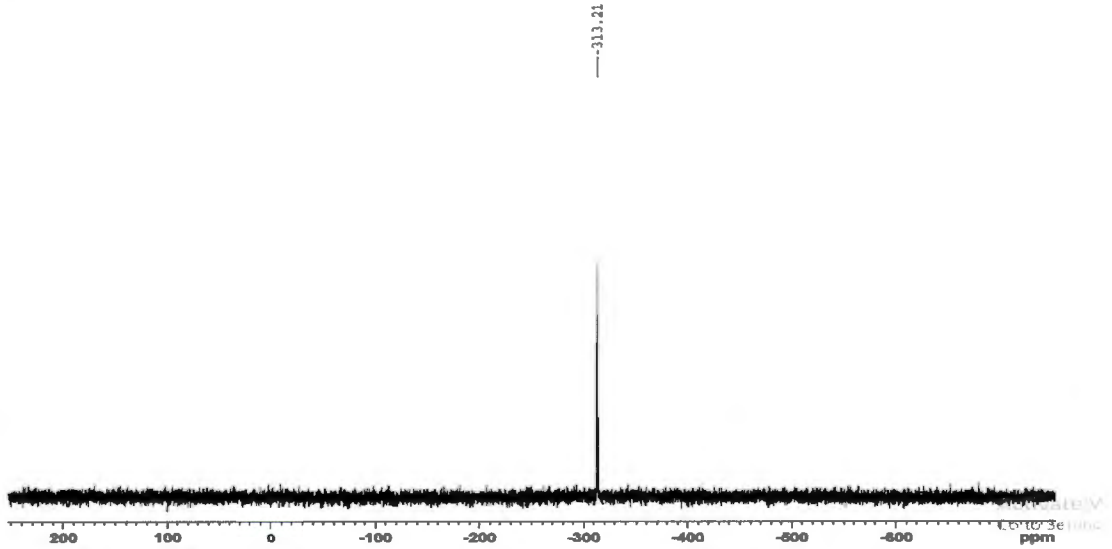

Figure 3.31: ^{119}Sn NMR spectrum of dimethyltin(IV) *N,N*-methyl phenyl-*N,N*-butyl phenyldithiocarbamate **(19).**

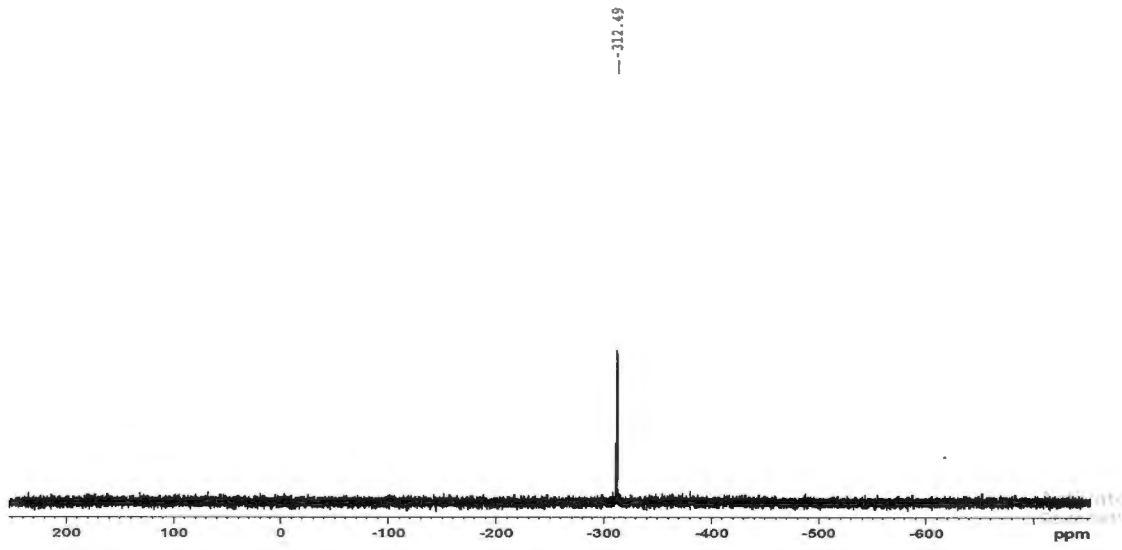

Figure 3.32: ^{119}Sn NMR spectrum of dimethyltin(IV) *N,N*-ethyl phenyl-*N,N*-butyl phenyldithiocarbamate **(20).**

3.12.4. Thermogravimetric analysis (TGA) of dimethyltin(IV) *N,N*-alkyl phenyl-*N,N*-butyl phenyldithiocarbamate (19) and (20)

The data obtained from the thermogravimetric plot of Figures 3.33 – 3.34 and presented in Table 3.13 show the varying mass changes in the complexes under heat treatment. Different decomposition patterns were observed for both complexes. Complex **19** followed two decomposition pathways, while complex **20** followed a single decomposition pathway. The first step of decomposition for **19** occurred from 85 – 208 °C, which resulted in 83.85% (Calc. 86.46%) loss of the starting mass. This mass loss was attributed to the release of a phenyl group (C_6H_5) from one of the ligand moiety which could have originated from the side with the weaker bonding to the metal center. The second and final step occurred in the range 209 to 327 °C to give a residue. The mass of the residue left was 24.08% of the starting mass which is in good agreement with the estimated value for SnS (26.36%). In complex **20**, the only decomposition step gave SnS residue in the temperature range of 98 to 305 °C. The mass of this residue was found to be 24.48% of the starting mass and was in good agreement with the calculated value of SnS (26.21%).

Therefore, complex **19** and **20** showed similar thermal stabilty between 85 – 327 °C with their final decomposition temperatures withing the range 282 - 298°C.

Table 3.13: Thermal analysis data of complexes **19** and **20**

Compounds	19	20
Temp. range of decom. (°C)		
1st stage	85 – 208	98 – 305
2nd stage	209 – 327	--------
DTG peak T(°C)		
1st stage	177	282
2nd stage	298	---------
Prod. obtained		
1st decomposition	$(CH_3)_2SnL^1(N\text{-}CH_3)$	SnS
2nd decomposition	SnS	---------
Mass of res.(mg) Found (Calc)		
1st stage	9.06 (9.34)	3.65 (3.98)
2nd stage	2.60 (2.85)	----------

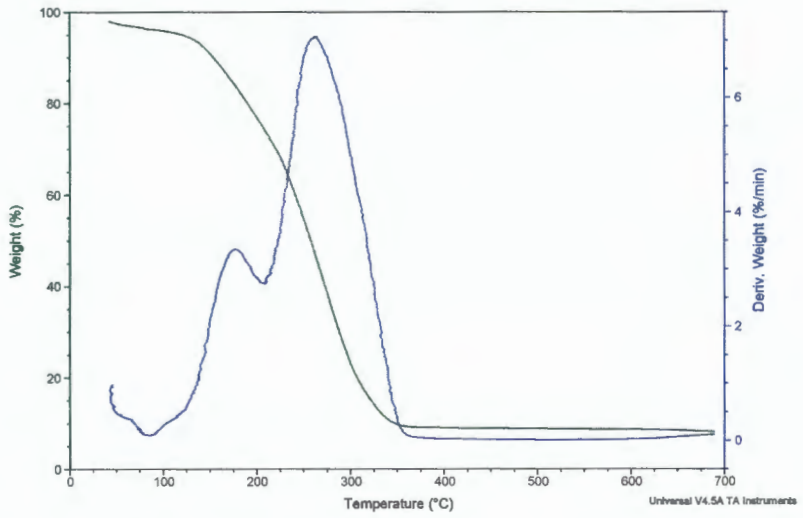

Figure 3.33: TG/DTG curves of complex **19** obtained under nitrogen atmosphere (75 mL/min), heating rate 10 °C/min.

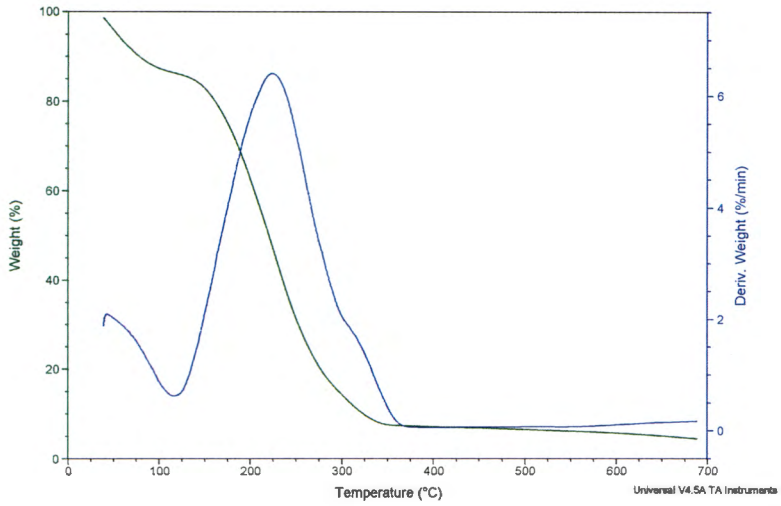

Figure 3.34: TG/DTG curves of complex **20** obtained under nitrogen atmosphere (75 mL/min), heating rate 10 °C/min.

3.13. Complexes of organotin(IV) with diallyldithiocarbamate

3.13.1. Synthesis of ammonium-*N, N*,-diallyldithiocarbamate, L^4

The preparation of the ligand (L^4) was achieved by slightly modifying a previously reported procedure [51]. *N, N*-diallylamine (1.25 mL, 0.01 mol) was introduced into a flask containing ammonium hydroxide solution (3 mL, 0.01 mol) placed in an ice bath. This mixture was allowed to stir for 5 min, then followed with the drop wise addition of carbon disulfide (0.6 mL, 0.01 mol). This mixture was stirred for 5–6 h, and the resulting precipitate was filtered. The product was rinsed with cold ethanol to remove unreacted compounds.

3.13.2. Synthesis of the organotin(IV) *N, N*,-diallyldithiocarbamate, $RSnClL_2$ and R_2SnL_2 ($R = CH_3, C_4H_9, C_6H_5$)

About 10 mL ethanoic solution of the respective organotin(IV) chloride (0.005 mol) was added to a 10 mL aqueous solution of ammonium *N,N*-diallyldithiocarbamate (0.01 mol) and stirred for 2 h. The white precipitates obtained were filtered off and rinsed with cold ethanol.

(21) $[(C_4H_9)ClSn(L^4)_2]$: Yield: 2.91 g (83.14%); M.pt.: 79 – 81 °C; Selected FTIR, υ (cm^{-1}): 1485 (C=N), 1238 (C_2-N), 992 (C=S), 2804 (-CH), 3115 (=CH), 549 (Sn-C), 356 (Sn-S); ^{1}H NMR ($CDCl_3$) δ ppm = 5.87-5.82 (ddt, 4H, β-C<u>H</u>), 5.81-5.27 (dd, 8H, γ-C<u>H</u>), 4.35-4.26 (d, 8H, α-C<u>H</u>), 2.25-2.33 (t, 2H, Sn-C<u>H</u>$_2$CH$_2$CH$_2$CH$_3$), 1.95-1.84 (m, 2H, Sn-CH$_2$C<u>H</u>$_2$CH$_2$CH$_3$), 1.46-1.42 (m, 2H, Sn-CH$_2$CH$_2$C<u>H</u>$_2$CH$_3$), 0.94-0.97 (t, 3H, Sn-CH$_2$CH$_2$CH$_2$C<u>H</u>$_3$); ^{13}C NMR ($CDCl_3$) δ ppm = 206.90 (N<u>C</u>S$_2$), 129.05 (β-<u>C</u>H), 120.41 (γ-<u>C</u>H$_2$), 57.03 (α-<u>C</u>H$_2$), 30.91 (Sn-<u>C</u>H$_2$CH$_2$CH$_2$CH$_3$), 29.71 (Sn-CH$_2$<u>C</u>H$_2$CH$_2$CH$_3$), 27.74 (Sn-CH$_2$CH$_2$<u>C</u>H$_2$CH$_3$), 13.64 (Sn-CH$_2$CH$_2$CH$_2$<u>C</u>H$_3$); ^{119}Sn NMR ($CDCl_3$): δ ppm = -304.40;
$C_{18}H_{29}ClN_2S_4Sn$ (555.86); C, 38.89; H, 5.26; N, 5.04; S, 23.07; Found: C, 38.16; H, 5.20; N, 5.04; S, 22.90.

(22) $[(CH_3)_2Sn(L^4)_2]$: Single-crystals suitable for X-ray diffraction analysis were obtained from chloroform-ethanol (4:1) solvent system. Yield: 3.03 g (94.9%); M.pt.: 80-82 °C; Selected FTIR, υ (cm^{-1}): 1468 (C=N), 1228 (C_2-N), 998 (C=S), 2914(-CH), 3078 (=CH), 550 (Sn-C), 358 (Sn-S); ^{1}H NMR ($CDCl_3$) δ ppm = 5.89-5.79 (ddt, 4H, β-C<u>H</u>), 5.29-5.21 (dd, 8H, γ-C<u>H</u>), 4.34-4.33 (d, 8H, α-C<u>H</u>), 1.54 (s, 6H, Sn-C<u>H</u>$_3$); ^{13}C NMR ($CDCl_3$) δ ppm = 201.34 (N<u>C</u>S$_2$), 130.75 (β-<u>C</u>H), 118.66 (γ-<u>C</u>H$_2$), 55.92 (α-<u>C</u>H$_2$), 15.34 (Sn-<u>C</u>H$_3$); ^{119}Sn NMR ($CDCl_3$): δ ppm = -330.49;

$C_{16}H_{26}N_2S_4Sn$ (493.36): C, 38.95; H, 5.31; N, 5.68; S, 26.00; Found: C, 38.89; H, 5.66; N, 5.23; S, 26.07.

(23) $[(C_4H_9)_2Sn(L^4)_2]$: Yield: 2.27 g (63.12%); M.pt.: 184 – 185 °C; Selected FTIR, υ (cm^{-1}): 1462 (C=N), 1224 (C_2-N), 991 (C=S), 2919 (-CH), 3082 (=CH), 550 (Sn-C), 429 (Sn-S); ^{1}H NMR ($CDCl_3$) δ ppm = 5.85-5.78 (ddt, 4H, β-C<u>H</u>), 5.25-5.17 (dd, 8H, γ-C<u>H</u>), 4.47-4.46 (d, 8H, α-C<u>H</u>), 2.16-2.07 (t, 2H, Sn-C<u>H</u>$_2$CH$_2$CH$_2$CH$_3$), 2.06-1.85 (m, 2H, Sn-CH$_2$C<u>H</u>$_2$CH$_2$CH$_3$), 1.56-1.41 (m, 2H, Sn-CH$_2$CH$_2$C<u>H</u>$_2$CH$_3$), 0.94-0.86 (t, 3H, Sn-CH$_2$CH$_2$CH$_2$C<u>H</u>$_3$); ^{13}C NMR ($CDCl_3$) δ ppm = 206.91 (N<u>C</u>S$_2$), 127.96 (β-<u>C</u>H), 118.38 (γ-<u>C</u>H$_2$), 55.879 (α-<u>C</u>H$_2$), 30.92 (Sn-<u>C</u>H$_2$CH$_2$CH$_2$CH$_3$), 29.71 (Sn-CH$_2$<u>C</u>H$_2$CH$_2$CH$_3$), 26.40 (Sn-CH$_2$CH$_2$<u>C</u>H$_2$CH$_3$), 14.12 (Sn-CH$_2$CH$_2$CH$_2$<u>C</u>H$_3$); ^{119}Sn NMR ($CDCl_3$): δ ppm = -333.61;
$C_{22}H_{38}N_2S_4Sn$ (578.1): C, 45.76; H, 6.63; N, 4.85; S, 22.2; Found: C, 44.90; H, 6.01; N, 4.00; S, 23.0.

(24) $[(C_6H_5)_2Sn(L^4)_2]$: Yield: 3.05 g (80.27%); M.pt.: 96 – 98 °C; Selected FTIR, υ (cm^{-1}): 1475 (C=N), 1230 (C_2-N), 976 (C=S), 2982 (-CH), 3084 (=CH), 554 (Sn-C), 444 (Sn-S); ^{1}H NMR ($CDCl_3$) δ ppm = 5.88-5.82 (ddt, 4H, β-C<u>H</u>), 5.28-5.20 (dd, 8H, γ-C<u>H</u>), 4.39-4.37 (d, 8H, α-C<u>H</u>), 7.78- 7.39 (m, 10H, C_6<u>H</u>$_5$); ^{13}C NMR ($CDCl_3$) δ ppm = 194.87 (N<u>C</u>S$_2$), 129.82 (β-<u>C</u>H), 119.16 (γ-<u>C</u>H$_2$), 53.51 (α-<u>C</u>H$_2$), 132.41–120.25 (Sn-<u>C</u>$_6$H$_5$); ^{119}Sn NMR ($CDCl_3$): δ ppm = -320.32;
$C_{26}H_{30}N_2S_4Sn$ (618.03): C, 50.57; H, 4.90; N, 4.54; S, 20.77; Found C, 51.01; H, 4.11; N, 4.72; S, 21.03.

(25) $[(C_6H_5)ClSn(L^4)_2]$: Yield: 1.79 g (49.86%); M.pt.: 115 – 116 °C; Selected FTIR, υ (cm^{-1}): 1461 (C=N), 1248 (C_2-N), 1007 (C=S), 2941 (-CH), 3067 (=CH), 557 (Sn-C), 417 (Sn-S); ^{1}H NMR ($CDCl_3$) δ ppm = 5.81-5.77 (ddt, 4H, β-C<u>H</u>), 5.20-5.18 (dd, 8H, γ-C<u>H</u>), 4.41-4.36 (d, 8H, α-C<u>H</u>), 7.75- 7.46 (m, 10H, C_6<u>H</u>$_5$); ^{13}C NMR ($CDCl_3$) δ ppm = 200.01 (N<u>C</u>S$_2$), 127.12 (β-<u>C</u>H), 120.16 (γ-<u>C</u>H$_2$), 54.51 (α-<u>C</u>H$_2$), 135.41–121.80 (Sn-C_6H_5); ^{119}Sn NMR ($CDCl_3$): δ ppm = -320.30;
$C_{20}H_{25}ClN_2S_4Sn$ (575.85): C, 41.71; H, 4.38; N, 4.86; S, 22.27; Found C, 41.01; H, 4.11; N, 4.82; S, 21.97.

3.14. Results and discussion on the organotin(IV) *N, N*,-diallyldithiocarbamate complexes (21 – 25)

3.14.1. Synthesis of organotin(IV) *N, N*,-diallyldithiocarbamate (R = CH_3, C_4H_9 , C_6H_5)

The reaction proceeded by the displacement of the chloride ion present in the organotin moiety by the *N,N*- diallyldithiocarbamato ligand, based on the mole ratio of the ligand to the metal salt used respectively as presented in scheme 3.3. White precipitates were obtained for the complexes formed except for the diphenyltin derivatives which gave a faint yellow colour. These complexes are soluble in dichloromethane, chloroform and sparingly soluble in alcohols.

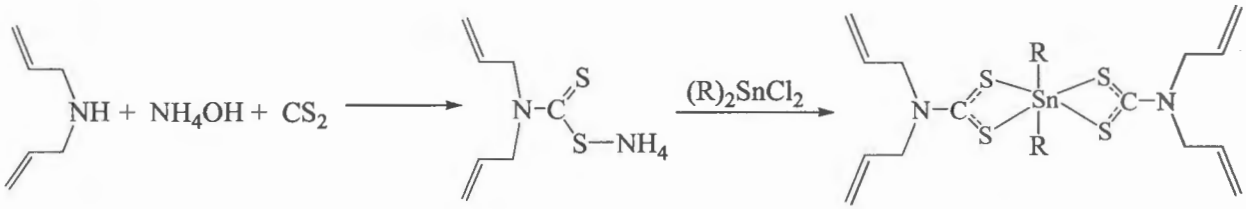

R = Cl, CH_3, C_4H_9, C_6H_5

Scheme 3.3: Schematic route for the synthesis of organotin(IV) *N, N*,-diallyldithiocarbamate complexes.

3.14.2. FTIR spectral studies of organotin(IV) *N, N*-diallyldithiocarbamate complexes

Common bands found in the IR spectra of the ligand (DTCs) were observed in the complexes: the stretching vibrational band of C–N group and the band attributed to the $–CS_2$ moiety. The vibrational frequency attributed to the ν(C–N) group was observed in the region 1485 - 1461 cm^{-1} in the complexes. This shows an increase in wavenumber when compared to the value in the precursor ligand observed at 1446 cm^{-1}[52], and has been attributed to an increase in the carbon–nitrogen double bond character as a result of chelation. The ν($–CS_2$) peak was observed within the range 1007 – 976 cm^{-1} as a single peak in the infrared spectra of the complexes. The presence of a single ν($–CS_2$) peak is attributed to the bidentate mode of bonding of the dithiocarbamate moiety to the tin(IV) ion [9]. A notable vibrational band often observed in organotin dithiocarbamate complexes is *ν*(Sn–S) which is found in the region 350 - 450 cm^{-1} in the IR spectra [53]. This band was observed in the spectra of each of the complexes in the region 358 - 444 cm^{-1}, showing that the organotin moieties are bonded to the ligand through the sulfur atoms of the dithiocarbamate.

3.14.3. Nuclear Magnetic Resonance studies of organotin(IV) *N, N*,-diallyldithiocarbamate complexes

The structure of the proposed complexes shown in Figure 3.35 reveals the various positions of the hydrogen atoms. From the dithiocarbamate moiety present in each of the complexes, βH protons of the vinylic group resonated as a doublet of doublets of triplet (ddt) in the range 5.89 – 5.77 ppm, while the terminal protons (γH) of the same vinylic group were found as doublet of doublets in the region 5.81 – 5.20 ppm. Doublet peaks in the range of 4.47 – 4.33 ppm, observed in each of the complexes were attributed to the allylic protons. A peak at 1.26 ppm was ascribed to the protons of the dimethyl group of complex **22** [54]; while the methylene protons of the butyl group in complex **21** and **23** resonated in the range 2.33 – 0.86 ppm [10]. In the spectra of complexes **21** and **23**, the butyl substituents of the former resonated at a slightly higher chemical shift compared to the later. This could be due to the unsubstituted electronegative chlorine atom still present in the complex. The phenyl protons resonated as a multiplet in the range 7.78 – 7.39 ppm in complexes **24** and **25**[12].

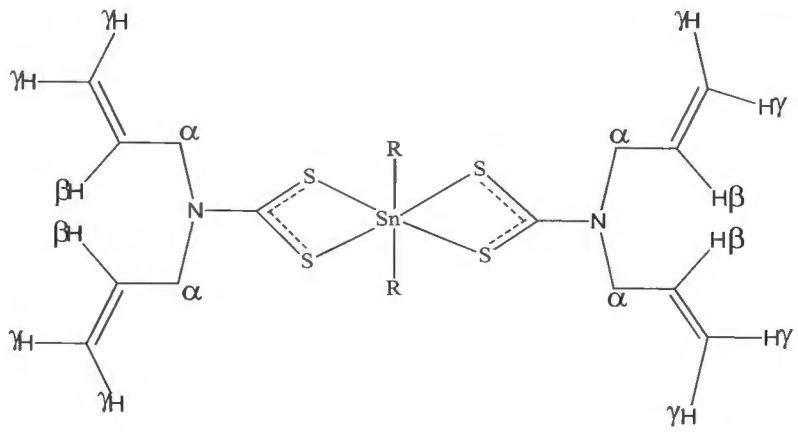

Figure 3.35: Schematic representation of the positions of hydrogen atoms in the complexes.

In the ^{13}C NMR spectra of the complexes, the carbon of the thioureide bond (-NCS_2) gave a weak signal in the range 194.87 - 206.91 ppm, due to the deshielding of the carbon atom upon complexation to the positive Sn(IV) centre [7]. The signals of the β- and γ- carbons of the allylic group appeared within 127.96 to 130.75 and 118.36 to 120.16 ppm respectively in the spectra of the complexes. The α-carbons signals were found in the region 53.51 – 57.03 ppm. The occurrence of peaks in this region could be attributed to the effect of the electronegative N atom bonded to the methyl group. Carbons of the dimethyl group of complex **22** gave a signal at 15.34 ppm [55]. The carbon signals due to the butyl groups in

complexes **21** and **23** were found within 13.64 and 30.92 ppm. The signals due to the aromatic carbons of complexes **24** and **25** gave signals in the range 135.41 – 120.25 ppm.

The spectra of ^{119}Sn NMR usually show a singlet which is significantly lower in the value of its chemical shift than corresponding organotin(IV) salts [11]. The chemical shifts values (δ) observed in all the complexes were from -210 to -400 ppm, which is suggestive of a hexa-coordinated geometry around the Sn metal. A representative spectra is shown in Figure 3.36.

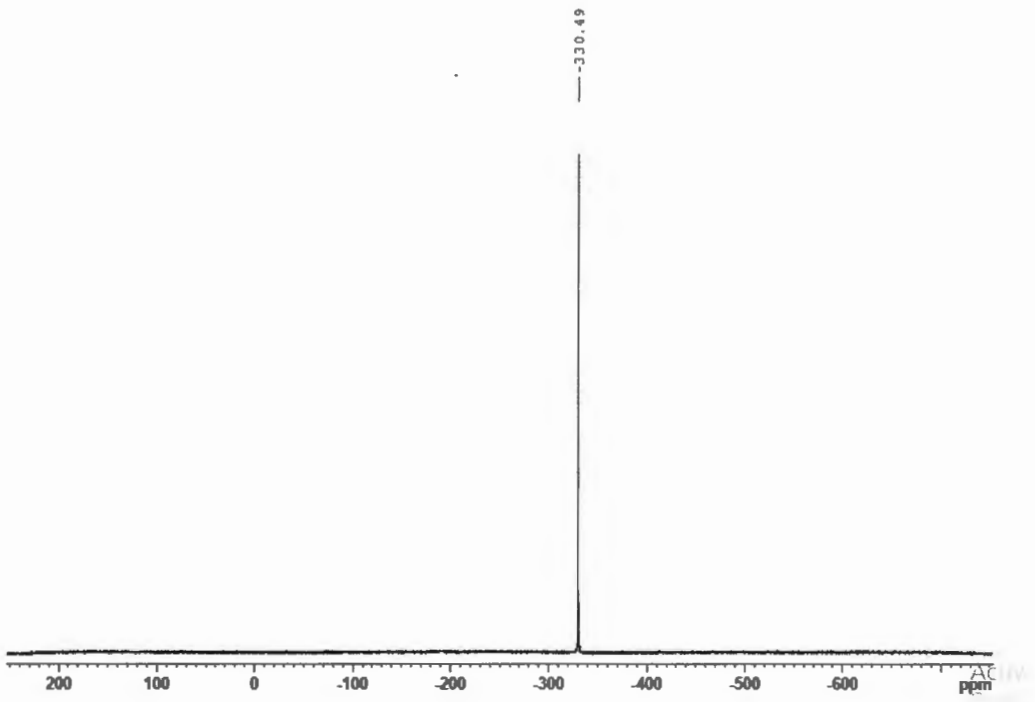

Figure 3.36. ^{119}Sn NMR spectrum of dimethyltin(IV) *N, N*,-diallyldithiocarbamate complexes **(22).**

3.14.4. X-ray crystallography of organotin(IV) *N, N*,-diallyldithiocarbamate complexes 22 and 23

Single crystals of complexes **22** and **23** were obtained by slow evaporation of a mixture of chloroform and ethanol at room temperature. Crystallographic information about the structure, data collection and refinement parameters are summarized in Table 3.14. Relevant bond lengths and angles are presented in Table 3.15. The ORTEP plots of the structure and the numbering scheme of the complexes are shown in Figure 3.37a and 3.38a, while Figure 3.37b and 3.38b show the crystal packing of these complexes. The complexes are monomeric with two molecules per unit cell, and six-coordinate geometry around the central Sn metal

atom which are in agreement with the ^{119}Sn NMR spectra of the complex. Two *N*, *N*,-diallyldithiocarbamate groups were attached to the organotin group through the two available sulfur atoms present in the ligand in a bidentate chelating fashion, resulting in an octahedral environment around the tin atom. Four sulfur atoms of the dithiocarbamate ligands present are attached unequally in both complexes to the tin atom as shown in the bond length differences of Sn-S. The Sn-S bond lengths are 2.9353(7) [Sn1-S12], 2.9353(7) [Sn1-S22], 2.553(8) [Sn1-S11] and 2.5250(7) Å [Sn1-S21] in complex **22**; 3.025(3) [Sn1-S12], 2.917(2) [Sn1-S22], 2.528(2) [Sn1-S11] and 2.528(2) Å [Sn1-S11] in **23**. These distances show that the ligand and the tin centre are asymmetrically coordinated as suggested by the IR spectra obtained. Although Sn1-S12 and Sn1-S22 bonds distances are appreciably longer than Sn1-S11 and Sn1-S21 in both complexes, these distances are considered as bonds (weak) because they are significantly less than the sum of the van der Waals radii (4.0 Å) [56]. These weak/longer Sn-S bonds are presumed to result from the low Lewis acidity of the tin atom in hexacoordinated complexes compared to those with lower oxidation number [57]. The observed interatomic distances of the Sn-S bonds are comparable to those observed in literature [18]. On both sides of the ligand moiety, S-Sn-S bonds have bite angles subtending at 64.83(2)° and 84.14(2)° for **22** and at 63.54(6)° and 81.73(7)° for **23**. This deviation from the expected angle, thus, supports the asymmetric coordination of the ligand molecule to the Sn atom. The bond lengths observed for Sn-C bond are 2.122(2) and 2.122(3) Å in complex **22,** and 2.110(8) and 2.13(2) Å for complex **23** are reasonably within the expected ranges reported for diorganotin(IV) complex of dithiocarbamate[32]. The bond angles of the methyl/methylene carbon (C-Sn-C) attached to the tin, occupying the axial position (144.94(11) and 129.5(5) Å), show that they do not exactly form a trans-axial coordination to the tin and this in turn contributes to the distortion of the expected octahedral geometry [22]. This cis–trans pathway is known to start its formation at a bond angle of 134° of the C–Sn–C bond [18]. The bond angles between S-Sn-C ranged between 101.77(10)° and 104.25(8)° in **22**; between 80.7(60)° and 111.0(5)° in **23**. These angles show the bending of the Sn-C bonds towards the longer Sn-S bond distances due to the repulsion between the central tin atom and the bonding electron pairs and thus leading to the distortion of these complexes from the expected octahedral geometry [22]. This bonding asymmetry of the dithiocarbamate ligands at both end of the complexes are further established by the association between the Sn-S bonds and the C-S bonds: the longer C-S bond is associated with the shorter Sn-S bond and vice versa. The geometry around the central Sn metal atom for these complexes can be best described as a distorted skew trapezoidal-bipyramidal due to the distortion. This

observed geometry is in good agreement with a previously reported organotin(IV) dithiocarbamate complex [18].

(a)

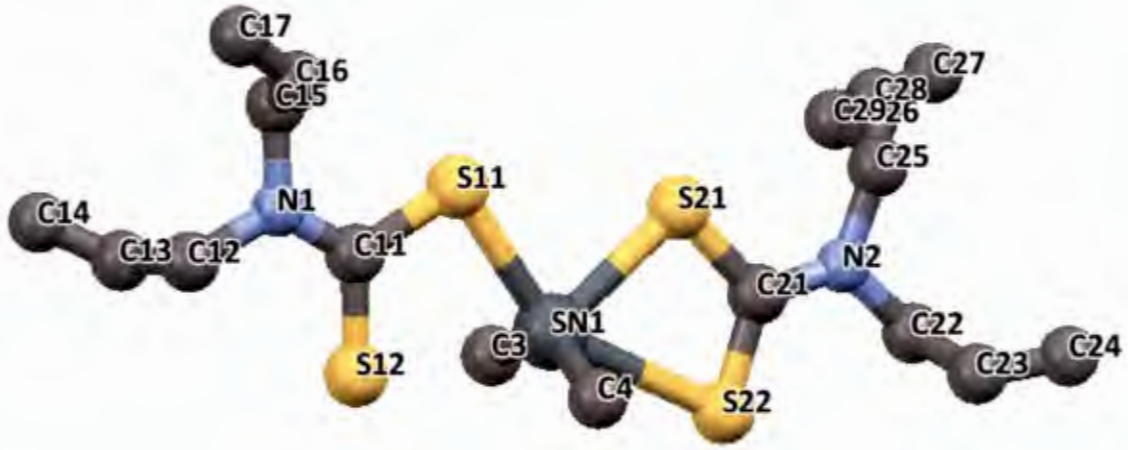

(b)

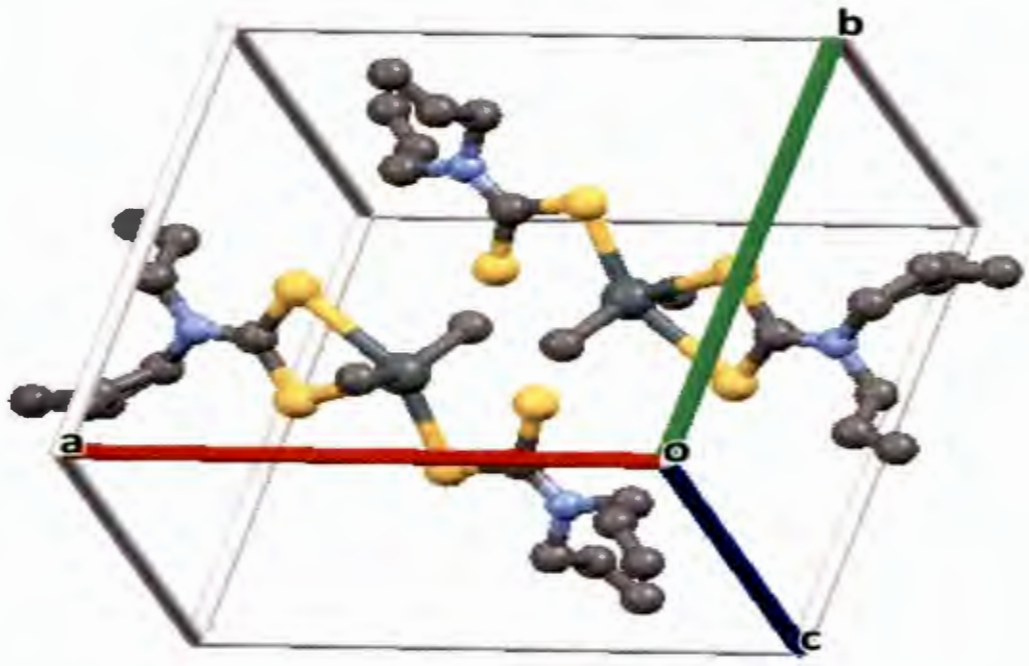

Figure 3.37: **(a)** Structure of dimethyltin(IV) *N, N*,-diallyldithiocarbamate complex **(22)** drawn at 50% probability level displacement ellipsoids (hydrogen atoms are excluded for clarity), and **(b)** the crystal packing viewed along the best axis.

(a)

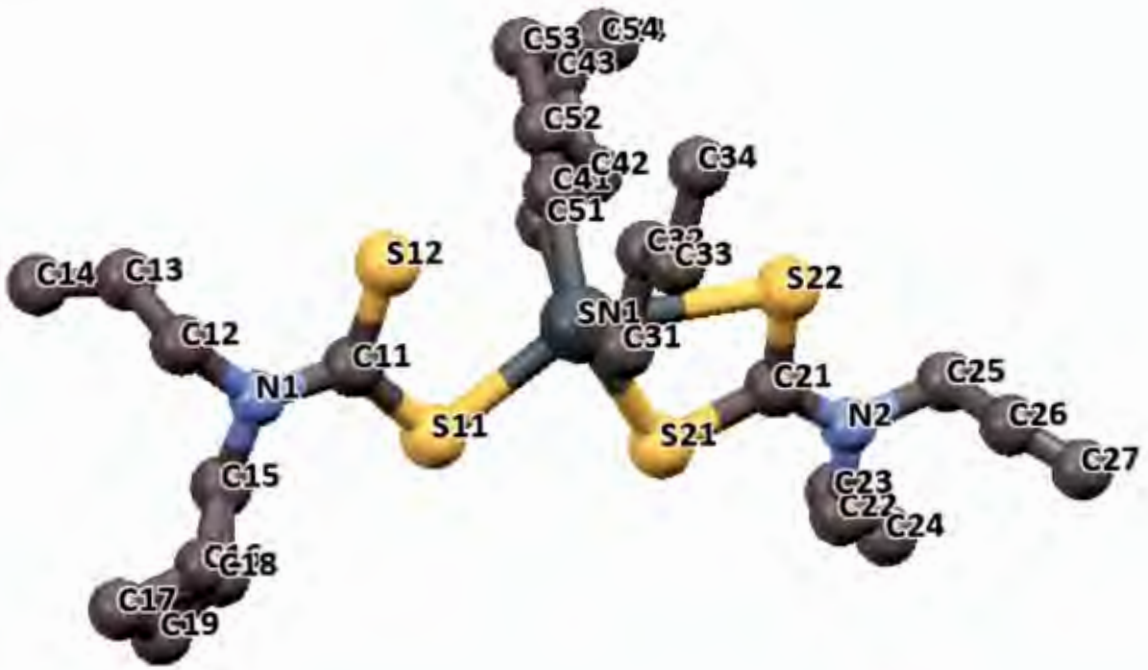

(b)

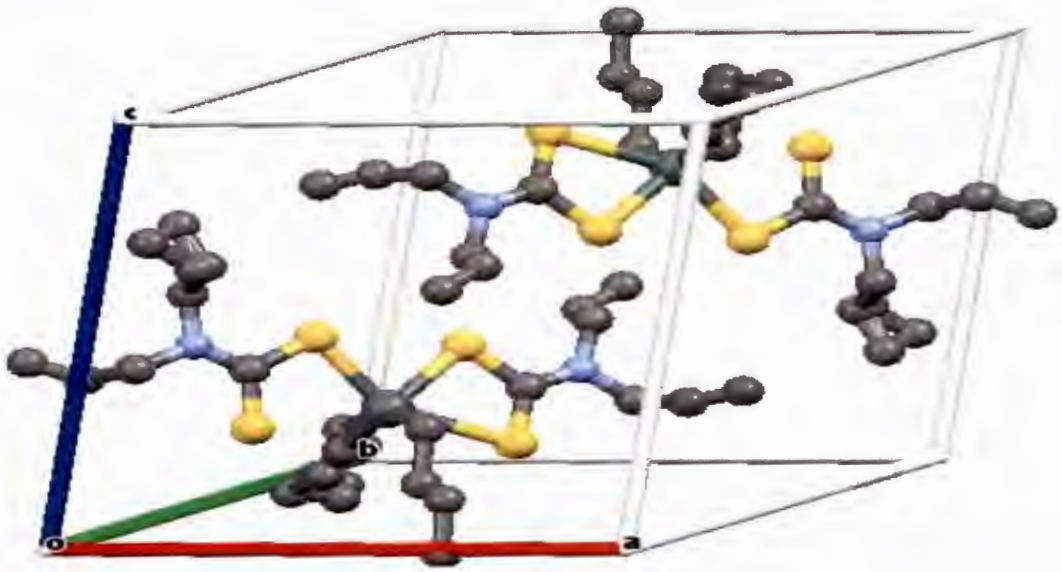

Figure 3.38: **(a)** Structure of dibutyltin(IV) *N, N*,-diallyldithiocarbamate complex **(23)** drawn at 50% probability level displacement ellipsoids (hydrogen atoms are excluded for clarity), and **(b)** the crystal packing viewed along the best axis.

Table 3.14: Crystal data collection and refinement parameters for complexes **22** and **23**

Complex	**22**	**23**
Empirical formula	$C_{16}H_{26}N_2S_4Sn$	$C_{22}H_{38}N_2S_4Sn$
Formula weight	493.34	577.49
Crystal size (mm)	0.22 x 0.34 x 0.52	0.28 x 0.38 x 0.62
Crystal system	triclinic	triclinic
Crystal habit	colorless needle	colorless needle
Space group	P-1 (No. 2)	P-1 (No. 2)
a (Å)	11.1822(10)	11.5592(18)
b (Å)	11.2706(10)	11.5680(17)
c (Å)	11.6522(10)	12.3219(19)
α (°)	118.125(3)	81.295(7)
β (°)	102.686(4)	82.641(7)
γ (°)	105.029(4)	63.785(6)
U (Å3)	1145.67(19)	1457.7(4)
Z	2	2
Dcalc (g cm-3)	1.430	1.316
F(000)	500	596
θ range (°)	2.1-28.3	1.7-28.4
Index range	-14:14 ; -15:15 ; -15:15	-15:14 ; -15:15 ; -16:16
Total, unique reflections	40037, 5672	58711, 7201
Observed reflections I > 2σ(I)	5119	4693
Number of parameters refined	229	259
Final R, wR2	0.0217, 0.0525	0.0676, 0.1518
Goodness-of-fit (GOF) S	1.07	1.06

Table 3.15: Selected interatomic distances and angles complexes **22** and **23**

Bond distances (Å)			
22		**23**	
Sn1-S11	2.5538(8)	Sn1-S11	2.528(2)
Sn1-S12	2.9353(7)	Sn1-S12	3.025(3)
Sn1-S21	2.5250(7)	Sn1-S21	2.514(2)
Sn1-S22	2.9006(8)	Sn1-S22	2.917(2)
Sn1-C3	2.122(2)	Sn1-C31	2.110(8)
Sn1-C4	2.122(3)	Sn1-C41	2.13(2)
S11-C11	1.738(2)	Sn1-C51	2.13(3)
S12-C11	1.698(3)	S11-C11	1.709(7)
S21-C21	1.745(3)	S12-C11	1.668(6)
S22-C21	1.695(2)	S21-C21	1.755(6)
N1-C11	1.337(3)	S22-C21	1.646(6)
N1-C12	1.476(3)	N1 -C11	1.374(9)
N1-C15	1.475(4)	N1 -C12	1.462(10)
N2-C21	1.330(3)	N1 -C15	1.454(9)
N2-C22	1.475(3)	N2 -C21	1.342(9)
N2-C25	1.462(4)	N2 -C22	1.453(9)
		N2 -C25	1.472(11)
Bond angles (°)			
S11-Sn1-S12	64.83(2)	S11-Sn1-S12	63.54(6)
S11-Sn1-S21	84.14(2)	S11 -Sn1-S21	81.73(7)
S11-Sn1-S22	150.19(2)	S11-Sn1-S22	146.84(6)
S11-Sn1-C3	103.85(7)	S11-Sn1-C31	104.9(2)
S11-Sn1-C4	101.77(10)	S11-Sn1-C41	109.7(6)
S12-Sn1-S21	148.81(2)	S11-Sn1-C51	98.2(10)
S12-Sn1-S22	144.97(2)	S12-Sn1-S21	145.20(6)
S12-Sn1-C3	83.60(6)	S12-Sn1-S22	149.56(6)
S12-Sn1-C4	86.06(9)	S12-Sn1-C31	83.1(2)
S21-Sn1-S22	66.07(2)	S12-Sn1-C41	80.7(6)
S21-Sn1-C3	101.82(7)	S12-Sn1-C51	88.0(10)
S21-Sn1-C4	104.25(8)	S21-Sn1-S22	65.24(6)
S22-Sn1-C3	84.27(7)	S21-Sn1-C31	109.4(2)
S22-Sn1-C4	85.29(9)	S21-Sn1-C41	111.0(5)
C3-Sn1-C4	144.94(11)	S21-Sn1-C51	95.3(9)
Sn1-S11-C11	93.94(9)	S22-Sn1-C31	84.4(2)
Sn1-S12-C11	82.25(8)	S22-Sn1-C41	86.1(6)
Sn1-S21-C21	92.73(8)	S22-Sn1-C51	88.2(10)
Sn1-S22-C21	81.55(8)	C31-Sn1-C41	129.5(5)
C11-N1-C12	122.0(2)	C31-Sn1-C51	148.2(10)
C11-N1-C15	122.8(2)	Sn1-S11-C11	95.0(2)
C12-N1-C15	115.2(2)	Sn1-S12-C11	79.4(2)
C21-N2-C22	122.0(2)	Sn1-S21-C21	92.9(2)
C21-N2-C25	123.2(2)	Sn1-S22-C21	81.8(2)
C22-N2-C25	114.70(19)	C11-N1-C12	122.9(5)
S11-C11-S12	118.97(14)	C11-N1-C15	123.1(6)
S11-C11-N1	118.89(18)	C12-N1-C15	114.0(6)
S12-C11-N1	122.15(17)	C21-N2-C22	125.1(6)
N1-C12-C13	111.5(2)	C21-N2-C25	121.1(5)
S21-C21-S22	119.65(13)	C22-N2-C25	113.7(7)
S21-C21-N2	118.21(18)	S11-C11-S12	122.0(4)
S22-C21-N2	122.14(19)	S11-C11-N1	117.9(5)
N2-C22-C23	110.99(18)	S12-C11-N1	120.1(5)
		N1-C12-C13	111.3(7)
		S21-C21-N2	116.1(4)
		S22-C21-N2	123.7(5)
		S21-C21-S22	120.1(4)
		N2 -C22 -C23	110.9(7)

Symmetry element i: 1-x,-y+1,-z

3.14.5. Thermogravimetric analysis of organotin(IV) *N, N*,-diallyldithiocarbamate complexes

The various decomposition temperature and corresponding weight losses have been summarized in Table 3.16. Complexes **21** and **25** showed a two-step decomposition pattern as presented in Figures 3.39 and 3.40. The first decomposition occurred for **21** in the temperature range of 92 and 213 °C, with weight loss of 12.84% attributed to the loss of $S(C_3H_5)$ [58]. This step was swiftly followed by decomposition in the range 216 – 313 °C leaving behind a solid residue identified stoichiometrically as SnS; the observed mass of 26.70% agrees favourably with the calculated value (27.02 %). The decomposition pattern of complex **25** is somewhat similar as observed in Figure 3.40. However, the decomposition proceeded via a single step decomposition step in the temperature range of 98 – 500 °C to give a SnS residue. The found mass residue of 26.05% agrees with the calculated value (25.96 %).

The TG/DTG graph of complexes **22, 23** and **24** in Figures 3.41 -3.43 showed that they decomposed in three steps. A sharp peak was observed from the DTG curve at 80 °C, which resulted from the melting of complex **22**. The first step of the decomposition for complexes **22, 23 and 24** occurred in the temperature ranges 93 – 206, 125 – 187 and 105 – 200 °C respectively. This decomposition resulted in the loss of 14.72, 12.25, and 14.43 % of the initial masses of complexes **22, 23 and 24** respectively. These mass losses were attributed to the loss of an allyl group and a sulfur atom $[S(C_3H_5)]$ from the ligand moiety [58]. This is probably due to the weak bond between the longer Sn-S bonds from the dithiocarbamate moiety as observed from the X-ray crystallographic structure, thus making the fission of the molecule possible. This was followed by a second decomposition in the temperature range of 207 – 259, and 188 – 245 °C for complexes **22** and **23** respectively and thus resulted in a weight loss of 42.67 and 60.40%, leaving behind about 57.40 and 39.60% of the initial masses respectively. The mass losses was attributed to the sequential loss of $S_2CN(C_3H_5)_2$ and C_3H_5 similar to the report by Ali *et. al*[58]; leaving behind a metal isothiocyanide intermediate $(NCSSn(CH_3)_2$ for **22** and $NCSSn(C_4H_9)$ for **23)**. However, for complex 24, the second decomposition step occurred in the temperature range 203 – 238 °C. The mass left was 73.93% of the starting mass which was in agreement with the loss of the two phenyl groups attached to the Sn metal atom (26.07%). The third and final decomposition step gave a residue of 31.31, 25.33 and 24.08% for complexes **22, 23 and 24** respectively from the initial masses in the temperature range 260 – 340, 246 – 300, 243 – 341 °C, attributed to SnS

which is in good agreement with the calculated value [30.38% (**22**), 26.49% (**23**), 24.22% (**24**)].

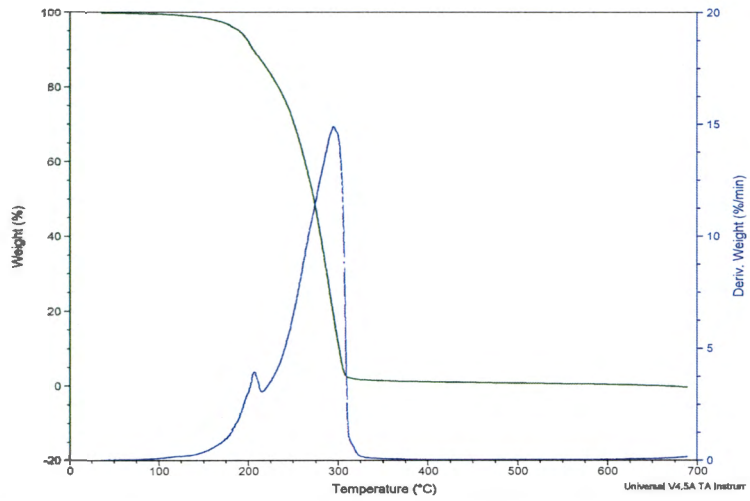

Figure 3.39: TG/DTG curves of complex **21** obtained under nitrogen atmosphere (75 mL/min), heating rate 10 °C/min.

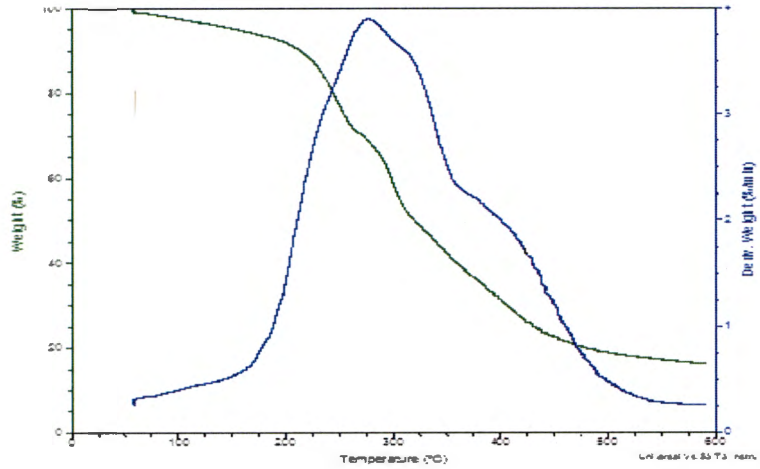

Figure 3.40: TG/DTG curves of complex **25** obtained under nitrogen atmosphere (75 mL/min), heating rate 10 °C/min.

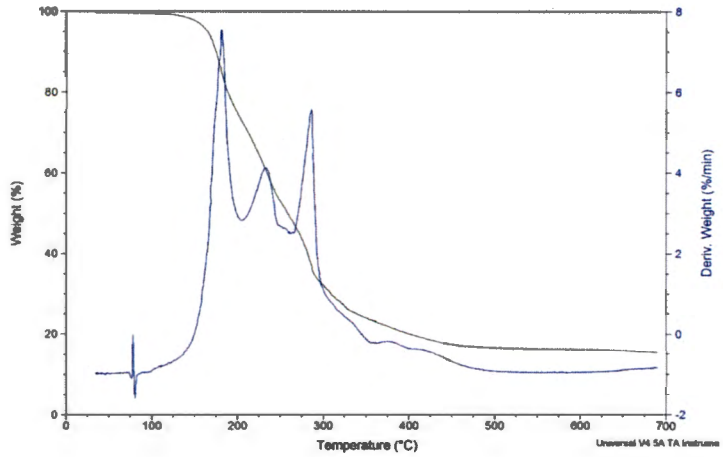

Figure 3.41: TG/DTG curves of **22** obtained under nitrogen atmosphere (75 mL/min), heating rate 10 °C/min.

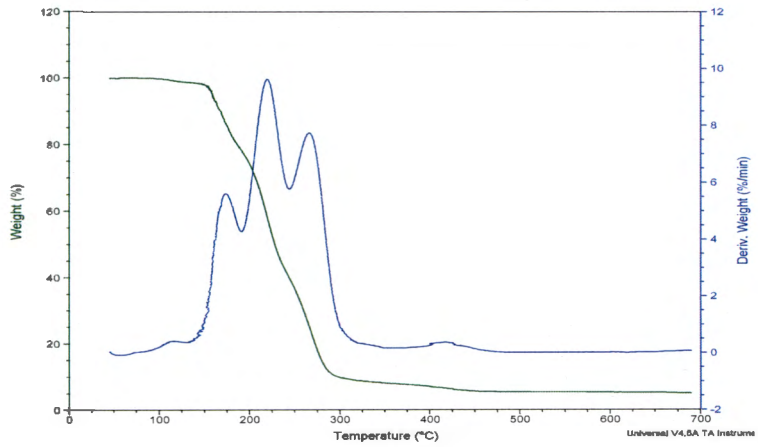

Figure 3.42: TG/DTG curves of complex **23** obtained under nitrogen atmosphere (75 mL/min), heating rate 10 °C/min.

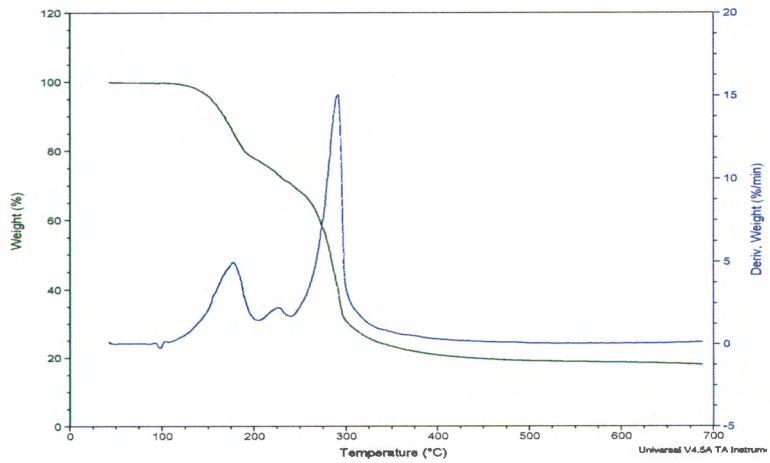

Figure 3.43: TG/DTG curves of complex **24** obtained under nitrogen atmosphere (75 mL/min), heating rate 10 °C/min.

Table 3.16: Thermal analysis data of organotin(IV) *N, N*,-diallyldithiocarbamate complexes **(22 -25)**

Complex	21	22	23	24	25
Temp range of decomp. (°C)					
1st stage	92 – 213	93 – 206	135 – 187	105 – 200	98 - 543
2nd stage	216 – 313	207 – 259	188 – 245	203 – 238	———
3rd stage	———	260 – 340	246 – 300	243 – 341	———
DTG peak T(°C)					
1st stage	206	180	172	177	423
2nd stage	284	239	245	223	———
3rd stage	———	317	266	341	———
Products obtained					
1st decomposition	$[(C_3H_5)_3(CN)_2S_3]Sn(C_4H_3)Cl$	$[(C_3H_5)_3(CN)_2S_3]Sn(CH_3)_2$	$[(C_3H_5)_3(CN)_2S_3]Sn(C_4H_9)_2$	$[(C_3H_5)_3(CN)_2S_3]Sn(C_6H_5)_2$	SnS
2nd decomposition	SnS	$SCNSn(CH_3)_2$	$SCNSn(C_4H_9)$	$[(C_3H_5)_3(CN)_2S_3]Sn$	———
3rd decomposition	———	SnS	SnS	SnS	———
Mass of residue (mg), Found (Calc)					
1st stage	1.87 (1.89)	13.53 (13.52)	2.18 (2.19)	9.70 (9.99)	2.79 (26.05)
2nd stage	3.89 (3.94)	9.32 (9.03)	6.99 (6.99)	8.38 (8.51)	———
3rd stage	———	4.97 (4.82)	4.46 (4.50)	24.08 (24.22)	———

3.15. Complexes of organotin(IV) and *p*-alkylphenyldithiocarbamate

3.15.1 Synthesis of sodium *p*-methyl phenyldithiocarbamate (L^5)

The preparation of the ligand $\mathbf{L^5}$ was achieved by slightly modifying a previously reported procedure [59]. *p*-methylaniline (0.01 mol) was dissolved in 10 mL of tetrahydrofuran and reacted with a 20 mL tetrahydrofuran solution of NaOH (0.01 mol) under nitrogen. Carbon disulfide (0.01 mol) was added dropwise via a syringe into the solution. This mixture was stirred for 4 – 5 h at room temperature and filtered. The residue obtained was washed with diethyl ether to afford pale yellow solids, which were dried under vacuum.

3.15.2. Synthesis of ammonium *p*-ethyl phenyldithiocarbamate (L^6)

P-ethyl aniline (0.01 mol) was dissolved in 20 mL of ethanol and reacted with a 20 mL ethanoic solution of NH_4OH (0.01 mol) in an ice bath for 30 min. Carbon disulfide (0.01 mol) was added dropwise via a syringe into the solution. This mixture was stirred for 6 – 7 h at room temperature and filtered. The residue obtained was washed with ethanol and diethyl ether.

3.15.3. Synthesis of the organotin(IV) *p*-ethyl phenyldithiocarbamate complexes ($R_2Sn(L^1)_2$ ($R = CH_3, C_4H_9, C_6H_5$)

The respective organotin(IV) chloride (0.005 mol) of the formula R_2SnCl_2 were dissolved in 10 mL cold ethanol and added drop wise to the freshly prepared ethanol solution of $\mathbf{L^5}$ or $\mathbf{L^6}$. The solution was stirred for about 2 h in an ice bath. White precipitates were formed for all the complexes. These precipitates were flitered, washed with excess ethanol and dried under vacuum for 24 h. Recrystallization was achieved in a mixture of dichloromethane and ethanol.

(26) $[(C_4H_9)_2Sn\ (L^5)_2]$: Yield: 2.63 g (73.66%); M.pt.: 190 – 191 °C; Selected FTIR, υ (cm^{-1}): 1516 (C=N), 1261 (C_2-N), 1004 (C=S), 2957 (-CH), 3085 (=CH), 3148 (N-H) 546 (Sn-C), 366 (Sn-S); ^{1}H NMR (DMSO) δ (ppm) = 7.47 - 7.12 (m, 8H, N-$C_6\underline{H}_4$), 2.50 (s, 6H, Ar–$C\underline{H}_3$), 5.29 (s, 2H, N-$\underline{H}$), 2.31 (t, 4H, Sn-$C\underline{H}_2CH_2CH_2CH_3$), 1.81 (m, 4H, Sn-$CH_2C\underline{H}_2CH_2CH_3$), 1.36 (m, 4H, Sn-$CH_2CH_2C\underline{H}_2CH_3$), 0.90 (t, 6H Sn-$CH_2CH_2CH_2C\underline{H}_3$); ^{3}C NMR (DMSO) δ (ppm) = 192 (-$N\underline{C}S_2$), 136.94, 133.29, 129.12, 123.50 (-$\underline{C}_6H_5$), 20.42 (Ar–$\underline{C}H_3$), 27.58 (Sn-$\underline{C}H_2CH_2CH_2CH_3$),

26.12 (Sn-$CH_2\underline{C}H_2CH_2CH_3$), 25.83 (Sn-$CH_2CH_2\underline{C}H_2CH_3$), 13.45 (Sn-$CH_2CH_2CH_2\underline{C}H_3$); ^{119}Sn NMR ($CDCl_3$): δ ppm = -312.06;

$C_{24}H_{34}N_2S_4Sn$ (598.06): C, 48.24; H, 5.74; N, 4.69; S, 21.47; Found: C, 47.84; H, 6.04; N, 4.19; S, 22.00.

(27) [$(C_6H_5)_2$Sn (L^5)$_2$]: Yield: 2.82 g (74.80%); M.pt.: 192 – 194 °C; Selected FTIR, υ (cm^{-1}): 1508 (C=N), 1247 (C_2-N), 998 (C=S), 2949 (-CH), 3056 (=CH), 3145 (N-H) 531 (Sn-C), 371 (Sn-S); ^{1}H NMR (DMSO) δ (ppm) = 7.48 - 7.20 (m, 8H, N-$C_6\underline{H}_4$-CH_3), 2.36 (s, 6H, Ar–$C\underline{H}_3$), 5.29 (s, 2H, N-$\underline{H}$), 7.58 – 7.49 (m, 10H, Sn-$C_6\underline{H}_5$); ^{13}C NMR (DMSO) δ (ppm) = 200.01 (-$N\underline{C}S_2$), 135.46, 130.20, 129.87, 125.51 (N-$\underline{C}_6H_4$-CH_3), 21.06 (Ar–$\underline{C}H_3$), 140, 135.61, 130.11, 128.74 (Sn-$\underline{C}_6H_5$); ^{119}Sn NMR ($CDCl_3$): δ ppm = -315.96;

$C_{28}H_{26}N_2S_4Sn$ (637.5): C, 52.75; H, 4.11; N, 4.39; S, 20.12; Found: C, 52.25; H, 4.29; N, 4.01; S, 19.99.

(28) [$(CH_3)_2$Sn(L^6)$_2$]: Yield: 2.51 g (73.18%), M.pt.: 155 – 156 °C; Selected FTIR, υ (cm^{-1}): 1511 (C=N), 1286 (C_2-N), 983 (C=S), 2956 (-CH), 3055 (=CH), 3285 (N-H) 555 (Sn-C), 388 (Sn-S); ^{1}H NMR (DMSO) δ (ppm) = 7.48 – 7.33 (m, 8H, N-$C_6\underline{H}_4$-CH_3), 2.59 (q, 4H, Ar–$C\underline{H}_2CH_3$), 1.26 (t, 6H, Ar–$CH_2C\underline{H}_3$), 5.29 (s, 2H, N-$\underline{H}$), 1.39 (s, 6H, (Sn-$C\underline{H}_3$)); ^{13}C NMR (DMSO) δ (ppm) = 202.97 (-$N\underline{C}S_2$), 137.46, 128.20, 128.50.87, 123.88 (N-$\underline{C}_6H_4$-CH_3), 31.16 (Ar–$\underline{C}H_2CH_3$), 16.08 (Ar–$CH_2\underline{C}H_3$), 16.14 (Sn-$\underline{C}H_3$); ^{119}Sn NMR ($CDCl_3$): δ ppm = -321.96;

$C_{20}H_{26}N_2S_4Sn$ (541.40) = C, 44.37; H, 4.84; N, 5.17; S, 23.69; Found: C, 44.01; H, 5.04; N, 5.18; S, 23.67.

(29) [$(C_4H_9)_2$Sn (L^6)$_2$]: Yield: 2.89 g (76.29%), M.pt.: 189 – 190 °C; Selected FTIR, υ (cm^{-1}): 1514 (C=N), 1275 (C_2-N), 1002 (C=S), 2958(-CH), 3063 (=CH), 3131 (N-H) 553 (Sn-C), 352 (Sn-S); ^{1}H NMR (DMSO) δ (ppm) = 7.41 - 7.28 (m, 8H, N-$C_6\underline{H}_4$-CH_3), 2.78 (q, 4H, Ar–$C\underline{H}_2CH_3$), 1.30 (t, 6H, Ar–$CH_2C\underline{H}_3$), 5.28 (s, 2H, N-$\underline{H}$), 2.19 (t, 4H, Sn-$C\underline{H}_2CH_2CH_2CH_3$), 1.68 (m, 4H, Sn-$CH_2C\underline{H}_2CH_2CH_3$), 1.47 (m, 4H, (Sn-$CH_2CH_2C\underline{H}_2CH_3$)), 0.96 (t, 6H, (Sn-$CH_2CH_2CH_2C\underline{H}_3$)); ^{13}C NMR (DMSO) δ (ppm) = 203.40 (-$N\underline{C}S_2$), 140.46, 129.84, 128.18, 126.33 (N-$\underline{C}_6H_4$-CH_3), 31.69 (Ar–$\underline{C}H_2CH_3$), 16.88 (Ar–$CH_2\underline{C}H_3$), 30.94 (Sn-$\underline{C}H_2CH_2CH_2CH_3$), 28.89 (Sn-$CH_2\underline{C}H_2CH_2CH_3$), 20.31 (Sn-$CH_2CH_2\underline{C}H_2CH_3$), 13.76 (Sn-$CH_3CH_2CH_2\underline{C}H_3$); ^{119}Sn NMR ($CDCl_3$): δ ppm = -278.66;

$C_{26}H_{38}N_2S_4Sn$ (625.56) = C, 49.92; H, 6.12; N, 4.48; S, 20.50; found C, 49.56; H, 6.19; N, 4.23; S, 20.66.

3.16. Results and discussion on the organotin(IV) *p*-alkylphenyldithiocarbamate complexes (26 – 29)

3.16.1. Synthesis of organotin(IV) and *p*-alkylphenyldithiocarbamate

Dithiocarbamates ligand obtained from primary amine sources are generally less stable compared to those obtained from secondary amine sources due to the presence of the acidic hydrogen on the nitrogen [59,60]. The synthesis of dithiocarbamate ligands from primary amine sources sometimes requires an inert atmosphere as in the case of the *p*-methyl dtc $\mathbf{L^5}$. However, $\mathbf{L^6}$ was synthesized in the air. The complexes were prepared by the reaction of the ligands with respective organotin salt, Scheme 3.4. The reaction proceeded by the equivalent replacement of the chloride ions of the organotin(IV) chloride salts by the ligand. The complexes were characteristically white, soluble in dichloromethane, chloroform, dimethylsulfoxide and sparingly soluble in alcohols.

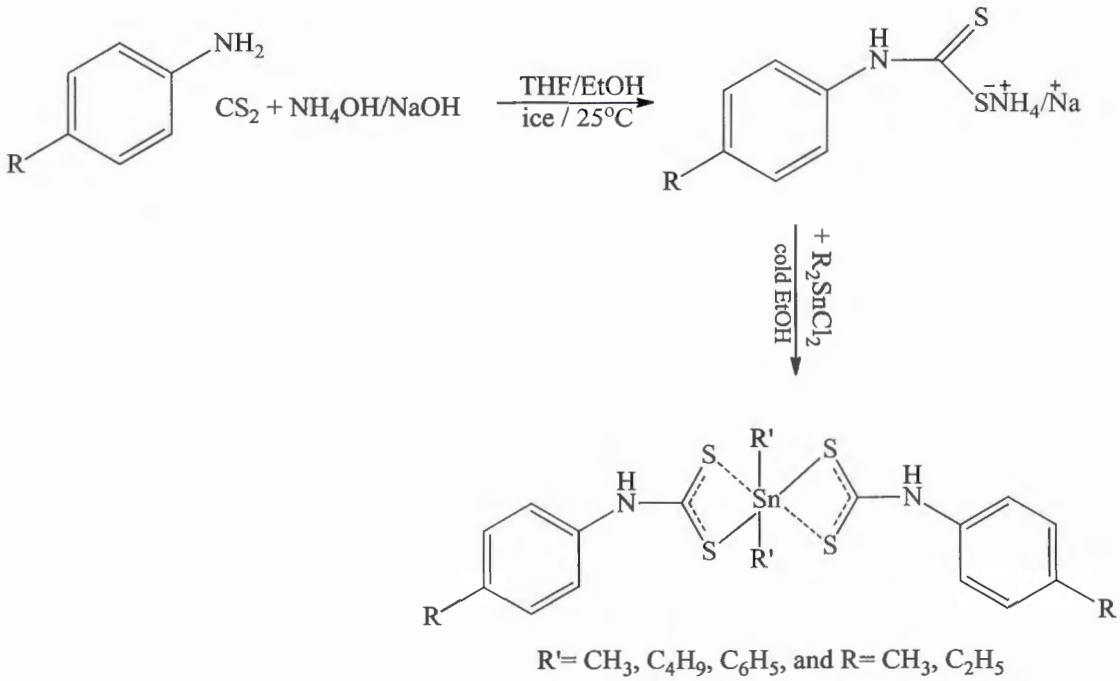

Scheme 3.4: Organotin(IV) complexes of *p*-alkyl phenyldithiocarbamate $\mathbf{L^5}$ and $\mathbf{L^6}$.

3.16.2. FTIR spectral studies of organotin(IV) *p*-alkylphenyldithiocarbamate complexes

Useful information has been deduced from the selected IR peaks due to the wide studies on dithiocarbamate and its complexes. The complexes showed bands around 1516 to 1508 cm^{-1}, which is indicative of a partial double bond character of C-N stretching vibration. A strong band in the frequency range of 1004 – 983 cm^{-1} ascribed to C-S stretching vibration was observed in all the complexes and this suggest a bidentate coordination between the organotin(IV) moiety and the dithiocarbamate ligand [61]. The band associated with the aromatic ring, which is expected around 1600 – 1450 cm^{-1}, were masked by the dithiocarbamate ligand[59]. In the complexes, a band around 555 – 531 cm^{-1} ascribed to the Sn-C bond was observed and, thus, supports the presence of the organotin(IV) moieties [43]. Furthermore, a low intensity peak around 366 – 388 cm^{-1} due to the presence of the Sn-S bond was also observed [17,62].

3.16.3. Nuclear Magnetic Resonance studies of organotin(IV)*p*-alkylphenyldithiocarbamate complexes

In the ^{1}H NMR, the aromatic protons were observed downfield as multiplet in the region 7.47 – 7.12 ppm. The peaks with the chemical shift in this region have been attributed to the proton signals ortho to the carbon of the thioureide group because they are more deshielded due to the electronegative N atom and the proximity to the $-CS_2$ group [59]. Signals between 2.20 -2.11 ppm were observed in the spectra and were ascribed to the protons of the methyl group in the para position of the ring in complexes **26** and **27** having $\mathbf{L^5}$ ligand moiety. The signals due to the methylene and the methyl groups in the para position for the complexes **28** and **29** with $\mathbf{L^6}$ were found around 2.78 – 2.35 and 1.30 – 1.26 ppm respectively. The signal observed at a higher frequency in all the complexes around 5.29 ppm, has been ascribed to the proton of the N-H; and the position was due to the electronegative N atom [63,64]. The signals due to the alkyl groups on the organotin moiety were found in their expected ranges: 1.39 ppm for the dimethyl ($Sn-CH_3$) [13], 2.31 – 0.90 ppm for the dibutyl ($Sn-C_4H_9$) [12], and as a complex multiplets between 140 and128 ppm for the diphenyl ($Sn-C_6H_5$).

In the ^{13}C NMR, a weak signal ascribed to the carbon of the thioureide ($-NCS_2$) group was found between 203 and 190 ppm in the complexes. The region in which these peaks occurred in the complexes suggested the contribution of the double bond character of the N-C bond in the dithiocarbamate moiety [59]. The aromatic carbon signals resonated in the range 136 – 123

ppm[63]. The signals ascribed to the para-methyl carbon in the complexes derived from $\mathbf{L^5}$ resonated around 21 ppm [59], while the methylene and methyl carbons of the para-ethyl group in the complexes derived from $\mathbf{L^6}$ resonated at approximately 31 and 16 ppm respectively. The signals due to the various carbons of the organotin moieties were found at 16.14 ppm (for the dimethyl group), around 30 – 13 ppm (for dibutyl group), and around 140 – 126 ppm for diphenyl group attached to the Sn atom [65]. The chemical shifts values (δ) as observed for all the complexes were from -312 to -322 ppm, which is suggestive of a hexa-coordinated geometry around the Sn metal.

3.16.4. Thermogravimetric Analysis (TGA) of organotin(IV) *p*-alkylphenyldithiocarbamate complexes

The TG/DTG plot of the complexes, show two decomposition pathways as presented in Figures 3.44 – 3.47. The data obtained from the thermogravimetric plots have been summarized in Table 3.17.

3.16.4.1. Thermal analysis of complexes 26 and 27

The first step of decomposition of complex **26** occurred between 98 – 162 °C, and this resulted into about 82.35% loss of the starting mass attributed to the mass of CH_3-C_6H_4 from the ligand group in the complex, which agree well with the calculated values (82.35%). After this stage, the mass further decomposed (in a second step) in the temperature range of 163 -188 °C to give a mass which was about 80% of the starting mass and this was attributed to the butyl group from the organotin moiety in the complex. This agrees with the calculated value of the butyl group. (81.17%). This step was subsequently followed by a third and final step in a temperature range of 211 – 303 °C. The mass of the residue found was 52.97% of the starting mass and this agrees well with the calculated value Sn_2S_3 (54.80%). The phase of tin sulphide residues observed here is similar to what has been reported in literature for organotin(IV) pyrrolidinedithiocarbamate complexes [66].

The decomposition pattern of complex **27** followed a two-step pathway. The first step occurred in the temperature range of 100 – 217 °C. The mass found at this stage was 82.98% of the starting mass and is attributed to the loss of CH_3-C_6H_4 from the ligand molecule in the complex. This agrees well with the calculated value (calc. 83.21%). This was followed by a second and

final decomposition in the range 230 – 321 °C to give Sn_2S_3. The mass found was 50.10% of the starting mass and this agreed well with the calculated value of Sn_2S_3 (calc. 52.10%) [66].

3.16.4.2. Thermal analysis of complexes **28** and **29**

In complex **29**, two decomposition pathways were observed. The first step occurred in the range of 72 – 171 °C which gave 80.08% of the starting mass. This mass loss corresponded to the mass of the butyl group on the organotin moiety which agrees well with the calculated value (calc. 81.48%). This step was immediately followed by a second and final decomposition step which gave SnS in the range of 172 – 301 °C. The mass of the residue found here was 21.25% of the starting mass which was in agreement with the calculated value for SnS (calc. 23.39%). A single step decomposition was observed in complex **28** in the range of 75 – 201 °C to give a final residue. The mass found was 23.11% of the starting mass which agreed with the calculated value of SnS (calc. 27.65%).

Generally, the decomposition of the complexes gave either Sn_2S_3 or SnS residue, and thus indicated their potential as a precursor for Sn_2S_3/SnS nanoparticles.

Table 3.17: Thermal analysis data of complexes **26 – 29**

Compounds	**26**	**27**	**28**	**29**
Temp. range of decom. (°C)				
1st stage	98 – 162	100 – 217	75 – 201	72 – 171
2nd stage	163 -188	230 – 321	———	172 – 301
3rd stage	211 – 303	———	———	———
DTG peak T(°C)				
1st stage	157	216	185	170
2nd stage	168	303	———	264
3rd stage	294	———	———	———
Prod. obtained				
1st decomp	$(CH_3\text{-}Ph)H(NCS_2)_2Sn(But)_2$	$(CH_3\text{-}Ph)H(NCS_2)_2Sn(Ph)_2$	SnS	$(C_2H_5\text{-}Ph\text{-}NHCS_2)_2Sn$
2nd decomp	$(CH_3\text{-}Ph)H(NCS_2)_2Sn$	Sn_2S_3	———	SnS
3rd decomp	Sn_2S_3	———	———	———
Mass of res.(mg) Found (Calc)				
1st stage	13.96 (13.96)	11.90 (11.93)	1.58 (1.89)	3.43 (3.49)
2nd stage	13.56 (13.76)	7.19 (7.47)	———	0.91 (1.03)
3rd stage	8.98 (9.29)	———		———

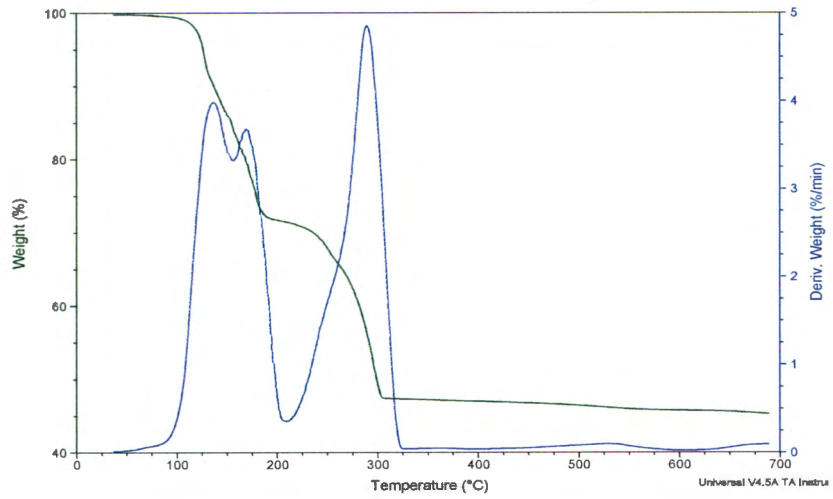

Figure 3.44: TG/DTG curves of complex **26** obtained under nitrogen atmosphere (75 mL/min), heating rate 10 °C/min.

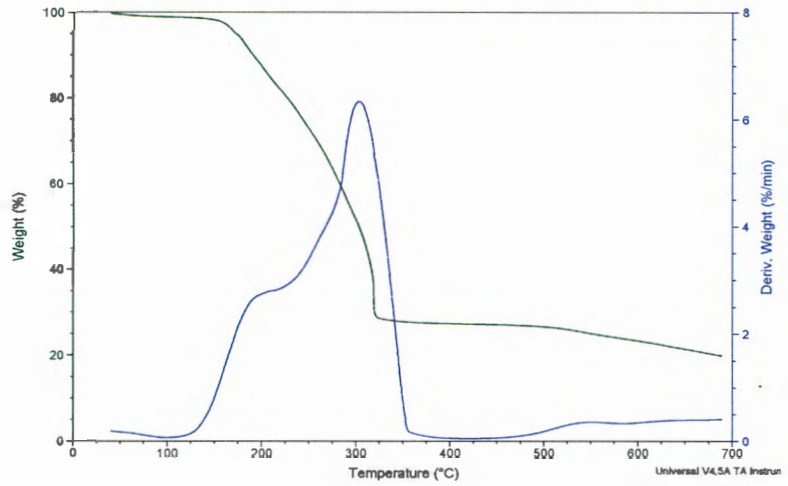

Figure 3.45: TG/DTG curves of complex **27** obtained under nitrogen atmosphere (75 mL/min), heating rate 10 °C/min.

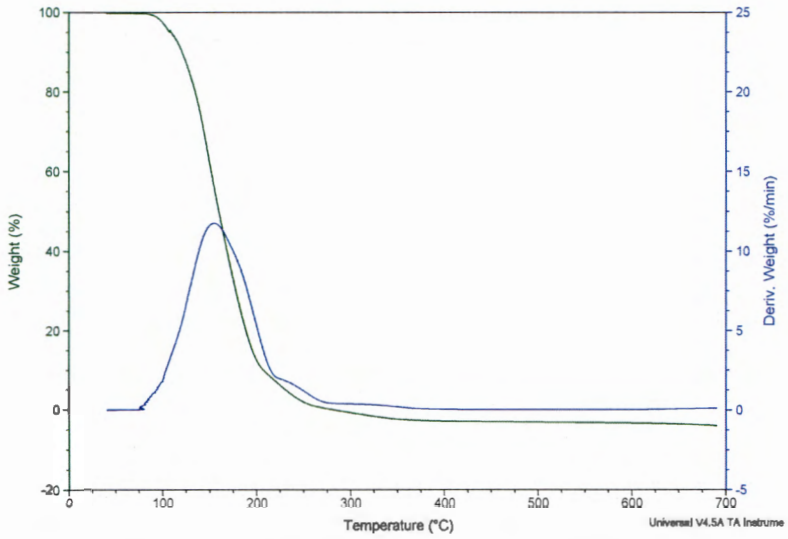

Figure 3.46: TG/DTG curves of complex **28** obtained under nitrogen atmosphere (75 mL/min), heating rate 10 °C/min.

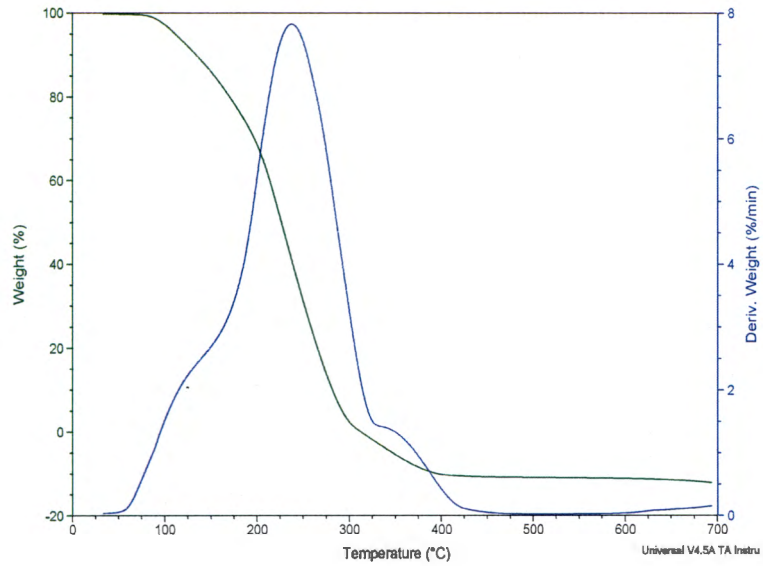

Figure 3.47: TG/DTG curves of complex **29** obtained under nitrogen atmosphere (75 mL/min), heating rate 10 °C/min.

3.17. Complexes of organotin(IV) and benzyl dithiocarbamate

3.17.1. Synthesis of ammonium *N*-benzyldithiocarbamate (L^7)

Benzylaniline (5.50 mL, 0.05 mol) was stirred with ammonium hydroxide (15 mL, 0.05 mol) for 30 min in ice bath. To this solution, cold carbon disulfide (3 mL, 0.05 mol) was added in drop wise and the mixture was stirred for 3 h while maintaining a temperature of about 4 °C. A yellowish-white solid crude substance precipitated out, separated using suction pump and rinsed severally, first with absolute ethanol and followed with ether. The white solid product was stored under reduced temperature.

3.17.2. Synthesis of organotin(IV) complexes ($R_2Sn(L^7)_2$ (R = CH_3, C_4H_9, C_6H_5)

About 10 mL ethanoic solution of the respective organotin(IV) chloride (0.025 mol) was added to a 10 mL aqueous solution of ammonium *N*-benzyldithiocarbamate (0.01 mol) and stirred for 2 h. The white precipitates obtained were filtered off and rinsed with cold ethanol.

30. **[$(CH_3)_2Sn(L^7)_2$]**: Yield, 2.21 g (71.29%); M.pt.: 125 – 126 °C; Selected FTIR, υ(cm^{-1}): 1503 (C=N), 1239 (C_2-N), 983 (C=S), 2912(-CH), 3147 (=CH),3378 (N-H), 508 (Sn-C), 451 (Sn-S); ^{1}H NMR (DMSO) d (ppm) = 7.47–7.24 (m, 10H, $C_6\underline{H}_5$-CH_2-NH), 4.62 (s, 2H, C_6H_5-CH_2-N$\underline{H}$), 3.93 (s, 4H, C_6H_5-C$\underline{H}_2$-NH), 1.53 (s, 6H, Sn-C$\underline{H}_3$); ^{13}C NMR (DMSO) d (ppm) = 202.77 (-N$\underline{C}S_2$) , 135.60, 134.23, 129.59, 127.56 ($\underline{C}_6H_5$-CH_2-NH), 52.83 (C_6H_5-$\underline{C}H_2$-NH), 15.04 (Sn-$(CH_3)_2$); ^{119}Sn NMR ($CDCl_3$): δ ppm = -335.09;
$C_{18}H_{22}N_2S_4Sn$ (513.35); C, 42.11; H, 4.32; N, 5.46; S, 24.98, Found; C, 41.91; H, 4.02; N, 5.06; S, 24.49.

31. **[$(C_4H_9)_2Sn(L^7)_2$]**: Yield, 2.68 g (74.65%); M.pt. 133 – 134 °C; Selected FTIR, υ(cm^{-1}): 1487 (C=N), 1237 (C_2-N), 1008 (C=S), 2954 (-CH), 3117 (=CH), 3300 (N-H), 512 (Sn-C), 440 (Sn-S); ^{1}H NMR (DMSO) d (ppm) = 7.47–7.24 (m, 10H, $C_6\underline{H}_5$-CH_2-NH), 4.85 (s, 2H, C_6H_5-CH_2-N$\underline{H}$), 3.56 (s, 4H, C_6H_5-C$\underline{H}_2$-NH), 2.35 (t, 4H, Sn-C$\underline{H}_2$$CH_2CH_2CH_3$), 1.76 (m, 4H, Sn-$CH_2C\underline{H}_2$$CH_2CH_3$), 1.48 (m, 4H, Sn-$CH_2CH_2C\underline{H}_2CH_3$), 0.88 (t, 6H, Sn-$CH_2CH_2CH_2C\underline{H}_3$); ^{13}C NMR (DMSO) d (ppm) = 201.07 (-N$\underline{C}S_2$),135.60, 134.23, 129.59, 127.56 ($\underline{C}_6H_5$-CH_2-NH), 52.83 (C_6H_5-$\underline{C}H_2$-NH), 31.25 (Sn-$\underline{C}H_2CH_2CH_2CH_3$), 27.82 (Sn-$CH_2C\underline{H}_2CH_2CH_3$), 23.34 (Sn-$CH_2CH_2C\underline{H}_2C\underline{H}_3$) 13.98 (Sn-$CH_2CH_2CH_2C\underline{H}_3$); ^{119}Sn NMR ($CDCl_3$): δ ppm = -351.06;

$C_{18}H_{22}N_2S_4Sn$ (598.06); C, 48.24; H, 5.74; N, 4.69; S, 21.47; Found; C, 47.94; H, 5.24; N, 4.26; S, 22.07.

32. $[(C_6H_5)_2Sn(L^7)_2]$: Yield, 2.93g (78.76%); M.pt. 135 – 137°C; Selected FTIR, υ (cm^{-1}): 1478 (C=N), 1229 (C_2-N), 996 (C=S), 2932 (-CH), 3119 (=CH), 3318 (N-H), 510 (Sn-C), 443 (Sn-S); ^{1}H NMR (DMSO) d (ppm) = 7.47–7.24 (m, 10H, $C_6\underline{H}_5$-CH_2-NH), 4.62 (s, 2H, C_6H_5-CH_2-N$\underline{H}$), 3.93 (s, 4H, C_6H_5-C$\underline{H}_2$-NH), 8.06–7.78 (m, 10H, Sn-($C_6\underline{H}_5$)$_2$). ^{13}C NMR (DMSO) d (ppm) = 200.71 (-N$\underline{C}S_2$), 135.60, 134.23, 129.59, 127.56 ($\underline{C}_6H_5$-CH_2-NH), 52.83 (C_6H_5-$\underline{C}H_2$-NH), 136.23, 135.37, 129.43, 128.96 (Sn-($C_6\underline{H}_5$)$_2$); ^{119}Sn NMR ($CDCl_3$): δ ppm = -343.90; $C_{28}H_{26}N_2S_4Sn$ (638.00); C, 52.75; H, 4.11; N, 4.39; S, 20.12; Found; C, 52.45; H, 3.99; N, 4.01; S, 20.32.

3.18. Results and discussion on organotin(IV)*N*-benzyldithiocarbamate complexes

3.18.1. Synthesis of organotin(IV) *N*-benzyldithiocarbamate complexes

The syntheses of the complexes were achieved in similar procedure presented in 3.3. Good yields were obtained and the stoichiometry of the reaction agrees with the elemental analysis of the complexes. These complexes were white, stable at room temperature and are soluble in dichloromethane, chloroform, dimethylsulfoxide but sparingly soluble in alcohols.

3.18.2. FTIR spectral studies organotin(IV) *N*-benzyldithiocarbamate complexes

The IR spectra of the three complexes showed the characteristic dithiocarbamate bands. A strong band assigned to the C–N vibration of the thioureide bond was found in the region between 1503– 1478 cm^{-1} for all the complexes due to delocalization of electron towards the tin centre in the complexes [7]. A single peak in the region 1008 – 996 cm^{-1} was attributed to the vibrational mode of C–S which is suggestive of a bidentate mode of coordination [9]. Stretching vibration due to the aromatic ring (=C–H) was found in the region 3147 – 3030 cm^{-1}, while the stretching vibration due to the CH_2 bond appeared in the region 2954 – 2912 cm^{-1}[67]. The N-H stretching vibration was found in the region 3300 – 3378 cm^{-1}[68]. In the far IR region, characteristic peaks

associated with organotin dithiocarbamate complexes were found in the region 512 – 508 cm^{-1} and 451 – 440 cm^{-1} ascribed to the stretching vibrations of Sn-C and Sn-S respectively [65].

3.18.3. Nuclear Magnetic Resonance studies of organotin(IV) *N*-benzyldithiocarbamate complexes

In the ^{1}H NMR of the complexes, the expected chemical shifts were found at their appropriate regions. The signals due to the aromatic protons from the ligand moiety were found as multiplet in the region 7.47 – 7.24 ppm for the complexes. Signals attributed to protons of methylene group appeared in the region 3.93 – 3.56 ppm due to the electronegative N atom, while signals in the region 4.85 – 4.62 ppm attributed to the proton on the N atom were found in all the spectra of the complexes. Signals of the proton in the organotin moiety appeared high field as a singlet at 1.53 ppm for the dimethyltin(IV) derivative and as a complex multiplet in the region 8.06 – 7.78 ppm in the diphenyltin(IV) derivative. The signals which appeared in the range 2.35 – 0.88 ppm were found in the dibutyltin(IV) derivative and were attributed to the methylene and methyl protons [47].

The ^{13}C NMR spectra showed a weak signal of the thioureide carbon (-NCS_2) for all the complexes between 202 and 200 ppm [7], while carbon signals of the phenyl moiety resonated between 135 and 125 ppm. The signal in the region 59.80 – 57.03 ppm was found in the spectra of the complexes and has been attributed to the methylene carbon close to the electronegative N atom. Carbons of the alkyl substituents in the complexes resonated at 13.94 ppm [55] in the spectra of the dimethyl complex; in diphenyl complex it showed in the range 136.23 to 128.96 ppm; and between 31.25 and 13.98 ppm in dibutyl complex [68]. The ^{119}Sn chemical shifts values (δ) for this group of complexes ranged from -335 to -350 ppm, which is suggestive of a hexa-coordinated geometry around the Sn metal.

3.18.4. Thermogravimetric Analysis (TGA) of organotin(IV) *N*-benzyldithiocarbamate complexes

The thermogravimetric plots of the complexes are presented in Figures 3.48 – 3.50. The change in the composition of each complex based on mass losses with their respective temperature changes is summarized in Table 3.18.

These complexes followed a two-step decomposition pathway except for **32** which has single step decomposition. The first step of decomposition in complexes **30** and **31** occurred from around 90 to 168, and 122 to 171 °C respectively. These led to the respective mass losses which corresponding to 82.70% and 89.57% of the starting masses. These mass losses have been attributed to the loss of two $-C_6H_5$ group from the ligand moiety of complex **30** and one $-C_4H_9$ group from the organotin moiety of complex **31**. The masses left in the complexes at this stage were in close agreement with the calculated values of the (83.74% for complex 30 and 90.55% for **31**). These remaining compounds undergo further decomposition in a second and final step for both complexes in the range 172 – 263 and 184 – 293 °C respectively. The mass of residues found were 14.42% (calc.; 16.87%) and 24.12% (calc.; 25.0%) of the starting masses for complexes **30** and **31** respectively; and these agreed well with the theoretical estimated value of SnS.

The thermogravimetric graph of complex **32** showed the decomposition to proceed in a single step pathway in the range of 57– 296 °C. The mass left was found to be 21.30% of the starting mass and this was in good agreement with the calculated weight (23.43%) of SnS. The thermal decomposition study therefore showed that all the complexes gave SnS residue and indicated their potential as precursors for SnS nanoparticles.

Table 3.18: Thermal analysis data of complexes **30 – 32**

Compounds	**30**	**31**	**32**
Temp. range of decom. (°C)			
1st stage	89 -168	122 – 171	57 - 296
2nd stage	172 – 263	184 – 293	---------
DTG peak T(°C)			
1st stage	167	161	253
2nd stage	242	274	------
Prod. obtained			
1st decomposition	$(CH_2\text{-}NHCS_2)_2Sn(CH_3)_2$	$(Ph\text{-}CH_3\text{-}NHCS_2)_2Sn(C_4H_9)$	SnS
2nd decomposition	SnS	SnS	------
Mass of res.(mg), Found (Calc)			
1st stage	8.09 (8.10)	9.17 (9.27)	1.71 (1.87)
2nd stage	1.41 (1.65)	2.47 (2.56)	----------

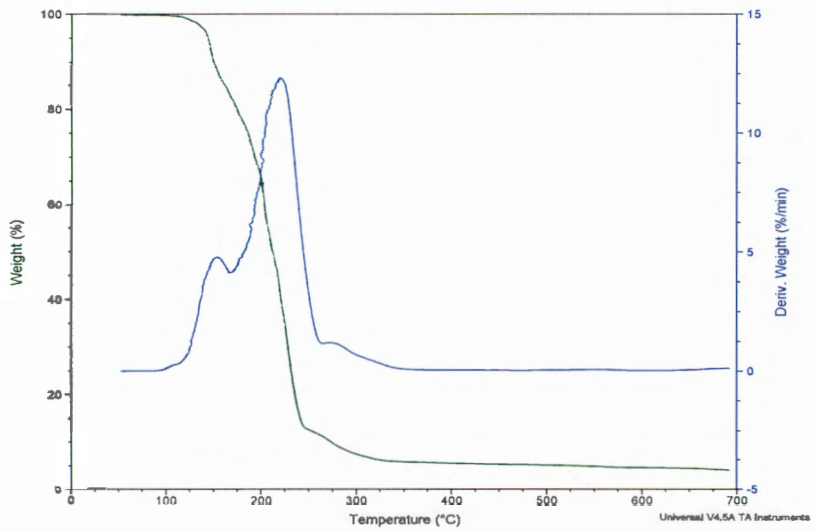

Figure 3.48: TG/DTG curves of complex **30** obtained under nitrogen atmosphere (75 mL/min), heating rate 10 °C/min.

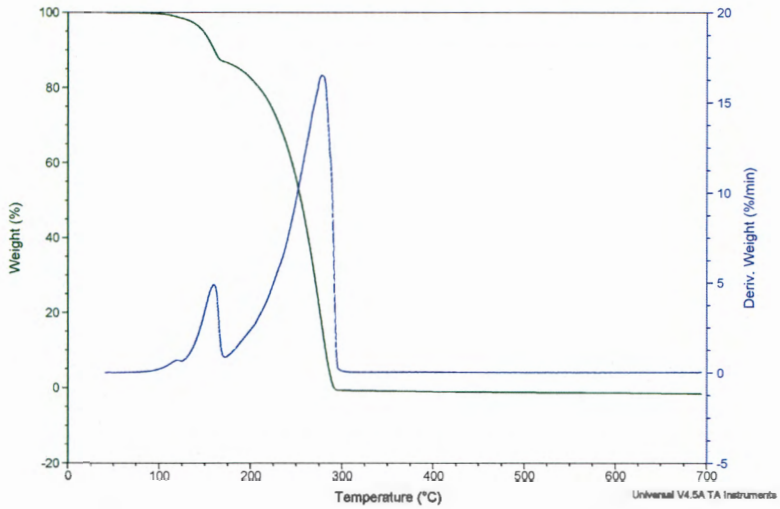

Figure 3.49: TG/DTG curves of complex **31** obtained under nitrogen atmosphere (75 mL/min), heating rate 10 °C/min.

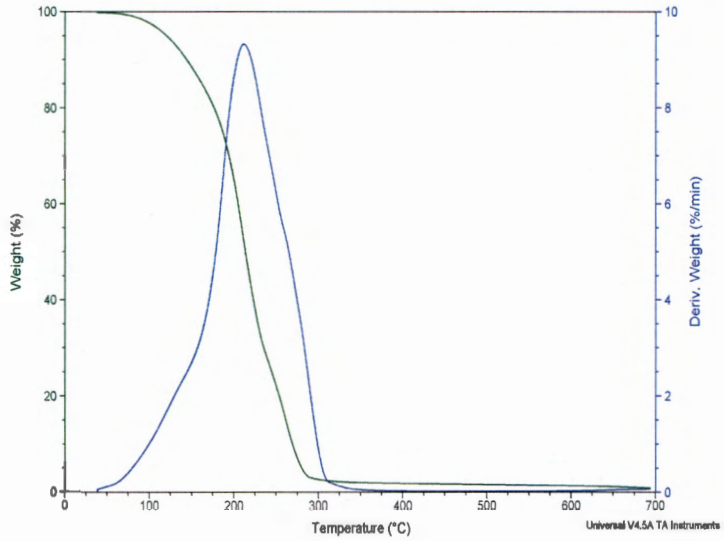

Figure 3.50: TG/DTG curves of complex **32** obtained under nitrogen atmosphere (75 mL/min), heating rate 10 °C/min.

3.19. Chapter conclusion

The salts of the dithiocarbamate ligands were prepared using a one pot reaction system and were obtained in good yield. The synthesis of the respective metal complexes of the ligand have been achieved by the chemical reaction of corresponding organotin(IV) chloride ($RSnCl_3$ and R_2SnCl_2) salts with the ligand ($\mathbf{L^1}$). A series of new organotin(IV) derivatives of dithiocarbamate ligand (*N*-methyl-*N*-phenyldithiocarbamate($\mathbf{L^1}$), *N*-ethyl-*N*-phenyldithiocarbamate ($\mathbf{L^2}$), *N*-butyl-*N*-phenyldithiocarbamate ($\mathbf{L^3}$), *N,N*-methyl phenyl-*N,N*-ethyl phenyldithiocarbamate ($\mathbf{L^1L^2}$), *N,N*-alkyl phenyl-*N,N*-butyl phenyldithiocarbamate ($\mathbf{L^1L^3}$) and ($\mathbf{L^2}$ $\mathbf{L^3}$) , *N,N*-diallyl dithiocarbamate ($\mathbf{L^4}$), *p*-alkyl phenyl dithiocarbamate ($\mathbf{L^5}$, $\mathbf{L^6}$), benzyl dithiocarbamate($\mathbf{L^7}$) have been successfully synthesized and characterized. The structures of some of the complexes have been established through their single crystal analysis. Two types of geometry were generally observed around the central tin atom. A six and five coordinate geometry, with a strong distortion around the tin centre were presented from the crystallographic parameters and data obtained. These geometries have been influenced by the electronic and steric demands of the bulky alkyl group attached to the tin metal and the asymmetric nature of dithiocarbamate ligands used. The thermal analysis showed similar decomposition product for a group of complex with the same parent ligand. However, the varying pattern of decomposition and intermediates obtained for these complexes showed the dissimilarities that exist in the thermal decomposition of structurally related organotin complexes. All the complexes gave different sulfides of the tin (SnS and Sn_2S_3) as their final residues. Thus, the synthesized complexes can be useful as precursor compounds for tin sulfide nanoparticles.

References

[1] APEX2, SAINT, SADABS. Bruker AXS Inc., Madison, Wisconsin, USA. (2007).

[2] G.M. Sheldrick, Acta Crystallogr. Sect. A Found. Crystallogr. 71 (2015) 3–8.

[3] G.M. Sheldrick, Acta Crystallogr. Sect. C Struct. Chem. 71 (2015) 3–8.

[4] A.C. Ekennia, D.C. Onwudiwe, C. Ume, E.E. Ebenso, Bioinorg. Chem. Appl. 2015 (2015) 1–10.

[5] J.P. Fuentes-Martínez, I. Toledo-Martínez, P. Román-Bravo, P.G. y. García, C. Godoy-Alcántar, M. López-Cardoso, H. Morales-Rojas, Polyhedron 28 (2009) 3953–3966.

[6] N. Singh, S. Bhattacharya, J. Organomet. Chem. 700 (2012) 69–77.

[7] Zia-ur-Rehman, N. Muhammad, S. Ali, I.S. Butler, A. Meetsma, Inorg. Chim. Acta 376 (2011) 381–388.

[8] S. Ali, Zia-Ur-Rehman, Muneeb-Ur-Rehman, I. Khan, S.N.A. Shah, R.F. Ali, A. Shah, A. Badshah, K. Akbar, F. Bélanger-Gariepy, J. Coord. Chem. 67 (2014) 3414–3430.

[9] F. Bonati, R. Ugo, J. Organomet. Chem. 10 (1967) 257–268.

[10] M.K. Gupta, H.L. Singh, S. Varshney, A.K. Varshney, Bioinorg. Chem. Appl. 1 (2003) 309–320.

[11] T. Sedaghat, K. Goodarzi, Main Gr. Chem. 4 (2005) 121–126.

[12] N. Awang, I. Baba, B.M. Yamin, M.S. Othman, N.F. Kamaludin, Am. J. Appl. Sci. 8 (2011) 310–317.

[13] N. Khan, Y. Farina, L.K. Mun, N.F. Rajab, N. Awang, Polyhedron 85 (2015) 754–760.

[14] P. Sebatian, D. Iv, Malaysian J. Anal. Sci. 15 (2011) 106–112.

[15] D.C. Onwudiwe, P.A. Ajibade, Int. J. Mol. Sci. 12 (2011) 1964–1978.

[16] P.A. Ajibade, D.C. Onwudiwe, M.J. Moloto, Polyhedron 30 (2011) 246–252.

[17] M. Sirajuddin, S. Ali, M.N. Tahir, Inorganica Chim. Acta 439 (2016) 145–158.

[18] R. Yadav, M. Trivedi, R. Chauhan, R. Prasad, G. Kociok-Köhn, A. Kumar, Inorg. Chim. Acta 450 (2016) 57–68.

[19] J. S. Morris; E. O. Schlemper, J. Cryst. Mol. Struct. 8 (1979) 295–307.

[20] P.A. Cusack, Chemistry of Tin, 2nd Editio, Blackie Academic and professional, London, 1997.

[21] D.C. Onwudiwe, P.A. Ajibade, B. Omondi, J. Mol. Struct. 987 (2011) 58–66.

[22] F. Shaheen, Zia-Ur-Rehman, S. Ali, A. Meetsma, Polyhedron 31 (2012) 697–703.

[23] N. Awang, I. Baba, N.S.A. Mohd Yousof, N.F. Kamaludin, Am. J. Appl. Sci. 7 (2010) 1047–1052.

[24] J.O. Hill, S. Chirawongaram, J. Therm. Anal. 41 (1994) 511–518.

[25] D.C. Onwudiwe, P.A. Ajibade, Polyhedron 29 (2010) 1431–1436.

[26] F. Bonati, S. Cenini, R. Ugo, J. Org. Chem. 9 (1967) 395–402.

[27] S. Thirumaran, V. Venkatachalam, K. Ramalingam, Transition Met. Chem 90 (1997) 89–90.

[28] S. Rathod, M. Phansekar, A. Bhagwan, G. Surve, Indian Drugs 50 (2013) 5–14.

[29] A. Al Bawab, A. Bozeya, F. Odeh, GSTF Int. J. Chem. Sci. 1 (2014) 32–39.

[30] P.A. Ajibade, D.C. Onwudiwe, J. Mol. Struct. 1034 (2013) 249–256.

[31] T. Sedaghat, K. Goodarzi, Phosphorus. Sulfur. Silicon Relat. Elem. 182 (2007) 2227–2233.

[32] A.N. Gupta, V. Kumar, V. Singh, A. Rajput, L.B. Prasad, M.G.B. Drew, N. Singh, J. Organomet. Chem. 787 (2015) 65–72.

[33] Kimoon Kim and James Ibers, Acta Cryst. 7 (1987) 2317–2319.

[34] E.R.T. Tiekink, Appl. Organomet. Chem. 22 (2008) 533–550.

[35] A.T. Kana, T.G. Hibbert, M.F. Mahon, K.C. Molloy, I.P. Parkin, L.S. Price, Polyhedron 20 (2001) 2989–2995.

[36] A.Z. Halimehjani, S. Torabi, V. Amani, B. Notash, M.R. Saidi, Polyhedron 102 (2015) 643–648.

[37] D.C. Onwudiwe, P.A. Ajibade, Polyhedron 29 (2010) 1431–1436.

[38] Damian C. Onwudiwe; Peter A. Ajibade, Asian J. Chem. 25 (2013) 10057–10061.

[39] N. Awang, N.F. Kamaludin, I. Baba, K.M. Chan, N.F. Rajaajab, A. Hamid, Orient. J. Chem. 32 (2016) 101–107.

[40] B.A. Prakasam, K. Ramalingam, R. Baskaran, G. Bocelli, A. Cantoni, Polyhedron 26 (2007) 1133–1138.

[41] M. Jabeen, S. Ali, S. Shahzadi, M. Shahid, Q.M. Khan, S.K. Sharma, K. Qanungo, J. Iran. Chem. Soc. 9 (2012) 307–320.

[42] R. Yadav, M. Trivedi, R. Chauhan, R. Prasad, G. Kociok-Köhn, A. Kumar, Inorg. Chim. Acta 450 (2016) 57–68.

[43] J.O. Adeyemi, D.C. Onwudiwe, A.C. Ekennia, R.C. Uwaoma, E.C. Hosten, Inorg. Chim. Acta 477 (2018) 148–159.

[44] P.A. Ajibade, D.C. Onwudiwe, J. Coord. Chem. 64 (2011) 2963–2973.

[45] I.P. Alimarin, V.I. Shlenskaya, Pure Appl. Chem. 21 (1970) 461–478.

[46] D.C. Onwudiwe, Y.B. Nthwane, A.C. Ekennia, E. Hosten, Inorg. Chim. Acta 447 (2016) 134–141.

[47] M.S. Ahmad, M. Hussain, M. Hanif, S. Ali, M. Qayyum, B. Mirza, Chem. Biol. Drug Des. 71 (2008) 568–576.

[48] N. Srinivasan, S. Thirumaran, S. Ciattini, J. Mol. Struct. 936 (2009) 234–238.

[49] S.P. Sovilj, G. Vučković, K. Babić, T.J. Sabo, S. Macura, N. Juranić, J. Coord. Chem. 41 (1997) 19–25.

[50] G. Hogarth, Mini Rev. Med. Chem. 12 (2012) 1202–1215.

[51] D.C. Onwudiwe, M. Hrubaru, E.E. Ebenso, J. Nanomater. 2015 (2015).

[52] D.C. Onwudiwe, J.N. Mugo, M. Hrubaru, E. Hosten, J. Sulfur Chem. 36 (2015) 36–47.

[53] L.C. Dias, M.M.M. Rubinger, J.P. Barolli, J.D. Ardisson, I.C. Mendes, G.M. De Lima, L. Zambolim, M.R.L. Oliveira, Polyhedron 47 (2012) 30–36.

[54] T. Sedaghat, Z. Shokohi-Pour, J. Coord. Chem. 62 (2009) 3837–3844.

[55] R.B. and A.K.R. Jyoti Sharma, Yashpal Singh, Polyedron 5387 (1995) 1097–1102.

[56] H.D. Yin, S.C. Xue, Appl. Organomet. Chem. 20 (2006) 283–289.

[57] O. Jung, J.H.W.A. Jeong, Polyhedron 8 (1989) 1413–1417.

[58] B.F. Ali, W.S. Al-Akramawi, K.H. Al-Obaidi, A.H. Al-Karboli, Thermochim. Acta 419 (2004) 39–43.

[59] R.J.K.D.C.O.T.A. Christien A. Strydom, Electrochim. Acta (2013) 19– 25.

[60] G. Hogarth, in:, Prog. Inorg. Chem. 53, (2005) 71–561.

[61] M. Sarwar, S. Ahmad, S. Ahmad, S. Ali, S.A. Awan, Transit. Met. Chem. 32 (2007) 199–203.

[62] N.K. Kaushik, B. Bhushan, A.K. Sharma, Transit. Met. Chem. 255 (1985) 250–255.

[63] D.C. Onwudiwe, T. Arfin, C.A. Strydom, R.J. Kriek, Electrochim. Acta 109 (2013) 809–817.

[64] M.A. Affan, M.A. Salam, F.B. Ahmad, F. White, H.M. Ali, Inorg. Chim. Acta 387 (2012) 219–225.

[65] N. Awang, I. Baba, B.M. Yamin, World Appl. Sci. J. 12 (2011) 630–635.

[66] D.C. Menezes, G.M. De Lima, A.O. Porto, C.L. Donnici, J.D. Ardisson, A.C. Doriguetto,

J. Ellena, Polyhedron 23 (2004) 2103–2109.

[67] R. Sharma, N.K. Kaushik, Indian J. Chem43A (2004) 769–772.

[68] M. Sirajuddin, S. Ali, V. Mckee, RSC Adv. 4 (2014) 57505–57521.

Chapter four

4.0. Biological application of the synthesized complexes.

Chapter Summary

The synthesized complexes reported in chapter three have been screened biologically for their antimicrobial, anticancer and antioxidant activities.

In this chapter, the biological studies (materials, methods, results and discussion) have been grouped into three studies:

- Antimicrobial studies
- Anticancer studies
- Antioxidant studies

4.1 Introduction

Metal based compounds continues to provide a platform for drug designs due to their wide range of geometries and coordination numbers which are better suited to target specific biological sites [1]. Organometallic compounds are one of such useful class of metal based compounds which have at least one metal to carbon bond within their molecules. Their diverse stereochemistry and structure have resulted in various promising biological activities [2]. The design of metal based drugs has taken center stage in the design of useful biologically active compounds in recent times, and this is ascribed to the synergy created from the organic drug and the metal moiety. This has consequently given rise to:

- enhanced biological activities of the organic fragment of the metal-drug due to the presence of the metal ion. This is possibly due to a longer retention time which allows these drugs to get to targeted biological site effectively, or due to formation of reactive oxygen species (ROS), among other effects.
- decrease in the associated metal toxicity towards the host cells. This is achieved since complexation with organic molecules facilitates the carrying of this metal ion to the specific action site, thus making it less available for undesired reactions (such as inhibition of enzymes, or other damaging reactions) which can be harmful to the general wellbeing of the organism [3].

Derivatives of organotin compounds, due to their diverse structural possibilities, have shown immense potentials in research as useful group of compounds. Various structures such as monomers, dimers, oligomers and polymers have been observed for complexes of organotin in earlier reports [4]. Recent works have slowly replaced this ligand with sulfur containing ligands due to their similarities to biologically active molecules such as amino acid and vitamins [4]. Prominent example with similar features as the carboxylate is the dithiocarbamate derivatives which possess two sulfur atoms (which replaced the two oxygen atoms in the carboxylate molecules). They are capable of binding in different fashions and also with the potential to generate a broad variety of molecular and supramolecular structures [5]. A large number of the metal dithiocarbamate complexes of both transition metals and lanthanides have been studied and proven to show useful biological applications [6,7]. However, their main group counterparts are less widely explored. Organotin(IV) dithiocarbamate belongs to this group of main group

dithiocarbamate complexes. Organotin(IV) dithiocarbamate complexes have been reported to exhibit biological properties such as antimicrobial, anticanacer, antiinflamatory and pesticidal activities [8–11]. The dithiocabamate, organotin moieties, and the coordination number of the centeral metal play crucial role in determining the biological proficiency of these group of complexes [4].

The useful biological properties of organotin compounds are structure dependent. The presence of an alkyl group often lowers the electron density in the complex, and, thus, affects their biological potential. Furthermore, a comparison of the electron density among various organotin complexes can be used to predict their interaction with bio-receptors[12]. Lengthening of the chain in the alkyl group attached to the tin metal, enhances the lipophilic character. The interaction of the bulky phenyl group with biomolecules within a cell can be achieved via π-π interactions because of the high lipophilicity observed for the phenyl group. Thus, due to lipophilicity, organotin can easily interact with cellular membranes with intracellular as well as cytoplasmic membrane being the possible site of action [12].

Organotin complexes are among the non-platinum compounds that have shown promising potential with diverse antitumor activity on diverse cancerous cell [13]. They have shown less toxicity as compared to the platinum compounds whilst displaying a non-cross-resistance [13]. Several di- and tri-organotin complexes have shown great *in vitro* antiplroliferating activities against solid and hematologic cancer, due to the possibilities for variation of the ligands attached to the central metal and the alkyl groups of the organotin moieties[14]. Both the ligand and the metal moieties play key roles in the transportation of the molecules to the target sites and cytotoxicity respectively[1]. Organotin moieties have shown, from literature, to bind to glycol proteins or to cellular proteins and also interact with DNA which consequently led to the death of such cell by apoptotic mechanism [13,14].

Some of the products continuously generated by the immune system in human body include reactive oxygen species and free radicals, which are responsible for protection against harmful oxidative compounds by ensuring the removal of dangerous or excessive unwanted radicals in the living system [15]. The partial reduction of oxygen in the body has continuously led to the generation of this reactive oxygen species such as superoxide, hydroxyl and hydrogen peroxides radical. Excessive production of these radicals leads to DNA, proteins and lipid damages which

consequently enhance ageing, cancer and some neuro and heart related diseases[16]. For example, complications associated with severe influenza have been associated with the formation of superoxide anions which are produced by the infiltration of the infected organs by macrophages. Dithiocarbamates belong to the class of metal chelating antioxidant [17], and have shown ability to stop the proliferation and remove unwanted superoxide anions [18]. Transition metal complexes of dithiocarbamates have shown promising antioxidative properties, but not much is known about the antioxidant properties of organotin(IV) complexes [19].

Thus, in this chapter the antimicrobial, the cytotoxicity and the antioxidant potentials of the organotin(IV) dithiocarbamate complexes are reported.

4.2. Antimicrobial studies

4.2.1. Methodology for antimicrobial studies

Clinical isolates of different microbial strains were collected from department of Microbiology, Federal Teaching Hospital, Abakaliki, Nigeria. The bacteria strains were Gram negative (*Escherichia coli, Klebsiella Pneumonia* and *Pseudomonas Aeruginosa*) and Gram positive (*Bacillus cereus and Staphylococcus aureus*) organisms. The fungi are *Candida albicans* and *Aspergillus flavus*. The microbial strains were selected based on their clinical and pharmacological relevance [20]. Antimicrobial screening was carried out using agar disc diffusion method [21]. The petri plates were prepared using sterile Muller–Hinton agar (MHA). The inocula of test cultures (10^6 CFU/mL) were streaked on to the condensed Muller Hinton agar in petri plates using a sterilized cotton swab, in order to ensure a uniform thick lawn or layer of growth, and allowed to dry for 15 min. About 10, 25 and 50 μg/mL concentrations of stock solutions of the complexes were prepared using 80% dimethylsulfoxide (DMSO) as diluent [22,23]. Consequently, wells were bored into the solidified agar surfaces on the petri dishes using 6 mm sterile cork borer and were impregnated with 25 μL of the sample stock solutions. About 20 μL of 1.25 mg/mL 3-(4, 5-dimethylthiazol-2-yl)-2, 5-diphenyltetrazolium bromide (MTT) (Sigma-Aldrich) was added to each plate and observed for a purple colouration [23]. The plates were incubated for 24 h at 37 °C for the bacteria and 48 h at 30 °C for the fungi strains. Control experiments were carried out under similar condition by using commercially available

antibacterial drug (Sulfamethoxazole) and an antifungal drug (Ketoconazole) as the positive control drugs, while 80% dimethylsulfoxide was used as a negative control.

The sensitivities of the microorganism species to the samples were determined by measuring the sizes of inhibitory zones (including the diameter of disk) on the agar surface around the disks, and values <6 mm were considered as inactive against the microorganisms. Thus, compounds that showed no activity (R) at 100 μg/mL or <15 mm were not screened (NS) at 50 μg/mL (see appendix). Zones of inhibition were recorded in millimetres and the experiment was repeated in quadruplet. Experimental results were given as mean ± S.D. of the four parallel measurements.

4.2.2. Results of antimicrobial activities of ligand L^1 - L^7 and complexes 1–32

Table 4.1: Summary of antimicrobial screening of ligand L^1 - L^7 and complexes 1–32

S/N	Compounds	*S. aureus*	*K. pneumonia*	*B. cerues*	*E.Coli*	*P. aeruginosa*	*C. albican*	*A. flavus*
L^1	*N*-methyl DTC	NA	NA	NA	NA	NA	NA	NA
L^2	*N*-ethyl DTC	NA	NA	NA	NA	NA	NA	NA
L^3	*N*-butyl DTC	NA	NA	NA	NA	NA	NA	NA
L^4	DiallylDTC	NA	NA	NA	NA	NA	NS	NA
L^5	*p*-methyl DTC	NA	NA	NA	NA	NA	NA	NA
L^6	*p*-ethyl DTC	NS	NA	NS	NA	NA	NS	NA
L^7	benzyl DTC	NS	NA	NS	NA	NA	NS	NA
SFMT	Sulfamethoxazole	23 ±0.7	26 ±0.0	26 ±0.4	30 ±0.4	28 ±0.0	NA	NA
KTCZ	Ketoconazole	NA	NA	NA	NA	NA	27 ±0.7	22 ±0.7
1	$[(C_4H_9)ClSn(L^1)_2]$	11 ±0.7	15 ±0.7	NA	15 ±1.4	17 ±1.4	NA	NA
2	$[(C_6H_5)ClSn(L^1)_2]$	11 ±0.7	15 ±0.7	11 ±0.0	12 ±2.1	15 ±0.7	11 ±0.7	11 ±2.1
4	$[(CH_3)_2Sn(L^1)_2]$	09 ±1.4	10 ±0.0	08 ±0.0	15 ±0.0	R	R	09 ±0.7
3	$[(C_4H_9)_2Sn(L^1)_2]$	10 ±0.7	16 ±0.7	R	17 ±2.1	17 ±0.7	R	R
5	$[(C_6H_5)_2Sn(L^1)_2]$	14 ±2.1	20 ±0.0	10 ±0.0	21 ±1.4	19 ±0.7	09 ±2.1	09 ±2.1
6	$[(CH_3)ClSn(L^2)_2]$	08 ±1.4	14 ±0.0	NA	17 ±2.1	NA	10 ±2.1	10 ±0.4
7	$[(C_4H_9)ClSn(L^2)_2]$	14 ±0.7	19 ±0.0	NA	21 ±0.0	18 ±0.7	15 ±0.7	11 ±1.4
8	$[(C_6H_5)ClSn(L^2)_2]$	15 ±0.7	19 ±0.7	10 ±0.7	18 ±0.7	20 ±0.0	14 ±0.4	17 ±0.4
9	$[(CH_3)_2Sn(L^2)_2]$	11 ±0.7	NA	NA	11 ±0.4	NA	NA	NA
10	$[(C_4H_9)_2Sn(L^2)_2]$	13 ±1.4	19 ±2.1	10 ±1.4	19 ±0.4	20 ±0.4	11 ±0.4	14 ±0.4
11	$[(C_6H_5)_2Sn(L^2)_2]$	16 ±0.0	23 ±0.4	13 ±0.4	23 ±0.4	18 ±0.0	15 ±0.4	16 ±0.7
12	$[(C_4H_9)ClSn(L^3)_2]$	15 ±0.7	21 ±0.7	17 ±0.0	23 ±0.0	19 ±0.7	17 ±1.4	13 ±0.0
13	$[(CH_3)_2Sn(L^3)_2]$	10 ±0.7	15 ±0.7	10 ±0.0	17 ±0.7	12 ±0.0	R	07 ±2.1
14	$[(C_4H_9)_2Sn(L^3)_2]$	15 ±0.0	20 ±0.7	13 ±0.0	21 ±0.7	17 ±2.1	13 ±0.0	11 ±0.7
15	$[(C_6H_5)_2Sn(L^3)_2]$	17 ±0.0	26 ±0.4	20 ±0.0	26 ±2.1	15 ±1.4	19 ±0.7	17 ±0.0

S/N	Compounds	*S. aureus*	*K. pneumonia*	*B. cerues*	*E. coli*	*P. aeruginosa*	*C. albican*	*A. flavus*
16	$[(CH_3)_2SnL^1L^2]$	NS	NS	NS	NS	07±0.7	NA	NS
17	$[(C_4H_9)_2SnL^1L^2]$	NS	NS	NS	08±0.0	NS	NS	09±0.7
18	$[(C_6H_5)_2SnL^1L^2]$	NS	15±0.0	NS	11±0.0	11±0.0	NS	NS
19	$[(CH_3)_2SnL^1L^3]$	NS	NS	NS	NA	11±0.0	NS	NS
20	$[(CH_3)_2SnL^2L^3]$	NS	NS	NS	NS	NA	NS	NS
21	$[(C_4H_9)ClSn(L^4)_2]$	NA	10 ±2.1	12 ±0.7	13 ±0.4	19 ±0.4	08 ±2.1	R
22	$[(CH_3)_2Sn(L^4)_2]$	11 ±0.0	14 ±2.1	10 ±0.0	15 ±0.7	11 ±0.7	07 ±2.1	R
23	$[(C_4H_9)_2Sn(L^4)_2]$	11 ±0.7	15 ±1.4	15 ±0.7	15 ±1.4	21 ±0.4	09 ±0.7	10 ±0.7
24	$[(C_6H_5)_2Sn(L^4)_2]$	13 ±0.5	16 ±1.1	16 ±0.5	16 ±0.5	23 ±0.7	09 ±0.3	11±0.7
25	$[(C_6H_5)ClSn(L^4)_2]$	09±0.7	NA	07±1.4	NA	NA	NA	NA
26	$[(C_4H_9)_2Sn(L^5)_2]$	13 ±0.7	18 ±0.7	17 ±0.4	21 ±1.4	15 ±0.7	07 ±0.4	NA
27	$[(C_6H_5)_2Sn(L^5)_2]$	15 ±0.7	23 ±0.7	20 ±0.4	25 ±0.7	20 ±0.7	10 ±0.4	11 ±0.7
28	$[(CH_3)_2Sn(L^6)_2]$	14±0.7	NA	10±0.0	11±0.7	11±0.7	09±2.1	11±1.4
29	$[(C_4H_9)_2Sn(L^6)_2]$	11±0.7	15±1.4	11±0.7	12±0.0	NA	09±2.1	13±1.4
30	$[(CH_3)_2Sn(L^7)_2]$	09±0.7	NA	NA	NA	09±0.7	NS	10±0.7
31	$[(C_4H_9)_2Sn(L^7)_2]$	10 ±0.7	07±0.7	R	10±2.8	11±0.7	09±1.4	10±0.7
32	$[(C_6H_5)_2Sn(L^7)_2]$	10±1.4	10±1.4	10±0.7	07±0.0	12±1.4	NA	11±0.0

50µg/mL(Triplicate results) ; NS = Not screened (compounds with less than 15mm inhibitory zones @100µg/mL concentration);NA=Not active

4.2.3. Discussion of the antimicrobial studies

The synthesized complexes 1 – 32 were screened *in vitro* for their antimicrobial activities against five bacterial strains (*S. Aureus*(G^+), *B. cerues*(G^+), *K. pneumonia*(G^-), *P. aeruginosa* (G^-)and *E. coli*(G^-)) and two fungi organisms (*C. albican* and *A. flavus*) at three concentrations of 10, 25 and 50 μg/mL. Significant antimicrobial activity (inhibitory zone >6mm) was observed at 50 μg/mL and the results obtained were taken as a measure of the antimicrobial potentials and minimum inhibitory concentration (MIC) of the complexes. The obtained data are presented in Table 4.1 and summarized as histogram in Figures 4.1 – 4.7 (the figures are based on ligand types). The antimicrobial activity was assessed by measuring the inhibition halo of microbial growth around the well, and the results were classified according to the following scale: inhibition zones down to 9 mm, inactive; 9–12 mm, moderately active; 13–18 mm, active; above 18 mm, very active [24,25]. Generally, the results showed that the bacterial organisms were more susceptible to the organotin complexes, although good to moderate activities were also recorded against the fungi organisms. The results obtained from the screening showed the free ligands are inactive against all tested microorganism at 50 µg/mL. However, upon complexation, the complexes gave appreciable antimicrobial activities against the used organisms. This observed enhanced antimicrobial activity upon complexation of the ligand with the organotin may be attributed to the Overton's concept and Tweedy's chelation theory [52,53]. It may also be based on the intrinsic biological effects of the organotin moiety [26,27]. According to Overton's concept, lipophicity of the complexes play a major role in the antimicrobial activity because lipid-soluble substances are favoured by the lipid cell membrane, i.e. it allows the permeation of hydrophobic material [28]. Furthermore, according to Tweedy's chelation theory, complexation reduces the polarity of metal ion. Thus, upon complexation, the lipophilic tendencies of the tin metal centre is enhanced which favours the permeation of these complexes through the cell membrane[29]. The partial sharing of positive charge of the metal ion with the sulfur donor atoms, the overlapping of the ligand's orbitals and the electron delocalization over the whole chelate are the two main factors contributing to the reduction in polarity of the metal center [28]. The mode of action as suggested for compounds containing the azomethine group (>C=N) may involve hydrogen bond formation with the active centre of the cell constituents through the azomethine group, which consequently interferes with the cell process and ultimately death [30].

Similarly, the pattern of the antibacterial results obtained for the complexes tend to suggest that the Gram negative bacterial organisms were more susceptible to the complexes compared to the Gram positive organisms. This could be attributed to the structural difference between the two bacterial organisms. The Gram positive bacteria possess cell wall. The complexity of the cell wall is due to an outer-lipid membrane formed from lipopolysaccharide contributing to the antigenic specificity, which does not permit easy penetration of the complexes into the bacteria [19,31–33]. The Gram negative bacterial organisms do not have cell walls but a simpler cell membrane that lacks the rigidity of the cell wall. Hence, they are more susceptible to the complexes compared to the Gram positive bacterial organisms.

The higher activities observed for the complexes with the phenyl rings in **2**, **5**, **8**, **11**, **15**, **24**, **25**, **27** and **32** may be attributed to the increase in lipophilic properties of the complexes through the lipid bilayer of the bacteria organisms due to the presence of the planar phenyl groups attached to the tin center [34]. The complexes with the weakest activities were **16** – **20**.

In the complexes obtained using *N*-alkyl-*N*-phenyldithiocarbamate ligands, the following structural activities were deduced

i. antimicrobial activity of the complexes increased with lengthening of the *N*-alkyl chain of the dithiocarbamate moiety. This was comparable to what has been reported for the organotin carboxylate complexes [35]. Thus, the nature of the anionic ligand may affect the biological activity of these complexes. Complexes show activity in this order $\mathbf{L^1<L^2<L^3}$

ii. antimicrobial activity increased as the alkyl moiety of the organotin(IV) salts increases. That is, the disubsitituted organotin salt (of the formular R_2SnCl_2). Complexes showed activity in the order $RSnCl_3 < R_2SnCl_2$ which agree well with those reported in literature [36].

iii. methyl derivatives of both mono and di-substituted organotin complexes have the least activity (with inhibitory zone range of 7 – 17 mm), while the phenyl derivative have the best antimicrobial activity (with inhibitory zone range of 9 – 26 mm) which agree with those observed in literature [37].
$(CH_3)ClSn <(CH_3)_2Sn <(C_4H_9)ClSn < (C_4H_9)_2Sn <(C_6H_5)ClSn < (C_6H_5)_2Sn$

iv. all the phenyl derivatives in the *N*-alkyl-*N*-phenyl dithiocarbamate compounds showed useful activity ranging from moderate to very active antimicrobial activity for both bacteria and fungi organisms used.

v. the complexes of the mixed *N*-alkyl derivatives showed no appreciable activity (complexes 16 – 20). Only complex 18 showed a moderate activity for *K. pneumonia, E. coli* and *P. aeruginosa*. This is due to the planar nature of the phenyl group which favours lipophilicity of this complex.

In complexes with *N,N*-diallyldithiocarbamate ligands, the following structural activities were deduced:

vi. the ligand has no activity (at the concentration used for the study), but upon complexation, moderate to good antimicrobial activity were observed in the inhibitory zone range of 7 – 21 mm

vii. the mono-substituted organotin derivatives were less active compared to the di-substituted derivatives. Thus, antimicrobial activity increases with increase in the number of alkyl substituents

viii. complexes **23** and **24** gave a moderate antifungal activity compared to others for both fungi while **21** and **22** gave weak activity for just *C. albican*.

For complexes derived from ligands which are of primary amine sources ($\mathbf{L^5}$-$\mathbf{L^7}$), the following structural activities were deduced

ix. complexes **26** and **27** showed good broad spectrum antimicrobial activity (with inhibitory zone range of 7 – 25 mm). However, complex **26** showed resistance against *A. flavus*. The best activity was shown by complex **27** (within the range of 10 – 25 mm) due to the reduced polarity of the tin centre caused by complexation. Overall, complex **27** gave the best antimicrobial activity for *E.coli* and *K. pneumonia.*

x. similarly, complexes **28** and **29** showed a moderate antimicrobial activity. However, both complexes showed good resistance against *K. pneumonia* and *P. aeruginosa.* . A weak antifungal activity was recorded for both complexes.

xi. complexes **30– 32** showed a weak antimicrobial activity towards the organism (with inhibitory zone range of 7 – 12 mm). The phenyl complex gave the best activity for this ligand ($\mathbf{L^7}$). The observed weak activity could be attributed to the nature of the ligand used.

In general, all the complexes showed better activity than their parent ligands which exhibited no activity at the concentration used in the study. The dissimilarity in the antimicrobial activities for a group of complexes with the same ligand, showed that some of them are specific to a particular group of bacteria [38]. It is expedient to note that the nature of the ligand used influenced the general activity of the complexes. The ligand derived from secondary amine sources generally gave a better activity than their primary counterpart. Also, the number of substitution of the chloride ion in the organotin(IV) moiety play a major role in the antimicrobial activity of the complexes similar to what has been reported for the carboxylate complex [36]. From the study, the organotin complexes with single chloride ion showed lower activity compared to their counterpart without chloride ion. This correlates well with what has been reported for the bactericidal activity of this class of compounds with similar number and type of organic groups bonded to the Sn(IV)-center ($R_3Sn^+ > R_2Sn_2^{2+} > RSn_3^{3+} > Sn_4^+$, bactericidal activity and toxicity scale) [36]. It is also noticeable that the biological activity of an organotin complex can decrease if the alkyl moiety attached to the tin metal is too large (e.g, octyl group) or too small (e.g, methyl group). Thus, in the search for an organotin complex with useful antimicrobial properties, the ratio between the lipophilicity and solubility properties of these complexes in an organism must be considered [39]. One major improvement often associated with the replacement of the chloride ion with an organic ligand is the reduction in side effect such as toxicity which could also reduce the antimicrobial activity. Thus, a right balance for the substitution and the availability of the chloride ion is needed.

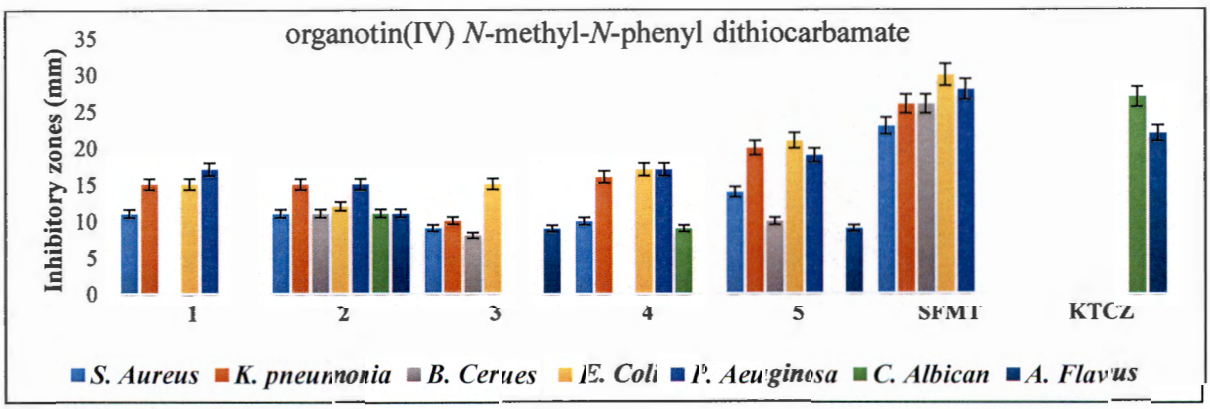

Figure 4.1: Histogram showing antimicrobial activities of the complexes **1 – 5**.

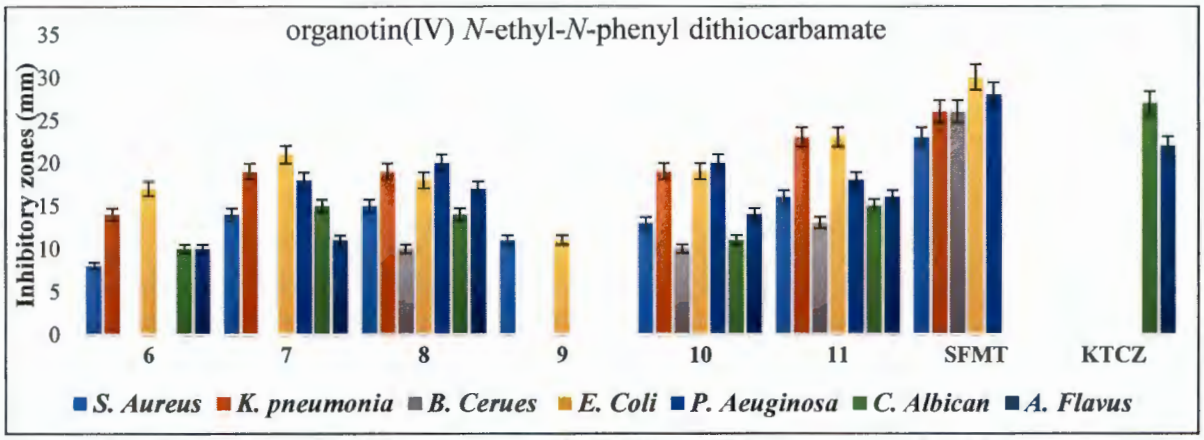

Figure 4.2: Histogram showing antimicrobial activities of the complexes **6 – 11**.

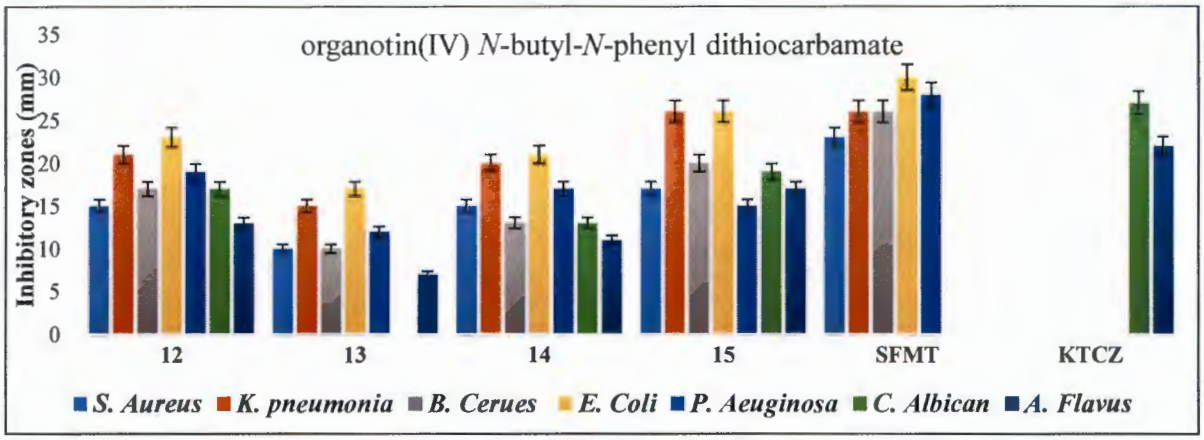

Figure 4.3: Histogram showing antimicrobial activities of the complexes **12 – 15**.

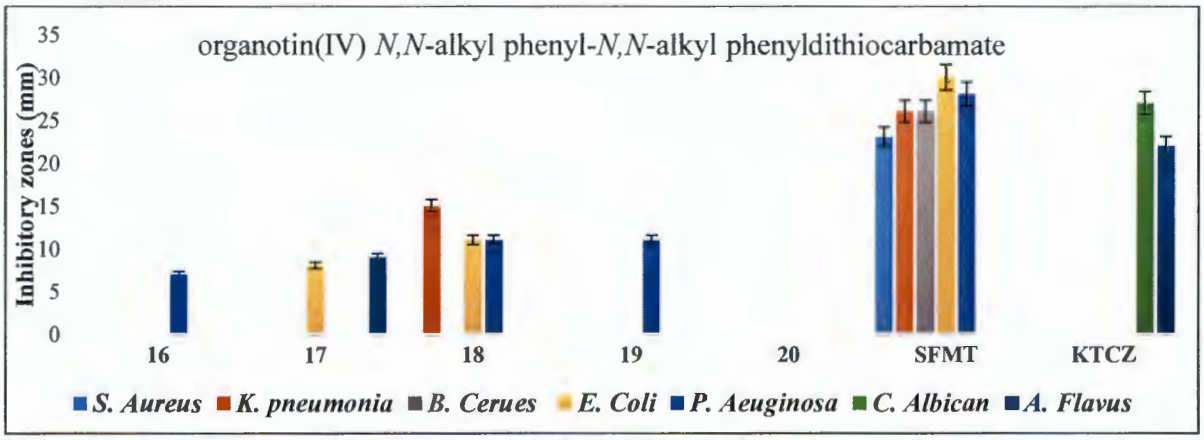

Figure 4.4: Histogram showing antimicrobial activities of the complexes **16 – 20**.

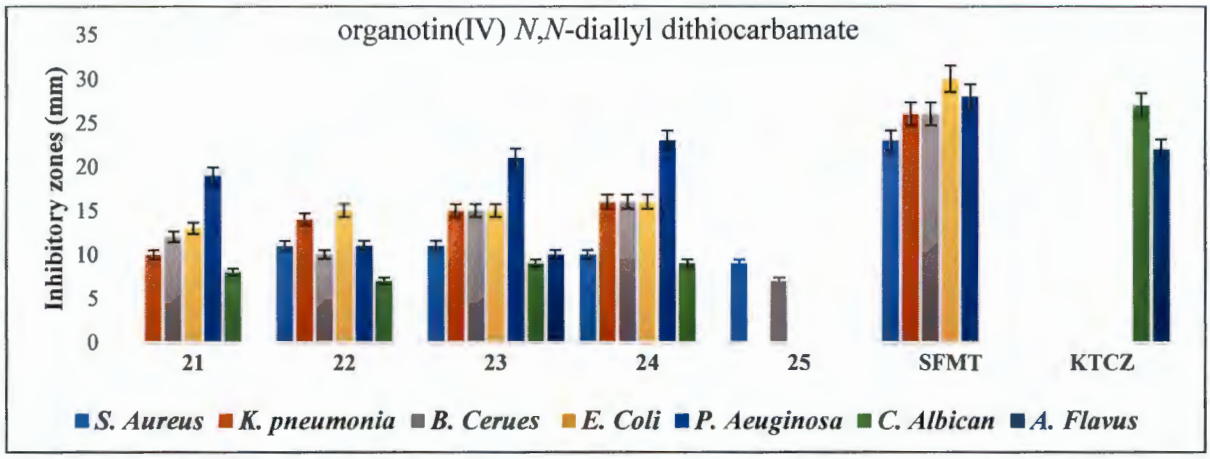

Figure 4.5: Histogram showing antimicrobial activities of the complexes **21 – 25.**

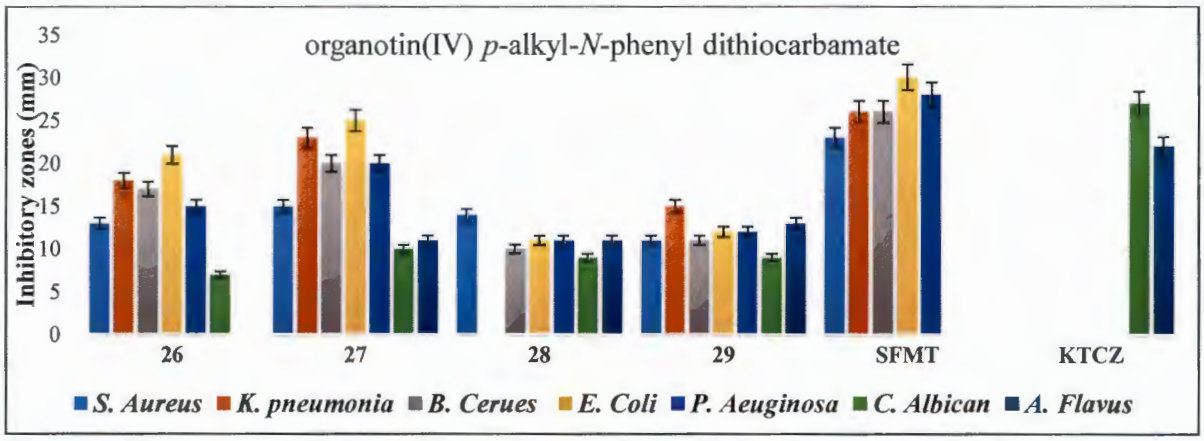

Figure 4.6: Histogram showing antimicrobial activities of the complexes **26 – 29.**

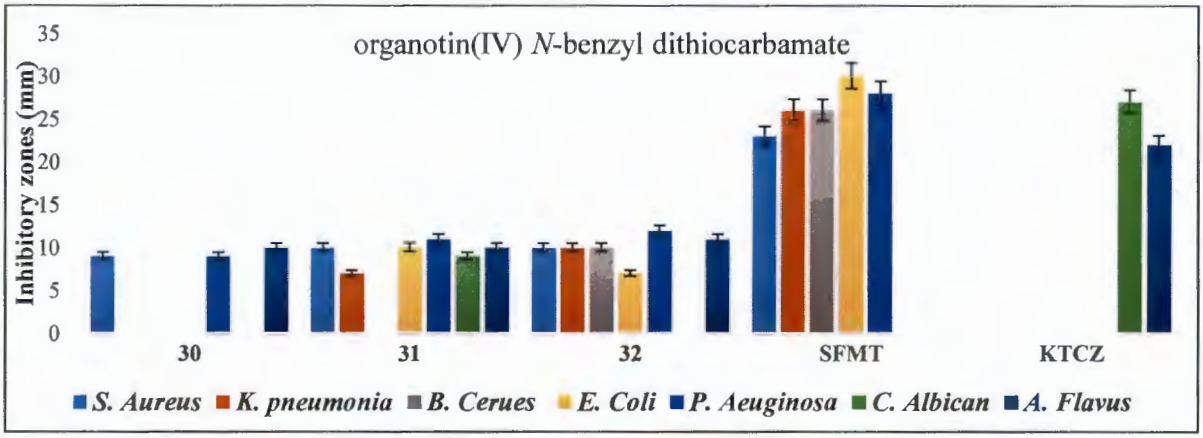

Figure 4.7: Histogram showing antimicrobial activities of the complexes **30 – 32.**

4.3. Antioxidant activity

4.3.1. Methodology for antioxidant activity evaluation

The antioxidant activities of the complexes were evaluated using the 2,2-diphenyl-1-picrylhydrazyl (DPPH) and reducing power assays [40]. The working solution (5 mg/mL) of the samples was prepared in dimethylsulfuoxide (DMSO), while gallic acid (1 mg/mL), used as standard, was dissolved in methanol. This method was used because of its general acceptance, simplicity, and the ability to compare with similarly reported complexes [41].

4.3.1.1. DPPH assay

About 100 μL of each sample and gallic acid were transferred into the first row of 96 well plates (containing 100 μL of DMSO) using automatic pipette. The samples were serially diluted by transferring 100 μL of the solution to the second well, and subsequently to other wells. A solution of DPPH (0.15 mM; 200 μL) was added to all the wells containing the samples, and the plates were kept in the dark for 30 min. The blank contained only DMSO and DPPH solution. The absorbance was measured at 517 nm using microplate reader (Versa max, China). Equation (1) was used to calculate the percentage antioxidant activity

$$\%AA = \frac{[Ab - As]}{Ab} x\ 100 \quad \ldots\ldots (1)$$

where Ab is the absorbance of the blank and As is the absorbance of the complexes or standard. A plot of the percentage antioxidant activity (AA) against concentration was used to extrapolate the 50% inhibition concentration (IC_{50}).

4.3.1.2. Reducing power assay

The complexes or gallic acid (5 mg/mL or 1 mg/mL; 100 μL) were transferred into the first row of the 96 well plates (containing 100 μL of DMSO) and then serially diluted using automatic pipette. Sodium phosphate buffer (0.2 M, pH 6.6; 50 µL) and aqueous potassium hexacyanoferrate (1%; 50 μL) were added to each well containing the complexes or gallic acid. After 20 min of incubation at 45 °C, 50 μL of 10% trichloroacetic acid was added to the mixture in each well. A portion (80 μL) of the mixture in each well was transferred to a new well plate containing 80 μL of deionized water. A solution of $FeCl_3$ (0.1% w/v; 16 μL) was

added to each well and absorbance was measured at 690 nm using microplate reader (Versa max, China). The blank contained deionized water instead of complexes. The concentration ($IC_{0.5}$) required for the complexes or standard to give an absorbance of 0.5 was obtained by plotting a graph of the absorbance against concentration [40].

4.3.2. Results of antioxidant activities of complexes 1 - 11 and 21 – 25.

Table 4.2: Antioxidant activities (μg/mL) of complexes **1-11** and **21 – 25**.

Samples Code	Sample	DPPH	Reducing power
$\mathbf{L^1}$	*N*-methyl DTC	131±2	NA
$\mathbf{L^2}$	*N*-ethyl DTC	127±2	NA
$\mathbf{L^3}$	*N*-butyl DTC	110±1.5	NA
$\mathbf{L^4}$	diallyl DTC	72±3.2	NA
GA	gallic acid	6.3±0.1	20.1±0.5
1	$(C_4H_9)ClSn(L^1)_2$	788±8	344±2
2	$[(C_6H_5)ClSn(L^1)_2]$	608±10	464±1
3	$[(CH_3)_2Sn(L^1)_2]$	187±2	561±3
4	$[(C_4H_9)_2Sn(L^1)_2]$	175±6	919±2
5	$[(C_6H_5)_2Sn(L^1)_2]$	62±2	349±3
6	$[(CH_3)ClSn(L^2)_2]$	117±2	242±5
7	$[(C_4H_9)ClSn(L^2)_2]$	245±7	538±4
8	$[(C_6H_5)ClSn(L^2)_2]$	256±3	640±1
9	$[(CH_3)_2Sn(L^2)_2]$	29±1	318±1
10	$[(C_4H_9)_2Sn(L^2)_2]$	59±1	507±2
11	$[(C_6H_5)_2Sn(L^2)_2]$	65±1	764±3
21	$[(C_4H_9)ClSn(L^4)_2]$	1136±22	NA
22	$[(CH_3)_2Sn(L^4)_2]$	31±2	206±2
23	$[(C_4H_9)_2Sn(L^4)_2]$	118±2	354±2
24	$[(C_6H_5)_2Sn(L^4)_2]$	60±1	231±0.6
25	$[(C_6H_5)ClSn(L^4)_2]$	171±1	NA

Data (n=3) expressed as mean ± standard error. NA: not active

4.3.3. Discussion of antioxidant activities

The 2,2-diphenyl-1-picrylhydrazyl (DPPH) radical scavenging assay has been widely employed in the study of antioxidant activities due to its simplicity and short time required in the analysis. DPPH is a stable free radical with odd numbers of electrons within its structure. The DPPH radical can be reduced through hydrogen transfer mechanism which involves the donation of a hydrogen atom by an antioxidant to the radical (see scheme 4.1) or by electron transfer mechanism that involves transfer of electron from the ligand or the metal centre.

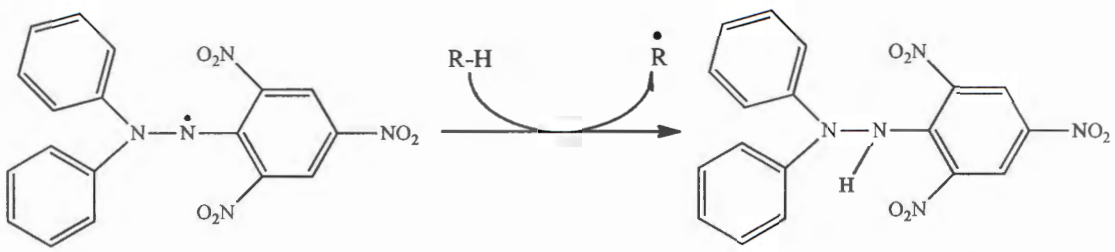

1,1-Diphenyl-2-picrylhydrazyl
(Free radical)

1,1-Diphenyl-2-picrylhydrazine
(Nonradical)

Scheme 4.1: General mechanism of DPPH reduction from a hydrogen-donating antioxidant

The antioxidant activities of the samples are measured through spectroscopic method by monitoring the reduction in the absorbance of the solution of the DPPH compared to the mixture of the DPPH radical and the antioxidant [41]. The results of the antioxidant studies (DPPH radical scavenging ability and reducing power) of the complexes are presented in Table 4.2. In the DPPH assay, complexes **5**, **9**, **10**, **11**, **22** and **24** exhibited the lowest IC_{50} in the range 29 - 65 μg/mL, which are better than their respective parent ligands. However, complexes **9** and **22** with IC_{50} values of 29 and 31 respectively, have the best antioxidant activities compared to other complexes; and this could be attributed to the small size of the alkyl (methyl) substituent of the organotin moiety [42]. Hence, variation in the nature of the alkyl group on the organotin moiety could affect the antioxidant activity of complexes [41,43]. Similarly, the nature of the ligands also played a major role in the antioxidant potential of these complexes. Although, the standard antioxidant drug (gallic acid) used in this study showed a better activity, on comparing with other standard antioxidant drug (for which gallic acid top the scale of activity), some of the complexes obtained showed comparable activity to the likes narigin, trolox and ascorbic acid at the same concentration [57]. In the reducing power assay, complexes **6**, **22** and **24** displayed the highest reducing activity. Complex **21** showed a very negligible antioxidant activity with no reducing power.

The antioxidant studies show that complexes **9** and **22** have the best DPPH radical scavenging and reducing abilities, indicative of their ability to donate protons so as to quench free radicals, and also donate electrons to oxygen species [44].

4.4. *In vitro* cytotoxicity assay

Tin complexes have shown promising antitumor activity among other metal complex derivatives. They have been found to induce cell apoptosis at very low concentrations and often have better or similar activities than currently available standard drugs [45].The search for a novel agent with the capacity to eliminate cancerous cells without affecting the normal cells is desirous via a programmed cell death. Cytotoxic studies on organotin(IV) dithiocarbamate complexes on various types of cancer often reveal useful activity in comparison with clinical available drugs [46]. The structural diversity of complexes of organotin(IV) salt have necessitated the wide antitumor study of this group of compounds with different ligands [47]. Molecules containing sulfur atoms have been widely studied as chemoprotectant in Pt-based chemotherapy, due to their promising modulating activity in cisplatin nephrotoxicity which has shown improved therapeutic index under acidic conditions. Thus, this feature may have significant implication in the treatment of cancer because the condition often observed in solid tumor is acidic due to the fermentation of glucose secreting acid in such tumor tissue [48]. Both organotin and dithiocarbamate moieties have been reported to play significant role in the cytotoxic activities of various cell lines. This may be attributed to the increased lipophilicity due to complexation or the transportation role played by the ligand which thus facilitating the movement of the metal to the site of action where the cytotoxic effect can be induced [45]. The electronic effect induced by the ligand alongside lipophilicity of the complexes also plays crucial roles in the cyto-selectivity exhibited by these complexes. Thus, in their right mix, these properties often give outstanding cytotoxic activities [47]. Furthermore, the nature, the length and the number of the alkyl substituents in the organotin moiety play crucial roles in inducing the desired cytotoxic effect on divers cell lines [45]. Organotin(IV) derivatives have been reported to show significant cytotoxicity in the following order $RSn^{3+} < R_2Sn^{2+} < R_3Sn^{+}$, with the Tri-substituted organotin showing the best activity. Mono-alkyl derivatives of organotin have been reported not to exhibit cyto-toxicaction [49].

4.4.1. Methodology for cytotoxicity activity evaluation (MTT Assay)

Human cervical carcinoma (HeLa) cells were obtained from the ATCC, Manasas, USA, and cultured in 25 cm^2 tissue culture flasks in EMEM (Lonza BioWhittaker, Verviers, Belgium). Containing 10% fetal bovine serum, 100 U mL^{-1} penicillin, and 100 μgmL^{-1}streptomycin.

Cell viability was investigated in the HeLa cell line using the MTT assay in a 96-well plate containing 2.5×10^2 cells/well in 100 µL EMEM. Cells were incubated overnight at 37 °C, and medium thereafter replaced, together with addition of the samples at various concentrations (25, 50, 100, and 1500 µg/ml). There were then incubated for 48 h at 37 °C, followed by the MTT assay. A positive control with untreated cells was included, together with 5-Fluorouracil as a standard. For the assay, the medium was replaced with fresh one containing 10% MTT reagent (5 mg/ml in PBS), and incubated for 4 h at 37°C. This was then removed, and the insoluble formazan crystals were dissolved in 100 µL of DMSO, followed by reading of the absorbance at 570 nm in a Mindray MR-96A microplate reader (Vacutec, Hamburg, Germany) using DMSO as the blank. Assays were done in triplicate.

4.3. Results of cytotoxicity study for complex 1 – 32

Table 4.3: Viabilities (%) of the HeLa cell lines at different concentration for complex **1 – 32.**

No	Complex	25 μg mL^{-1}	50 μg mL^{-1}	100 μg mL^{-1}	150 μg mL^{-1}	IC_{50} μM
Control 1	Cell only	100.00±0.79	100.00±0.79	100.00±0.79	100.00±0.79	-
Control 2	Cell + 10 μl DMSO	104.09±2.43	104.09±2.43	104.09±2.43	104.09±2.43	-
5FU	5-Fluorouracil	36.57±4.15	27.47±6.14	23.54±2.90	17.72±4.34	**40**
1	$[(C_4H_9)ClSn(L^1)_2]$	50.57±13.72	48.94±8.86	44.62±3.96	45.76±5.93	**31.6**
2	$[(C_6H_5)ClSn(L^1)_2]$	58.43±4.24	51.92±0.60	49.29±8.64	50.62±7.93	**81.6**
3	$[(CH_3)_2Sn(L^1)_2]$	27.2±18.53	26.4±8.32	26.0±18.94	24.0±13.92	**0.867**
4	$[(C_4H_9)_2Sn(L^1)_2]$	53.13±6.60	47.57±14.19	42.85±9.59	40.53±14.16	**37.0**
5	$[(C_6H_5)_2Sn(L^1)_2]$	80.8±2.05	79.9±11.24	79.1±5.83	75.1±5.91	**1995**
6	$[(CH_3)ClSn(L^2)_2]$	83.14±3.22	82.21±3.08	81.38±6.54	80.54±1.27	**>4000**
7	$[(C_4H_9)ClSn(L^2)_2]$	36.28±3.15	33.23±10.00	21.22±13.33	21.33±14.54	**8.12**
8	$[(C_6H_5)ClSn(L^2)_2]$	32.23±8.32	25.18±21.23	27.98±14.20	25.18±18.55	**4.37**
9	$[(CH_3)_2Sn(L^2)_2]$	31.13±10.67	30.44±2.24	31.28±5.49	30.21±13.06	**12.30**
10	$[(C_4H_9)_2Sn(L^2)_2]$	41.68±5.61	39.78±14.60	30.62±13.75	26.56±14.37	**11.75**
11	$[(C_6H_5)_2Sn(L^2)_2]$	32.33±6.10	30.65±9.01	29.30±7.17	28.16±8.25	**0.01**
12	$[(C_4H_9)ClSn(L^3)_2]$	47.87±0.98	56.24±3.35	59.09±7.34	58.78±0.96	**12**
13	$[(CH_3)_2Sn(L^3)_2]$	29.84±5.72	45.13±7.81	44.00±12.77	39.85±6.57	**400**
14	$[(C_4H_9)_2Sn(L^3)_2]$	62.25±3.14	65.52±6.84	62.98±6.88	65.82±12.16	**25**
15	$[(C_6H_5)_2Sn(L^3)_2]$	58.23±3.71	58.63±4.84	78.60±4.90	73.85±6.26	**15**
16	$[(CH_3)_2SnL^1L^2]$	17.60±9.36	24.39±19.99	15.99±32.28	22.27±12.65	**5**
17	$[(C_4H_9)_2SnL^1L^2]$	11.59±3.77	22.20±11.43	27.45±3.32	19.48±6.70	**25**
18	$[(C_6H_5)_2SnL^1L^2]$	17.47±9.12	13.27±10.87	16.16±4.95	26.22±11.72	**12**

19	$[(CH_3)_2\ SnL^1L^3]$	19.56±16.18	20.54±18.17	29.14±9.20	28.16±7.89	**2000**
20	$[(CH_3)_2SnL^2L^3]$	15.46±7.59	18.88±9.92	23.63±19.13	33.54±4.22	**1258**
21	$[(C_4H_9)ClSn(L^4)_2]$	4.12±15.25	6.58±12.69	5.90±6.94	37.61±21.74	**758**
22	$[(CH_3)_2Sn(L^4)_2]$	6.53±12.15	5.90±14.79	88.30±8.50	147.64±5.64	**56**
23	$[(C_4H_9)_2Sn(L^4)_2]$	65.77±2.87	59.27±2.83	57.57±2.25	15.40±11.46	**288**
24	$[(C_6H_5)_2Sn(L^4)_2]$	16.57±27.74	11.41±22.43	2.03±24.00	6.81±15.79	**2**
25	$[(C_6H_5)ClSn(L^4)_2]$	9.75±19.97	6.71±14.76	19.53±16.67	44.17±9.90	**316**
26	$[(C_4H_9)_2Sn(L^5)_2]$	67.116.42	62.92±4.95	62.02±7.50	49.66±12.06	**148**
27	$[(C_6H_5)_2Sn(L^5)_2]$	76.91±5.26	76.38±3.08	69.79±3.06	63.60±14.07	**1230**
28	$[(CH_3)_2Sn(L^6)_2]$	9.55±10.28	13.02±21.45	21.27±17.06	24.91±5.86	**3000**
29	$[(C_4H_9)_2Sn(L^6)_2]$	13.50±9.86	16.21±4.17	24.06±8.05	34.57±5.16	**1000**
30	$[(CH_3)_2Sn(L^7)_2]$	17.17±6.73	11.34±13.80	561.49±4.98	741.00±1.81	**40**
31	$[(C_4H_9)_2Sn(L^7)_2]$	9.05±13.98	4.75±9.64	6.87±14.81	5.14±10.68	**0.019**
32	$[(C_6H_5)_2Sn(L^7)_2]$	10.81±6.35	17.67±5.09	30.978±9.18	37.51±4.85	**330**

4.4.3. Discussion of cytotoxicity results

Several possible mechanisms have been described for the action of anticancer drug [50]. However, the lipophilicity of this drug plays a crucial role in their interaction with the cells. An increase in the length of the carbon chain in an organotin compounds often increase its cytotoxicity towards cancerous cells [37,48]. Thus, the nature of the alkyl/aryl group on the tin metal center often influences lipophilicity. The phenyl group in an organotin molecule can induce a π-π interaction with biomolecular cells. Furthermore, The outstanding cytotoxicity of phenyl derivatives in an organotin complexes with at least two phenyl group, also contributes to the enhanced lipophilicity [48]. Other routes of interaction have been put forward for the interaction of compounds with cancerous cell. These include interaction with nitrogenous bases, which consequently interferes with the DNA replication and transcription or by affecting the multi-enzymes complexes which also helps in DNA transcription and replication, thus inhibiting cell proliferation [11]. Hence, DNA may be the likely targets of these complexes as reported in literature [51].

HeLa cell is a cell line obtained from common human cervical cancer. It is an immortal cell line often used for research. From the study, the IC_{50} levels of the complexes in the HeLa cell line obtained have been summarized in Table 4.3. This result obtained showed that most of the complexes displayed a concentration dependent profile with some good activity toward this cell line. Some of the complexes also showed cyto-selectivity against the HeLa cell line. Some of the IC_{50} values obtained were much better than the standard drug, 5-Fluorouracil (**5FU**), with an IC_{50} value of 40 μM. However, some of these complexes displayed high IC_{50} values which are comparable due to selectivity or low cytotoxic activity as the case may be. Generally, the organotin complexes with the di-substituted alkyl/aryl group induced better cytotoxicity than their mono-substituted alkyl/aryl counterpart similar to what has been reported [52,53]. However, the phenyl containing organotins (either in its diphenyltin(IV) or the phenyltin derivatives), have very good activities. However, due to selectivity, few of these complexes showed poor activity towards HeLa cell line. In some cases, mono-substituted alkyl/aryltin complexes uncharacteristically showed good to moderate activities especially those of butyl and phenyl derivatives.

Therefore, possible structural-activity relationships have been deduced as follows:

1. All organotin(IV) complexes derived from *N*-alkyl-*N*-phenyldithiocarbamate ($\mathbf{L^1}$, $\mathbf{L^2}$, $\mathbf{L^3}$) exhibited good antitumor activity towards HeLa cell which were better in some cases than the standard drug, except for complexes **5**, **6**, and **13**, which is due to the selectivity and nature of alkyl group respectively.

2. Complexes derived from *N*-ethyl-*N*-phenyldithiocarbamate showed very good cytotoxic activities, except complex **6** which gave an IC_{50} value greater than 4000 μM. Amongst the organotin(IV) *N*-alkyl-*N*-phenyldithiocarbamate complexes, the phenyltin derivatives (**2, 8, 11** and **15**), complex **11** showed the best activity amongst this group of organotin(IV) dithiocarbamate compound, with an IC_{50} value of 0.01, which is 4000 times better than the standard drug (**5FU**) used. This has been attributed to the enhanced lipophilicity caused by the presence of more than one phenyl group in the complex. The order of activity for this group follows thus:

11>3>8>7>10>12>9>15>14>1>4

Increasing order of activity better than **5FU**

3. The mixed dithiocarbamate ligand complexes of *N*-alkyl-*N*-phenyldithiocarbamate ($\mathbf{L^1L^2}$) also gave good cytotoxic activities better than the standard drug. Complex **16**, which is a dimethyltin derivative showed a better activity for these group, perhaps due to its high selectivity towards this cell line than the diphenyl and dibutyltin counterpart. The IC_{50} observed was 8 times better than the standard drug for complex **16**. However, the dimethyltin(IV) *N*-alkyl-*N*-phenyldithiocarbamate complexes (**19** and **20**), showed poor cytotoxicity (with IC_{50} values greater than >1000) in both cases. This was probably due to poor selectivity of this cell line towards these complexes.

4. The IC_{50} values obtained for complexes **21** to **25** ranged from 2.0 to 758 μM in the HeLa cell line compared to that of the standard drug (**5-FU**) with an IC_{50} value of 40 μM. Complexes **21**, **23** and **25** gave exceptionally high IC_{50} values. For complex **21** and **25**, the high IC_{50} values observed could be attributed to the effect of the mono-alkyl

substituent present in the organotin moiety, which often induces weaker activity compared to the di and the tri-alkyl organotin derivatives. In the case of complex **23,** which is a dibutyltin derivative, the somewhat high IC_{50} value observed could be best attributed to the cyto-selectivity of this complex for the HeLa cell line. However, from the observed IC_{50} values, both complex **22** and **24** showed good cytotoxic activity compared to other members in this series. Complex **24** produced a value much lower than that of 5-FU, which is 20 times more effective than the standard drug used, based on their IC_{50} values obtained. The outstanding cytotoxicity of complex **24** could be attributed to the presence of two phenyl groups which often enhances lipophilicity [48]. Cytotoxic activity have shown from studies to be related to the degree of lipophilicity [54]; i.e. complexes with high lipophilicity often have high cytotoxicity. Therefore, complex **24** showed the highest cytotoxicity among these complexes.

5. In the complexes derived from dithiocarbamate which are of primary amine sources (**26 – 29**), the IC_{50} values were very high even though all the complexes were derived from diorganotin(IV) sources. Thus, these groups of complexes showed poor selectivity towards this cell line compared to other ligands from secondary amine sources.
6. In the case of organotin(IV) benzyldithiocarbamate complexes (**30 – 32**), complexes **30** and **31** (which are dimethyl and dibutyltin(IV) complexes) gave good cytotoxic activity better than 5-Fluorouracil drug used. The best activity for this complexes was observed for dibutyltin(IV) benzyldithiocarbamate which had an IC_{50} values 2100 times better than the standard drug. Due to selectivity, the diphenyl derivative gave a poor activity against the HeLa cell line.

The cytotoxic activity observed for organotin(IV) compounds against the HeLa cell line generally indicated remarkable anti-tumoral activity upon complexation with diverse dithiocarbamate ligands. Thus, show potentials as anticancer agents upon further screening and clinical trials. From these obtained preliminary results, it is safe to say that further optimizations or modifications and testing of all compounds in other cells lines as well are required.

4.5. Chapter conclusion

The evaluation of the antimicrobial, cytotoxic and antioxidant activities of the synthesized complexes have been achieved. These complexes showed some outstanding activity against a wide range of bacterial (+/- Gram) and two fungi organisms with complexes **2**, **5**, **8**, **11**, **15**, **24**, **25**, **27** and **32** (phenytin(IV) derivatives) showing the best activities due to the lipophilic nature of their molecules in biological system. These complexes, through a weak intermolecular contact with cell membranes, may alter the cell membrane of the organisms, thus causing death by interrupting the transportation of useful nutrients into their cell by deprivation. Similarly, the cytotoxicity study of these complexes favours the molecules with longer chain and those of aryl derivatives due to the increased lipophilicity upon complexation. The organtin(IV) *N*-alkyl-*N*-phenyl dithiocarbamate complexes exceptionally showed a good selectivity towards the HeLa cell line with outstanding activity better than the standard 5-Fluorouracil drug used. In this study, complexes **11** and **31** gave an IC_{50} value of 0.01 and 0.019 respectively, which are 4000 and 2100 times better than the standard 5-Fluorouracil drug. Furthermore, the antioxidant activity tests carried out on some of the complexes showed that complexes **9** and **22** have the lowest IC_{50} values attributed to the small size of the methyl substituent of the organotin moiety but less than the value obtained for gallic acid.

From the relationship deduced from structural-activity of the complexes, it is therefore apparent that the biological activity of organotin(IV) dithiocarbamate complexes is highly influenced by the number and the nature of alkyl/aryl group attached to the tin metal alongside lipophilcity and selectivity. Thus, the nature of the ligand moiety is important in their functionality as useful biological molecules [49]. The results obtained in these studies showed that these molecules, upon further screening *in vivo,* may lead to development of a new drug against cancer cells and also act as a broad spectrum antimicrobial agent with antioxidant potential.

References

[1] A. Alama, B. Tasso, F. Novelli, F. Sparatore, Drug Discov. Today 14 (2009) 500–508.

[2] G. Gasser, I. Ott, N. Metzler-Nolte, J. Med. Chem. 54 (2011) 3–25.

[3] A.B. Caballero, J.M. Salas, M. Sánchez-Moreno, Met. Ther. Leishmaniasis (2014) 1–28.

[4] M. Mahato, S. Mukherji, K. Van Hecke, K. Harms, A. Ghosh, H.P. Nayek, J. Organomet. Chem. 853 (2017) 27–34.

[5] A. Torres-Huerta, B. Rodríguez-Molina, H. Höpfl, M.A. Garcia-Garibay, Organometallics 33 (2014) 354–362.

[6] G. Hogarth, in: Prog. Inorg. Chem. Vol. 53, 2005, pp. 71–561.

[7] G. Hogarth, Mini Rev. Med. Chem. 12 (2012) 1202–1215.

[8] D.C. Menezes, F.T. Vieira, G.M. de Lima, A.O. Porto, M.E. Cortés, J.D. Ardisson, T.E. Albrecht-Schmitt, Eur. J. Med. Chem. 40 (2005) 1277–1282.

[9] T.S.B. Baul, Appl. Organomet. Chem. 22 (2008) 195–204.

[10] Sadiq-Ur-Rehman; Sadia Saeed Kiani; Muhammad Aziz Choudhary; Khawaja Ansar Yasin; Muhammad Safdar, A. Journal, Asian J. Chem. 23 (2011) 1497–1502.

[11] M. Sirajuddin, F. Shaheen, M. Sirajuddin, S. Ali, J. Organomet. Chem. 856 (2017) 13–22.

[12] H. Iqbal, S. Ali, S. Shahzadi, Chem. J. 06 (2016) 59–73.

[13] F. Arjmand, S. Parveen, S. Tabassum, C. Pettinari, Inorg. Chim. Acta 423 (2014) 26–37.

[14] M.M. Shoukry, S.S. Hassan, Sci. J. 2013 (2013) 1–7.

[15] T.K. Komarnisky, L. A., Christopherson, R. J. and Basu, Nutrition 19 (2003) 54–61.

[16] D.C. Onwudiwe, A.C. Ekennia, Res. Chem. Intermed. 43 (2017) 1465–1485.

[17] H. Nabipour, S. Ghammamy, S. Ashuri, Z.S. Aghbolagh, Org. Chem. J 2 (2010) 75–80.

[18] E.A. Hassan, S.E. Zayed, Phosphorus, Sulfur Silicon Relat. Elem. 189 (2014) 300–323.

[19] F. Javed, M. Sirajuddin, S. Ali, N. Khalid, M.N. Tahir, N.A. Shah, Z. Rasheed, M.R. Khan, Polyhedron 104 (2016) 80–90.

[20] W.P.. Ross, P.W. and Malbrook, Clinical and Oral Microbiology, Hemispher Publishing Corporation, New York, 1982.

[21] M. Balouiri, M. Sadiki, S.K. Ibnsouda, J. Pharm. Anal. 6 (2016) 71–79.

[22] B. Fernández-torres, I. Inza, J. Guarro, Antimicrob. Agents Chemother. 49 (2005) 2116–2118.

[23] H.J. Simon, E.J. Yin, Appl. Microbiol. 19 (1970) 573–9.

[24] T.M. de A. Alves, A.F. Silva, M. Brandão, T.S.M. Grandi, E. de F.A. Smânia, A. Smânia Júnior, C.L. Zani, Mem. Inst. Oswaldo Cruz 95 (2000) 367–373.

[25] A.C.O. Silva, E.F. Santana, A.M. Saraiva, F.N. Coutinho, R.H.A. Castro, M.N.C. Pisciottano, E.L.C. Amorim, U.P. Albuquerque, Evidence-Based Complement. Altern. Med. 2013 (2013) 1–9.

[26] C. Pellerito, L. Nagy, L. Pellerito, A. Szorcsik, J. Organomet. Chem. 691 (2006) 1733–1747.

[27] T. Sedaghat, M. Aminian, M. Azarkish, Phosphorus. Sulfur. Silicon Relat. Elem. 190 (2015) 352–359.

[28] H. Zafarian, T. Sedaghat, H. Motamedi, D. Trzybiński, K. Woźniak, J. Organomet. Chem. 853 (2017) 184–192.

[29] T. Sedaghat, L. Tahmasbi, H. Motamedi, R. Reyes-Martinez, D. Morales-Morales, J. Coord. Chem. 66 (2013) 712–724.

[30] R. Prabhakaran, A. Geetha, M. Thilagavathi, R. Karvembu, V. Krishnan, H. Bertagnolli, K. Natarajan, J. Inorg. Biochem. 98 (2004) 2131–2140.

[31] A.C. Ekennia, D.C. Onwudiwe, A.A. Osowole, L.O. Olasunkanmi, E.E. Ebenso, J. Chem. 2016 (2016) 1–12.

[32] S. Jabbar, I. Shahzadi, R. Rehman, H. Iqbal, Qurat-Ul-Ain, A. Jamil, R. Kousar, S. Ali, S. Shahzadi, M.A. Choudhary, M. Shahid, Q.M. Khan, S.K. Sharma, K. Qanungo, J. Coord. Chem. 65 (2012) 572–590.

[33] Y. Anjaneyulu, R.P. Rao, Synth. React. Inorg. Met. Chem. 16 (1986) 257–272.

[34] F. Shaheen, Zia-Ur-Rehman, S. Ali, A. Meetsma, Polyhedron 31 (2012) 697–703.

[35] Sadiq-ur-Rehman, S. Ali, A. Badshah, M. Mazhar, X. Song, G. Eng, K.M. Khan, Synth. React. Inorg. Met. Chem. 34 (2004) 1379–1399.

[36] A.S.L. Barbosa, J. de S. Guedes, D.R. da Silva, S.M.P. Meneghetti, M.R. Meneghetti, A.E. da Silva, M.V. de Araujo, M.S. Alexandre-Moreira, T.M. de Aquino, J.P. de Siqueira Junior, R.S.A. de Araújo, R.M.D. da Cruz, F.J.B. Mendonça-Junior, J. Inorg. Biochem. 180 (2018) 80–88.

[37] S.K. Hadjikakou, N. Hadjiliadis, Coord. Chem. Rev. 253 (2009) 235–249.

[38] H.K. Adli, N.M. Sidek, N. Ismail, W.M. Khairul, Chiang Mai J. Sci. 40 (2013) 117–125.

[39] L.C. Dias, G.M. de Lima, J.A. Takahashi, J.D. Ardisson, Appl. Organomet. Chem. 29

(2015) 305–313.

[40] C.P. Anokwuru, I.D.I. Ramaite, P. Bessong, African J. Tradit. Complement. Altern. Med. 12 (2015) 21–27.

[41] A. Corona-Bustamante, J.M. Viveros-Paredes, A. Flores-Parra, A.L. Peraza-Campos, F.J. Martínez-Martínez, M.T. Sumaya-Martínez, Á. Ramos-Organillo, Molecules 15 (2010) 5445–5459.

[42] R. Apak, M. Özyürek, K. Güçlü, E. Çapanoɨlu, J. Agric. Food Chem. 64 (2016) 997–1027.

[43] M. Jabeen, S. Ali, S. Shahzadi, M. Shahid, Q.M. Khan, S.K. Sharma, K. Qanungo, J. Iran. Chem. Soc. 9 (2012) 307–320.

[44] L.P. Bhuyan, S. Sabhapondit, B.D. Baruah, C. Bordoloi, R. Gogoi, P. Bhattacharyya, Food Chem. 141 (2013) 3744–3751.

[45] N.F. Kamaludin, N. Awang, I. Baba, A. Hamid, C.K. Meng, Pakistan J. Biol. Sci. 16 (2013) 12–21.

[46] M. Sirajuddin, V. McKee, M. Tariq, S. Ali, Eur. J. Med. Chem. 143 (2018) 1903–1918.

[47] X. Shang, B. Zhao, G. Xiang, M.F.C. Guedes da Silva, A.J.L. Pombeiro, RSC Adv. 5 (2015) 45053–45060.

[48] R. Kadu, H. Roy, V.K. Singh, Appl. Organomet. Chem. 29 (2015) 746–755.

[49] P. G. Harrison, Chemistry of Tin, 2nd Ed, Springer Netherlands, Dordrecht, 1998.

[50] P. Zhang, P.J. Sadler, J. Organomet. Chem. 839 (2017) 5–14.

[51] F. Shaheen, M. Sirajuddin, S. Ali, Zia-ur-Rehman, P.J. Dyson, N.A. Shah, M.N. Tahir, J. Organomet. Chem. 856 (2018) 13–22.

[52] E.R.T. Tiekink, Appl. Organomet. Chem. 22 (2008) 533–550.

[53] Y. Yang, M. Hong, L. Xu, J. Cui, G. Chang, D. Li, C.Z. Li, J. Organomet. Chem. 804 (2016) 48–58.

[54] M. Tariq, M. Sirajuddin, S. Ali, N. Khalid, M.N. Tahir, H. Khan, T.M. Ansari, J. Photochem. Photobiol. B Biol. 158 (2016) 174–183.

Chapter five

5.0. Conclusion and recommendations

The chemistry and useful synergy created by the individual moieties of organotin(IV) and dithiocarbamate compounds has led to the enhanced biological activity of organotin(IV) dithiocarbamate complexes. A major attribute of these complexes is their ability to increase the coordination number around the tin center and thus, influence the geometry in the complexes. Their geometries are not exactly perfect, but are distorted due to the asymmetric nature of the dithiocarbamate ligand which consequently leads to unequal distances between the tin-sulfur bonds. The possibilities for several resonance structure of the dithiocarbamate moiety explain their outstanding stability. Numerous application of dithiocarbamate compounds stems from the ease of replacing the cations ($K^+/Na^+/NH_4^+$) in a coordinate bond to form complexes with metals. Thermal studies of these complexes have shown that they can be useful single source precursors for tin-sulfide nanoparticles which could exists as SnS, SnS_2, or Sn_2S_3. Hence, these compounds also found relevance in Materials chemistry.

In the reported studies, thirty-two new organotin(IV) dithiocarbamate complexes have been successfully synthesized from seven different ligands according to the set aim and objectives. All complexes were characterized by spectroscopic techniques (^1H, ^{13}C and ^{119}Sn NMR; and FTIR), thermogravimetric analysis and single crystals X-ray diffraction. The spectroscopic techniques showed a high degree of coordination about the tin centre. Single crystals, obtained by slow evaporation of these complexes in a mixture of solvent at room temperature, aided the prediction of the geometries about the tin atom. The geometries were mostly between distorted five or six coordinate geometry, due to the asymmetric nature of dithiocarbamate compounds and the stearic hindrances on the tin metal.

The biological studies carried out showed that the complexes have great potential as useful biological agents. This improved biological potentials observed in the complexes in comparisons to the ordinary organic ligand of dithiocarbamate, can be associated with the replacement of the chloride ion in the organotin salt with the respective ligand used. Thus, resulting in a fine tuning effect of both the ligands and the organotin(IV) chloride salts. This leads to improvement in biological properties. The synthesized complexes showed promising antimicrobial, antioxidant and cytotoxic activities at lower concentration with an appreciable IC_{50} value, lower or comparable to some of the available standard drug used in this work. Thus, the need for the *in*

vivo studies of these complexes in order to ascertain their possible usage as antimicrobial and anticancer agents. Furthermore, they need to be screened against other cancerous cell lines to ascertain their suitability in the treatment of other types of cancerous cells.

The diverse biological activity of these group of complexes indicates that the strategy of substituting bioactive organic ligand into an organotin(IV) compound can successfully overcome the challenge of lack of alternative drugs as antimicrobial agent. In addition, the complexation of already available organic antimicrobial agent with organotin(IV) compounds can allow for the renewed usage of these sets of compounds. Therefore, the various biocidal activities of organotin(IV) dithiocarbamate complexes are worthy of development and utilization. Their usage should not only be limited to their application in the industries, agriculture and material science, but could be further explored for the treatment of diseases as described and enumerated in this work. The use of these complexes in drug design could make a significant contribution to human lives, and also provide alternative medication which might be cheaper and more efficient than the currently available drugs. The world health organization (WHO, 2017) recently gave an alarming report about the low availability of antibiotics and the alarming encroachment of resistance for the modified existing class of the currently used antibiotics. Hence, the need for new therapeutic agents to combat this menace is imperative. Although, organtin(IV) dithiocarbamate complexes could be useful in the fight against antimicrobial resistance and treatment of cancerous cells and against other infectious diseases., considerable effort must be made to understand their specific mechanism of actions and side effects. These factors are still drawbacks which negates their usage. Regardless of the side effects, these complexes could offer a platform for the design of novel therapeutic agents. Thus, new approaches/ideas and detailed studies are needed to outwits these challenges.

Appendices

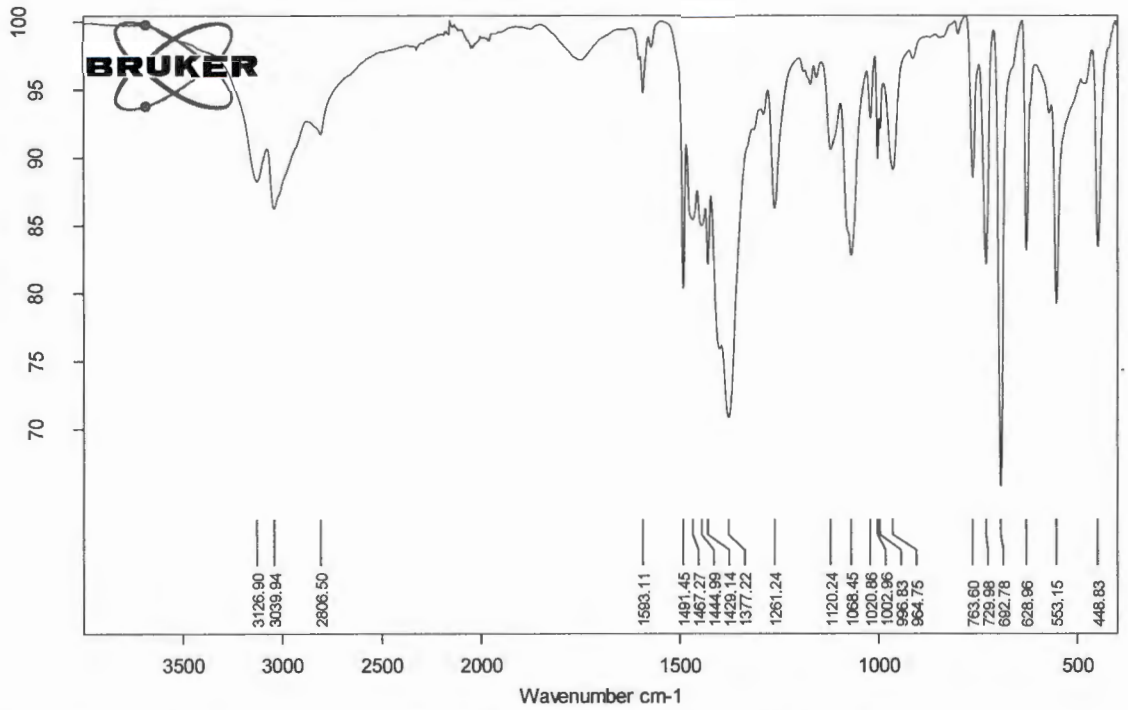

Figure S1: FTIR spectrum of phenyltin(IV) *N*-methyl-*N*-phenyl dithiocarbamate (**2**)

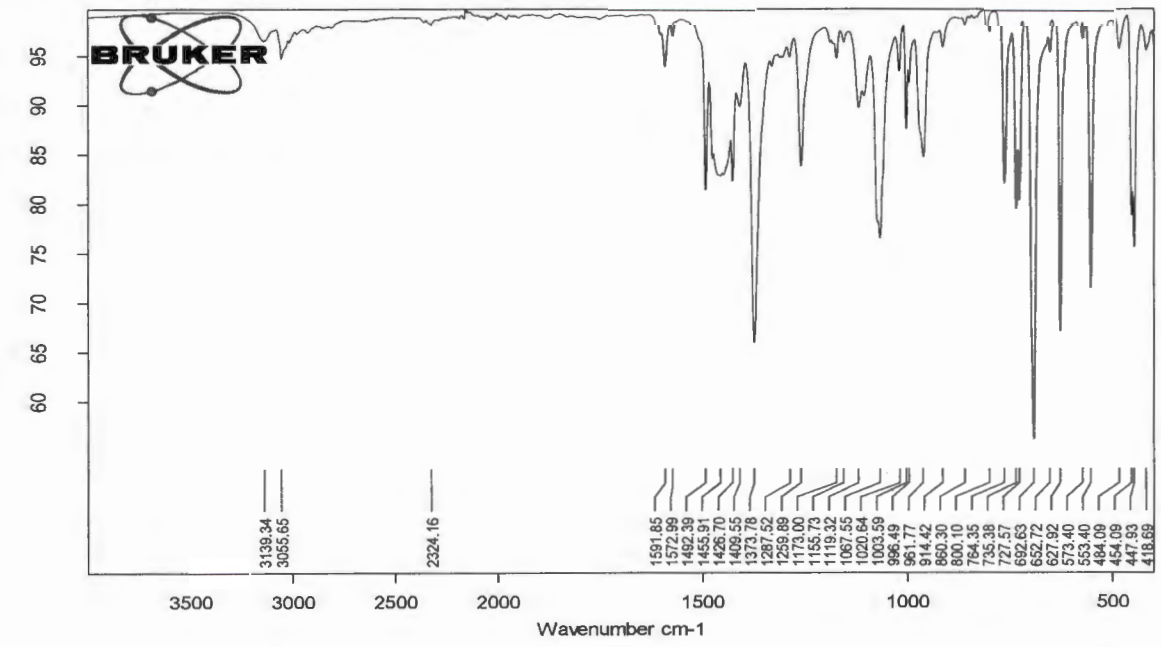

Figure S2: FTIR spectrum of diphenyltin(IV) *N*-methyl-*N*-phenyl dithiocarbamate (**5**)

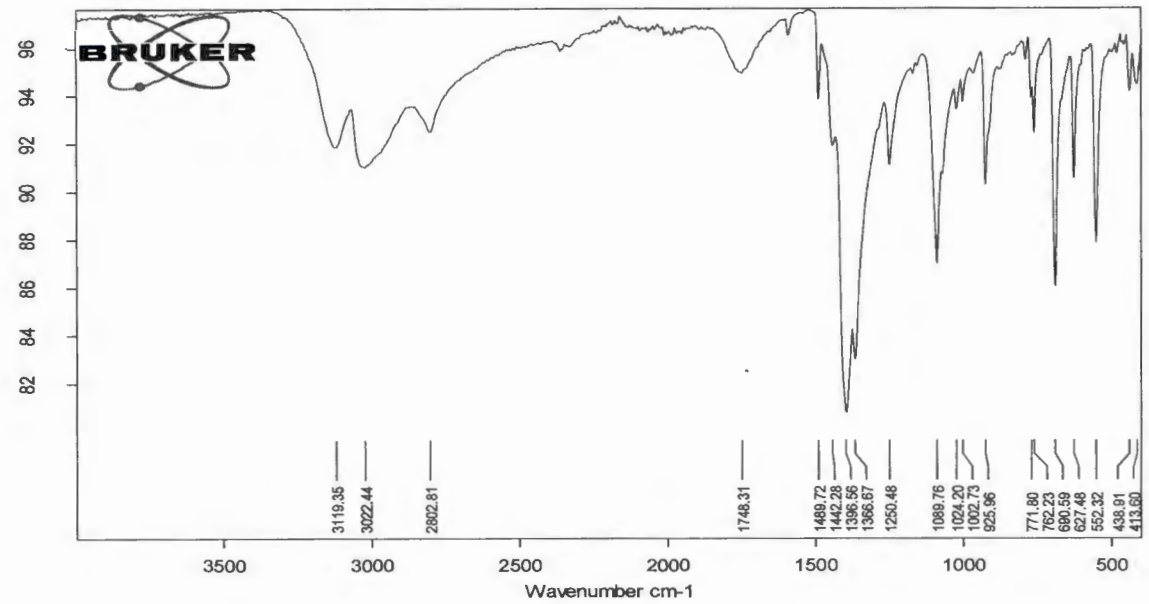

Figure S3: FTIR spectrum of chlorobutyltin(IV) *N*-ethyl-*N*-phenyl dithiocarbamate (**7**)

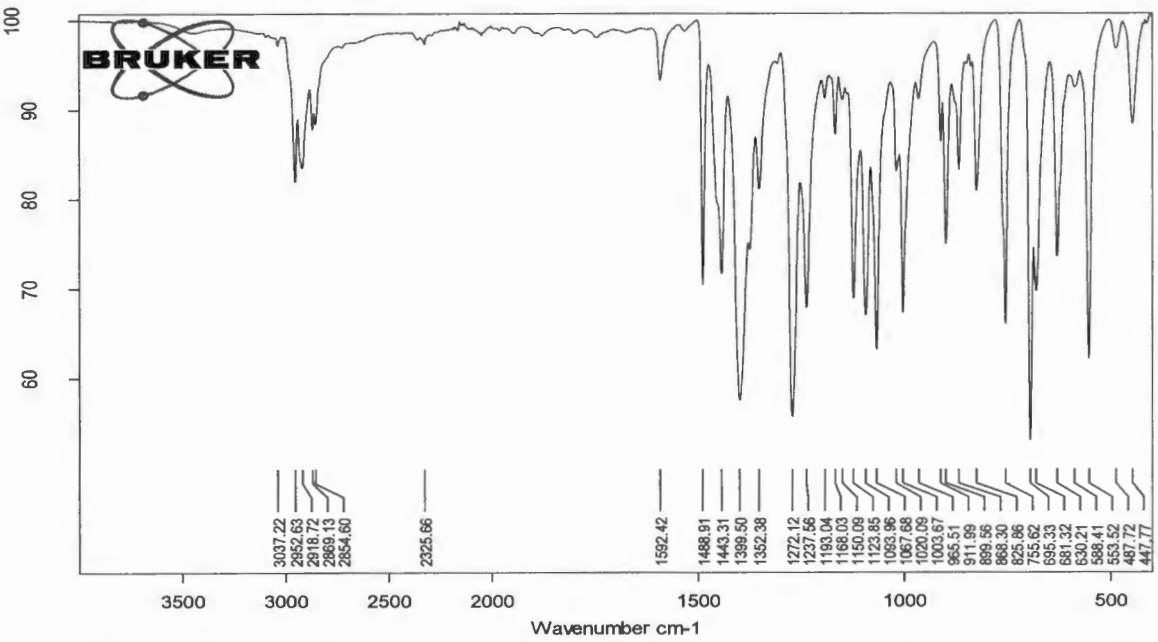

Figure S4: FTIR spectrum of dibutyltin(IV) *N*-ethyl-*N*-phenyl dithiocarbamate (**10**)

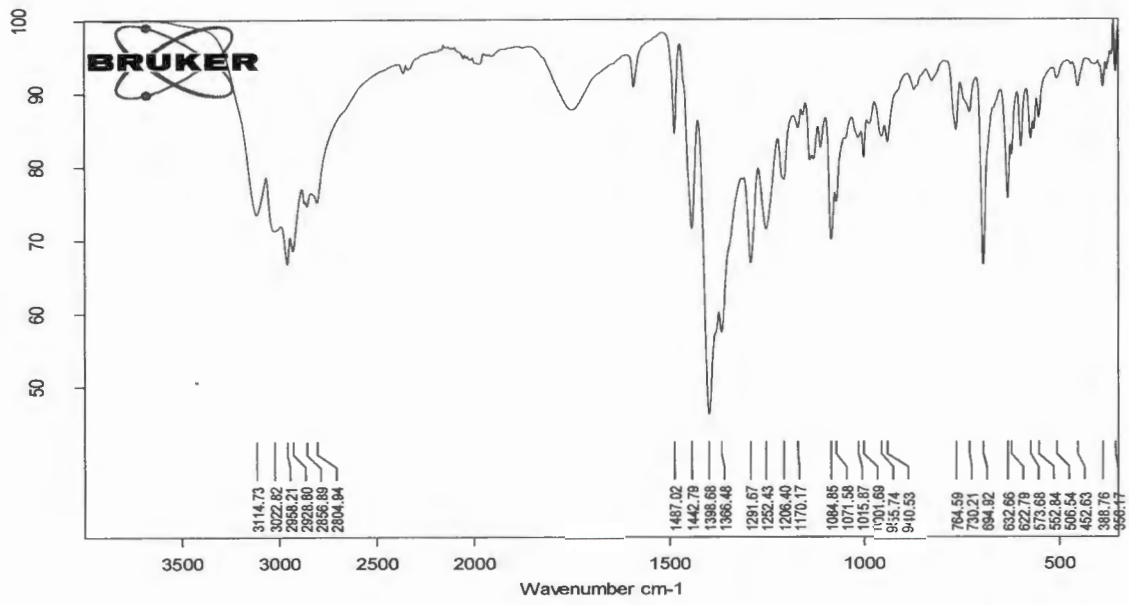

Figure S5: FTIR spectrum of butyltin(IV) *N*-butyl-*N*-phenyl dithiocarbamate (**12**)

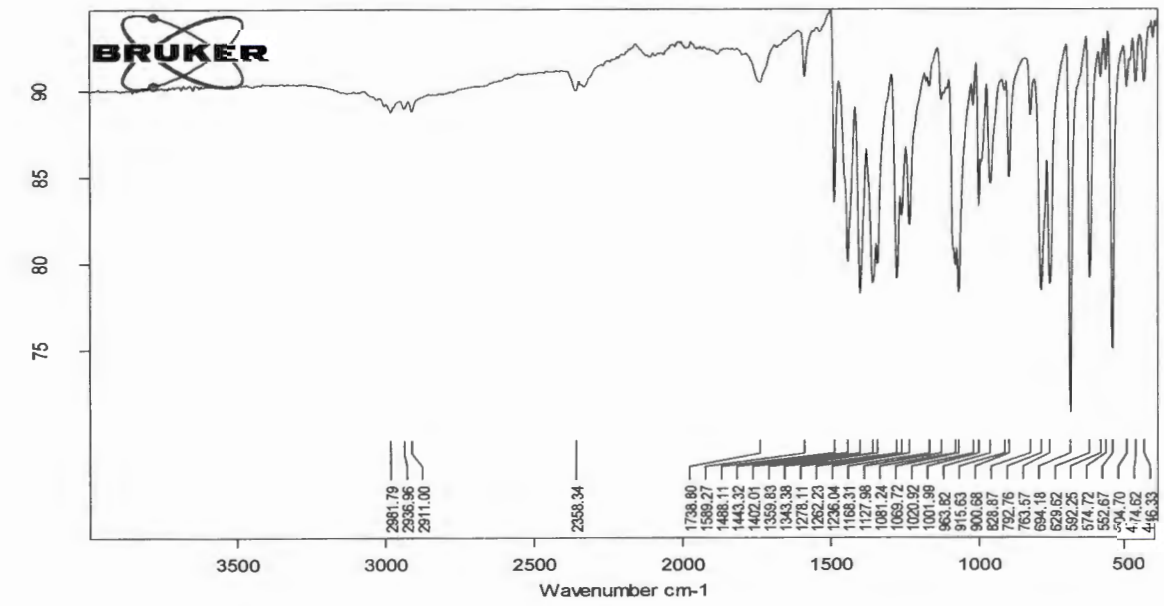

Figure S6: FTIR spectrum of dimethyltin(IV) *N,N*-methyl phenyl-*N,N*-ethyl phenyl dithiocarbamate (**16**)

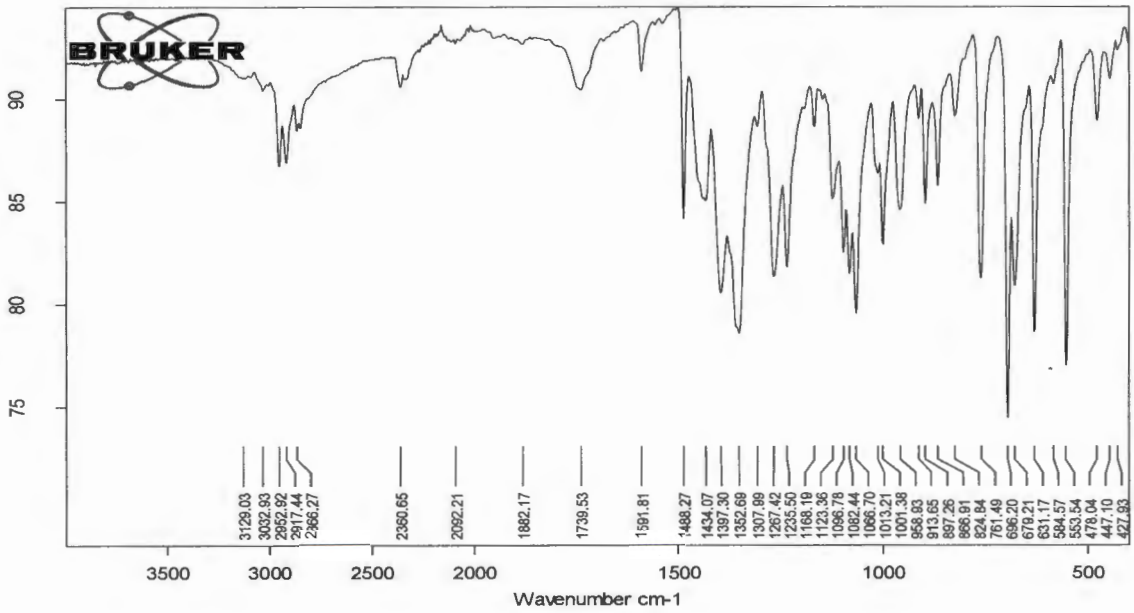

Figure S7: FTIR spectrum of dibutyltin(IV) *N,N*-methyl phenyl-*N,N*-ethyl phenyl dithiocarbamate (**17**)

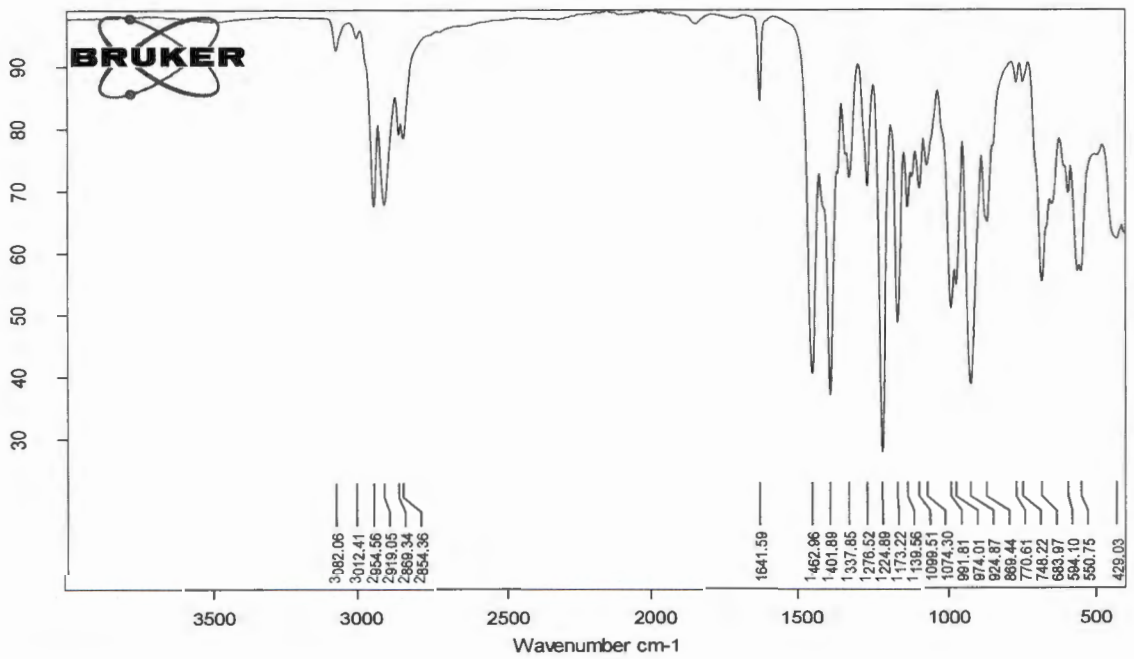

Figure S8: FTIR spectrum of dibutyltin(IV) *N,N* diallyldithiocarbamate (**23**)

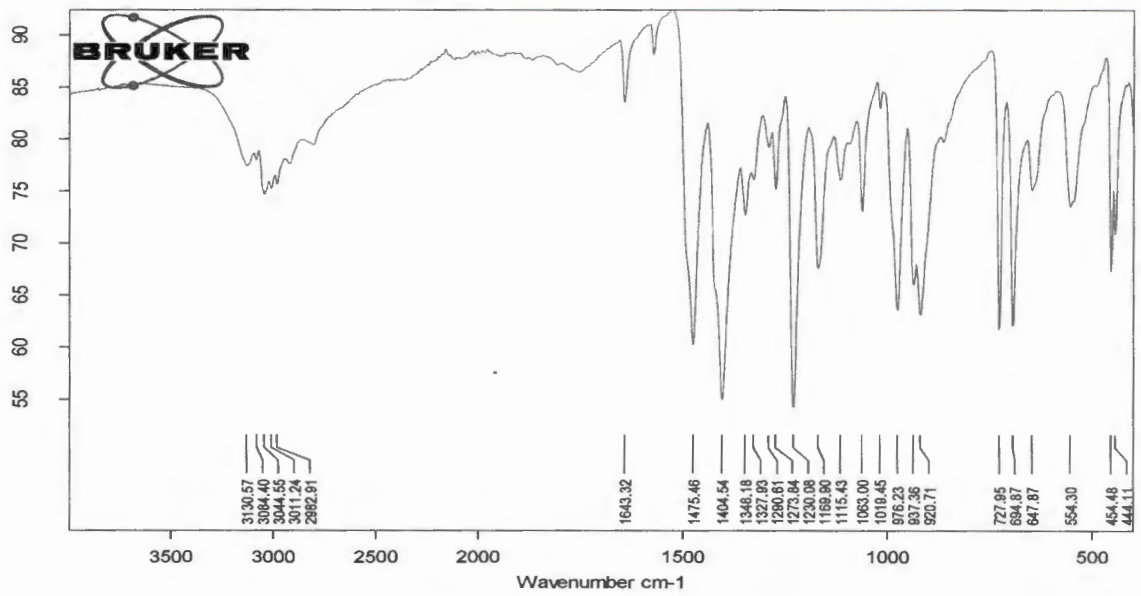

Figure S9: FTIR spectrum of diphenyltin(IV) *N,N* diallyl dithiocarbamate (**24**)

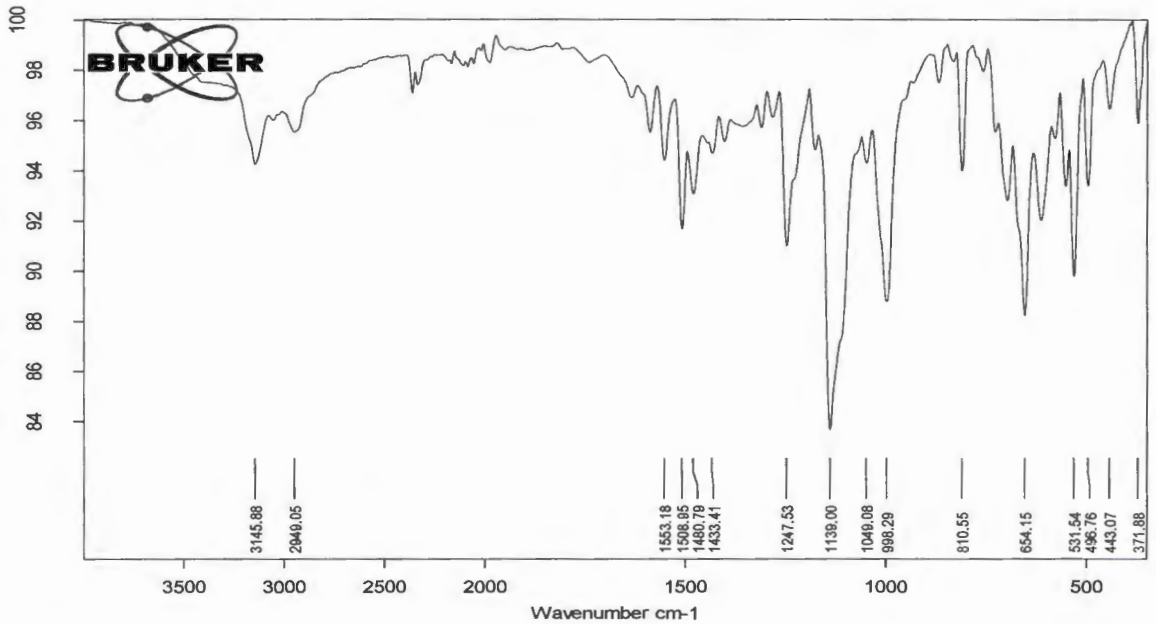

Figure S10: FTIR spectrum of diphenyltin(IV) *p*-methylphenyl dithiocarbamate (**27**)

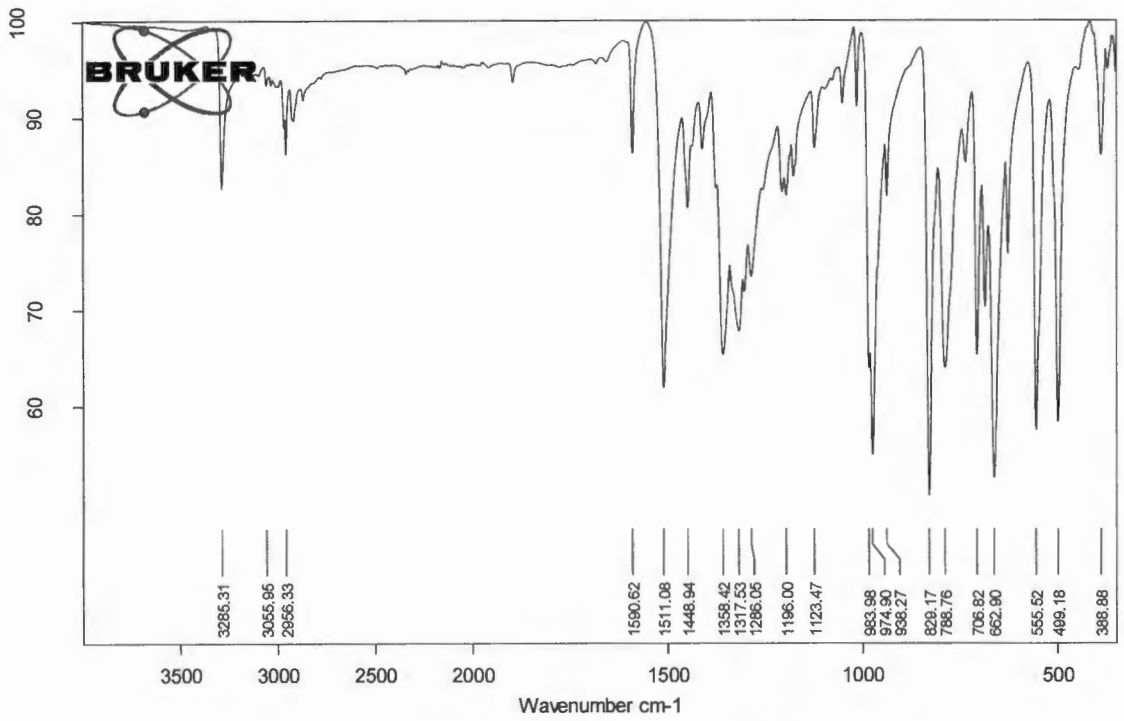

Figure S11: FTIR spectrum of dibutyltin(IV) *p*-ethylphenyl dithiocarbamate **(28)**

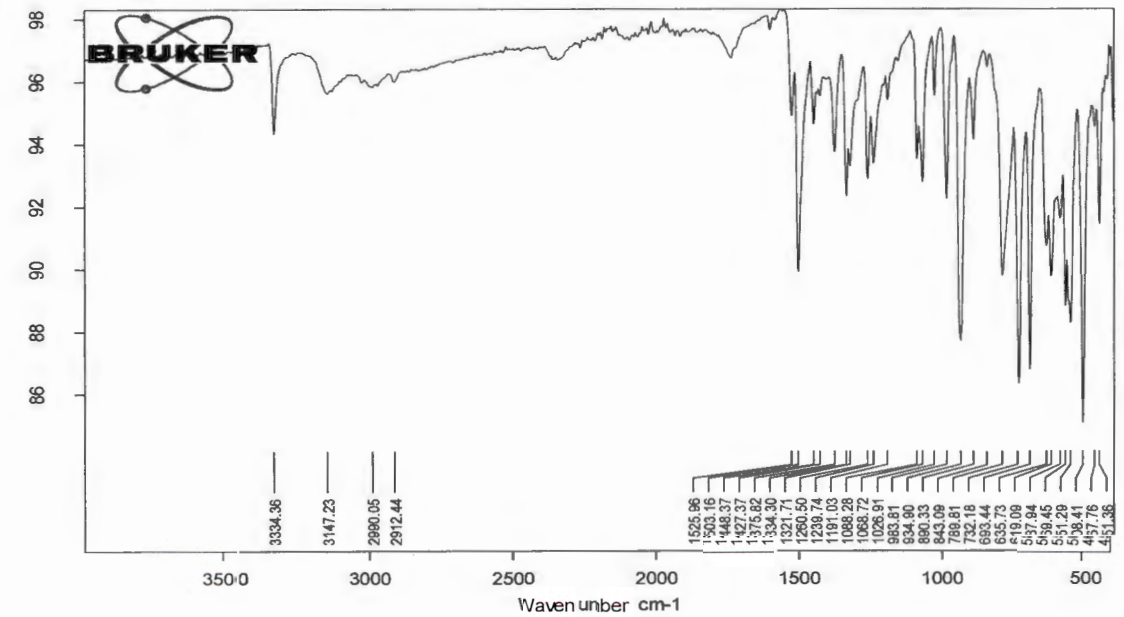

Figure S12: FTIR spectrum of dimethyltin(IV) *N*-benzyl dithiocarbamate **(30)**

(a)

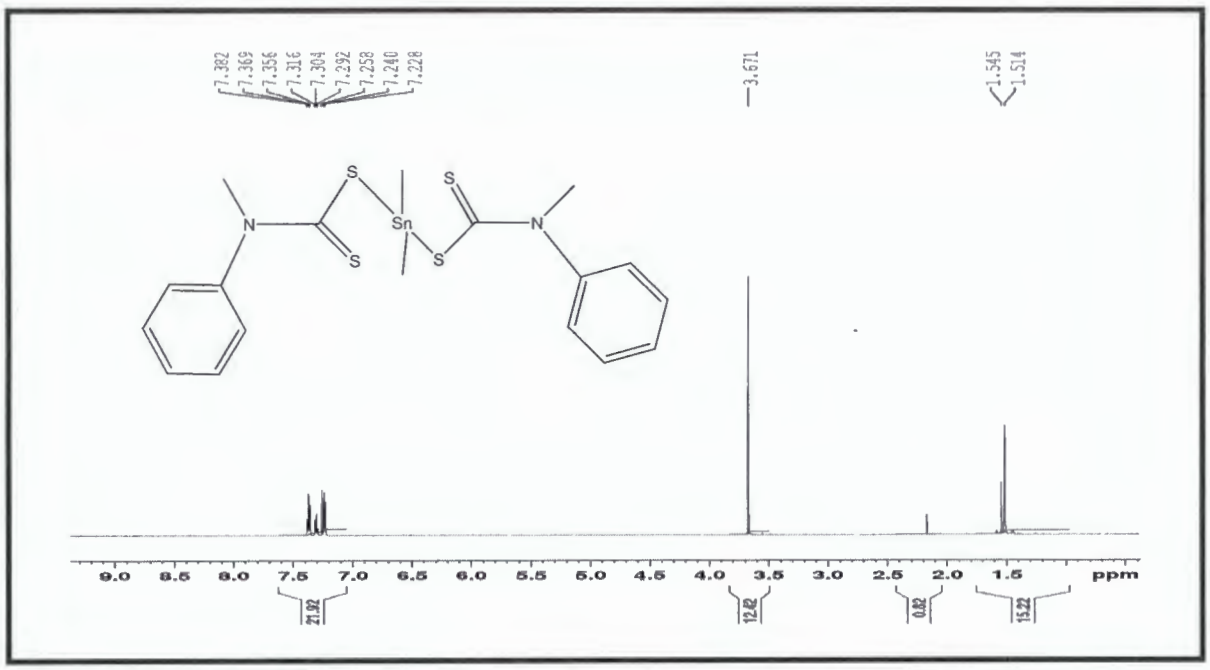

(b)

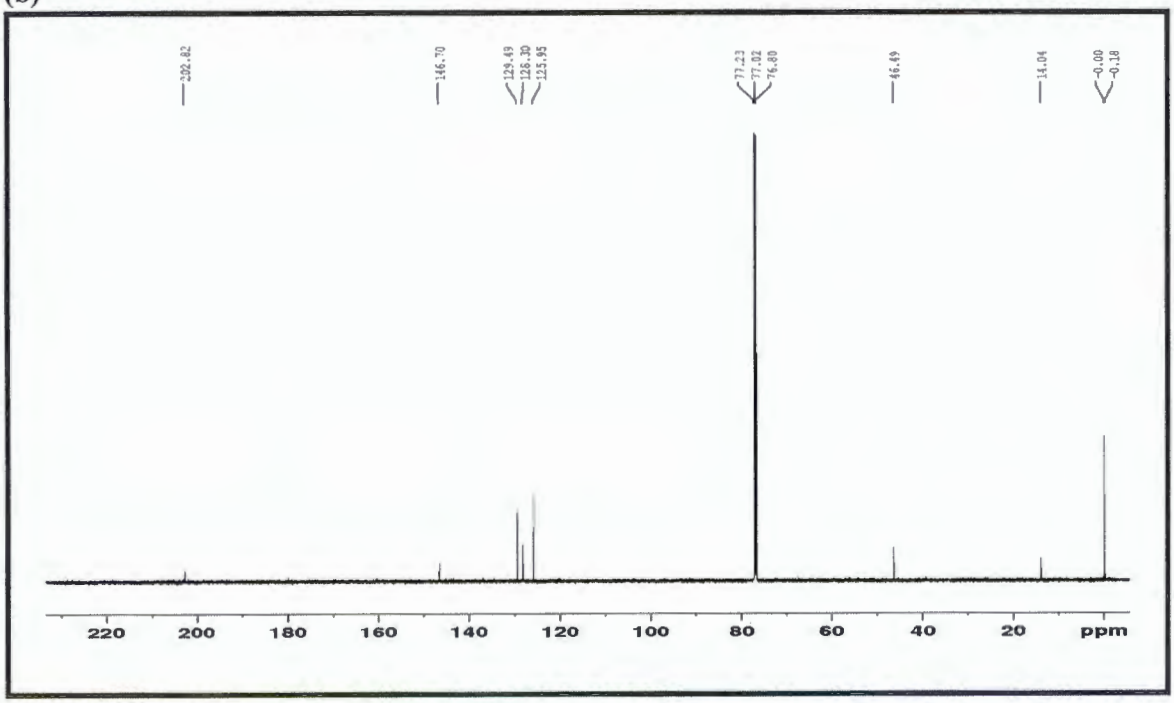

Figure S13: ^{1}H **(a)** and ^{13}C **(b)** spectra of dimethyltin(IV) *N*-methyl-*N*-phenyl dithiocarbamate **(3)**

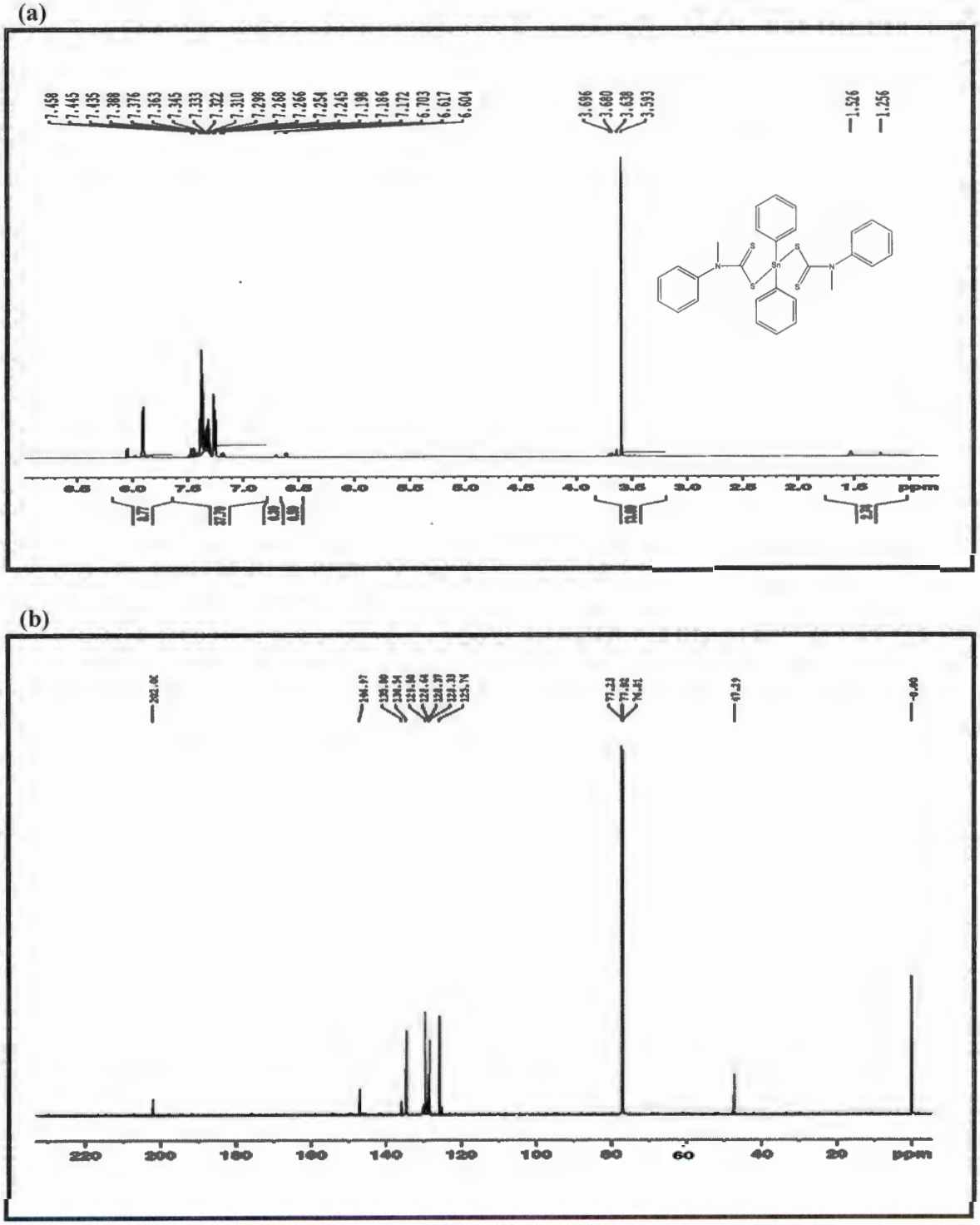

Figure S14: ^{1}H **(a)** and ^{13}C **(b)** spectra of diphenyltin(IV) *N*-methyl-*N*-phenyl dithiocarbamate **(5)**

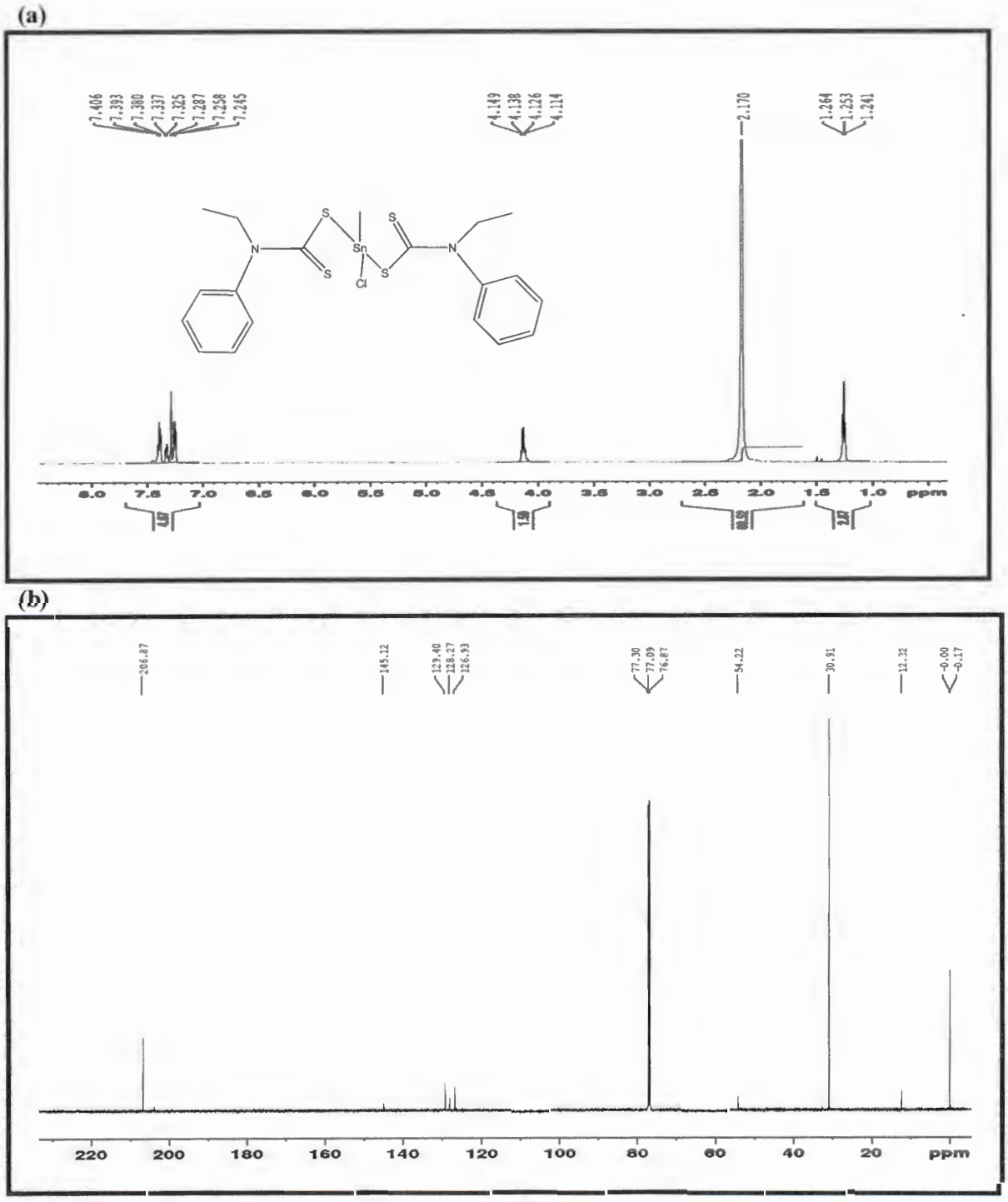

Figure S15: ^{1}H **(a)** and ^{13}C **(b)** spectra of chloromethyltin(IV) *N*-ethyl-*N*-phenyl dithiocarbamate **(6)**

(a)

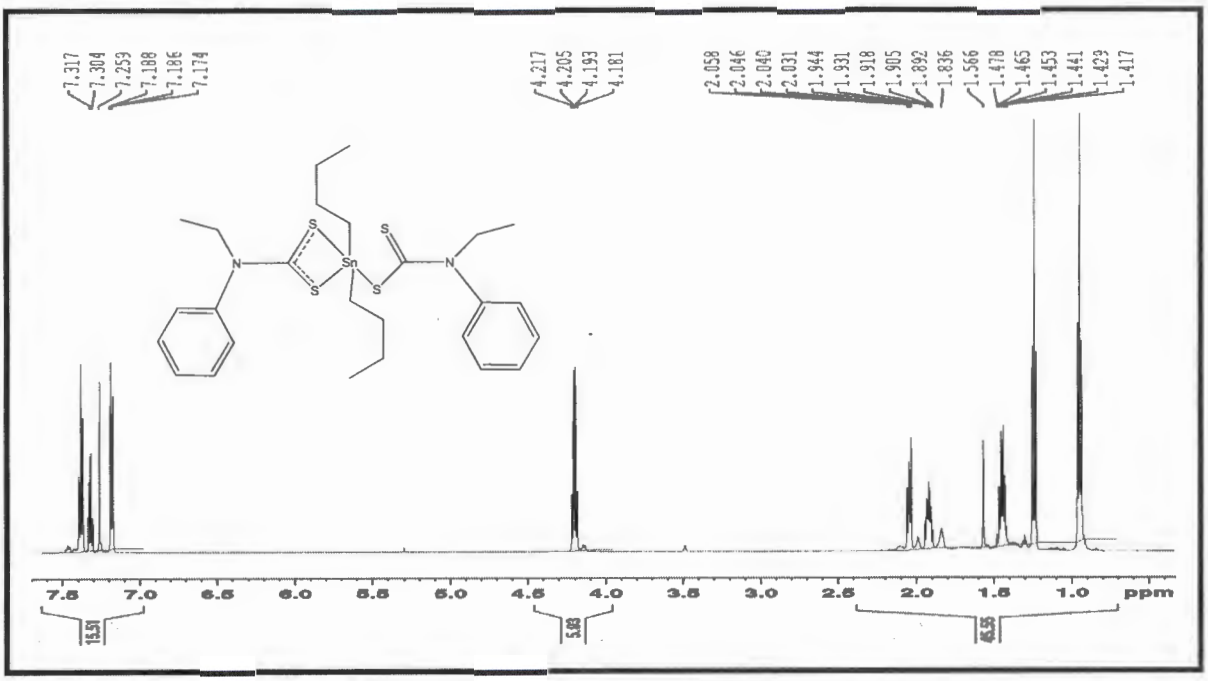

(b)

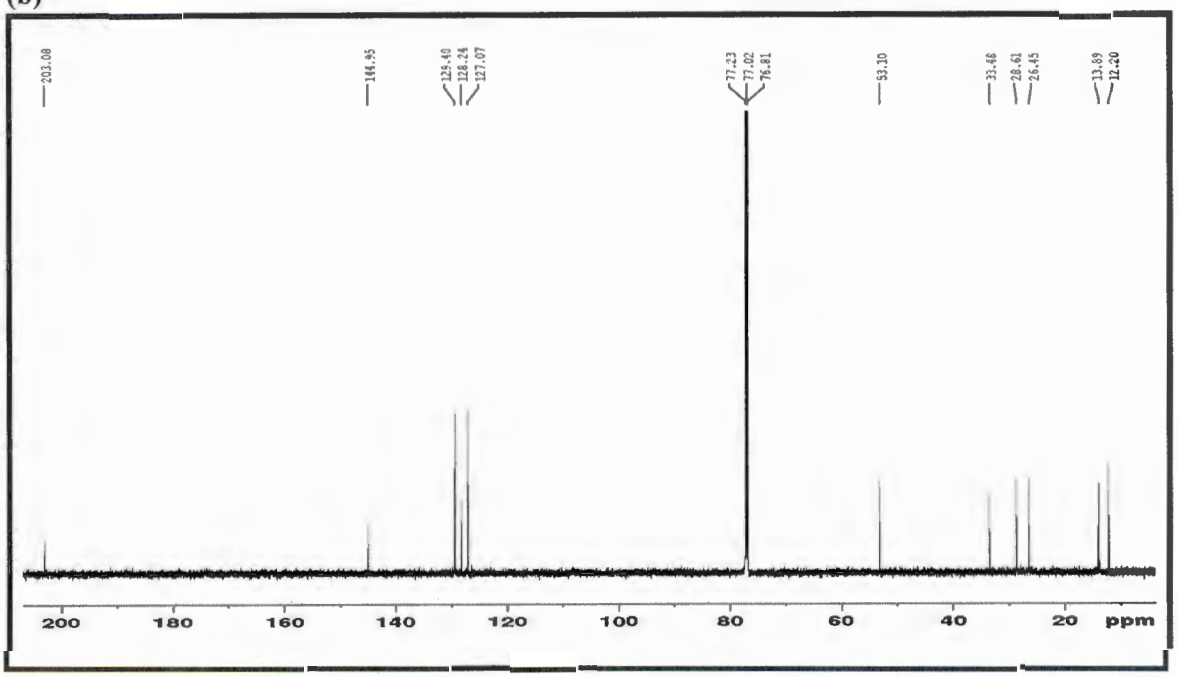

Figure S16: ^{1}H **(a)** and ^{13}C **(b)** spectra of dibutyltin(IV) *N*-ethyl-*N*-phenyl dithiocarbamate (**10**)

(a)

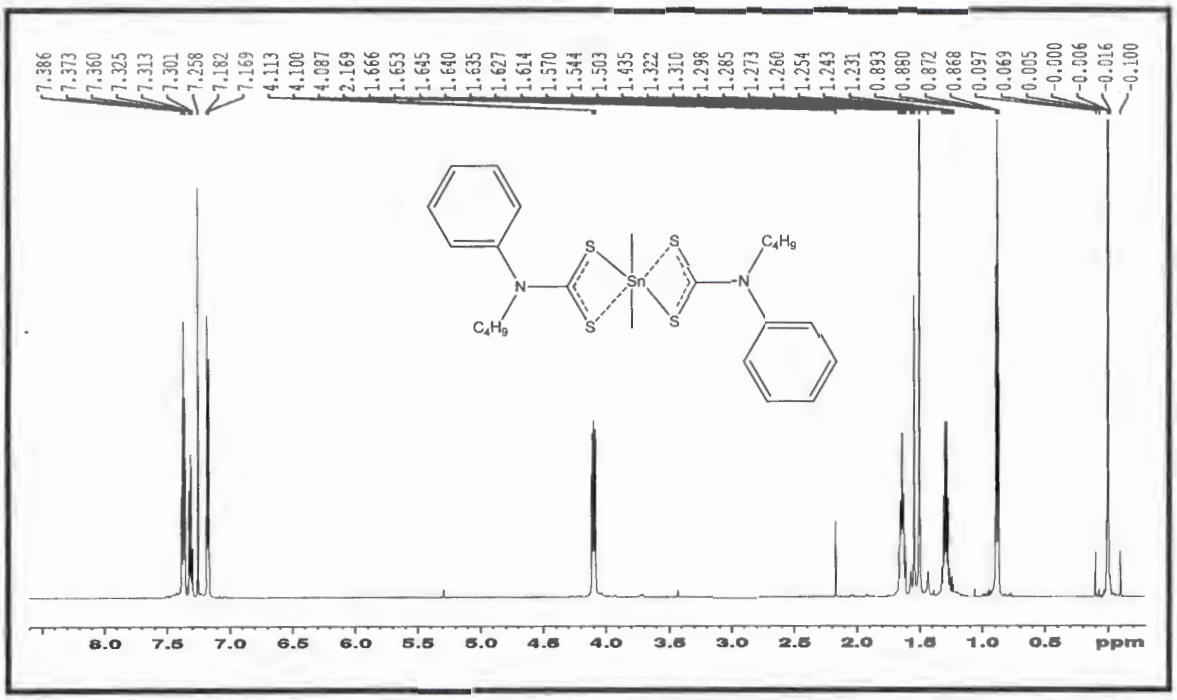

(b)

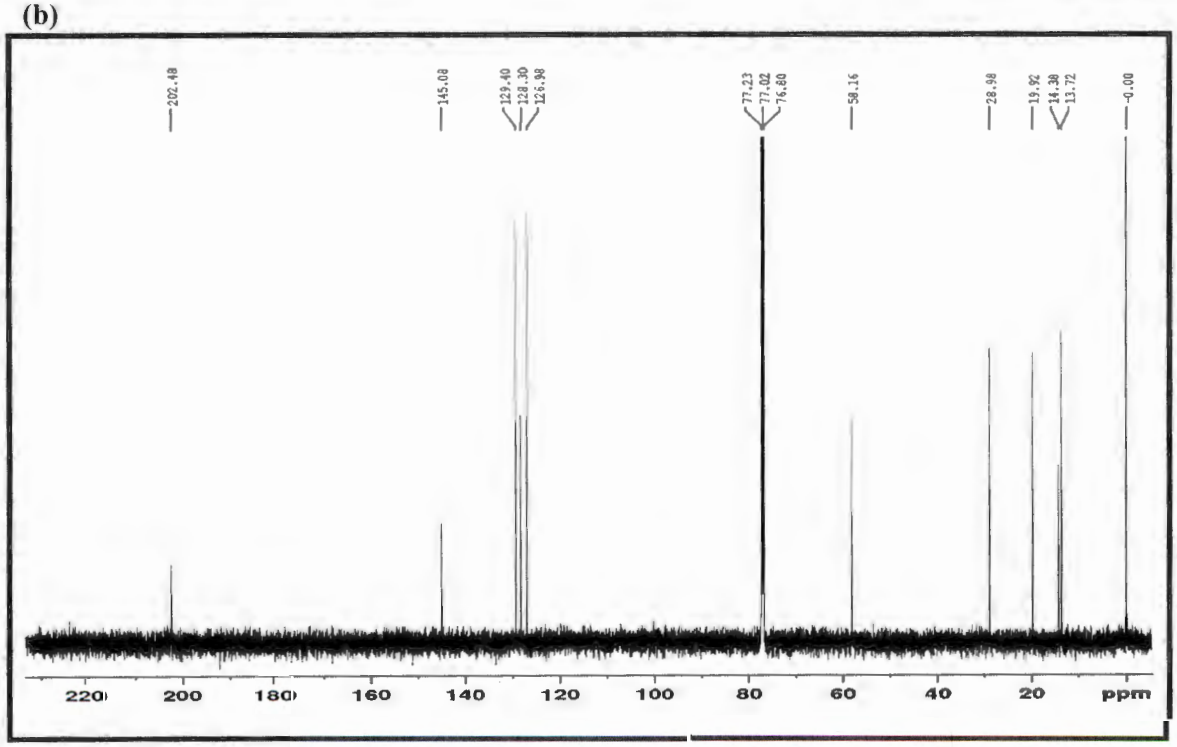

Figure S17: ^{1}H **(a)** and ^{13}C **(b)** spectra of dimethyltin(IV) *N*-butyl-*N*-phenyl dithiocarbamate **(13)**

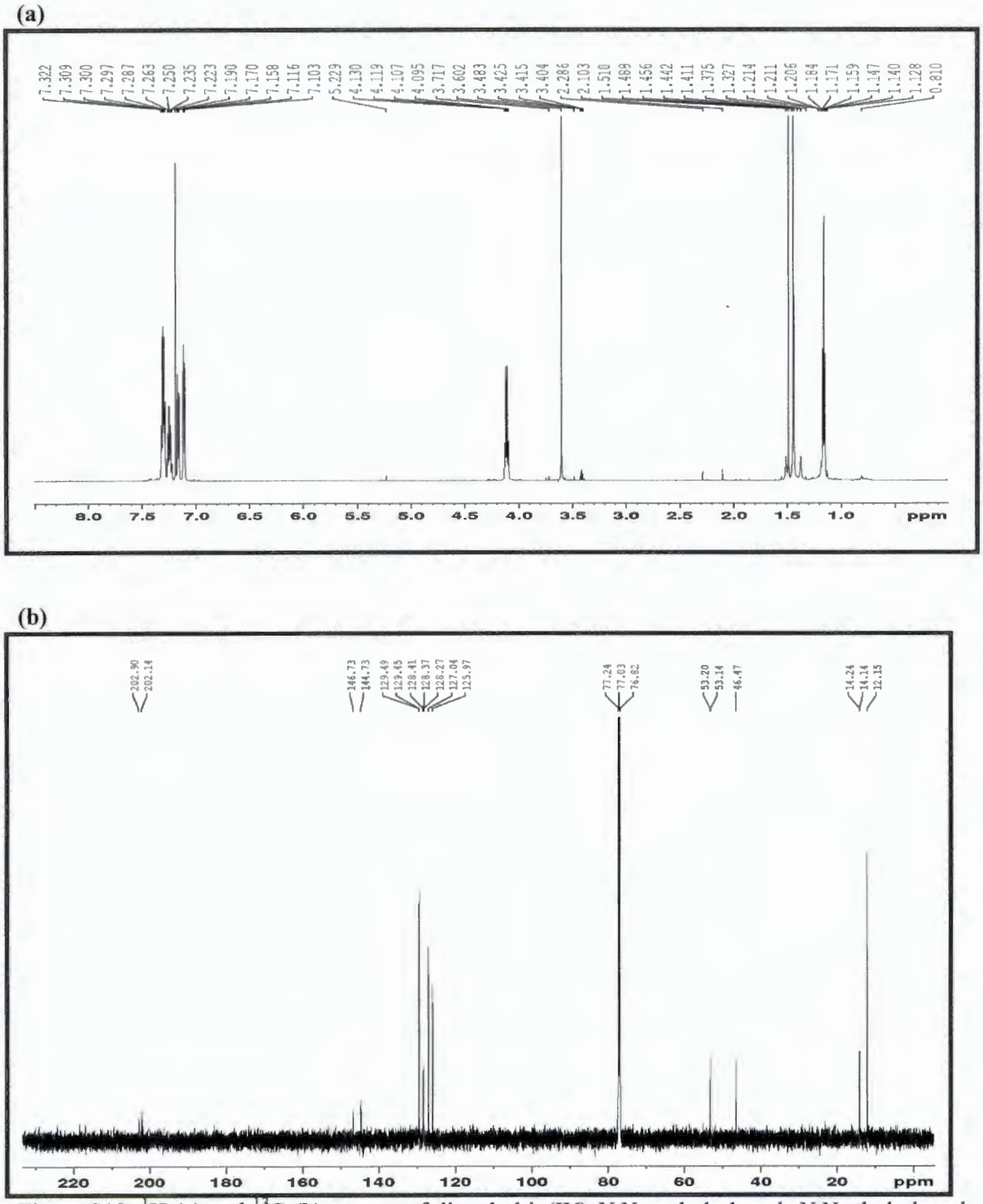

Figure S18: ^{1}H (**a**) and ^{13}C (**b**) spectra of dimethyltin(IV) *N,N*-methyl phenyl, *N,N*-ethyl phenyl dithiocarbamate (**16**)

(a)

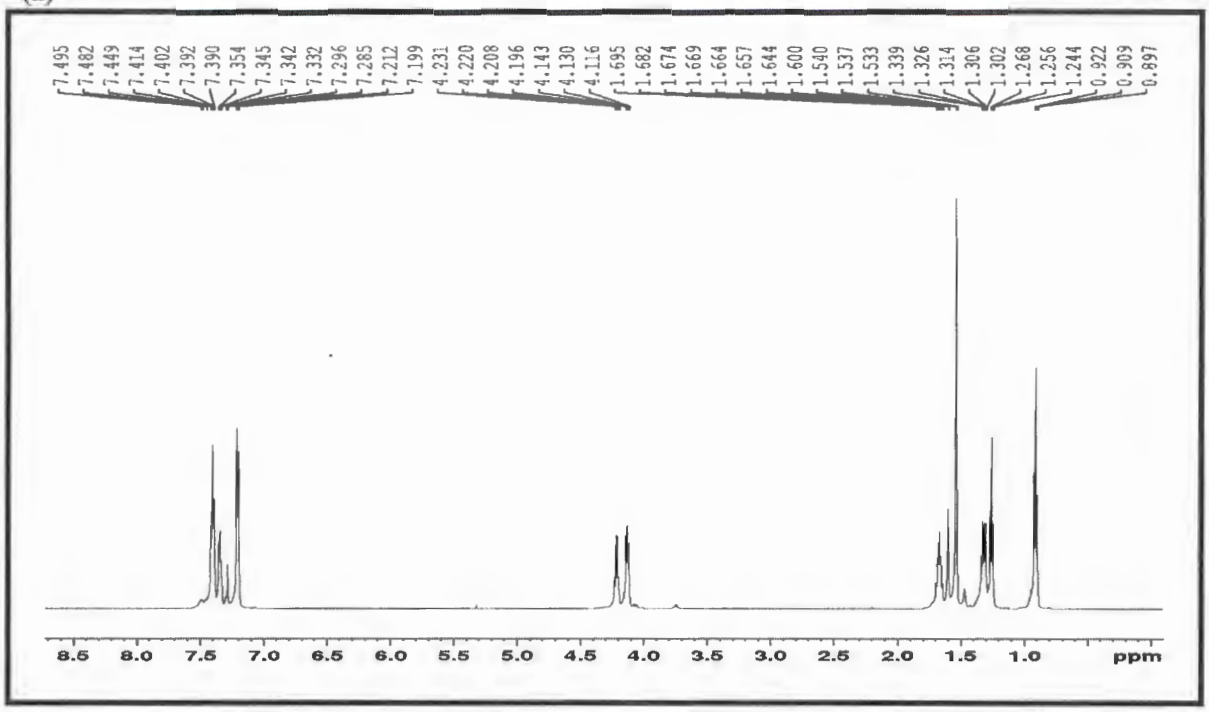

(b)

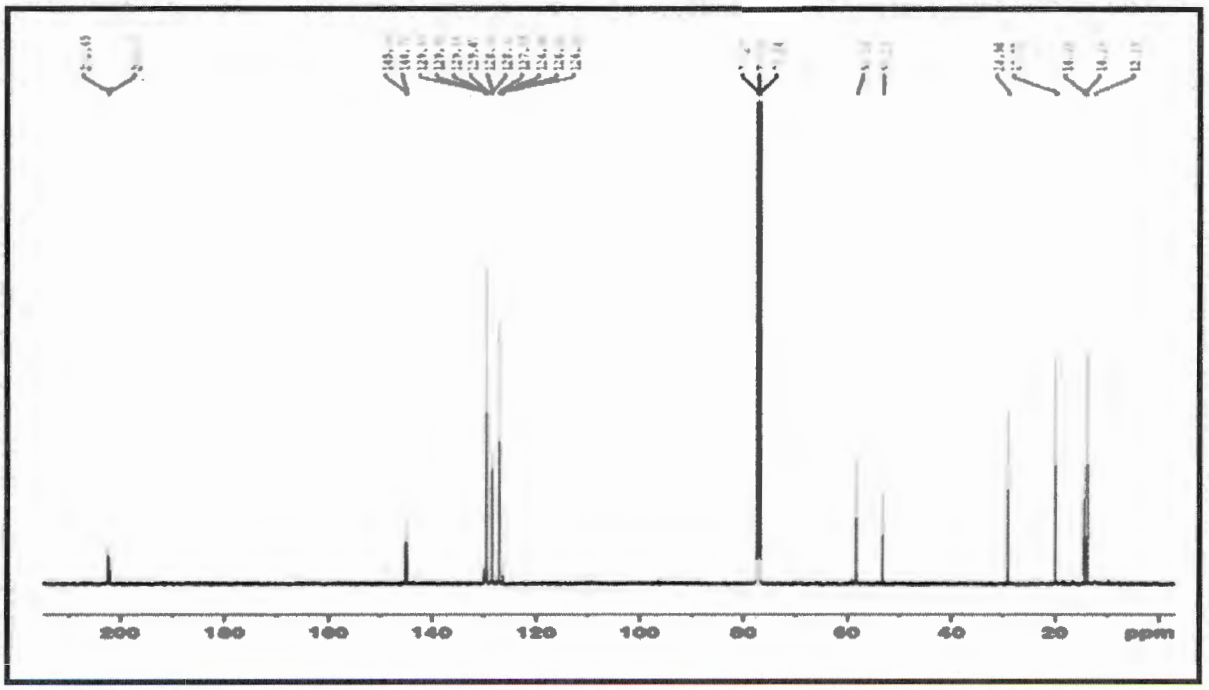

Figure S19: ^{1}H **(a)** and ^{13}C **(b)** spectra of dimethyltin(IV) *N*,*N*-butyl Phenyl *N*,*N*-ethyl phenyldithiocarbamate (**20**)

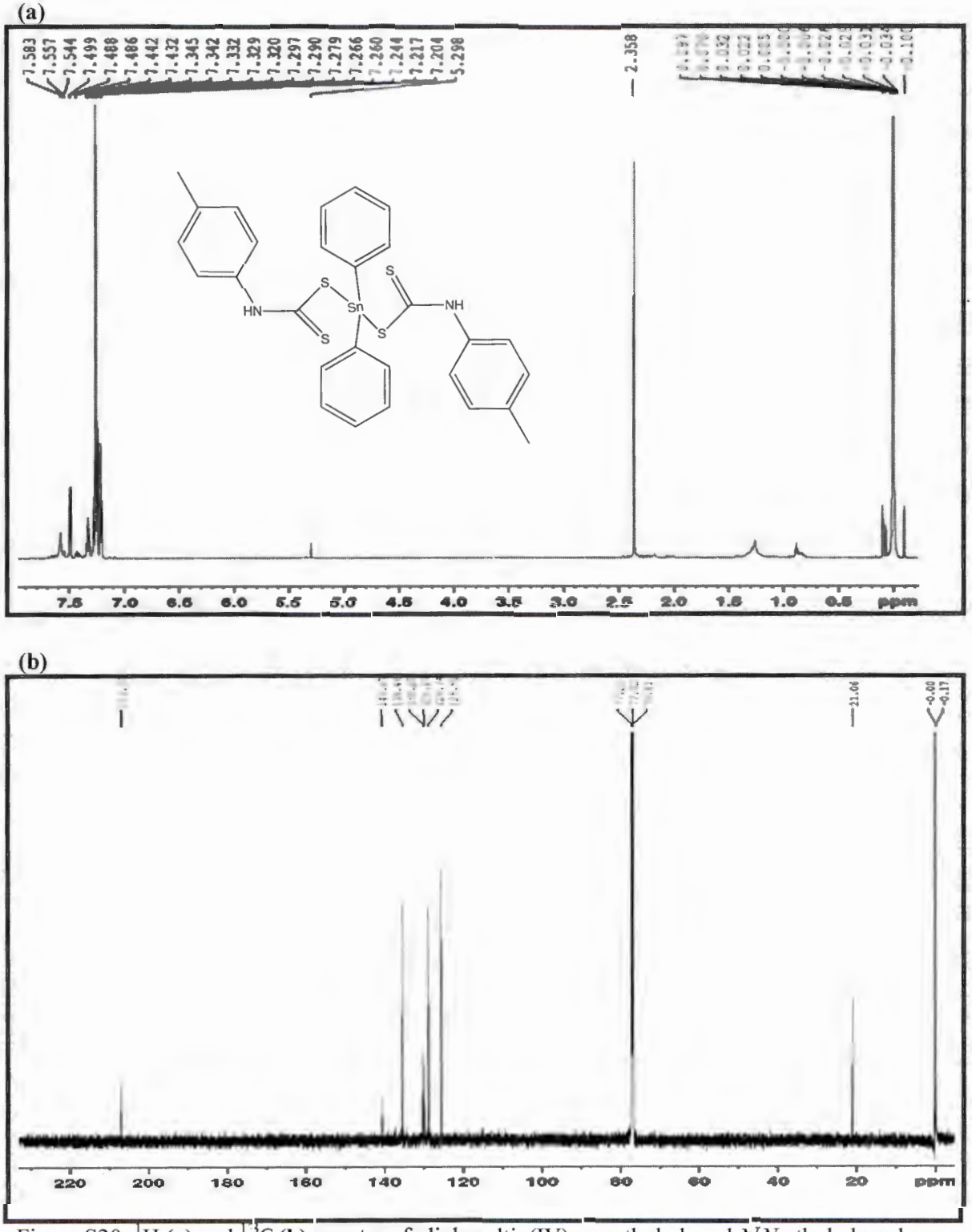

Figure S20. ^{1}H (**a**) and ^{13}C (**b**) spectra of diphenyltin(IV) *p*-methyl phenyl *N,N*-ethyl phenyl dithiocarbamate (**27**)

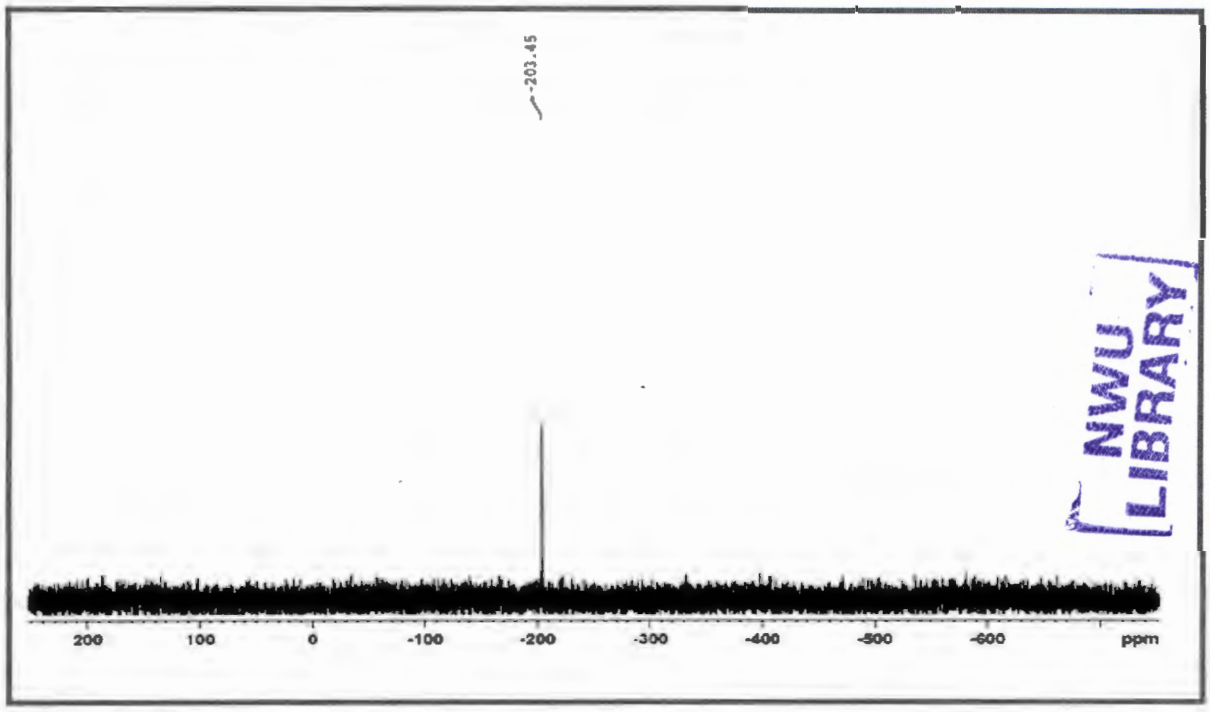

Figure S21: ^{119}Sn NMR spectrum of chorobutyltin(IV) *N*-methyl-*N*-phenyl dithiocarbamate (**1**)

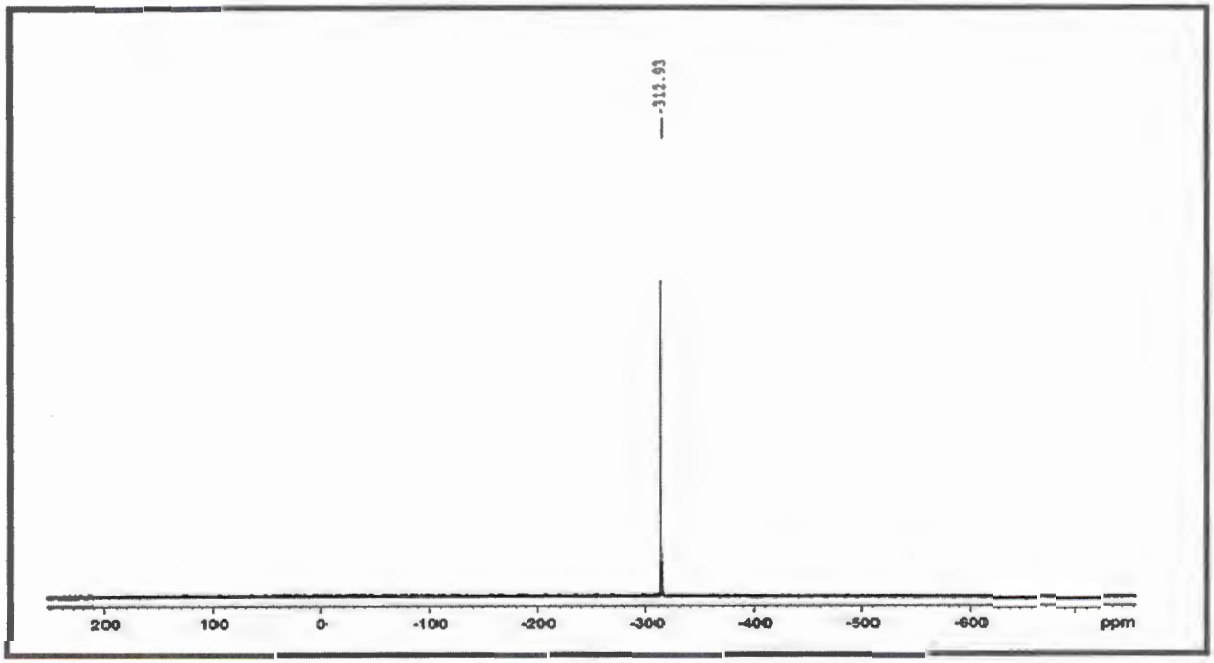

Figure S22: ^{119}Sn NMR spectrum of dimethyltin(IV) *N*-methyl-*N*-phenyl dithiocarbamate (**3**)

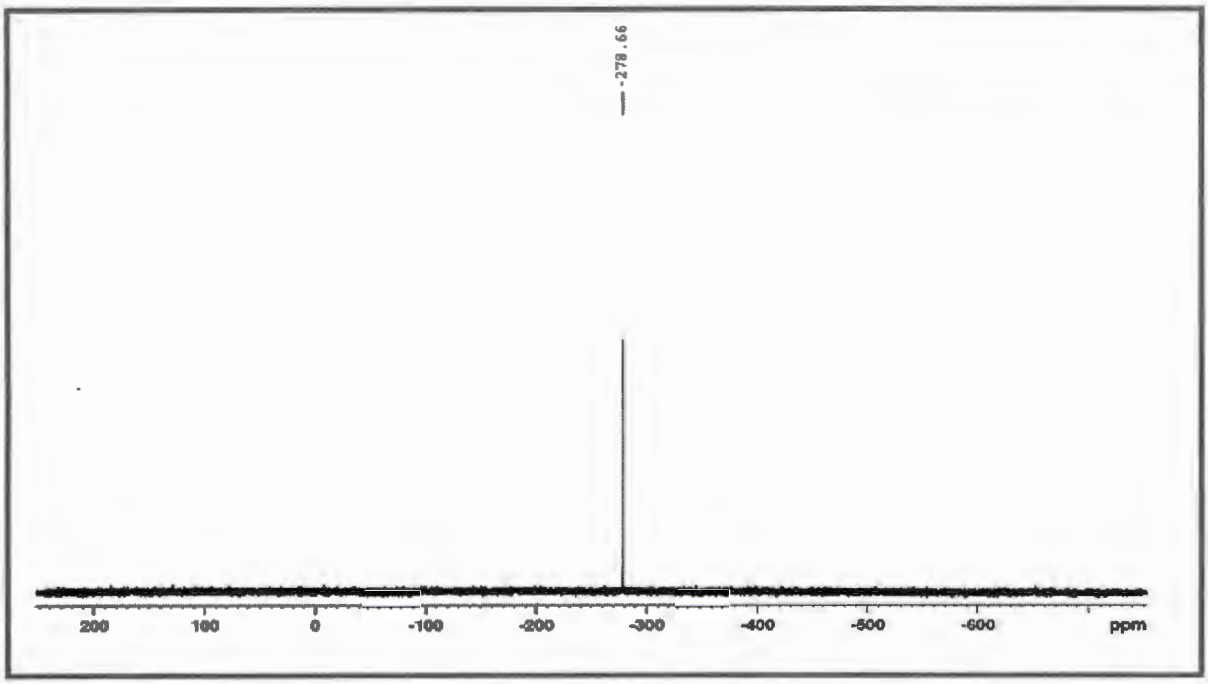

Figure S23: ^{119}Sn NMR spectrum of chorobutyltin(IV) *N*-methyl-*N*-phenyl dithiocarbamate (**7**)

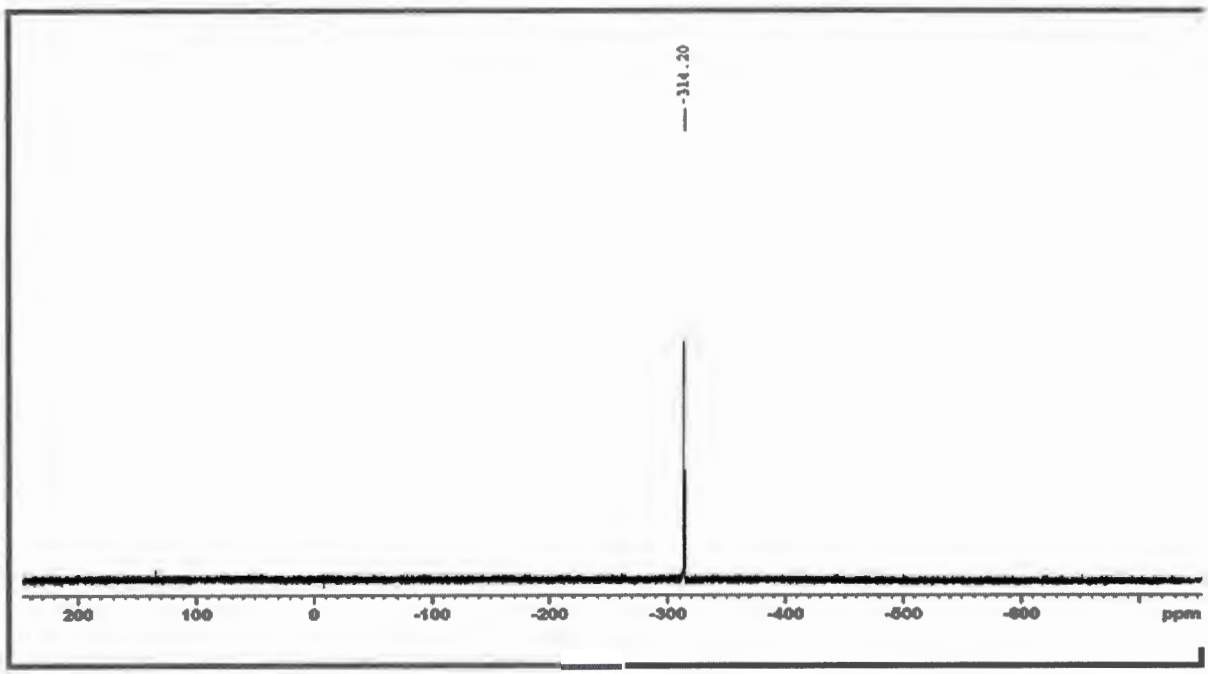

Figure S24: ^{119}Sn NMR spectrum of dibutyltin(IV) *N*-butyl-*N*- phenyl dithiocarbamate (**14**)

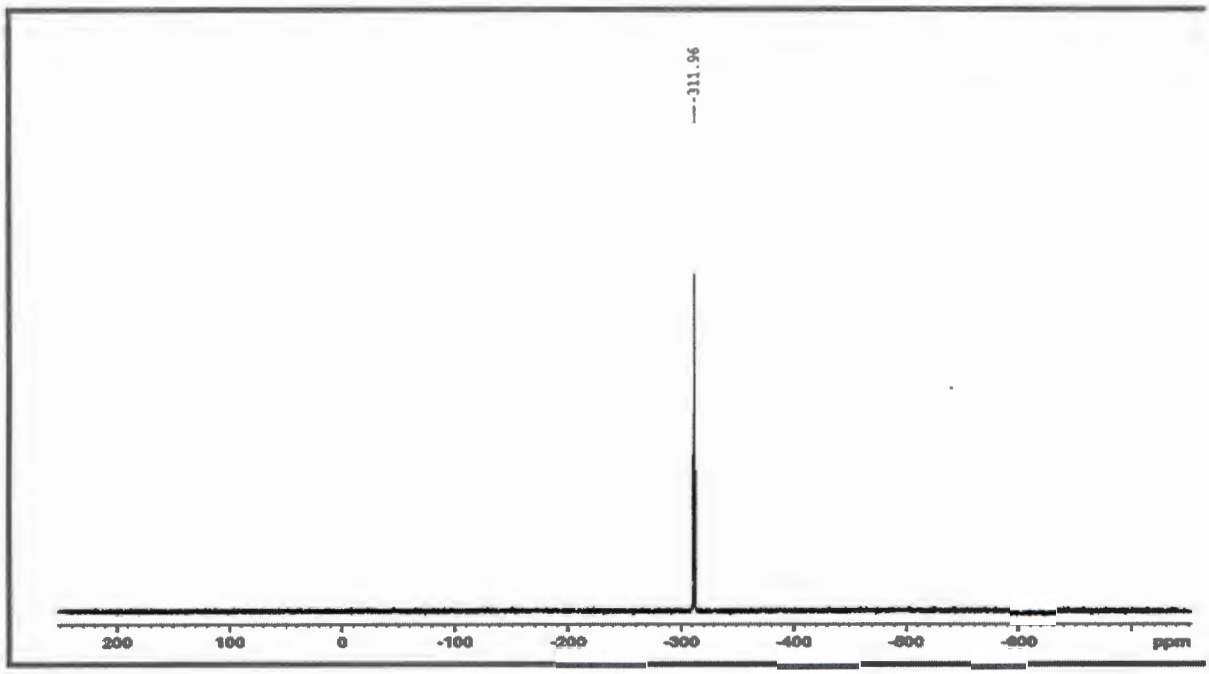

Figure S25: ^{119}Sn NMR spectrum of dimethyltin(IV) *N,N*-methyl phenyl *N,N*-ethyl phenyl dithiocarbamate (**16**)

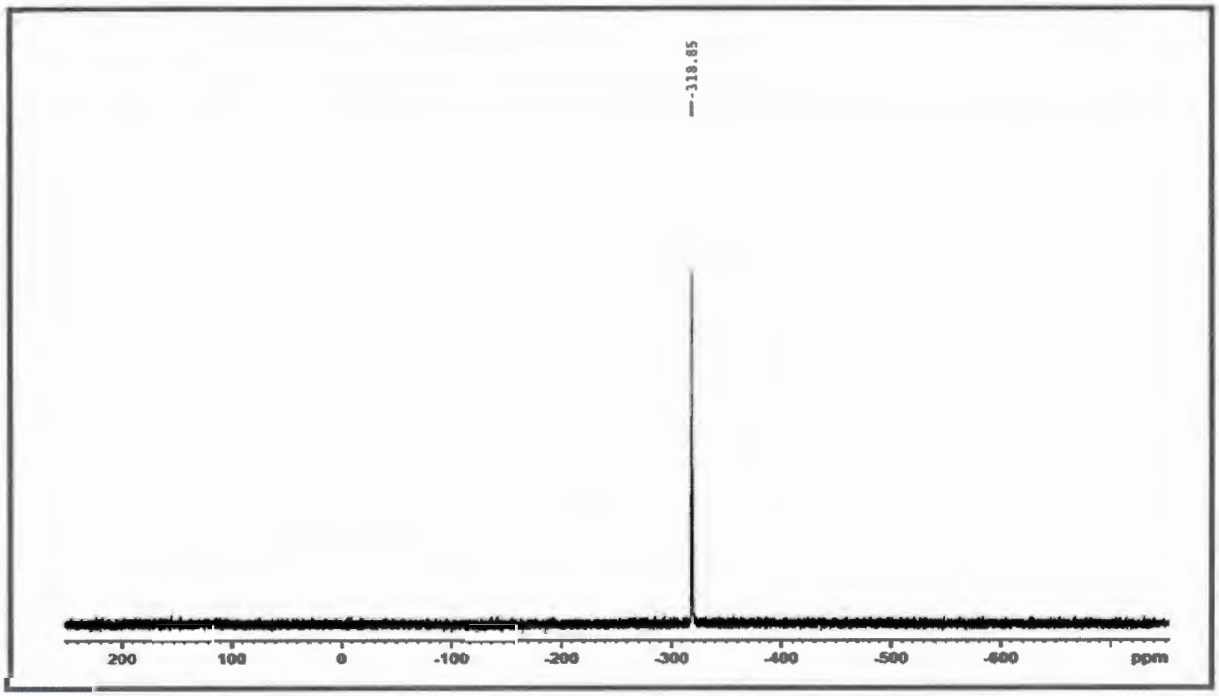

Figure S26: ^{119}Sn NMR spectrum of dibutyltin(IV) *N,N*-methyl phenyl *N,N*-ethyl phenyl dithiocarbamate (**17**)

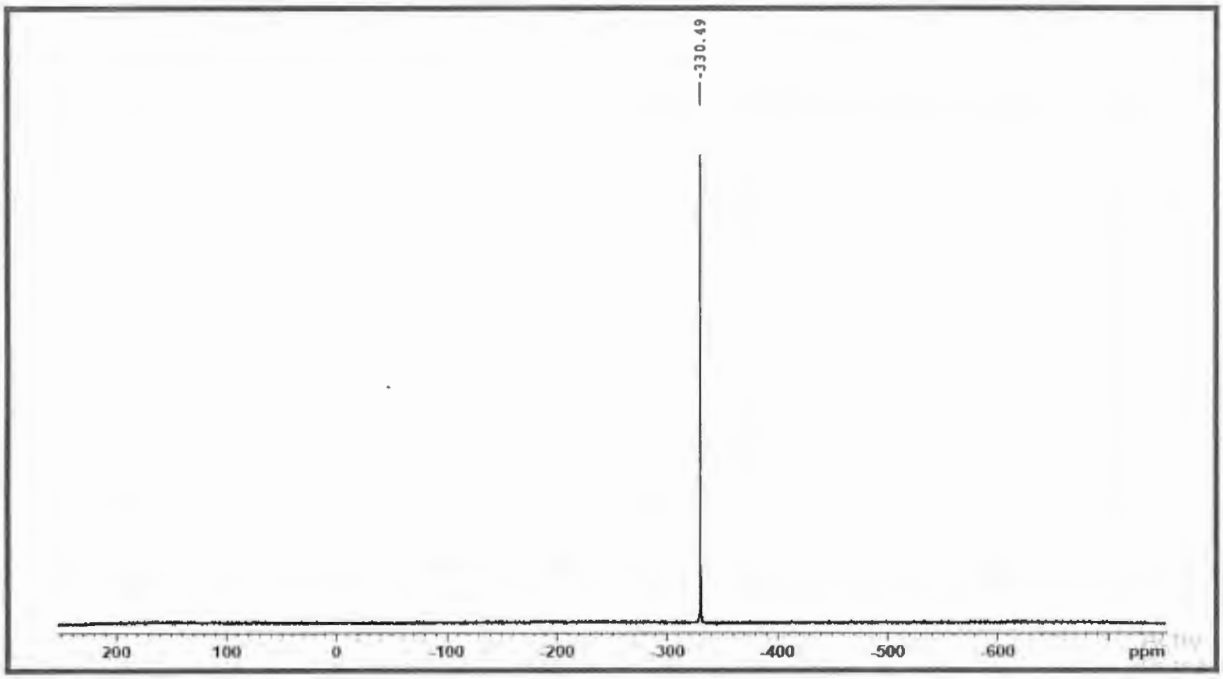

Figure S27: ^{119}Sn NMR spectrum of dimethyltin(IV) N,N-diallyl dithiocarbamate (**22**)

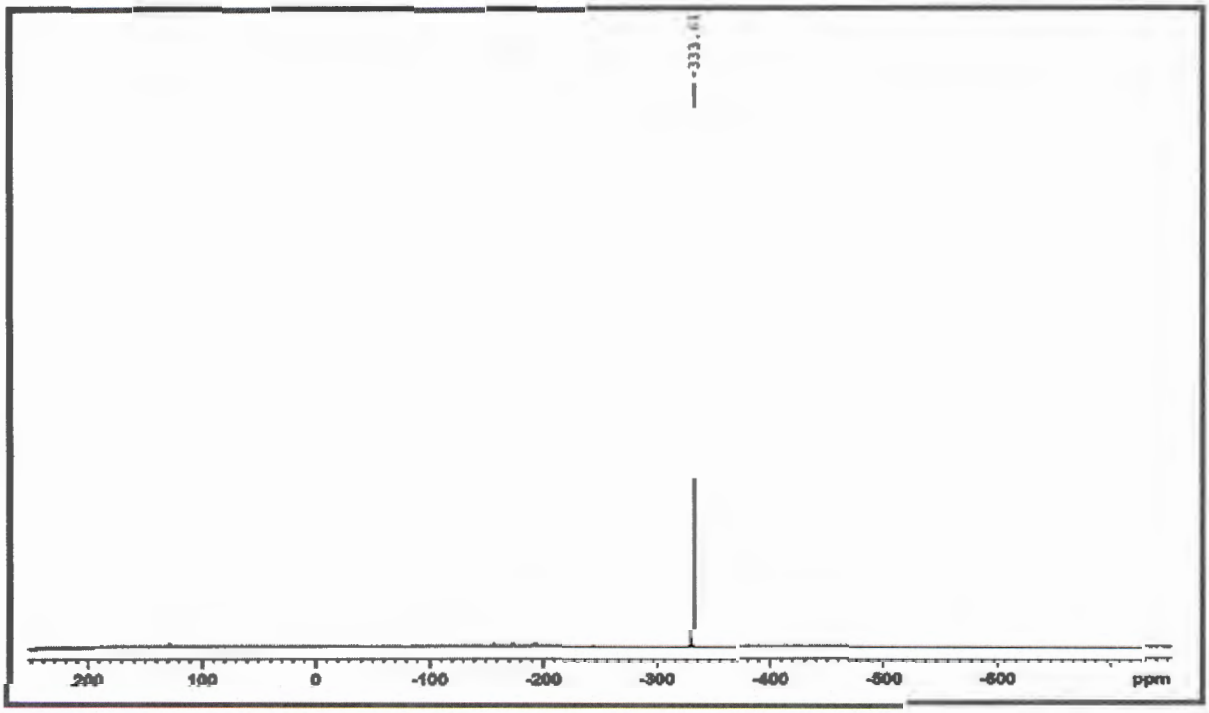

Figure S28: ^{119}Sn NMR spectrum of dibutyltin(IV) *N,N*-diallyl dithiocarbamate (**23**)

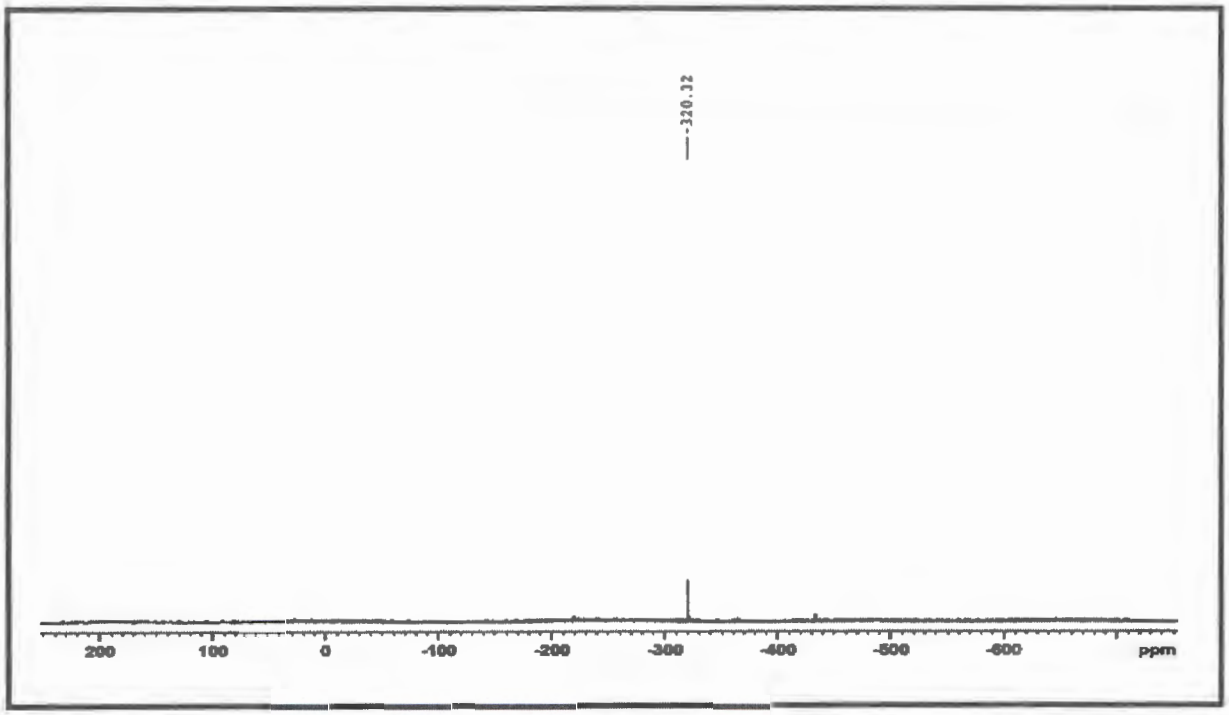

Figure S29: ^{119}Sn NMR spectrum of dibutyltin(IV) *N,N* diallyl dithiocarbamate (**25**)

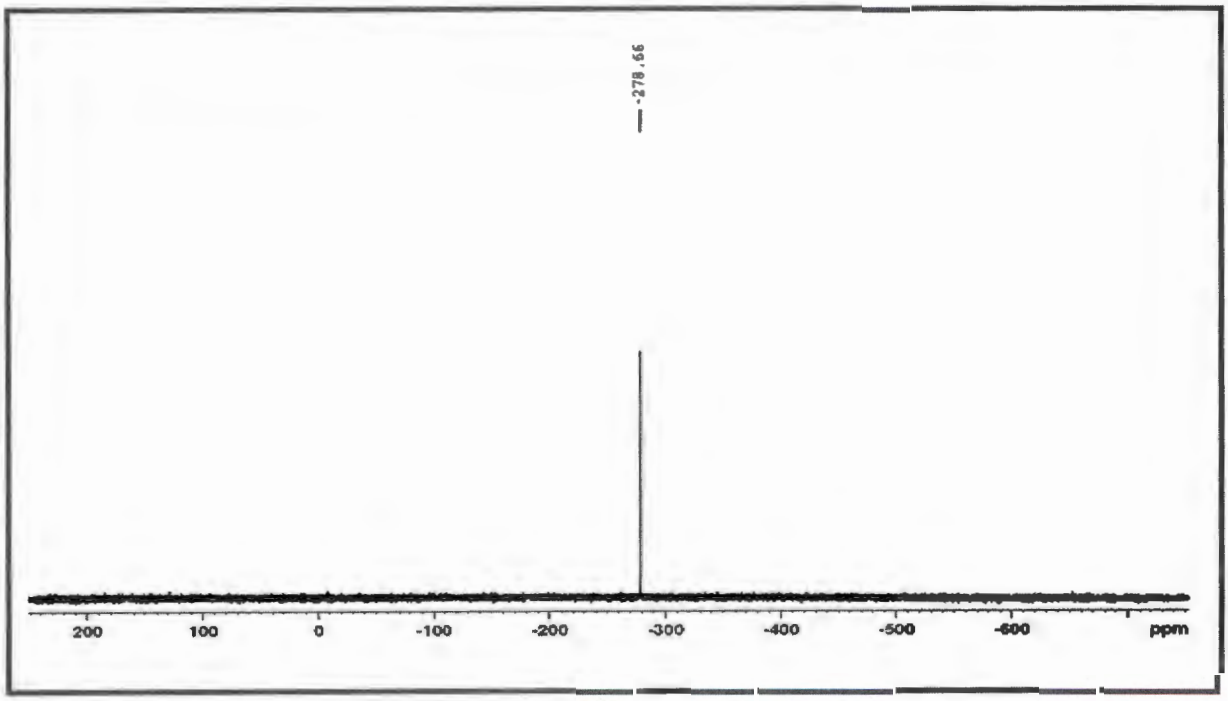

Figure S30: ^{119}Sn NMR spectrum of dibutyltin(IV) *p*-ethyl phenyl dithiocarbamate (**29**)

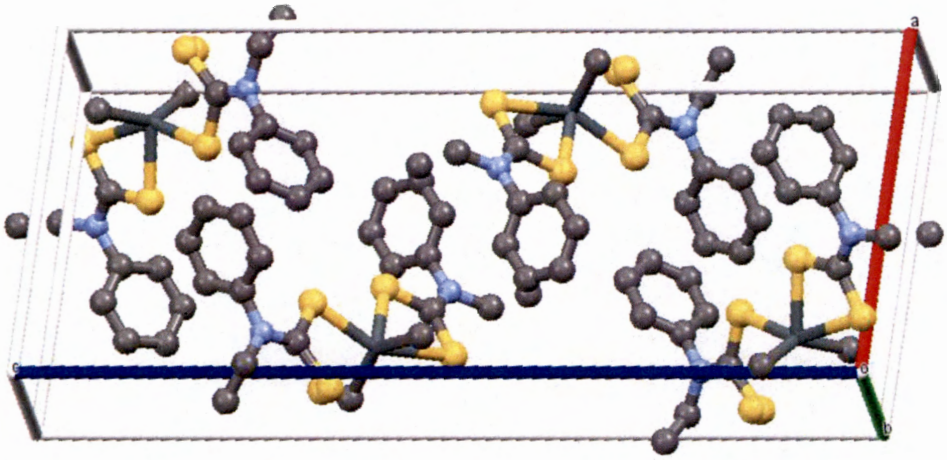

Figure S31: Crystal packing of dimethyltin(IV) *N,N*-methyl phenyl, *N,N*-ethyl phenyl dithiocarbamate (**16**) viewed along the best axis.

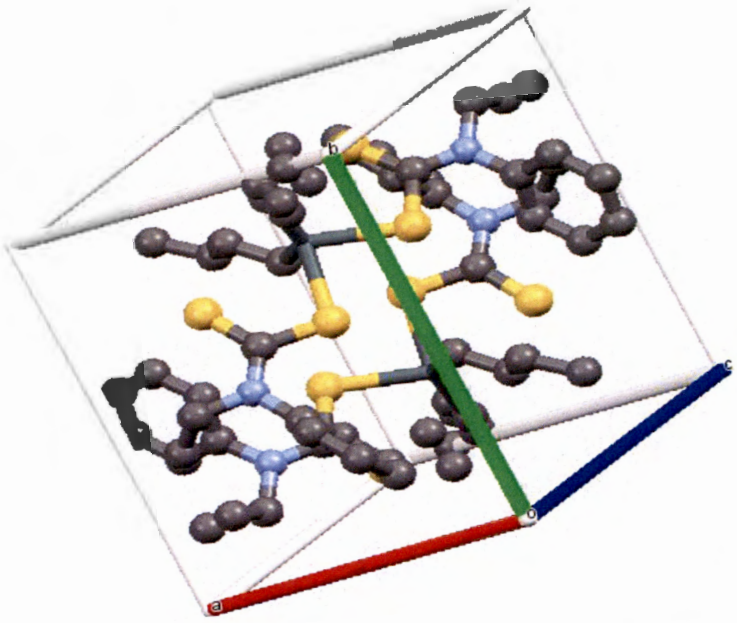

Figure S32: Crystal packing of dibutyltin(IV) *N,N*-methyl phenyl, *N,N*-ethyl phenyl dithiocarbamate (**17**) viewed along the best axis.

Supplementary data of organotin(IV)*N*-methyl-*N*-phenyldithiocarbamate complex

Crystallographic data of the complexes have been deposited with the Cambridge Crystallographic Data Center allocated with the deposit number CCDC 1551583 and 1551584 for complex **3** and **4**. Copy of the data can be obtained free of charge on application to CCDC, 12 Union Road, Cambridge CB2 1EZ, UK, fax: +44 1223 336033, email:deposit@ccdc.cam.ac.uk

Supplementary data of organotin(IV)*N*-ethyl-*N*-phenyldithiocarbamate complex

Crystallographic data of the complexes have been deposited with the Cambridge Crystallographic Data Center allocated with the deposit number CCDC 1551581 and 1551582 for complex **9** and **10**. These data can be obtained free of charge from The Cambridge Crystallographic Data Centre via www.ccdc.cam .ac.uk/data_request/cif.

Supplementary data organotin(IV)*N*-butyl-*N*-phenyldithiocarbamate complex

Crystallographic data of the complexes have been deposited with the Cambridge Crystallographic Data Center allocated with the deposit number CCDC 1551526 and 1834806 for complex **13** and **14**. Copy of the data can be obtained free of charge on application to CCDC, 12 Union Road, Cambridge CB2 1EZ, UK, fax: +44 1223 336033, email:deposit@ccdc.cam.ac.uk.

Supplementary data of organotin(IV)*N,N*-methylphenyl-*N,N*-ethylphenyl dithiocarbamate complexes

Crystallographic data for the structural analyses have been deposited with the Cambridge Crystallographic Data Centre, CCDC 1831463 and 1831466 contains the supplementary crystallographic data for complex **16** and **17**. These data can be obtained free of charge from The Cambridge Crystallographic Data Centre via http://www.ccdc.cam.ac.uk/structures

Supplementary data of the organotin(IV)*N, N*,-diallyldithiocarbamate complexes

Crystallographic data for the structural analyses have been deposited with the Cambridge Crystallographic Data Centre, CCDC Nos 1576822 and 1844959 for complexes **22** and **23**. Copies of this information may be obtained free of charge from: The Director, CCDC, 12 Union Road, Cambridge CB2 1EZ, UK [fax: (int. code) +44 1223-336- 033; e-mail: deposit@ccdc.cam.ac.uk or www: http://www.ccdc. cam.ac.uk].

Table S1: Summary of antimicrobial screening of complexes of the Ligands used at 100 µg/mL

S/N	Compounds	*S. aureus*	*B. Cereus*	*K. Pneumonia*	*E.Coli*	*P.Aeruginosa*	*C. Albican*	*A. flavus*
1	*N*-methyl PDTC	11±0.0	11±0.0	13±0.7	15±0.0	13±0.7	10±0.7	11±2.1
2	*N*-ethyl PDTC	13±0.7	10±2.1	15±0.0	15±2.1	16±0.7	13±1.4	10±0.0
3	*N*-butyl PDTC	16±2.1	12±2.1	15±0.7	19±1.4	16±0.0	11±0.7	11±1.4
4	*N,N*-diallyl DTC	13±0.3	11±0.1	16±0.6	13±0.3	11±0.5	R	09±1.1
4	*p*-methyl ligand	12±0.7	10±0.7	14±0.0	14±0.0	11±0.7	10±0.0	10±1.4
6	*p*-methyl ligand	R	R	10±0.0	11±2.1	13±0.7	R	09±2.1
5	benzyl ligand	R	R	10±1.4	10±1.4	13±0.0	R	07±2.1

100µg/mL; Double screening; R = Resistant

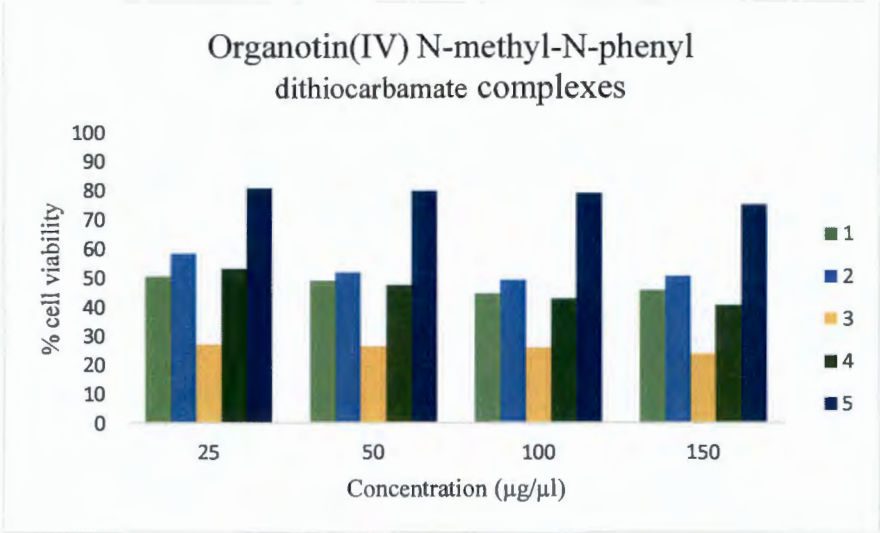

Figure S33: Histogram representation of %cell viability to concentration for complex 1-5

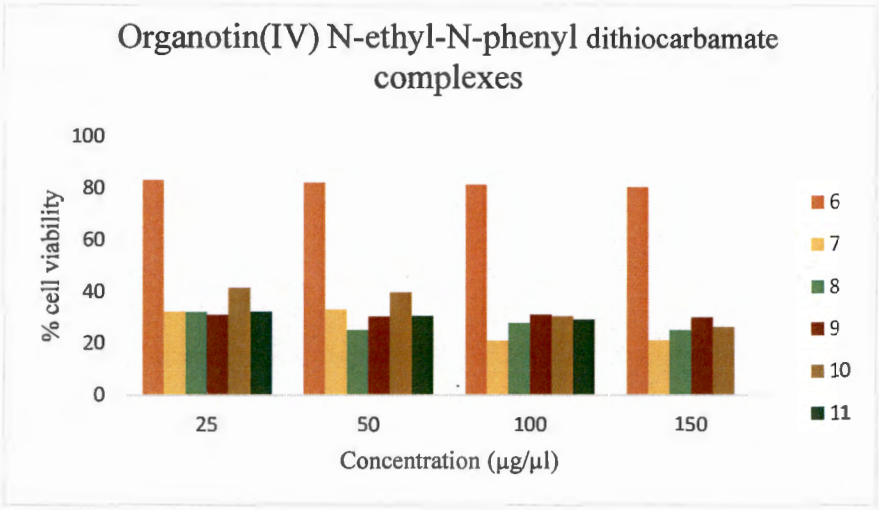

Figure S34: Histogram representation of %cell viability to concentration for complex 6-11

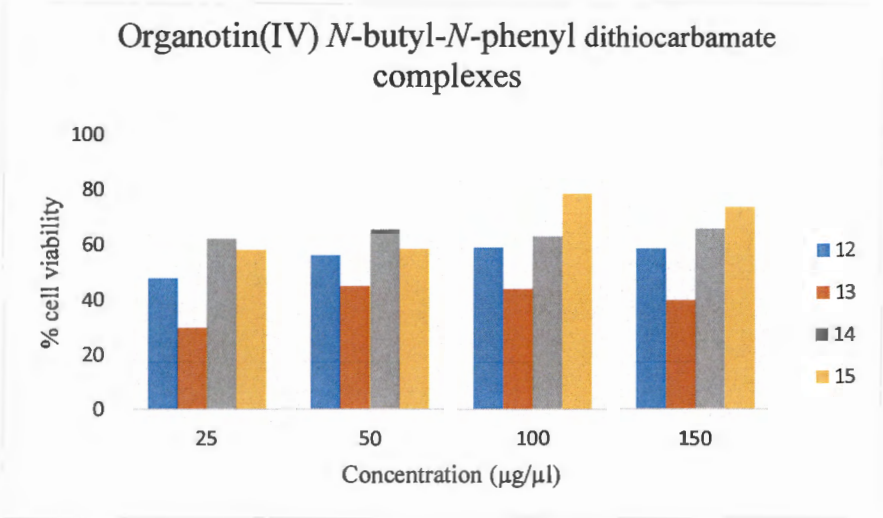

Figure S35: Histogram representation of %cell viability to concentration for complex 12 - 15

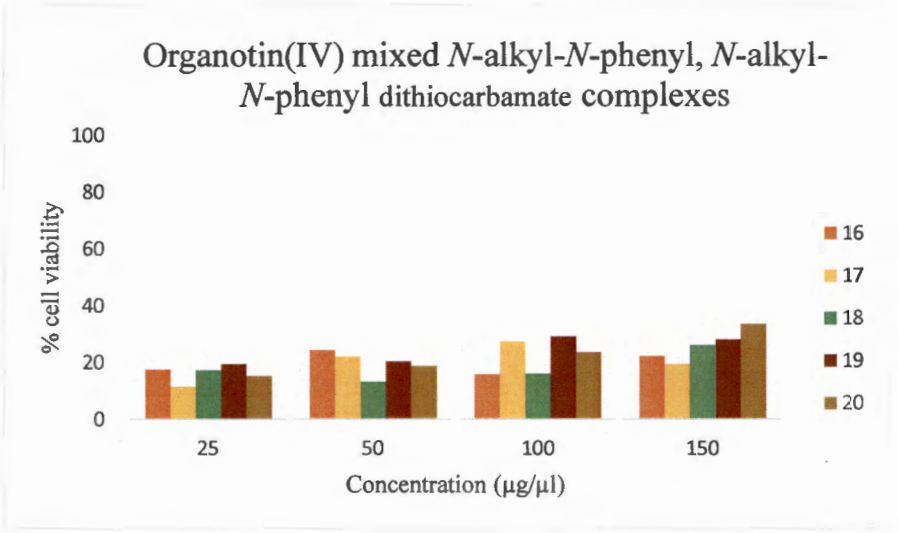

Figure S36: Histogram representation of %cell viability to concentration for complex 16-20

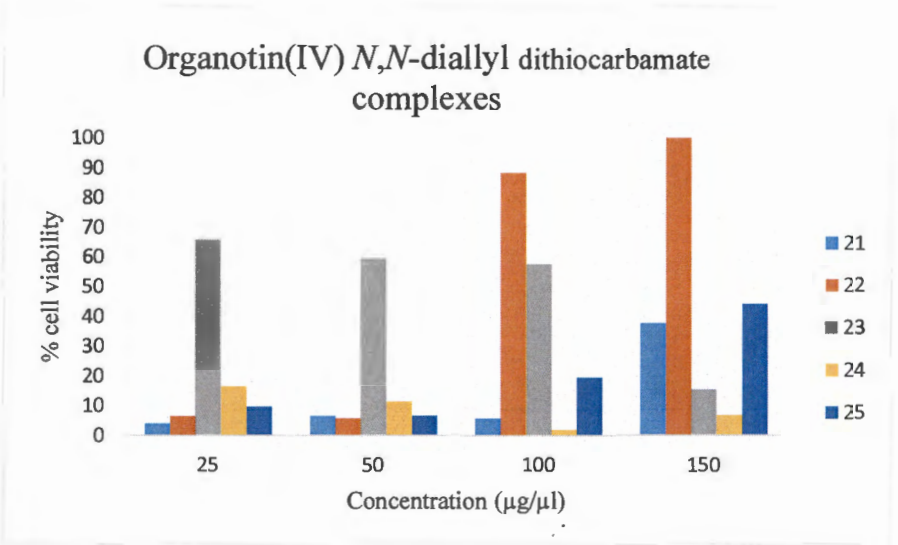

Figure S37: Histogram representation of %cell viability to concentration for complex 21-25

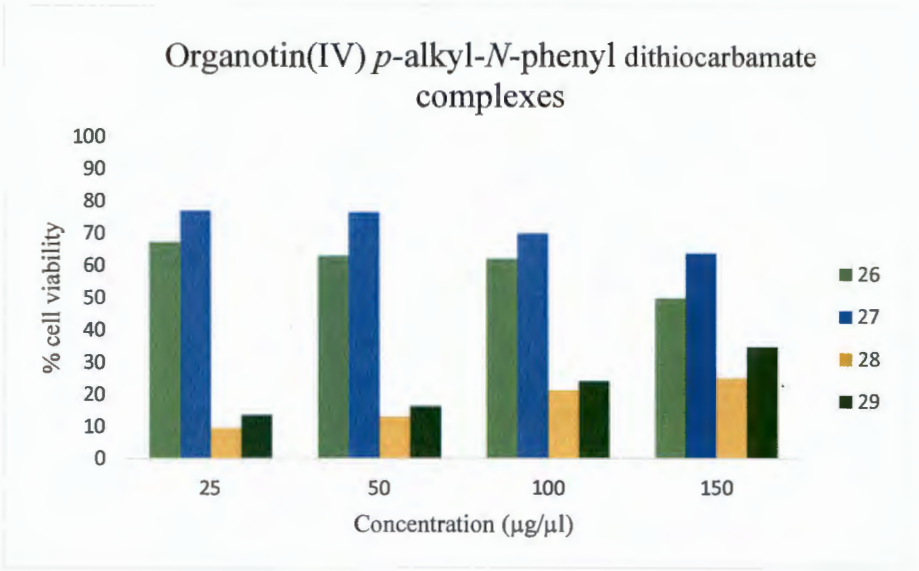

Figure S38: Histogram representation of %cell viability to concentration for complex 26-29

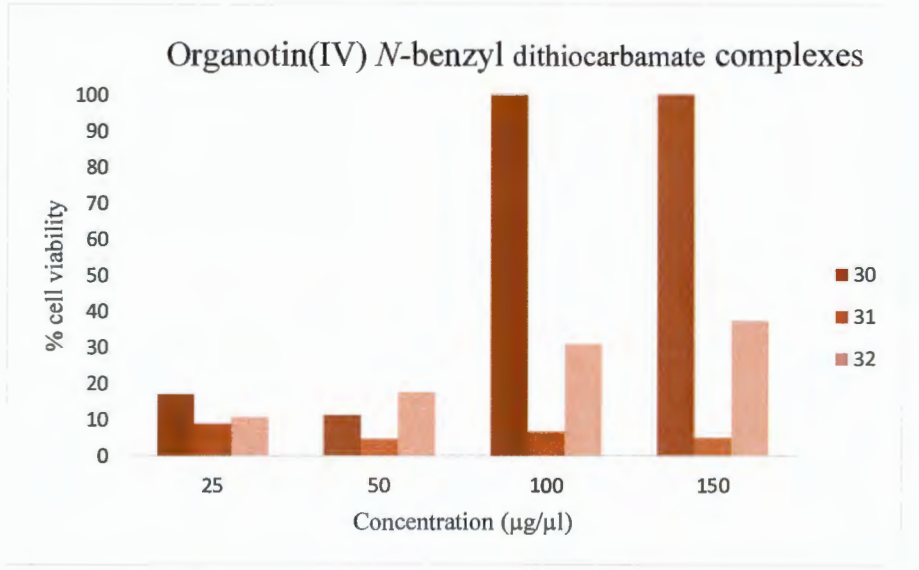

Figure S39: Histogram representation of %cell viability to concentration for complex 30-32